

Final Design Report
Deployable Cover for CubeSat FUV Imager



Senior Project Team:

Edwin Rainville – erainvil@calpoly.edu

Jeff Wagner – jwagne19@calpoly.edu

Patrick Whitesel – pmwhites@calpoly.edu

Project Advisors:

Dr. Eltahry Elghandour – Cal Poly

Jason Grillo- Co-Advisor, Cal Poly Graduate Student

Project Sponsors:

University of California, Berkeley – Space Sciences Laboratory

Kodi Rider – UCB, SSL

Dr. Thomas Immel – UCB, SSL

December 6, 2019

Table of Contents

1. Abstract	6
2. Introduction.....	7
3. Background	7
4. Objectives and Engineering Specifications	12
4.1 Objectives	12
4.2 Engineering Specifications and Testing	12
4.3. Boundary Diagram.....	14
4. Concept Design Development	15
4.1 Design Function.....	15
4.2 Brainstorming and Ideation.....	16
4.3 Early Prototyping.....	26
4.4 Idea Refinement.....	27
5. Final Design	38
5.1 Bottom Mirror Assembly	39
5.2 Top Mirror Assembly	41
5.3 Top Mirror Hinge Assembly	43
5.4 GSE Integration	47
6. Manufacturing, Assembly, and Integration	47
6.1 Procurement	47
6.2 Manufacturing	47
6.3 Assembly	48
7. Design Verification Plan.....	48
7.1 GEVS Testing.....	48
7.2 Optical Alignment Testing.....	49
8. Project Management	49
9. Conclusion & Recommendations	50
References	52
Appendices.....	53
Appendix A: Quality Function Development House of Quality	54
Appendix B: Gantt Chart.....	55

Appendix C: MATLAB Script.....	58
Appendix D: Morphological Matrix Design Concepts	63
Appendix E: Assembly Plan.....	64
Appendix F: Indented Bill of Materials	68
Appendix G: Flexure Analysis Calculations	69
Attachment H: Bottom Mirror Assembly Plan	71
Attachment I: Optical Alignment Test Plan	77
Appendix J: Bottom Mirror Assembly Finite Element Analysis	80
Appendix K: Deployable Cover Drawing Package.....	88

List of Figures

Figure 1. Front optics assembly designed by previous senior project group.	8
Figure 2. Release door mechanism on ICON FUV ^[1]	9
Figure 3. Example design of destructive wire burning showing burning element and tensioning components in cross section ^[7]	11
Figure 4. Flexure mounting of circular mirror, Smithsonian Astrophysical Observatory. ^[9]	12
Figure 5. Boundary Diagram of the Deployable Cover for the UV Imager CubeSat.	14
Figure 6. Final Volumetric Envelope for Deployment Cover Subsystem	15
Figure 7. Extended Mirror Concept Sketch for Mirror Alignment and Mounting Brainstorming	17
Figure 8. Auto-Alignment, Coupled Mirror Concept Sketch for Mirror	18
Figure 9. Mirror Orientation Double Door Concept Idea	19
Figure 10. Mirror Mounting Concept Design, Bolted Pattern	20
Figure 11. Mirror Mounting Concept Design, Epoxy Recession	21
Figure 12. Actuation and Lockout Design Idea #1	22
Figure 13. Actuation and lockout design idea #2.	23
Figure 14. Concept design for actuation of top cover deployment with a Miga Motor	24
Figure 15. Design Prototype #1	26
Figure 16. 1U Sheet Metal Cube for Subsystem Scale Visualization.....	27
Figure 17. Given space envelope by UCB SSL.	30
Figure 18. Initial schematic of concept design with variables used to determine a validated solution for the concept design.	31
Figure 19. Possible solutions that pass or fail the constraint for each crucial variable including: (A) length of mirror 1 L_{m1} , (B) length of mirror 2 L_{m2} , (C) angle between the lower corner of mirror 1 and the corner of the front baffle assembly, β , (D) angle between the back top corner of mirror 1 and the front corner of the CubeSat, Ψ , (E) angle between the lower corner of mirror 2 and the front corner of the CubeSat, ϕ , and (F) total solutions where all variables simultaneously meet all constraints which does not have any possible solutions.	33

Figure 20. Possible solutions that satisfy all remaining design constraints showing which iteration number passes all constraints as a blue line while the blank space is showing iterations that do not satisfy the requirements.	34
Figure 21. FOV of second mirror clipped by CubeSat front panel.....	35
Figure 22. FOV interference with Front Optics Assembly.....	36
Figure 23. CAD Depiction of Need for Translation and Rotation of Top Mirror for Preliminary Design	36
Figure 24. Preliminary layout and motion of deployable cover.	37
Figure 25. Preliminary dimensions of geometric layout.....	38
Figure 26. Final Deployable Cover design	39
Figure 27. Final bottom mirror assembly	39
Figure 28. Lower and upper mirror tangential flexure cantilever beam model	40
Figure 29. Top mirror in stowed position	41
Figure 30. Frangibolt mounting location	42
Figure 31. Deployable cover in open position	42
Figure 32. Top Mirror Hinge Assembly Overview	43
Figure 33. Top Mirror Hinge Assembly: Tower.....	44
Figure 34. Top Mirror Hinge Assembly: Shaft.....	44
Figure 35. Top Mirror Hinge Assembly: Top Clamp	45
Figure 36. Top Mirror Hinge Assembly: Spring	46
Figure 37. Top Mirror Hinge Assembly: Journal	46

List of Tables

Table 1. Table of Customer Requirements Organized by Category	8
Table 2. Preliminary List of Engineering Specifications Defined by UCB SSL	13
Table 3. Table of Verifying Tests	14
Table 4. Pugh matrix for mirror orientation and mounting.	28
Table 5. Pugh matrix from Morphology results.....	29
Table 6. Design 6 (Preliminary Design) Sub-Function Summary	29
Table 7. Summary of Variables Used to Validate Design Geometry	32
Table 8. Gantt chart summary of deadlines and task sections.	50

Nomenclature

CAD: Computer Aided Design

CCD: Charge-Coupled Device

FOA: Front Optics Assembly

FOD: Foreign Object Debris

FOM: Figure of Merit

FUV: Far Ultraviolet

GEVS: Goddard Space Flight Center General Environmental Verification Standard

ICON: Ionospheric Connection Explorer

PCB: Printed Circuit Board

SOW: Scope of Work

TVAC: Thermal Vacuum

UCB SSL: University of California, Berkeley – Space Sciences Laboratory

UV: Ultraviolet

1U: 10x10x10cm Volume

1. Abstract

The goal is to develop a deployable cover for a far ultraviolet imager cube satellite that will be used to map the earth's auroras in the ionosphere. The deployable cover is used to protect the Far Ultra-Violet (FUV) sensor and lenses, house two mirrors which are used to filter unwanted light and expose optics when deployed. The deployable cover consists of a door, an actuator, a lockout mechanism, and an "open position" indicator. This project also includes designing a fixture for testing the optical alignment of the deployable cover after launch and during orbital conditions. The subassembly is required to be contained within a 1U volume (10x10x10cm) with the existing front optics assembly, have minimal mass, and provide reliable optical alignment. The final design showed that two mirrors can be packaged into the given footprint if the second mirror is deployed outwards into position via a spring-driven door and the front panel is deployed to allow for full field of view. Although this project proved that a reliable design solution is possible and made long strides towards a finalized design, another design revision is suggested for the springs, front panel hinge, flexures, and mirror bonding fixtures to bring the system up to flight ready status.

2. Introduction

UC Berkeley-Space Sciences Laboratory (UCB-SSL) develops scientific instruments and satellites that allow them to research the Earth's atmosphere and beyond. SSL's Ionospheric Connection Explorer (ICON) team is interested in exploring the Earth's ionosphere. The ionosphere is an upper region of the Earth's atmosphere that is drastically impacted by Earth's weather and the Sun's radiation. There is a high amount of electrical activity in the ionosphere, and the ICON team is looking to study these phenomena. Imaging of these electrical activities prove to be rather challenging, but recent development in science has found imaging in ultraviolet provides excellent mapping capabilities ^[1]. Despite this finding, previous satellites with far ultraviolet (FUV) technology have been rather large and expensive, which make it a challenge for large scale mapping. ICON is looking to develop a cost-effective FUV imager in the CubeSat format which would have the capability of simultaneous large-scale mapping of Earth's auroras.

The senior project team at Cal Poly will develop a deployable cover to protect optical hardware and act as point of entry for light. By sealing the satellite during launch and pre-deployment, the cover will keep Foreign Object Debris (FOD) from contaminating the optical hardware during launch and orbit. This cover will provide mounting and alignment of entry mirrors, used for filtering unwanted wavelengths of light and providing indirect exposure to internal optics. This design will be subjected to thermal and vibrational loading during launch and orbit, requiring design validation through thermal vacuum (TVAC) and vibrational testing. In order to perform TVAC and vibration testing, our team will build a working prototype and an optical alignment test fixture.

This document provides our Preliminary Design Report (PDR) for our senior project's contribution to the development of the FUV imager. To begin, the background of the project will be discussed along with a literature review of design solutions and specification documents for satellites. Following the literature review, the main project objectives will be reviewed, which include the initial problem statement and design specifications. Using these design requirements, the concept design process is discussed. Finally, this document concludes with the next steps for our project and how we structure our project management.

3. Background

During initial project briefings, the group has learned that the project's objective is to validate a mechanical design of a deployable cover for a 2U CubeSat. This year will be the 2nd year of development of the FUV imager. A previous senior project group had design and verified the front optics assembly for the satellite, as seen in Figure 1.

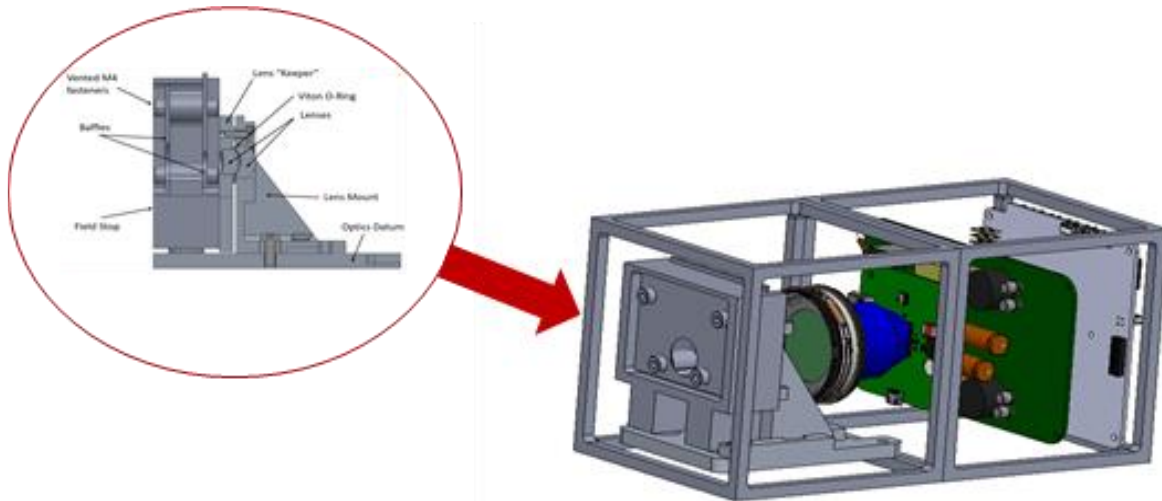


Figure 1. Front optics assembly designed by previous senior project group.

During the meeting, we spoke with Dr. Thomas Immel and Kodi Rider from SSL about what level of design the sponsor was expecting from our group. They indicated that a mechanically validated prototype was sufficient for our project scope, completed by mid-November 2019. The requirements of a successful design are listed below:

Table 1. Table of Customer Requirements Organized by Category

Category	Requirement
Performance	The UVI instrument shall be designed to allow the deployment of a protective cover post launch.
Performance	The UVI cover assembly shall contain two turn mirrors.
Performance	The UVI cover optics shall accommodate a 30 degree circular field of view (FOV).
Performance	The UVI cover shall suppress out of field stray light to <5%.
Performance	The UVI boresight shall remain aligned to within 0.25 degrees post launch with respect to its initial on-ground alignment.
Configuration	The UVI instrument shall fit within 2U, with the cover, optics, and baffles accommodating no more than 1U.
Configuration	The mass of the UVI cover shall be reported at pre-delivery to UCB.
Configuration	All remove before flight items shall be colored red and marked with "Remove before flight!".
Functional	The UVI cover shall maintain Allowable Flight Temperatures (AFTs), and successfully deploy at temperature extremes.
Functional	The UVI cover shall provide a positive indication of "open position" after deployment.
Ground Support Equipment (GSE)	Appropriate mechanical GSE to perform instrument alignment and I&T shall be designed and implemented.

In order to satisfy these requirements, we were pointed towards SSL's ICON FUV imager instrument. The instrument on-board the ICON satellite is a FUV imager that absorbs two different

wavelengths of ultra-violet light. The opto-mechanical design consists of entrance assembly where light is let in, an intricate mirror assembly that directs and filters light, and a CCD detector that absorbs the remaining UV light. Although ICON is a verified design, for low cost and large-scale scientific use it is not a viable option as it is too heavy (32kg) and complex to scale into the CubeSat form factor.

Despite the difference in satellite scale, ICON informed us that the controlled actuation of the deployment cover will likely be the largest design hurdle that we face. The ICON FUV door was purely a cover for particles and did not play a role into the optical alignment of the instrument. The cover for this project will not only be a functional mechanical door but it will also be port of entry for the light to be let into the satellite. This provides quite a challenge as the optics system in the FUV imager requires a tight optical angle tolerance to be functional. The door will have to be actuated and controlled in a manner that is functional in a space environment and is accurate to the desired angle tolerance.

From this design, we were able to see a functional actuation for a similar satellite. This design for a removable cover will be leveraged off this heritage design, as shown in Figure 2

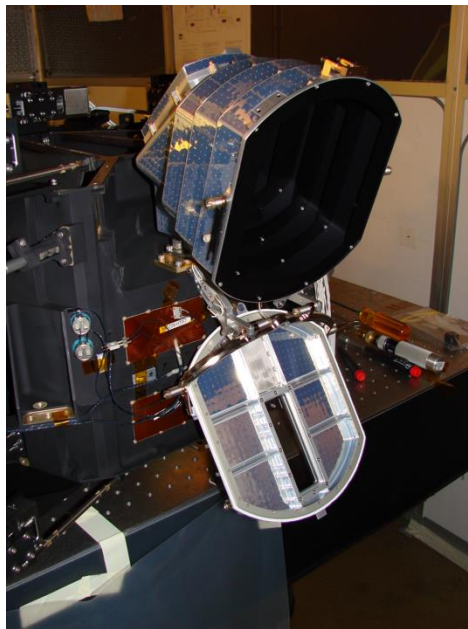


Figure 2. Release door mechanism on ICON FUV ^[1].

Despite the difference in satellite scale, this informed us that the controlled actuation of the deployment cover will likely be the largest design hurdle that we face. The ICON FUV door was purely a cover for particles and did not play a role into the optical alignment of the instrument. The cover for our project will not only be a functional mechanical door but it will also be port of entry for the light to be let into the satellite. This provides quite a challenge as the optics system in the FUV imager requires precise optical alignment. The door will have to be actuated and

controlled in a manner that is functional in a space environment and is accurate to the desired angle tolerance.

We also gained insight into industry standards for actuation and deployment technology. The list we uncovered during our literary review includes but is not limited to Frangibolts, Miga Motor actuators, wire burning, pin pullers, and circuit destruction. The Frangibolt is a non-explosive release device that uses shape memory alloys to shear conventional bolts with the application of a heat actuator. These are commonly used in many aerospace applications. Frangibolts eliminate the need for pyrotechnics which provide a major risk for spacecraft failure ^[3]. Another non-pyrotechnic actuation device is the Miga Motor. Miga Motors are small motors that can be used to replace standard motors and solenoids. These motors also use shape memory alloys (Nickel Titanium) to produce considerable power for their small size. Miga Motors are ideal in high force, electrical driven situations where weight needs to be considered ^[4]. This actuation technology is important to integrate to our design as it provides a high force, small size movement with a relatively low cost.

In order to fully verify an operational mechanical design of a deployable cover, standardized testing will be completed to check full functionality and reliability. For any space bound payloads and/or components, The Goddard Space Flight Center General Environmental Verification Standard (GEVS) provides requirements and guidelines for verifying satisfactory hardware and gives acceptable test methods for executing the conditions ^[5]. Within the GEVS, standards for vibrational and thermal testing for flight hardware are included. These tests will need to be performed to meet the prototype qualification standards.

With the small form-factor and low cost of CubeSat technology, SSL prefers the FUV to be within the 2U CubeSat size. By conforming to this standard, the accessibility to launches is greatly increased. Numerous aerospace companies such as ULA and Space X include CubeSat launchers on their spacecraft. These companies have created rideshares for research institutions to take scientific instruments into space. Never before has it been so accessible for scientific missions to study space. Pertaining to the CubeSat standards allows SSL to spend less time integrating hardware into a large-scale NASA mission and more time focusing on the technical scientific details. The CubeSat program has been highly structured since its creation around 2000. NASA has released a document detailing the technical requirements for CubeSats to be able to be integrated into a NASA mission. Included in the document are lists of functional and reliability tests that are needed to be performed before a CubeSat design is fully verified ^[6]. This document will be able to serve us as a guidebook through the testing phase of our project.

Other potential design solutions can be found in NASA tech briefs. The most common design mentioned in the NASA literature was destructive wire burning. Figure 3 shows the mechanism and how it operates.

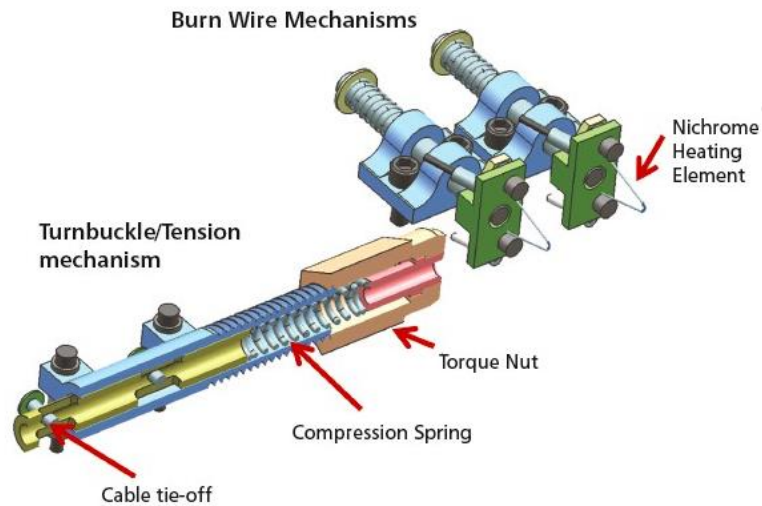


Figure 3. Example design of destructive wire burning showing burning element and tensioning components in cross section ^[7].

This design consists of a tensioned wire that when attached locks the design in place. The wire is then burned through electrical resistive heating. The destruction of this wire releases the energy in a kickback spring and deploys the door ^[7]. A variation on this design that appears to be more complex, yet more reliable, involves destroying a plastic circuit through resistive heating. The idea is to manufacture in a weak point into the circuit, then use resistive heating to fracture the PCB, releasing spring potential energy ^[8]. Both ideas follow the same general concept seen in products such as Miga Motors, pin pullers, and Frangibolts: permanently alter the system to release stored potential energy. These actuation methods are preferred to others as they allow for the satellite to be structurally contained during flight. Once in orbit, then the satellite can be deployed, and the satellite internals can be open to the space environment.

Another challenging function of the deployable cover will be the method of mirror mounting on the CubeSat. In order to create a clear image to the UV sensor, vibrations will be needed to be dampened by the mirrors. If the mirrors are mounted rigidly to the structure, there is a risk for vibrations to distort the image. If the image is slightly distorted by vibrations caused either by satellite electronics or the space environment, more complex software would be needed to clarify the image. There are various solutions to this issue, one being to mount the mirrors with flexures. In this design, the flexures take the vibration from the rigid structure and allow for the mirrors to not be distorted ^[9]. See Figure 4 for an example of how mirrors flexures are laid out.

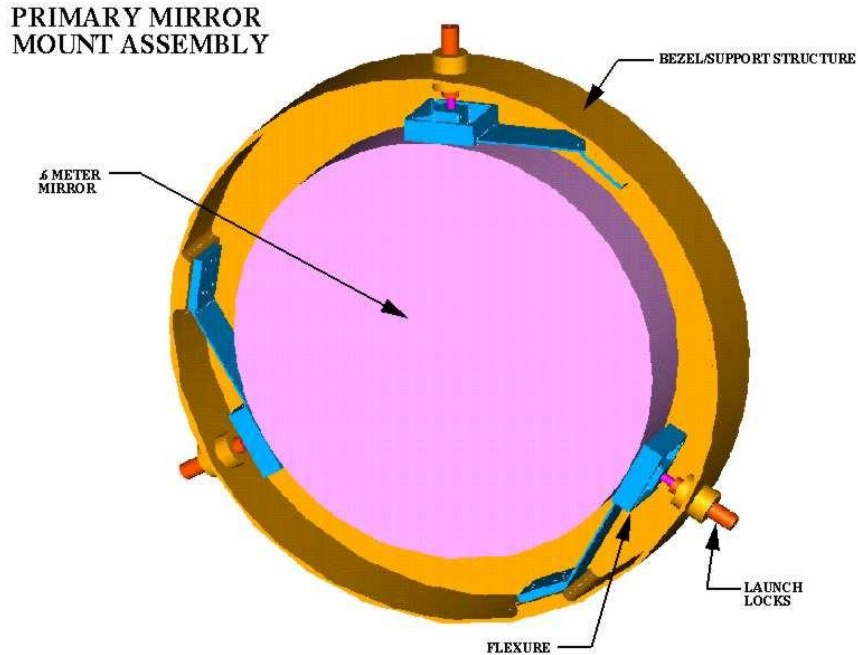


Figure 4. Flexure mounting of circular mirror, Smithsonian Astrophysical Observatory. ^[9]

Figure 4 shows flexure mounting for a circular mirror. Flexures can be configured to various mirror geometries, thus not being limited to use with circular mirrors. Despite vibrations being a challenge in image distortion, there are ways to design a mirror mount without the need to include flexures. In NASA's ICON FUV, designed by UCB SSL, image distortion was prevented with the use of intermediate damping material between the mirror and the rigid structure ^[10]. This method of vibration dampening was validated with extensive testing.

4. Objectives and Engineering Specifications

4.1 Objectives

The objective of this senior project will be to provide a validated mechanical design for a deployable, optical entrance cover for a FUV, 2U CubeSat that will provide reliable optical alignment for internal lenses and seal the internal optics from contamination. The deployable cover subassembly will be contained in approximately a half-U volume. The other physical project deliverable outside of documentation and design validation is an optical alignment test fixture.

4.2 Engineering Specifications and Testing

Breaking down the design requirements found in Table 1, preliminary specifications are used to quantify whether a requirement is met. The breakdown of this specification list can be seen in below and is derived from personal communication with UCB SSL.

Table 2. Preliminary List of Engineering Specifications Defined by UCB SSL

Specification Number	Specification	Requirement or Target	Tolerance	Risk	Compliance
1	Size	1U (10cm x 10cm)	MAX	L	I
2	Mass	TBD	MAX	L	I
3	Field of View	30° Circular Field of View	TBD	M	A,T
4	Boresight Alignment	0°	± 0.25°	H	A,T
5	Allowable Flight Temperatures (AFTs)	0 °C - 40 °C	TBD	M	T,I
6	GSE Alignment	TBD	TBD	L	T
7	Stray Light Suppression	< 5%	TBD	H	A,T
8	Contains Mirrors	Two Turning Mirrors	0	L	I
9	Protective Cover	TBD	TBD	M	A,T
10	Add "Remove Before Flight" Tags	N/A	N/A	L	I
11	Positive Indication of "Open Position" after Cover Deployment	Go/No-Go	N/A	H	T
12	Ground Support Equipment (GSE) for Instrument Alignment	N/A	N/A	L	T

While shows all the physical quantities necessary to adequately satisfy UCB SSL's needs, there are also more general design practice challenges such as ease of manufacturing and assembly that will need to be considered for our project to succeed. The customer wants/needs along with these design practices should all be considered to make the best final product possible, however a practical design will likely find a balance between the considerations as many may require tradeoffs. In order to evaluate the weight of importance that should be given to each consideration, a Quality Function Diagram (QFD) was used. This not only provides a weight to all design considerations, but also allows us to plan how we will evaluate whether our design adequately satisfies the customer needs/wants. The full QFD can be found in Appendix A, but the summary of the evaluation methods needed can be found in Table 3.

Table 3. Table of Verifying Tests

Test	Specification Evaluated	Description
TVAC Cycling with Deployment	5	Thermal cycling of subsystem as well as deployment at temperature extremes.
Post-Vibration Deployment	4	Deployment of cover after subsystem subjected to vibrational loading.
Optical Alignment Baseline	4	Provides deployment to optical alignment verification.
Simulation	Preliminary design verification for both specification 4 and 5	FEA and Thermal simulations to verify loads do not cause structural concerns as well as inform weak points to watch during TVAC and vibes testing.

4.3. Boundary Diagram

After initial review of UCB SSL design requirements, the subcomponents necessary to accomplish all tasks are illustrated in Figure 5 using a boundary diagram.

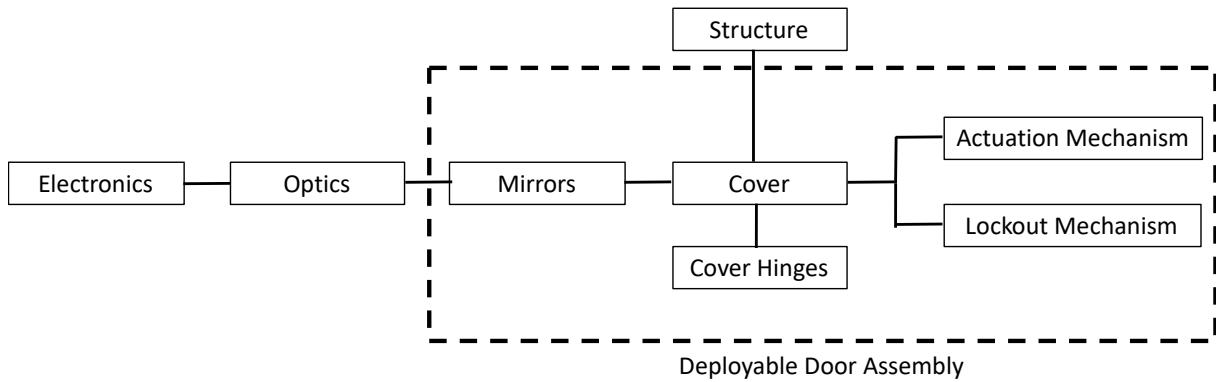


Figure 5. Boundary Diagram of the Deployable Cover for the UV Imager CubeSat.

The connections in Figure 5 show the interfaces that will have to be considered in our design process. Figure 5 will provide structure to the conceptualization of design process as it will allow our team to come up with ways to satisfy each subcomponent on the individual level as well as their integration into the subassembly as a whole.

4. Concept Design Development

The purpose of the following concept development stage is to pick a preliminary design that fulfills all project requirements. The concept design established during this phase will provide structure for detailed analysis and component level design decisions in the next stages of the project. To get from the project statement to the concept design, we first brainstorm on solutions to various assembly functions to generate a broad base of possibilities. Then we created a quick prototype of a single concept design to gain insight into physical assembly properties. From here, we compiled all reasonable solutions and refine through merit metrics. Finally, we verified solution feasibility through geometry calculations. Each of these steps are described in further detail in the following sections.

4.1 Design Function

Before ideation could begin, the list of requirements as seen in Table 2 had to be filtered into which requirements were fundamental enough to be included in the barebones conceptual design and which are accessories to be dealt with in a detailed design setting. Four fundamental requirements were identified to be included in the scope of the ideation process: FOV coverage, reliable boresight alignment, provide a particulate barrier, and most importantly, fit within the confines of the volumetric envelope.

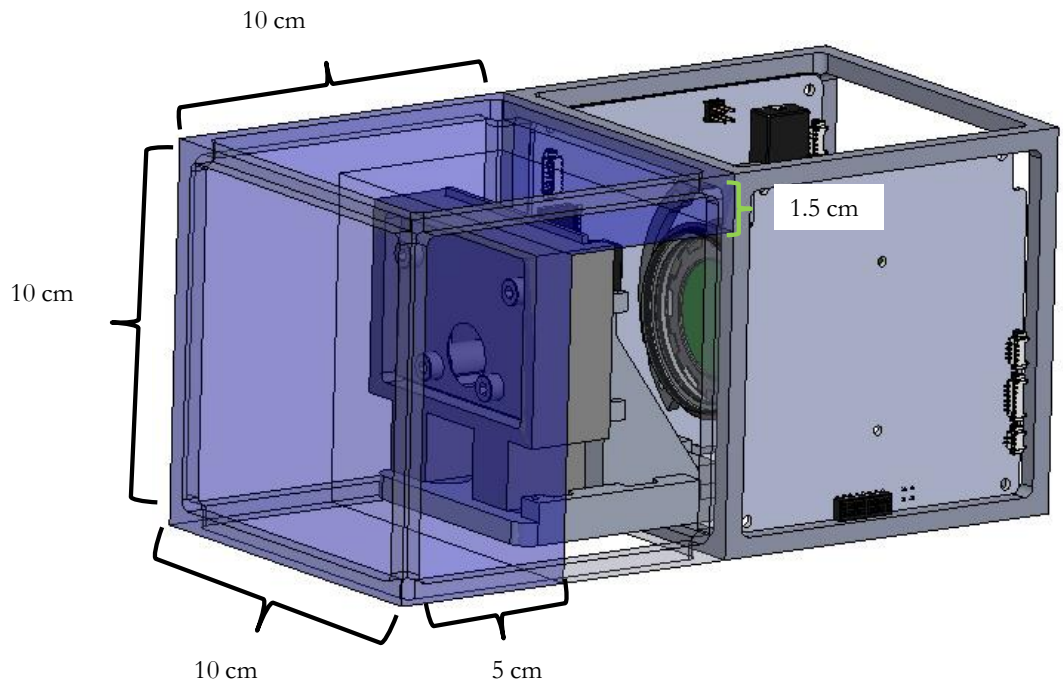


Figure 6. Final Volumetric Envelope for Deployment Cover Subsystem

Although Figure 6 illustrates the final volumetric envelope for our system, this design envelope has shrunk and expanded throughout the ideation process before settling upon this volume shown.

The fundamental requirements necessitate a basic set of functions be performed. Specifically, in order to fulfill the set of fundamental design requirements, our system will need to be held in a stowed, closed position and then lock into a final deployed position. In the stowed position, the mirrors should be contained within the assembly envelope and a seal should be created between the interior environment and the particulate contamination of the exterior. The lockout, or deployed, position will need to be defined position that stops mirror travel at a known location in order to provide optical alignment. The device(s) that hold the mirror in the stowed position and initiate the motion of the mirrors is called the actuator. Similarly, the device(s) that keep the mirrors in their deployed position is called the lockout mechanism. With these components necessary to fulfill the fundamental requirements of our problem statement in hand, we were able to start on the ideation process.

4.2 Brainstorming and Ideation

Initial brainstorming was performed in two stages: one for mirror mounting and orientation, the other for actuation and lockout methods. Although providing a particulate barrier was identified as another fundamental requirement of the project, this was included in the concept evaluation process instead of the ideation process itself. The methodology used for brainstorming was individual ideation with sketches and descriptions. These individual ideas were then presented to the larger group in hopes that the sheer quantity of design possibilities would spur further combination ideas within the group. This brainstorming format was largely based on the foundation laid by Stanford ^[11]. A challenge that was faced during the ideation process of this project was the varying subsystem envelope, which changed three times during this phase. Despite forcing extra brainstorming sessions on the group, the volatility in subsystem envelope drove us to come up with a diverse portfolio of design ideas as illustrated by the sample of design solutions showcased in the following sections.

4.2.1 Mirror Orientation

The first brainstorming session performed by the team dealt with mirror orientation. This session's primary goal was to investigate how the mirrors can stow in the system envelope during pre-deployment and how they will look upon deployment. There were three unique solutions that came out of this brainstorming session worth mentioning here.

The first mounting scheme was titled extended mirror. The concept was that the bottom mirror would be mounted stationary in its deployment position and only the top mirror would rotate. The hinge of the top mirror was not at the base of the mirror however, and thus the base of the top mirror would rotate into the CubeSat structure upon deployment. This concept can be further seen in Figure 7 below.

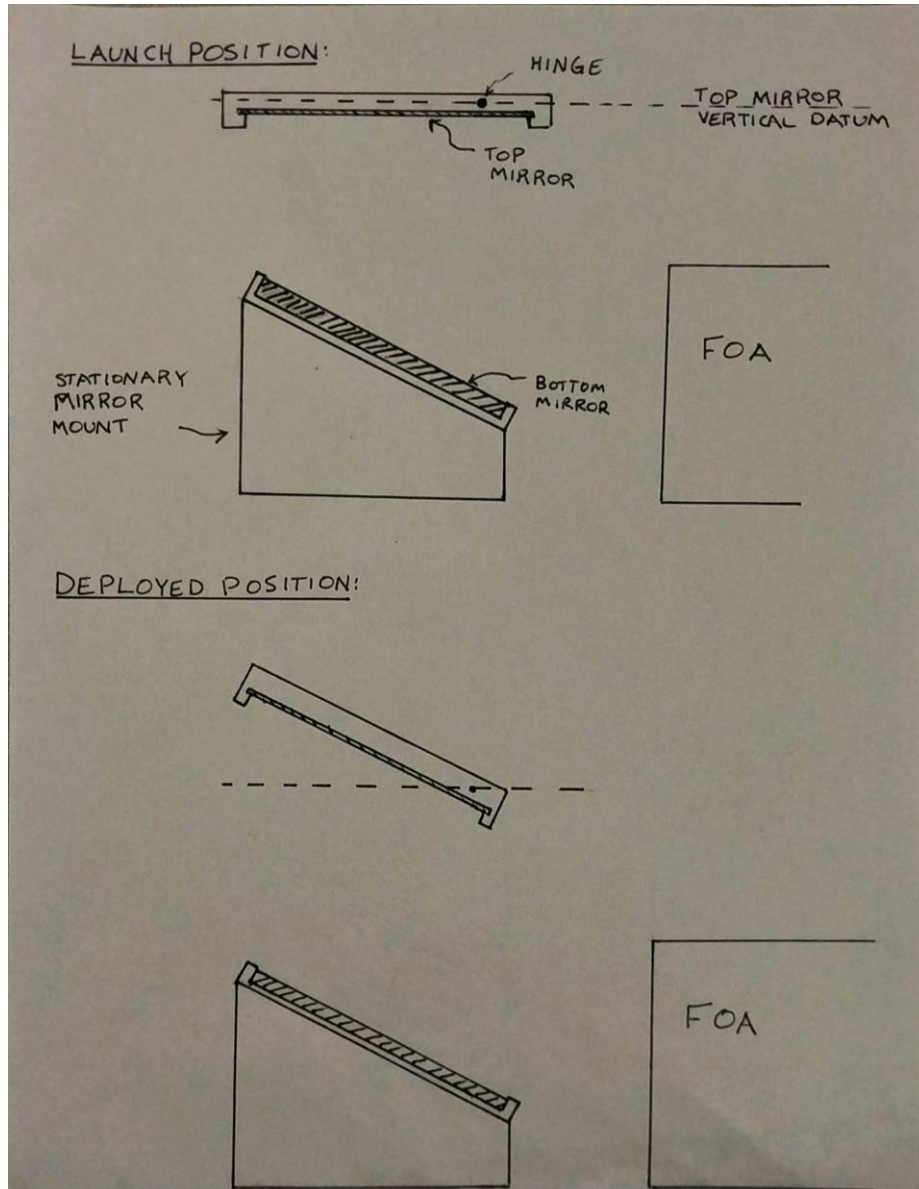


Figure 7. Extended Mirror Concept Sketch for Mirror Alignment and Mounting Brainstorming

The mirror orientation shown in Figure 7 permits a small distance between the top and bottom mirror by shifting the hinge location of the top mirror away from the corner. This is important for the FOV requirement as a greater distance between the two mirrors will allow the FOV to grow and will cause increased geometry concerns. Although great for the FOV, this concept poses challenges to the requirements of fitting within the 1U structure and providing a protective barrier for the internal optics. The stowed and deployed volume of this mirror orientation are the same due to the stationary bottom mirror, which causes concern of how big the bottom mirror needs to be in order to reflect the full FOV. Additionally, by splitting the top mirror into two sections with an off-corner hinge (the front portion rotating above the CubeSat and the back portion rotating below) poses a complication for sealing as it does not allow for a single-sided, full perimeter gasket to be compressed from one side.

The second design of interest was having two coupled, moving mirrors as shown in the sketch below.

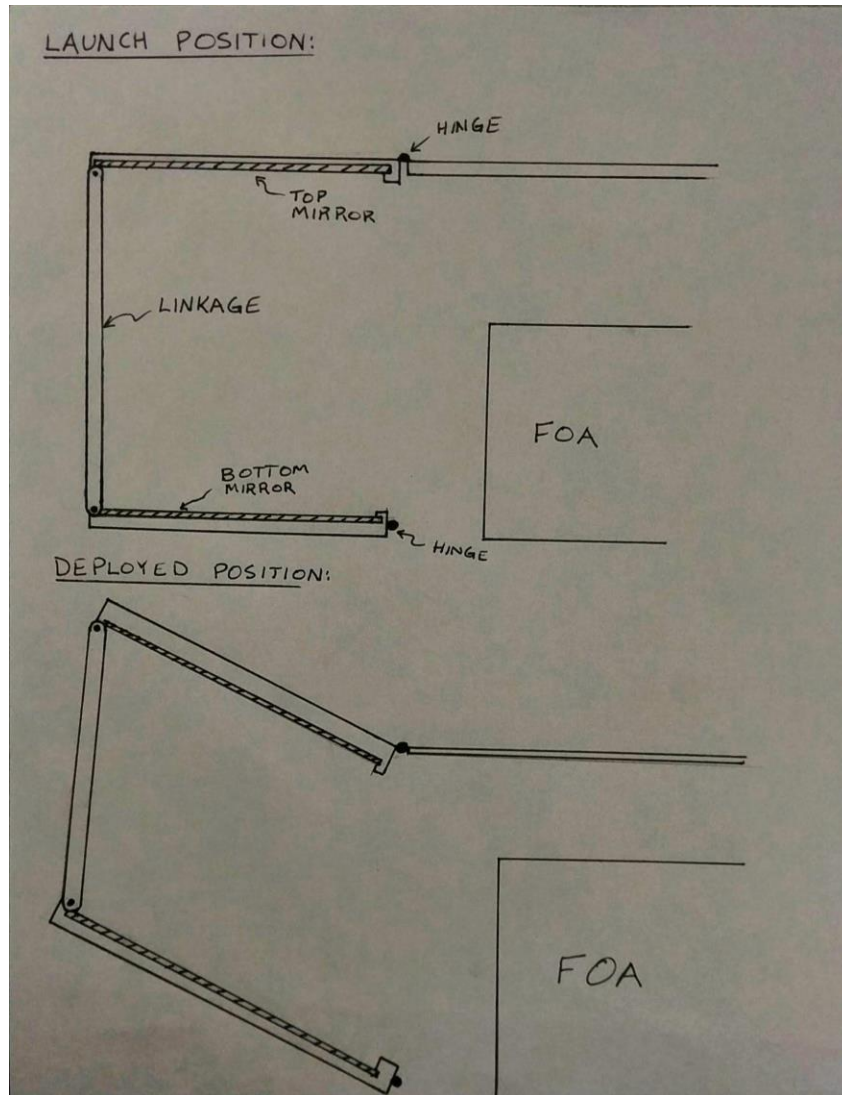


Figure 8. Auto-Alignment, Coupled Mirror Concept Sketch for Mirror Orientation and Mounting Brainstorming

The concept is that both mirrors would be stowed to fit within the sealed CubeSat upon launch, and then move together through a rigid linkage to their final deployed position for FUV imaging. Although the stowed position of the bottom mirror shown in Figure 8 is horizontal, the orientation of the bottom mirror could be changed to vertical and the linkage would be designed to accommodate this change. Having coupled mirror movement as shown in Figure 8 has the great advantage of allowing for play in individual mirror alignment. If both mirrors were to lockout with an equal, small deviation from their nominal lockout position, the resulting boresight after traveling through both mirrors would be aligned due to the complimentary reflections off of the misaligned mirrors. This could eliminate tolerance stack-up concerns and greatly aid in meeting

the boresight alignment requirement. However, there is a concern with optical reliability as there are three distinct, moving members in this system, and the addition of movement increases likelihood of system failure by compounding reliability of each component [12]. Also, this concept does have the advantage allowing simple sealing. Because the top mirror shown in Figure 8 is hinged on the base of the mirror, a planar sheet of gasketing could be applied to the inboard side of the top mirror mount to seal in the stowed position.

The final viable concept design came from the early concern that our volumetric envelope for our subsystem had a thickness of only 5mm. Early on in the ideation process, it came to the team's attention that there had been a communication gap between the actual volumetric constraints vs. the volumetric constraint we had been brainstorming with. Through the SOW process and into the ideation phase, we had assumed that our subsystem could take up a space of 1U. However, Jason Grillo brought it to our attention that we shared that 1U with the previous senior project's FOA. From the position that the previous senior project left their FOA, we actually had for our subassembly. This drastic change in subassembly envelope led to creative design solutions such as the one seen in Figure 9.

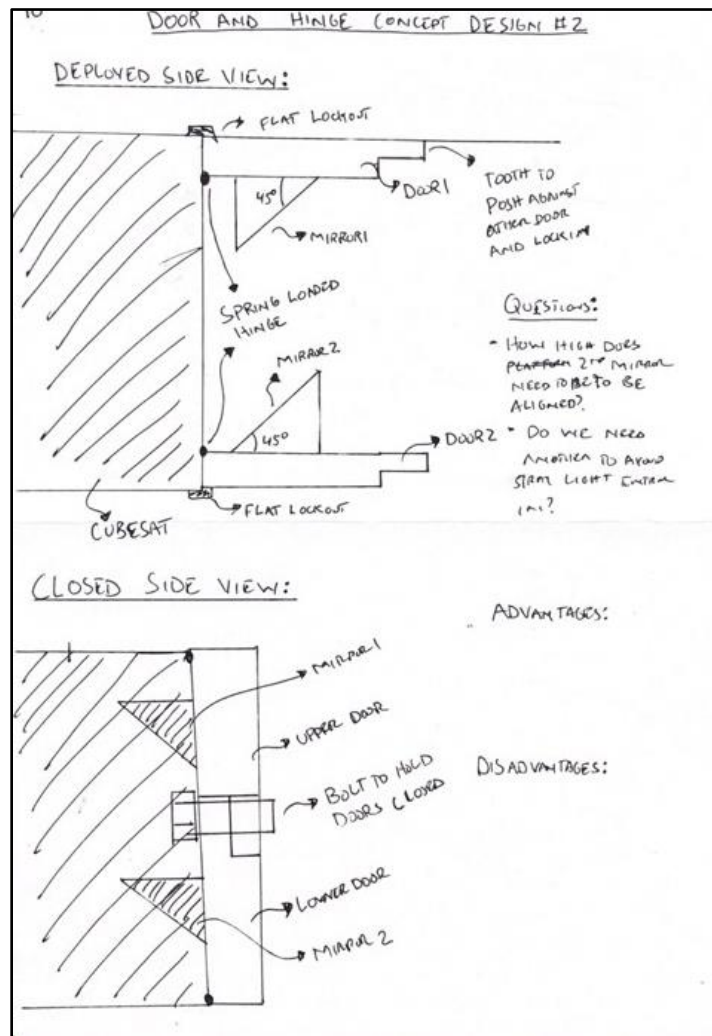


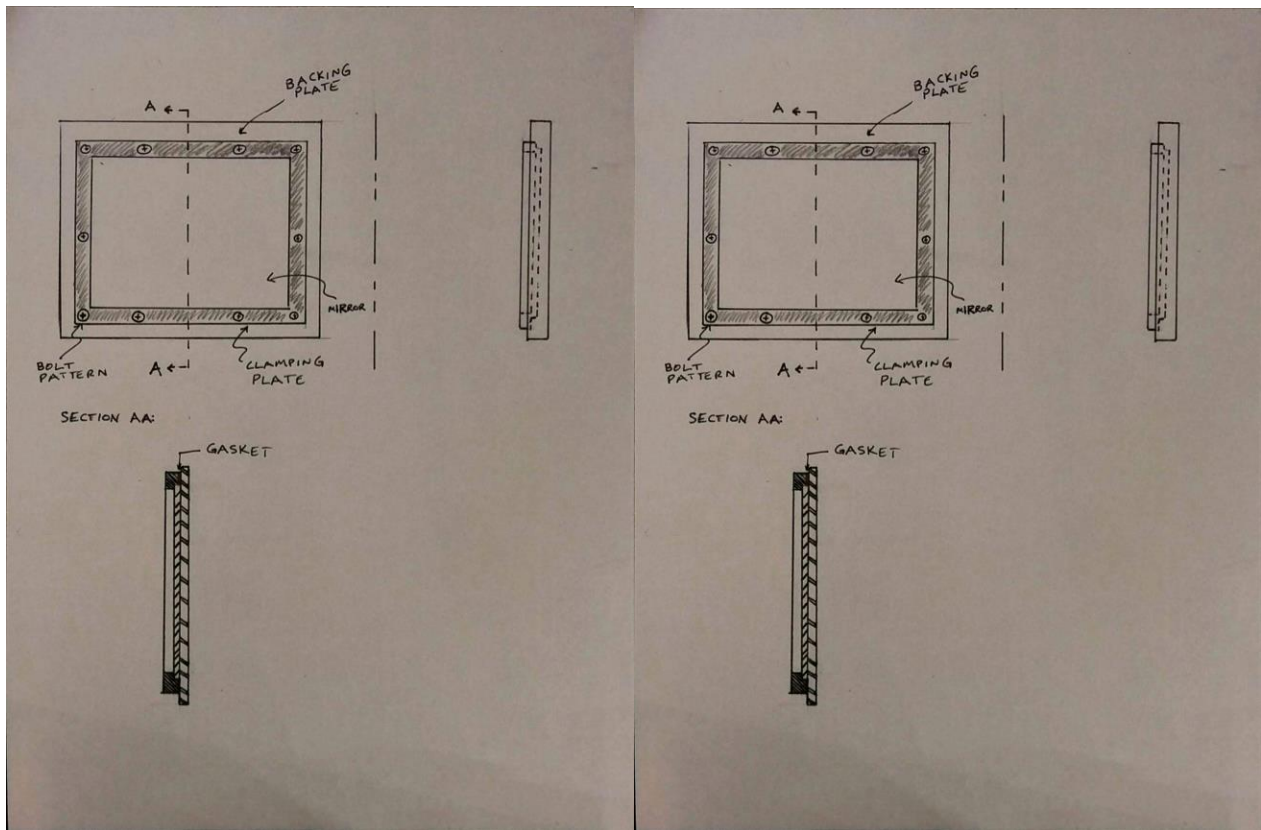
Figure 9. Mirror Orientation Double Door Concept Idea

The above design has both mirrors mounted to the front panel of the CubeSat. The advantage of this is that both mirrors stow vertically, reducing the stowed volume. The mirrors then deploy with the front cover opening to its lock-out position. This design relies on the mirrors being small enough to share the front panel space.

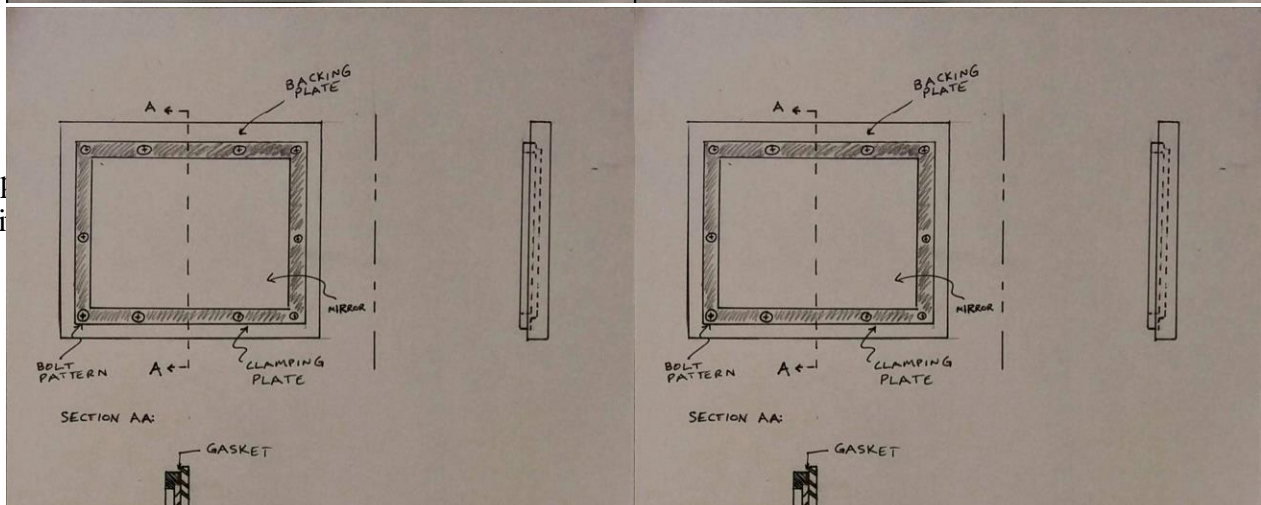
4.2.2 Mirror Mounting

The second brainstorming session included how we can mount the mirrors to a structural component and how the mirrors would be oriented relative in the available space, although the question was not expanded to include structural integration to the CubeSat body itself. There were three unique mounting schematics that appealed to the group: a bolted clamp, an epoxy recess, and flexures.

The first mirror mounting concept shown in Figure 10 is a bolted mirror pattern. This mounting scheme is inspired by the mounting seen in ICON's design review [9].



a p
wi



loads to the mirror perimeter which could cause deformation in the mirror surface and the accompanying image distortions.

The second mirror mounting concept formed in the ideation phase was to mount the mirrors using only epoxy. The resulting mounting schematic is illustrated by Figure 11.



Figure 11. Mirror Mounting Concept Design, Epoxy Recession

The advantage of epoxy recession mounting is that there are no moving parts nor fasteners. All critical geometry can be controlled by machining the backing plate properly and, theoretically, no static stress would be held within the mirror. The downfalls of this design are that it complicates the assembly process as the volume of epoxy used would have to be tightly controlled and its rigid connection to the mounting plate exposes the mirror to vibrational loading during launch. The epoxy recession as seen in Figure 11 allows for a nominal volume for epoxy to take up. If the epoxy deposited were to be less than the allotted volume, voids would form in the epoxy matrix which would reduce the strength of the bond. Conversely, if the epoxy deposited were to be greater than the available volume, it would likely find a gap and try to escape around the mirror surface. This would result in contamination of the mirror datum and possibly improper seating of the mirror. Although there are ways to mitigate the risks of applying too much or too little epoxy, it is nevertheless a complication to the manufacturing process. The rigid connection between the backing plate and the mirror would also transmit any vibrational load seen by the backing plate directly to the mirror. Since the mirror is brittle and the backing plate will likely see high vibrational loads during the launch process, this is a major concern.

The final mirror mounting concept formed in the ideation phase was to mount both mirrors using flexures. Flexures were encountered during our background research into optical systems and an illustration of flexures can be seen in Figure 4. The advantage to mounting our mirrors with flexures is that it provides an elastic connection between the mirror and CubeSat structure. By doing so, it can damp vibrational loads seen by the CubeSat structure if properly designed. The goal of designing with flexures would be that they transmit all the load and that there is no load seen by the brittle mirror. This would help greatly during launch vibrations to reduce mirror failure risk.

4.2.3 Actuation Mechanism and Lockout

The final brainstorming session focused on how the mirrors would be held in their launch and deployment positions. The actuation schemes brainstormed here were mostly integration ideas of researched, existing methods. The lockout mechanism did not leverage from off the shelf package designs and thus had a wide variety of solutions. Although both the actuation and lockout

mechanism were brainstormed at the same time, it became evident that they were independent design solutions and thus we could mix and match solution components.

The first concept built off the mirror orientation shown in Figure 7: involving a bottom stationary mirror and a top mirror that rotates. The conceptual sketch of this design can be seen in Figure 12.

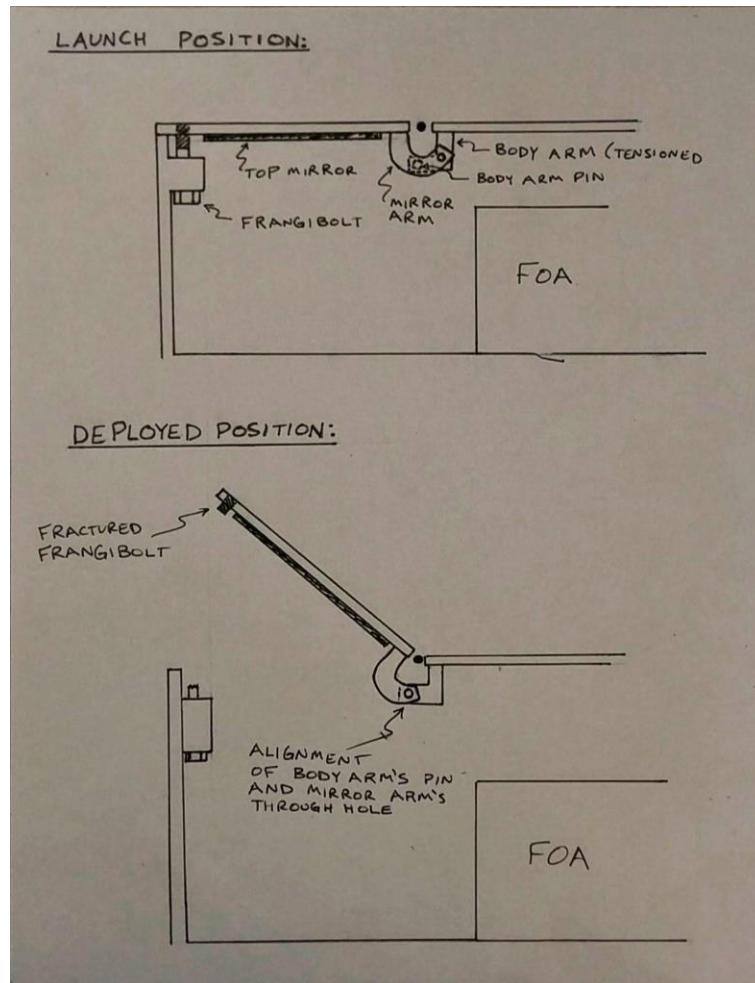


Figure 12. Actuation and Lockout Design Idea #1

This concept incorporates a Frangibolt as the actuation mechanism and a tensioned pin for lockout. To keep the top mirror in its stowed position, a Frangibolt is placed through a tab in the front panel of the CubeSat and threaded into the top mirror mounting panel. To hold the Frangibolt on the front cover after actuation occurs, a bracket would need to be designed. Upon Frangibolt fracture, a piece of thread would remain attached to the mirror mount as seen depicted in the deployed (bottom) sketch in Figure 12. This residual thread would need to be considered to make sure that it does not extend into the field of view. Also, the mirror mount design would need to be thick enough to allow for adequate thread engagement of the Frangibolt. The lockout mechanism considered in this concept involves a tensioned flange hanging off the body with an indexing pin

attached to the end. This arm is kept in constant tension against the arm hanging off the mirror. As the top mirror deploys, the top mirror's arm travels relative to the tensioned body flange. The pin of the body arm rides along the rigid mirror arm until it is positioned over the through hole in the mirror arm. At this point, the tension in the flange forces the pin through the hole in the mirror arm to lock the top mirror in the deployed position. This lockout mechanism would be mirrored to be incorporated on either side of the top mirror for more rigidity in the system. This method is an active lockout method as it is held in place in all directions, providing optical reliability through any vibrational loading that may occur after mirror deployment. However, boresight alignment in a complicated lockout system such as the one shown above would likely decrease as there are many moving parts and tolerances that would have to be designed, manufactured, and assembled to perfection in order to achieve the desired deployment position of the top mirror.

The second design solution of interest when brainstorming actuation and lockout mechanisms contains a Frangibolt, similar to the solution shown in Figure 12, but involves a passive lockout system as it does not resist motion in either direction but rather relies on spring force to hold it in the deployed position. An overview of the design solution can be seen in Figure 13 below.

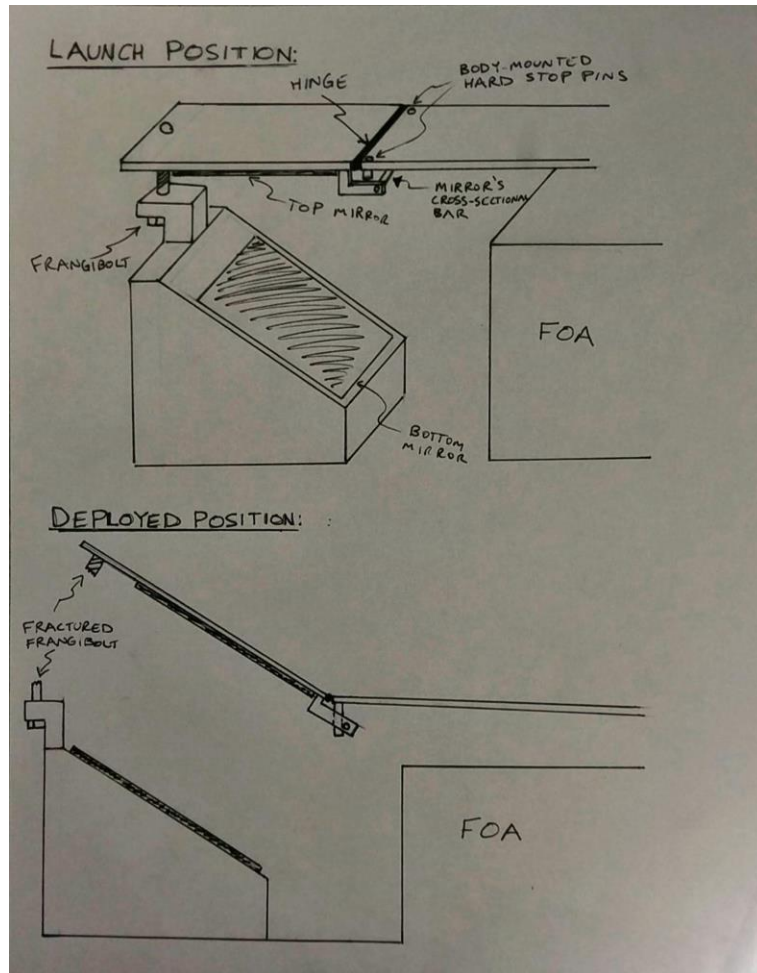


Figure 13. Actuation and lockout design idea #2.

Although this design also incorporates a Frangibolt as the actuation device, it differs from the design of Figure 12 in the Frangibolt position. This design houses the Frangibolt in the mounting structure of the bottom mirror. The advantage of this is it keeps all actuation dependencies to only our subsystem. This not only reduces the design requirements we impose on the CubeSat structure, but also eases the testing procedure of our subsystem as it does not require a 1U structural mockup. The downsides to this type of design include the potential to move the bottom mirror slightly upon preload release of the Frangibolt and the excess material required in the bottom mirror mount to house the Frangibolt. The lockout mechanism has a bar attached to the rotating top mirror and a static pin on the CubeSat body. As the top mirror rotates, the bar comes into contact with the pin. Upon contact, there will likely be kickback and oscillation of the mirror, but the rotational spring in the top mirror hinge will always drive the top mirror back to the pin and friction in the system will cause the oscillation to stop with the mirror held against the locating pin. The advantages to this passive design are that it does not require any tensioned lockout component that could fail during the lockout phase of deployment and the deployed position is driven by easily machined surfaces. The major downside to this lockout design is that any vibrational loads experienced by the CubeSat during post-deployment would cause the mirror to vibrate. The degree to which vibrational loads should be accounted for during post-deployment is a factor that would have to be considered if this design were to be the selected preliminary design.

The final actuation concept design of interest included a Miga Motor instead of a Frangibolt. Miga Motors were first encountered during the background research on CubeSat deployment methods. An illustration of the actuation design concept can be seen in Figure 14.

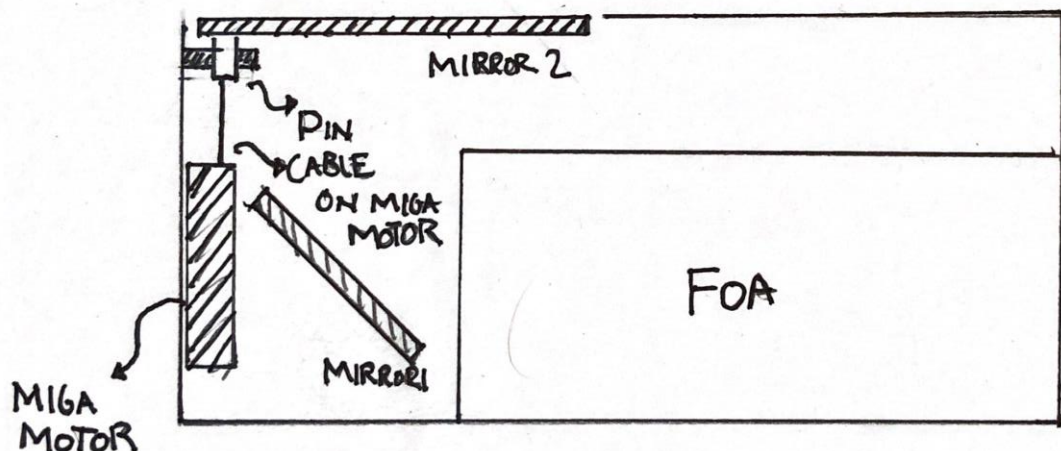


Figure 14. Concept design for actuation of top cover deployment with a Miga Motor

The Miga Motor, shown in Figure 14, is mounted to the front panel of the CubeSat. A pin is used to hold mirror 2, the top mirror, in the launch position. The Miga Motor would then be activated to pull on a cable and pull the pin out of its hole. The design shown in Figure 14 relies only on static friction to hold the pin in place during launch, but the design could be expanded upon to include a rigid bar instead of a cable to add additional support to the pin. The advantage of a Miga Motor actuation device such as the one seen above is in the integration with the CubeSat. While a Frangibolt takes up a cylindrical volume and special mounting brackets have to be designed to constrain the Frangibolt upon fracture, the Miga Motor only needs threaded holes to mounting of the PCB. Another advantage of this design is that it is not destructive and thus the design can be tested rigorously with full functionality. The disadvantage of the Miga Motor is that it does not have an inherent locking mechanism to hold the top mirror in launch position. Rather, it only provides the force necessary to initiate the actuation component. The leading concept for a Miga Motor-actuation system is a pin puller like the one seen in Figure 14.

4.2.4 Top Mirror Movement

Upon completion of the geometry validation of our preliminary design, it became evident that in order to fit within the volumetric envelope the top mirror would have to translate as well as rotate between the launch and deployed positions. This deviated from our previously assumed top mirror movement of pure rotation. To accommodate the new top mirror movement, another brainstorming session was performed. There were three leading concepts on how to achieve this movement: a linear rail/cart, a shaft/collar, and a slot/pin.

The rail and cart concept was to use an off-the-shelf system to give our top mirror the linear motion necessary. The mirror would then be mounted to the cart via a spring-loaded hinge that would provide the additional rotational motion. The shaft and collar idea is the same concept but allows for some play of collar rotation about the shaft. The advantage of both of these concepts is that they would be reliable as they rely heavily on existing products. The linear rail was found to be advantageous over the shaft as it provided more rigidity, and thus less tolerance error, to the hinge location. The third idea was to achieve the top mirror movement via a slot and pin. In this design, the pin would be allowed to translate directly in a machined slot. The pin would then be mounted rigidly to the mirror and act as the mirror hinge. The whole system would be spring loaded in such a way that the translation of the hinge would also drive the rotation of the top mirror. This concept has the advantage of minimizing components but has a disadvantage when it comes to reliability. Because this design does not utilize off-the-shelf precision linear guides, the precision of the movement will be at the mercy of the machining tolerances and material choices.

The top mirror movement brainstorming session concluded with the group leaning heavily towards incorporation of a linear rail and cart to achieve the top mirror's necessary translation and rotation. This concept is believed to provide the most reliable motion and simplest manufacturing.

4.3 Early Prototyping

After a handful of design ideas satisfied the fundamental requirements were selected, the next step was to build prototypes which demonstrating the functionality of the different ideas. The first prototype was built rapidly using Foam board, Popsicle sticks, and pins to create a physical form of the leading design idea at the time. Figure 15 below highlights this first, rough prototype.

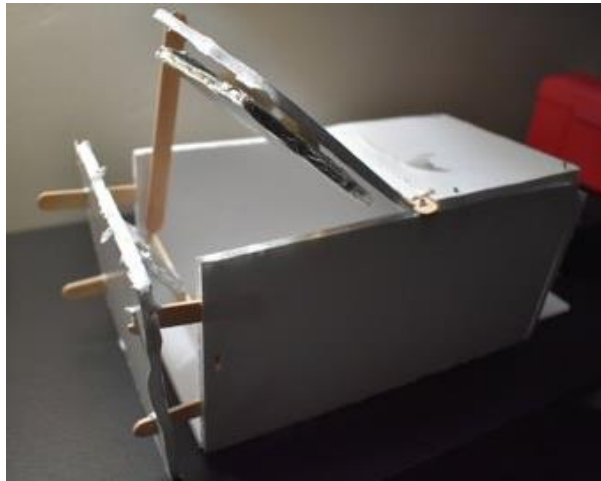


Figure 15. Design Prototype #1

The above figure highlights the best design the group brainstormed when the given space envelope was 0.5x10x10cm. The key features of this design were a deployable front and top cover, top cover which rotates and linear travels, and a bottom mirror which moves according to the deployment of the front cover. Later in the design phase, when our subsystem volume had been increased to 5x10x10cm, a second prototype of a full 1U structure was made of sheet metal to better visualize scale. This prototype is depicted in Figure 16.

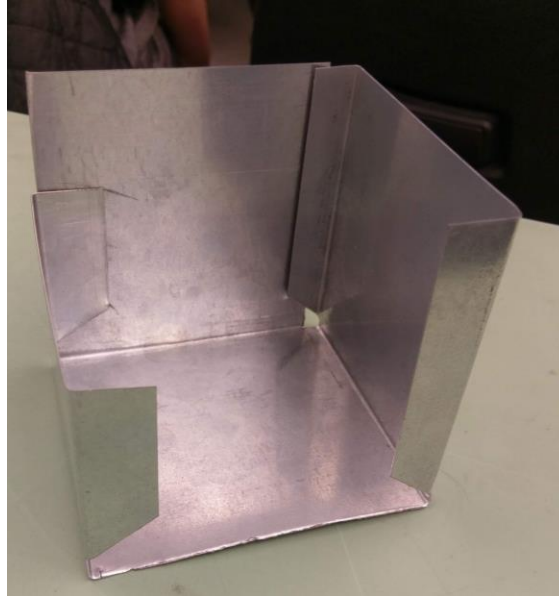


Figure 16. 1U Sheet Metal Cube for SubsystemScale Visualization

The 1U cube shown in Figure 16 proved quite useful when discussing design changes as it added tangible scale to CAD models. The left side of the CubeSat was left open in order to see inside the structure.

4.4 Idea Refinement

Once the ideation of possible solutions was performed and prototypes were created to get a better understanding of design functionality, we set out to narrow down the design direction. The design solutions for the fundamental functions were categorized and ranked. This process was performed initially with a decision matrix for mirror mounting and orientation, allowing preliminary design decisions to be made from the matrix results and engineering rationale. In addition, a morphology matrix paired with a weighted decision matrix was used to rank more unique design ideas.

4.4.1 Pugh Matrix

The first decision matrix was created to decide on the best idea for the mounting and orientation of the mirrors. The group agreed the rest of the design was contingent on how the mirrors were positioned with respect to the rest of the satellite. Five different factors were included in the Pugh matrix, each having a weight varying from 1-5. All designs were given a rating against the parameters. A rating of 1 means the design excels in the factor, 0 signifies the design is adequate in the parameter, and a rating of -1 shows the design poses risk against the defined factor. The weights of the factors are multiplied by the ratings given and added into the Design Figure of Merit (FOM). The design with the highest FOM should be the best solution from this idea refinement process.

Table 4. Pugh matrix for mirror orientation and mounting.

Factors	Small Footprint	Optical Reliability	Debris Sealing	Interface with Structure	Assembly Ease	Design FOM
Weights	4	5	2	3	1	
Two Moving, Linked Mirrors	-1	1	0	0	-1	0
Stationary Bottom Mirror Top Mirror Hinged	-1	0	0	1	1	0
French Double Doors #1	1	-1	-1	-1	0	-6
French Double Doors #2	1	-1	-1	-1	0	-6
Stationary Bottom Mirror, Front CubeSat Deployment	1	0	-1	0	0	2
Hidden Door	-1	0	0	1	1	0
Stationary Bottom Mirror, Top Mirror Removing Front Panel	0	0	0	1	1	4

As seen in the table above, the design idea with the bottom mirror being stationary and the top mirror existing on a removable panel performed the best. This concept was an idea originally proposed to the group by UCB SSL. The design integrates the best with the rest of the existing system. The team also agrees it be easier to manufacture as compared to other design ideas. With only having one mirror moving, this allows the cover mechanism to have fewer moving parts and be much more reliable. With each factor of the design justified with engineering rationale, this design became the base of our preliminary design.

4.4.2 Morphology Matrix

Previous refinement techniques were used in order to choose a particular design solution from the pool of existing solutions generated during the ideation phase, but those methods did not generate any more design ideas. A process was necessary to iterate on design possibilities which were not considered before. Therefore, a morphology matrix was used to create hundreds of designs with six sub-functions. Since it would take too long to go through hundreds of designs and some ideas were not feasible, the top ten designs from the morphology matrix were chosen to be analyzed.

Our Morphology Matrix [See Appendix D] contains the top ten designs along with the six unique sub-functions. The six functions are top mirror movement (1), actuation method (2), gasketing method (3), mirror mounting (4), baffling (5), and lockout (6). These six design

functions were decided as the most important parameters to the project. After the top ten designs for the overall system were organized into the morphology matrix, a rating was needed to be done to understand the best design among the ten. To do so, we went back to a Pugh Matrix and ranked the designs based on the requirements or factors that the design would need to meet.

Table 5. Pugh matrix from Morphology results.

Factor	Simplicity of Movement	Ease of Manufacturing	Cost	Lockout Integration	Interface with Structure	Small Footprint	Design FOM
Weights	6	2	1	4	3	5	
Design 1	-1	0	-1	1	-1	-1	-11
Design 2	0	1	-1	1	0	1	10
Design 3	0	1	0	0	-1	-1	-6
Design 4	1	1	0	0	1	1	16
Design 5	0	-1	0	0	-1	-1	-10
Design 6	1	0	0	0	1	1	14
Design 7	0	1	-1	1	-1	0	2
Design 8	0	0	-1	1	-1	0	0
Design 9	0	-1	-1	-1	-1	-1	-15
Design 10	-1	-1	-1	-1	-1	-1	-21

Looking at the Design FOM of Table 5, it can be seen Design 6 received the highest rating. The sub-functions included in Design 6 are summarized in Table 6 below.

Table 6. Design 6 (Preliminary Design) Sub-Function Summary

Sub-Function	Function Concept
Top Mirror Movement	Pin and Slot W/ Moving Hinge
Top Mirror Actuation	Direct Pin-Puller Mounting
Sealing	Continuous Top Mirror Gasket W/ Mirror Recess
Mirror Mounting	Circular Flexures
Stray Light Deterrence	Bottom Mirror Baffle
Lockout Mechanism	Linear Hard stop Block

This design contained many functions which the group was confident would work, and since the engineering rationale agreed with the Pugh Matrix FOM, the design was chosen as our complete preliminary design. In order to visualize and validate this design, CAD and a geometry analysis was performed.

4.5 Initial Design Analysis

4.5.1 Mirror Sizing Concept Validation

Once a mirror and door concept design were converged upon, the idea needed validation to confirm that the concept would be possible to satisfy all the requirements given by our sponsor. The most important requirements that needed to be validated were if the mirrors would fit within the given envelope of space, if the mirrors could be deployed at the correct angles, and that the design could maintain a full 30° field of view to the instrument iris. The envelope of space given to the senior project group is shown in Figure 17.

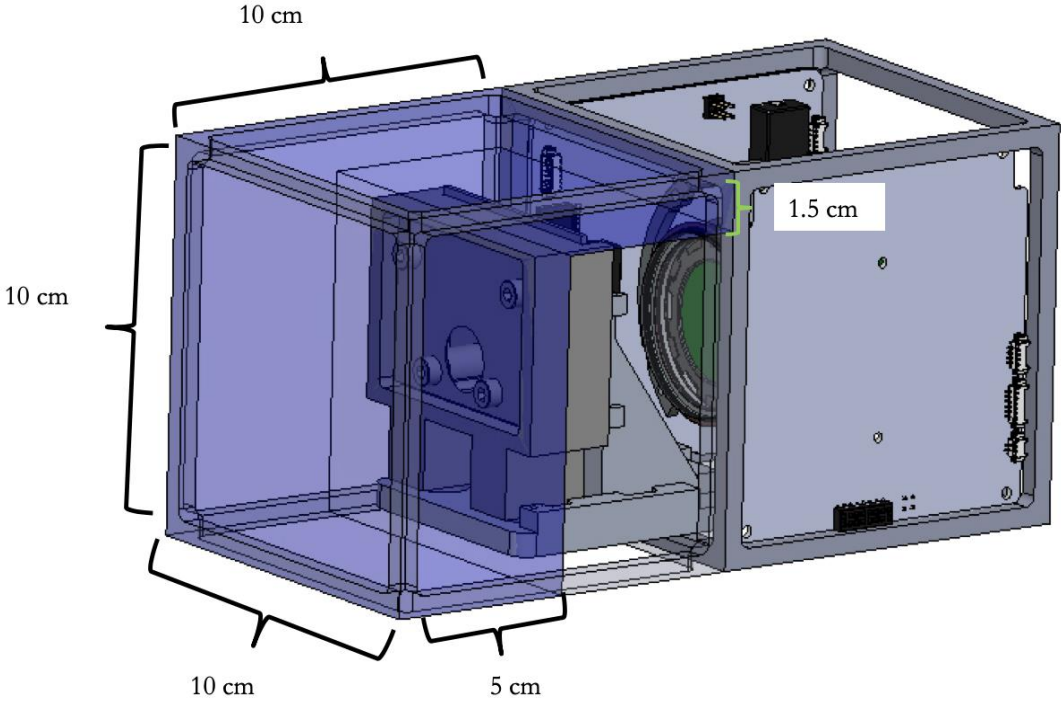


Figure 17. Given space envelope by UCB SSL.

In order to validate this design, we developed a series of variables that defined the location, orientation and size of the mirrors relative to the housing structure as shown in Figure 18.

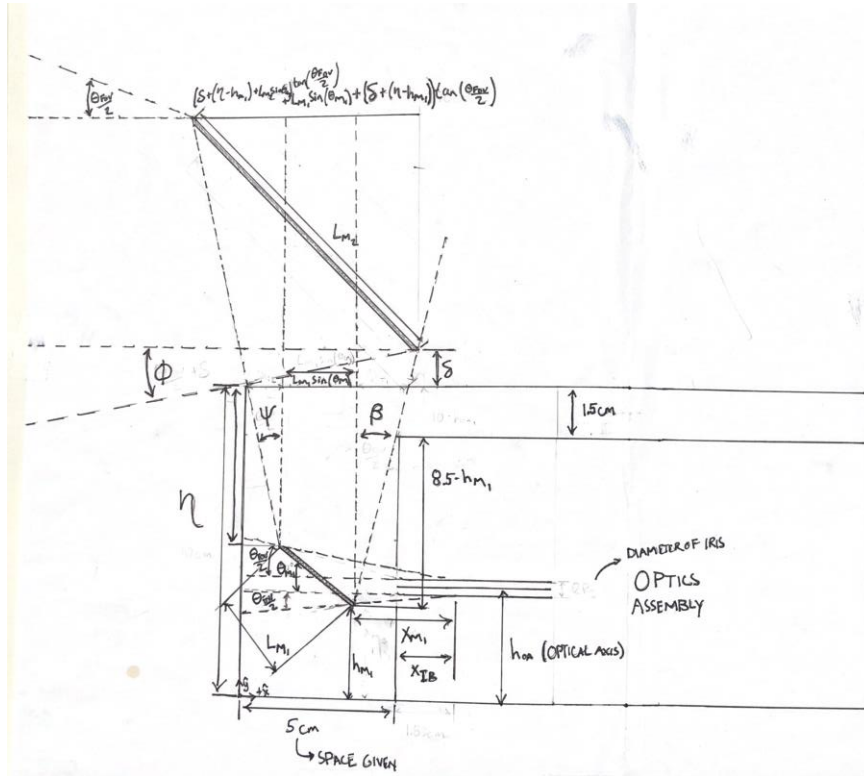


Figure 18. Initial schematic of concept design with variables used to determine a validated solution for the concept design.

The variables listed in Figure 18 are summarized in the table below.

Table 7. Summary of Variables Used to Validate Design Geometry

Variable	Description
θ_{FOV}	Field of View Angle
x_{m1}	Horizontal Position of Bottom Mirror Relative to Iris
h_{OA}	Vertical Height of the Optical Axis from Base of Cubesat
L_{m1}	Length of Bottom Mirror in Central Cross Sectional Plane
L_{m2}	Length of Top Mirror in Central Cross Sectional Plane
η	Height of CubeSat's Front Panel
δ	Vertical Distance of Top Mirrors Corner from Top Panel of CubeSat
β	Angle between Bottom Corner of Bottom Mirror and FOA
φ	Angle between Top Corner of Bottom Mirror and CubeSat Front Panel
ϕ	Angle between Bottom Corner of Top Mirror and CubeSat Front Panel

Each variable was defined in relation to a structural datum within the CubeSat and then possible solutions were solved for over a range of chosen values. The possible solutions were then compared to the requirement constraints to confirm that the set of dimensions fits within all of the constraints of the CubeSat including mirror sizes, angles and a maintained field of view. This process is shown in the MATLAB script attached in Appendix C.

After initial calculations for a larger range of all chosen variables, we discovered that there were no possible solutions for our original concept design that fit all of the constraints that this design must fulfill as shown in Figure 19.

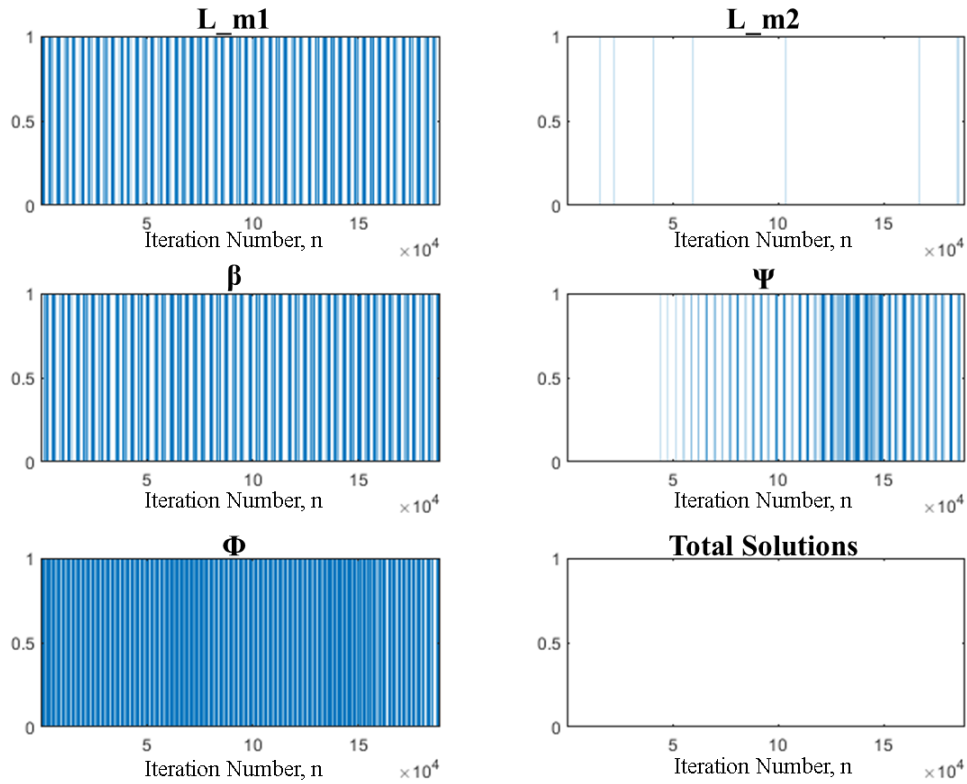


Figure 19. Possible solutions that pass or fail the constraint for each crucial variable including: (A) length of mirror 1 L_{m1} , (B) length of mirror 2 L_{m2} , (C) angle between the lower corner of mirror 1 and the corner of the front baffle assembly, β , (D) angle between the back top corner of mirror 1 and the front corner of the CubeSat, Ψ , (E) angle between the lower corner of mirror 2 and the front corner of the CubeSat, ϕ , and (F) total solutions where all variables simultaneously meet all constraints which does not have any possible solutions.

In Figure 19, a blue line suggests that the variable passes the design constraint for that variable while a blank space suggests that the variable does not pass for that iteration. Since there were no possible solutions that met all crucial constraint conditions for this design, we started to investigate which variable was the limiting factor. We found that the angle β between the lower corner of mirror 1 and the top corner of the front baffle assembly as well as angle ϕ , between the bottom corner of mirror 2 and the front corner of the CubeSat were the limiting factors. In order to find a solution for all for the constraints, we then included the idea to redesign the top corner of the front baffle assembly to allow for more space and maintain the field of view. We also decided to remove a portion of the front cover upon deployment in order to maintain the field of view. These design decisions then led to multiple possible solutions that fulfilled all design constraints. In order to look at solutions that meet all design constraints with our new design decisions, we neglect the requirements of β and of ϕ since we will redesign the top of the front baffle assembly and remove a section of the front cover of the CubeSat. Through neglecting these constraints, we find many possible solutions that satisfy the remaining constraints as shown in Figure 20.

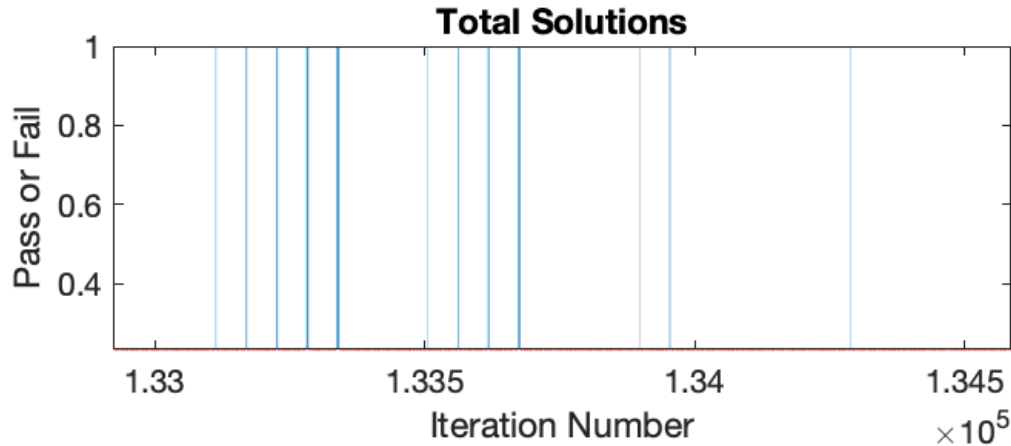


Figure 20. Possible solutions that satisfy all remaining design constraints showing which iteration number passes all constraints as a blue line while the blank space is showing iterations that do not satisfy the requirements.

We initially chose a possible solution that would minimize the size of mirror 2 in order to allow for more space for mounting fixtures on the top cover. After choosing this solution we found that mirror 1 would have to be too close to the front baffle assembly and would cause a major front baffle assembly redesign as opposed to a small redesign near the top of the baffle. We then chose a design that both minimized the size of mirror 2 and maximized angle β to reduce the amount of front baffle redesign necessary. This solution we then implemented in a 3-D model to visualize the actual dimensions and design a preliminary solution completely. This solution led to the final design concept that we chose to move forward with in.

4.5.2 Proposed Preliminary Design

Based off the MATLAB analysis of the geometry of the deployable cover interfacing with the CubeSat structure, the group was able to decide on an initial preliminary design. This design incorporates the changes needed from issues which resolved in the MATLAB geometry analysis. One issue found in the geometry investigation was no physical arrangement existed within the parameters of the system where the FOV of the second (top) mirror was not clipped by the front panel of the CubeSat. Figure 21 is an illustration of the problem area. To resolve this problem, the front panel will have to be partially deployed to have the full field of view.

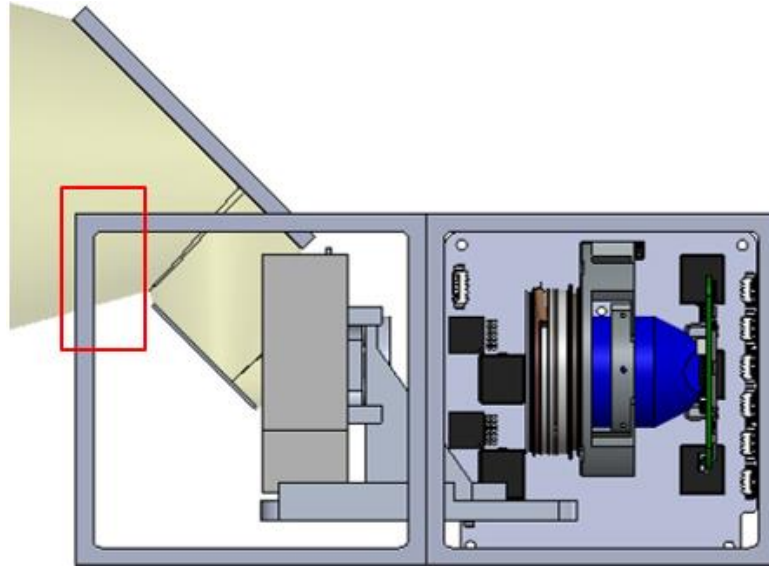


Figure 21. FOV of second mirror clipped by CubeSat front panel

Another predicament which arose was the light rays between the bottom and top mirror interfere with the Front Optics Assembly (FOA). In the iterations of the geometries to converge on a solution within the design conditions, no solution was found which did not involve a small redesign of the FOA. The light only caused a hindrance on the outermost baffle of the FOA. Figure 22 highlights where the light is interfering with the FOA. The assembly was overdesigned with three total baffles to limit stray light into the instrument. With a simple chamfer of the FOA at the problem of interference, the field of view would no longer be cut off. This action does not appear to pose a problem to the overdesigned FOA, and by cutting through one baffle, would maintain the integrity of the baffles' stray light suppression. Consultation with the project sponsor and advisors will be made before any revisions of the FOA will be made.

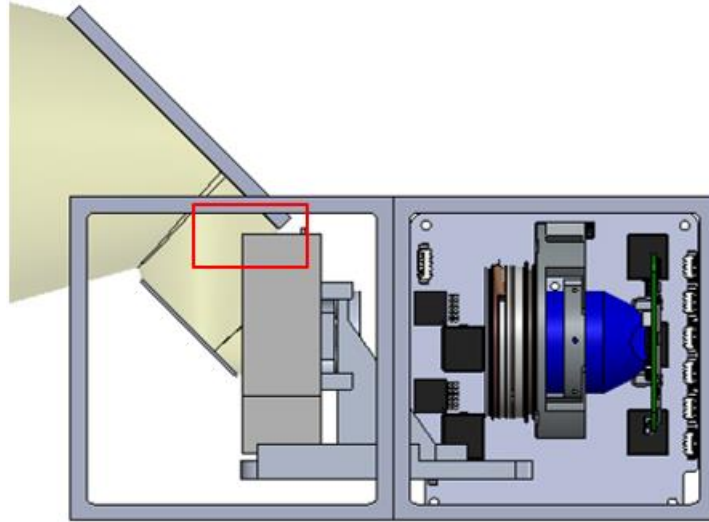


Figure 22. FOV interference with Front Optics Assembly

With the previously mentioned changes to not cut off the field of view, a physical layout of mirrors can be constructed, but with a cost of the top mirror having two degrees of freedom. In order to position the top mirror in the desired location, the front cover will need to linear travel and rotate. As shown in Figure 23, the top mirror cannot align with the bottom mirror purely by a rotation of a hinged joint.

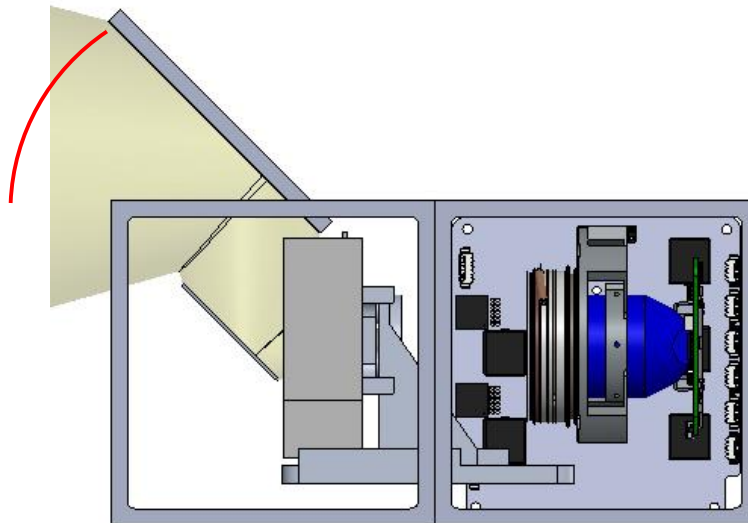


Figure 23. CAD Depiction of Need for Translation and Rotation of Top Mirror for Preliminary Design

Figure 23 shows the need to be extended to reach the deployed position. These two degrees of movement complicates the top mirror actuation. See section 4.2.4 for the initial brainstorming of the top mirror movement. A decision by the team was made to move forward with a linear rail and cart idea to perform this movement. The concept is that a linear rail and cart will be used to get precise translation of the top mirror, which can be spring loaded to occur upon deployment. The cart however will be outfitted with a spring-loaded hinge to introduce rotation of the top mirror. This solution bridges the gap between the horizontal, launch position mirror 2 and the deployed mirror 2 as shown in Figure 24 below.

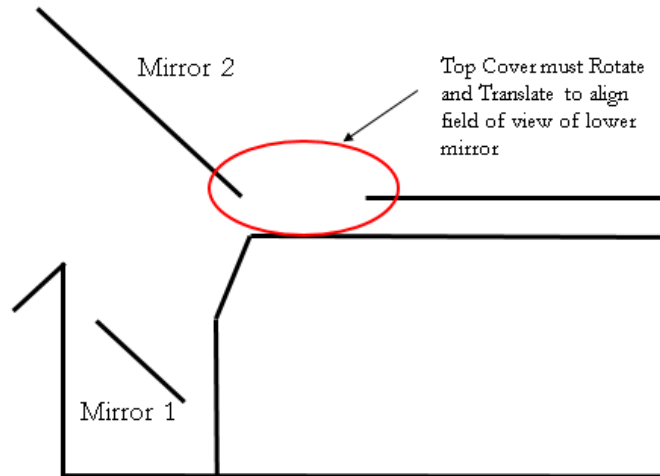


Figure 24. Preliminary layout and motion of deployable cover.

Based upon the other ideas for top cover movement, the linear rail and cart design proved to be the most simple and feasible. The detailed design of this top mirror movement will need to be performed in the critical design phase to validate this solution.

Actuation methods were previously brainstormed upon, and design choices were needed to be made. Out of the two leading actuation systems—Frangibolt or a Miga Motor driven pin puller—the pin puller and Miga Motor combination was chosen. The pin puller with the Miga Motor provides the highest flexibility for integration with the structure. The Miga Motor size and shape provides excellent mounting capabilities and strength in actuation. Additionally, the pin puller is a non-destructive device, so reliability testing can be repeatedly performed with full functionality.

In conclusion, the team had decided on a stationary bottom mirror and a top mirror which both linear translates and rotates. In order to have both linear and rotational movement of the top mirror, a linear rail and cart design is being explored. A pin puller with a Miga Motor was chosen as the actuation device. This allows the team to use the pin puller for ease in reliability testing and Miga Motor actuation force. Figure 25 shows the overall preliminary dimensions of the deployable cover and mirror locations.

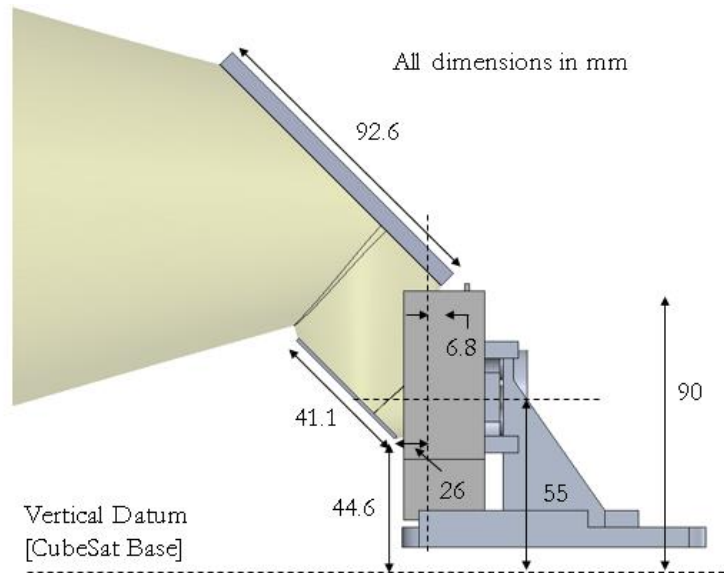


Figure 25. Preliminary dimensions of geometric layout.

The dimensions of Figure 25 are likely to change during the detailed design of the deployable cover, however the design decisions will be kept and validated through a critical design review process.

5. Final Design

The final design presented below is the culmination of all aforementioned design considerations. The important assemblies that reside within our final design are the bottom mirror assembly, the top mirror assembly, the actuation assembly, and the lockout assembly. An overview of the final design can be seen in Figure 26 below, and each assembly will be discussed in detail in the following sections.

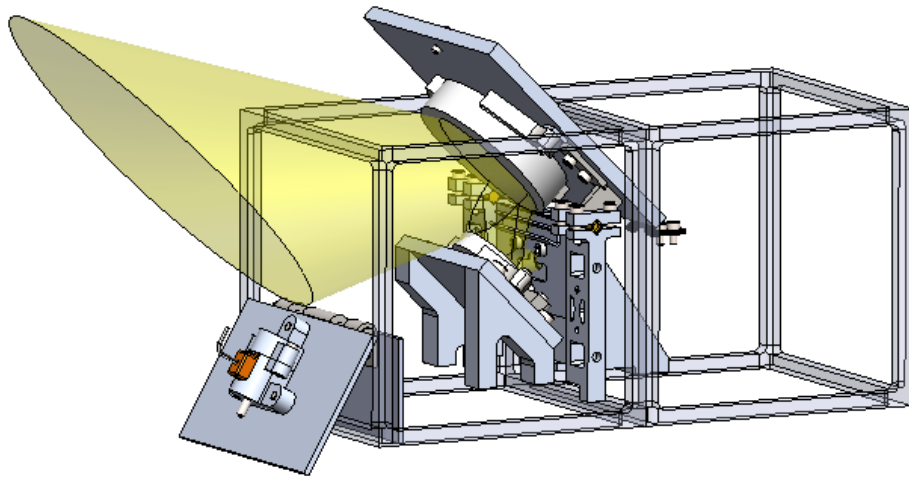


Figure 26. Final Deployable Cover design

5.1 Bottom Mirror Assembly

The bottom mirror assembly is kept as a static mirror at 45 degrees for the final design. An overview of the final design can be seen in Figure 27 below.

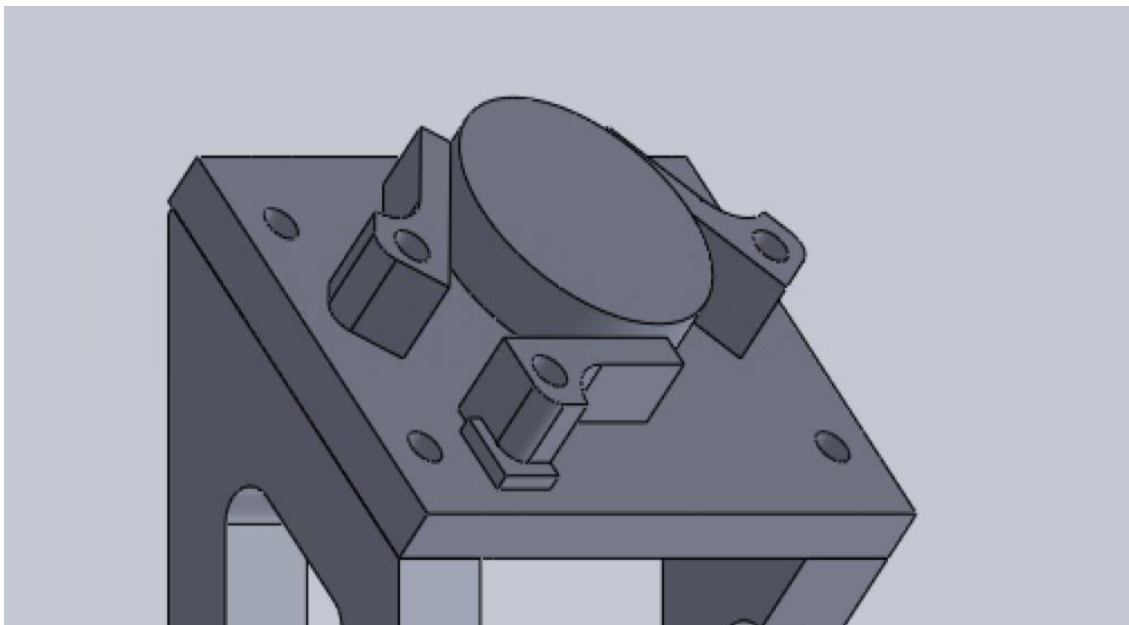


Figure 27. Final bottom mirror assembly

The main components of the bottom mirror assembly is the mirror itself, the flexures, and the mirror mount. To gain insight into the design decisions, each will be discussed in detail below.

The mirror shown in Figure 27 above is a zero-der, 1" diameter, flat mirror. Zero-der mirrors have flight heritage on ICON due to the low coefficient of expansion and good optical properties [13]. A flat mirror was chosen due to infeasibility of off-axis parabolic mirror application to our project due to our large field of view. The mirror geometry was chosen to be 1" diameter for stock availability. Choosing an off-the-shelf mirror geometry will drive down cost and ease upcoming prototyping efforts.

Flexures were chosen to secure the mirror in place while taking any vibrational loads expected during operation. There will be three independent flexures holding the bottom mirror in its nominal position. The number of flexures was chosen to define the mirror plane without over constraining the motion of the mirror. The flexures themselves are designed as a cantilever beam with a fillet in them. Their thin cross-section combined with their long moment arm will allow them to flex when loaded transversely by mirror deflection. A simplified model of these flexures can be seen in Figure 28.

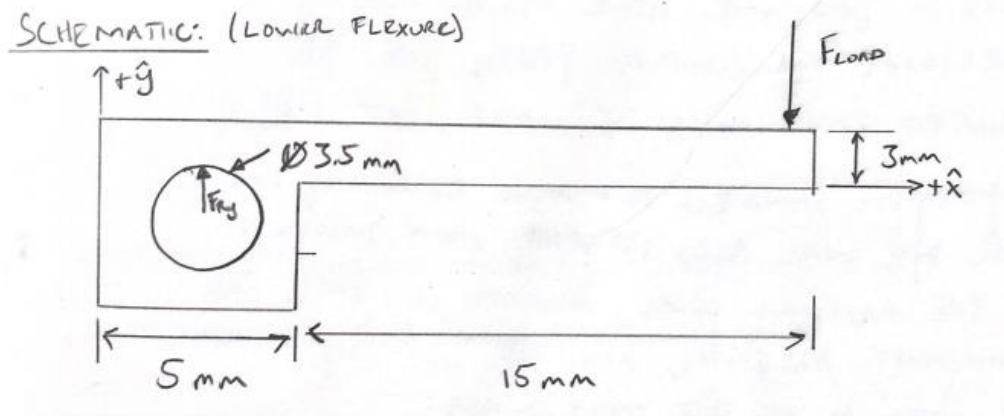


Figure 28. Lower and upper mirror tangential flexure cantilever beam model

The material chosen for these flexures is 301 stainless steel to give the proper stiffness to absorb vibrational loads while keeping the mirror from hitting the surrounding structure. For the complete flexure analysis used to size the cross section and choose the material properties, see Attachment G. The relative spatial orientation of the flexures is symmetric at 120 degrees between flexure placements. This is to provide the most even distribution of deflection between flexures for any given load.

Lastly, the bottom mirror mount is specifically designed for assembly and calibration of the bottom mirror's location relative to the lens. The bottom mirror mount is designed to be integrated directly on top of the optics datum, which also defines the height of the lens keeper. This precision datum will define the nominal location of the bottom mirror through the mount's three legs. The number of legs was chosen in order to allow for planar definition of the bottom mirror through iterative shimming of the individual legs. Due to the large oversize of the mirror

compared to the required field of view of the camera, no nominal shims are incorporated into the final design.

- Flow holes
- Shimming surfaces

5.2 Top Mirror Assembly

The top mirror assembly is a hinged assembly which positions the top mirror in the 45° position after the fracture of a Frangibolt. The assembly will be initially in a stowed position with a gasketed surface being compressed. Figure 29 highlights this stowed position of the top cover. The CubeSat will only be in this position during storage and in launch.

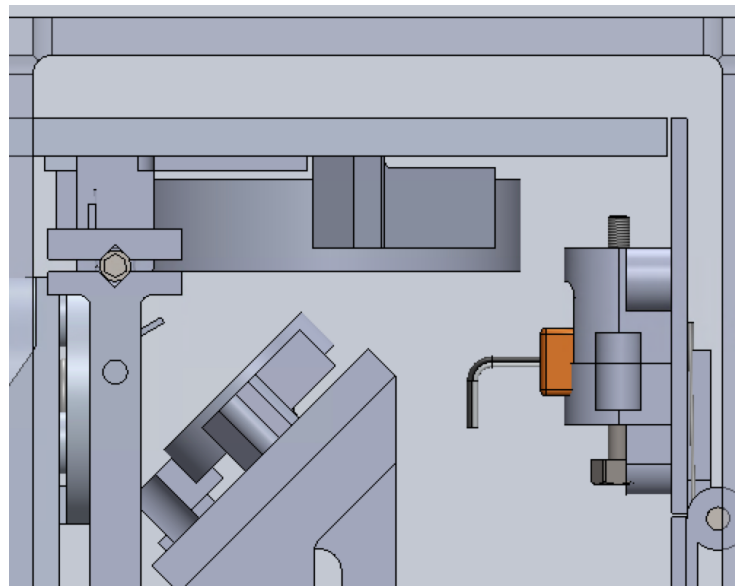


Figure 29. Top mirror in stowed position

Actuation of the top mirror assembly will occur when the Frangibolt is signaled to shear. Figure 30 illustrates the Frangibolt mounting location. As seen in the figure, the Frangibolt is tangentially mounted to the front panel of the CubeSat. This mounting allowed us to leverage off of ICON's Frangibolt mounting design.

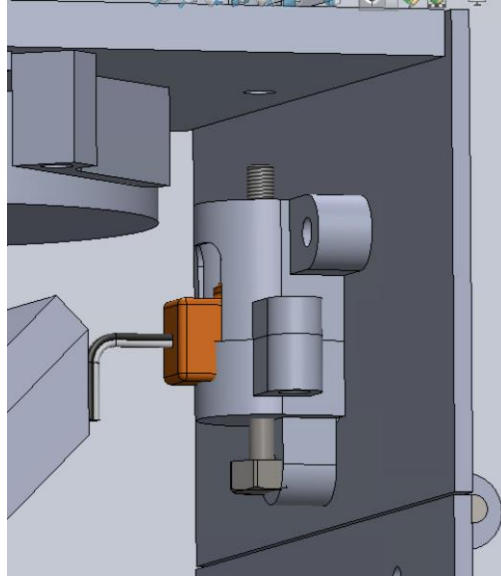


Figure 30. Frangibolt mounting location

The bolt is threading through the top cover of the satellite. The preload of the bolt on the top cover keeps the gasket compression on both the front panel and top cover. One bolt will be sufficient as only enough preload is needed to keep foreign particles outside of the CubeSat. A vacuum is not needed, so one preloaded bolt will provide sufficient compression for both panels. Once deployed, the Frangibolt housing assembly travels with the front panel, out of the way of the field of view. Figure 31 shows the top cover assembly in the deployed position with the Frangibolt housing outside of the satellite. The position of the Frangibolt housing in the deployed position provides an excellent mitigation to a potential issue. When the Frangibolt fractures, there is heat that is produced by the fracture in the housing. By pushing the housing outside of the satellite upon opening, the heat dissipates into the ionosphere and does not heat up the internal components.

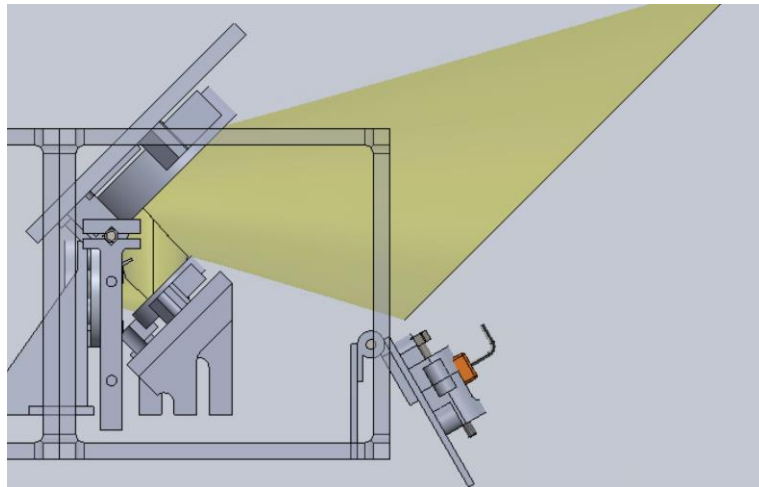


Figure 31. Deployable cover in open position

5.3 Top Mirror Hinge Assembly

In order to achieve the necessary motion of the top mirror assembly, a complex hinge assembly was designed to rotate the top mirror from the stowed to the deployed position. This hinge assembly is shown in Figure 32.

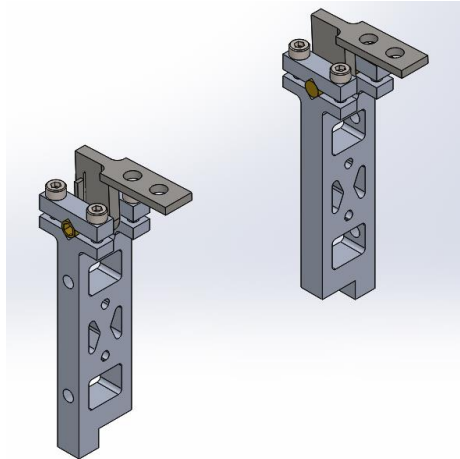


Figure 32. Top Mirror Hinge Assembly Overview

The biggest challenge in the top mirror hinge design was keeping the top mirror clear of the keeper. In order to achieve the 2" sizing of the top mirror, it is necessary the back corner of the top mirror 1.11 mm off the keeper top. Because the top mirror has to rotate 45° between the horizontally stowed position and the deployed position, the axis of rotation has to nearly coincide with the back corner of the top mirror. If it were to coincide perfectly with this corner, the corner of concern would not move at all upon deployment as it would have no radius from the rotational axis. It is this geometric constraint that drove the rest of the hinge design. Because the location of that top mirror is set relative to the keeper, the hinge mounts were split in two to sit on the sides of the keeper. Similarly, the hinge shaft itself had to be cut into two sections as it would interfere with the top mirror and top mirror flexure if it stretched the width of the cube. With these three design considerations made—it needs to mount on the sides of the keeper, it needs to have a split shaft, and it needs to have its rotational axis about the back corner of the mirror—the tower mechanism was created. The tower hinge design consists of a symmetric, double hinge, with each hinge consisting of five parts.

The first part is the tower itself. The tower provides structural support, mounting to the structure, and location to the optical datum for the hinge. The tower can be shown in Figure 33

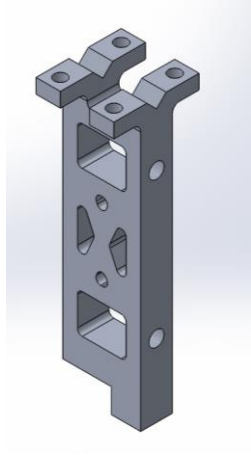


Figure 33. Top Mirror Hinge Assembly: Tower

It has a kinematic mount on top to interface with the hinge shaft. This allows the location of the axis of rotation of the shaft to be known relative to the tower without having to drill locational pins. It also has two threaded mounting holes that interface with the surrounding CubeSat structure. These holes will be mated with M3 screws that will go through a slot in the structure to allow for calibration. Lastly, the tower also includes the interface of the hinge to the optical datum. It has three critical surfaces that define its absolute position: the bottom of the leg defines the height of the hinge off the optical datum, the side tab makes contact with the optical datum to ensure symmetry, and the front of the tower interfaces with a planar optical datum feature to establish front-back alignment of the tower. The two interfaces that will allow for shimming are the vertical position of the mirror and the front-back position of the mirror. Both are being designed with a nominal 0.010 inch shim so that they can be shimmed up or down based on need.

The second part is the shaft, shown in Figure 34. The shaft performs three key functions: to allow smooth rotation, to constrain the spring into a tensioned position, and to allow for adjustment of spring preload.

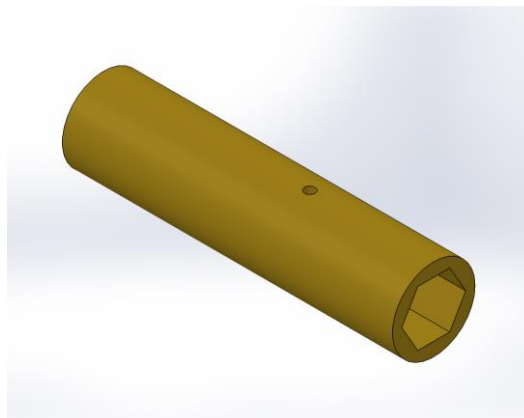


Figure 34. Top Mirror Hinge Assembly: Shaft

The material choice of machined brass will provide the smooth rotational surface relative to the journal. The spring is constrained by the shaft by a radial through hole. This through hole will constrain one of the free ends of the spring relative to the shaft. Tuning of the spring torque may be necessary during calibration and assembly, thus a M2 allen wrench key is cut into the end of the shaft. This will allow the assembler to rotate the shaft, which will in turn rotate a constrained end of the spring and adjust the angular deflection of the spring.

The third part is the top clamps that secure the shaft relative to the tower, seen below in Figure 35.

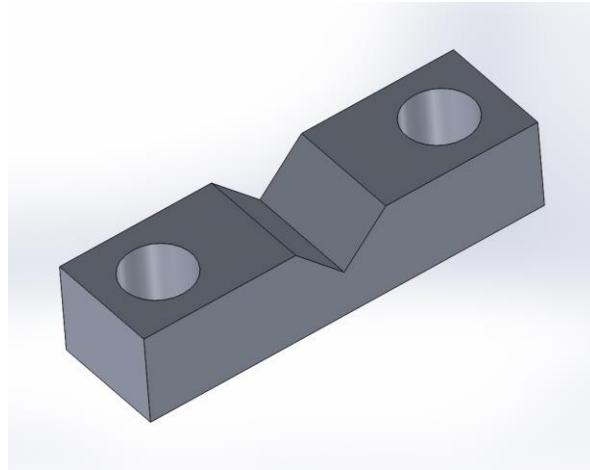


Figure 35. Top Mirror Hinge Assembly: Top Clamp

There are two of these parts per tower, four total. Since the shaft needs to spin to adjust the spring torque, no bolting or pins were used to interface with the shaft. Instead, the kinematic mount design was applied again. With sufficient clearance for either binding holes that mate to the tower, this top kinematic mount will fall into its natural location over the shaft without forcing it out of alignment with the tower. Once the screws are tightened down, the four points of contact between the kinematic mounts and the shaft will completely constrain the rotation and translation of the shaft.

The fourth part of interest is the spring. The spring provides the actuation force necessary to deploy the top mirror upon frangibolt shearing. Figure 36 is CAD rendering of the mentioned spring.



Figure 36. Top Mirror Hinge Assembly: Spring

The material choice for the hinge is 302 stainless steel for its non-corrosive properties. One of the ends was previously dictated by the shaft to be an axial free end. The other end, which is the side turning the journal, is chosen to be a tangential end. This will allow for large surface contact between the journal and the spring. The spring stiffness necessary is approximated using the heritage spring stiffness used for ICON and the ratio of the respective springs' supported mass. Due to the complex free end geometry of this spring, a custom spring will need to be procured.

The last part of the top mirror hinge assembly is the journal, highlighted in Figure 37. The journal provides interface of the hinge to the top mirror as well as rotates about the shaft.

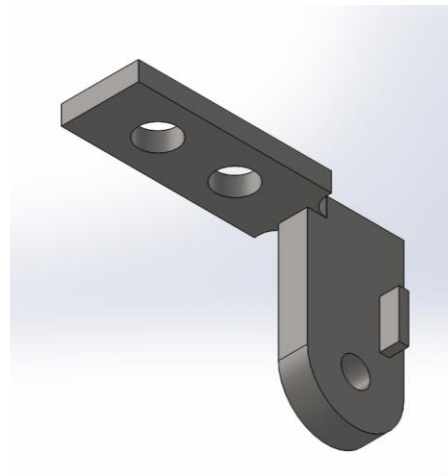


Figure 37. Top Mirror Hinge Assembly: Journal

The geometry of the journal is largely driven by spacial constraints of the hinge and backing plate of the mirror. The width of the journal surface is driven by the need to fit the spring and the journal side by side along the shaft. The length of the mounting surface to the backing plate was dictated by the location of the top mirror flexures. The key features included on the journal are the spring retention tab on the side and the journal surface itself. The spring retention tab will interface with the spring's free end to cause journal rotation. Because it is interfacing with a stainless steel spring, the material choice for the entire journal is stainless steel as well. The journal surface is a H7 fit with the shaft, allowing for temperature change while maintaining a close running fit. The journal

surface will be electrolessly, PTFE-Nickel plated to ensure the lowest friction possible when sliding on the brass shaft surface. This design is expected to change slightly as the constraints of the electroless process are not greatly understood by the team. The goal is to get the design in front of the manufacturing team by two weeks from the submission of the CDR to initiate this conversation.

In conclusion, the top mirror hinge consists of five independent parts: the tower, the top clamps, the shaft, the spring, and the journal. Each part integrates into a two-tower design to rigidly connect the top mirror via the optical datum and provide a hinge point about the back corner of the mirror.

5.4 GSE Integration

For testing purposes, an alignment fixture is needed to hold the Deployable Cover assembly and simulate the mechanism which will be on the future CubeSat UV Imager. The alignment fixture will be used in GEVS and designed tests. Due to the final 2U structure of the UV Imager not being finalized, the GSE will need to have structure to secure various parts of the Deployable Cover. Currently, the GSE alignment fixture is being finalized.

6. Manufacturing, Assembly, and Integration

Manufacturing of the CubeSat was performed after the detailed design was finalized, and the approval for all purchases was made. Most of the machined components of the deployable cover were allocated to be fabricated by the machine shop at UCBSSL. Other components were bought from third party vendors. This section of the report details the components which were machined and procured, and how the team unified the components into a functional assembly.

6.1 Procurement

A tabulated list of materials and components necessary for the manufacturing of each design was made. Most of the stock metal and fasteners were purchased from McMaster-Carr, while the optical and electrical components were purchased from Thorlabs and Digi-Key, respectively. See Appendix F for the specific procured components being integrated into the deployable cover assembly.

6.2 Manufacturing

The beginning of the design for manufacturing started with the resources we had gathered during our literature review. Leveraging off of other projects, including the first year development of the CubeSat UV Imager, we knew machined components were going to be made from 6061-aluminum. 6061 has an excellent weight to strength ratio, which is very important as our picosatellite needs to be as light as possible. Two major characteristics of aluminum is it is a very good reflector of light and conductor of heat. Thermal stability within the satellite is important as the internal electronics do not operate outside of the ranges specified by the manufacturers. Due to this satellite being used for imaging purposes, no stray light is wanted within the satellite. The reflectance of light is not preferred, therefore, portions of the machined aluminum components will be anodized to purely absorb light and not reflect it into the satellite.

Once the main type of material used in fabrication was chosen, the method of machining components needed to be decided upon. The main aspects we considered were lead time, and precise tolerancing. Many of components required very tight tolerances, including geometric dimensioning and tolerancing. For these reasons, CNC machining was chosen as the primary

manufacturing method. The capabilities of meeting the desired tolerances with CNC machining is unmatched when compared to conventional mills and lathes.

A major design consideration for manufacturing is no parts could be fabricated with materials which were at risk to outgas. Any parts that could outgas would be a risk to the optical system, and therefore inhibit the functionality of the satellite. As a result, no lubricates or materials with coatings that outgas were to be considered for manufacturing. Without the ability to use lubricants, a large issue arises when considering fasteners. For weight saving considerations as discussed above, the main structure is aluminum. Because we need to use stainless steel fasteners due to their high strength and anti-oxidation properties, a stainless insert needs to be used to provide a durable mating surface for the threads. Threading stainless steel fasteners into stainless hardware causes galling, or chemical adhesion, of the two components. To mitigate this issue without the use of anti-galling lubricants due to their outgassing, Nitronic 60 helicoil inserts are used. Nitronic 60 is an austenitic stainless steel which is well known for its wear and galling resistance. Helicoil inserts allow us to use standard fasteners with the low risk of thread wear, galling, and stripping.

6.3 Assembly

Assembly will be completed by the Cal Poly senior project group upon the arrival of procured and fabricated parts. An assembly plan has been drafted and is attached in Appendix E of this report. One of the most complex subsystems to assemble is the mirrors. The detailed assembly plan for the mirrors can be found in Appendix H.

7. Design Verification Plan

The testing of the UV Deployable Cover will be performed to validate the mechanical design of the subassembly. The types of testing involved include NASA's GEVS along with designed test methods specific to the design of the Deployable Cover. The designed tests include boresight alignment and a general field of view test.

7.1 GEVS Testing

In order to simulate the environmental conditions of space flight, thermal vacuum and vibrational testing will be performed on the Deployable Cover subassembly at Cal Poly. GSE will be used to house the subassembly and provide a datum for the subassembly to mount to test equipment. According to GEVS, testing will be performed on the subassembly level.

7.1.2 Thermal Vacuum Testing

The Cal Poly Space Environments Lab will be used to perform thermal vacuum testing. The purpose of this testing is to verify the assembly functions at extreme temperatures. At the lowest extreme temperature of 0°C, the stiffness of mechanical components is highest and the main top cover journal has the most amount of clearance. At the highest extreme temperature of 40°C, the stiffness of mechanical components will be the lowest and the stiction in the journal will be greatest. All of these characteristics are of risk to the functionality of the assembly, and will be tested properly to mitigate that risk. The GSE with the Deployable Cover mechanism will be mounted inside the thermal vacuum chamber. Testing will be performed to verify functionality at the temperatures extremes of 0°C and 40°C, respectively. Thermocouples will be mounting at

various parts of the GSE to verify the test temperature is at steady state. Deployment tests will be ran at the two extreme temperatures. Verification of a functioning Deployable Cover will be read by the signaling of the limit switch within the assembly.

7.1.3 Vibrational Testing

The Cal Poly Mechanical Engineering department vibrations lab will be used to perform vibrational testing on the entire assembly. The vibrational analysis consists of both component and overall assembly level vibration analysis to verify that the structure will withstand launch and orbital environments. The vibration testing will consist of sine burst, sine sweep, and random vibration testing. The sine burst testing is used to test the strength of the component and assembly as opposed to using static pull testing. The sine sweep test is use to determine natural frequencies and resonance to verify that the structure will not resonant during the launch or orbital conditions. The random vibration testing is used to verify that the structure can withstand the large variety of vibrations that can be experienced during launch and orbital conditions and the random nature of the testing simulates the launch environment. The vibration testing is crucial to the design of this structure since space environments are inherently vibrational and this structure must maintain optical alignment through the large variety of environmental forcing. The optical alignment will be tested after each subsequent test and each type of test will be repeated multiple times to ensure a large sample size and thus the conclusions will be adequate to determine reliability of the optical alignment.

7.2 Optical Alignment Testing

Optical testing will be coupled with the GEVS testing. Essentially, the test is to determine the opto-mechanical functionality of the deployable cover after experiencing environmental loads. In addition, this test allows our group to calibrate the cover into alignment. Optical alignment will be tested by mounting a laser behind the GSE. The laser will translate outside of the GSE in order to shine onto a polar plot sitting a known distance away. Moving this polar plot closer to the laser will allow for the tip and tilt of the laser to be adjusted properly. With the laser's tip and tilt confirmed, the laser will be translated back to the center of the bottom mirror and be reflected onto another polar plot. Shimming can then be performed to align the bottom mirror at this point. The top mirror is then added to the system, and it is aligned similarly using a polar plot and shimming. A complete procedure for how optical alignment was performed can be found in Appendix I.

8. Project Management

The design process that will be used to guide our resources towards a final prototype will generally follow a traditional process: brainstorm, design, simulate, manufacture, test, and report. The status of our work will be tracked using a Gantt chart through TeamGantt. This status will then be reported out to the sponsor weekly during meetings. Appendix B contains an outline of our project schedule and each objective group will be populated with individual tasks closer to the date. A summary of the critical dates is provided in the table below.

Table 8. Gantt chart summary of deadlines and task sections.

Task/Milestone	Date
Ideation Phase	2/1-2/10
Concept Visualization and Layout	2/10-3/8
Preliminary Design Review (PDR)	3/8
Simulation and FEA	3/8-5/3
Critical Design Review (CDR)	5/3
All Drawings to UCB	6/6
Assembly and Testing	9/19-10/31
Final Report Delivered to UCB	11/14

To keep our team on track towards milestone completions, a project manager position will be assigned biweekly to an individual member of the group. This member will set additional meeting times, follow up on all communication requirements with team members/sponsors, and update/assign daily tasks to group members. By switching off the responsibility between teammates, we hope to all gain insight into the responsibilities and difficulties of a managerial role.

The immediate action item for the group transitioning out of the CDR stage is to finalize our design and to begin the detailed drawings for manufacturing. Due to the drawings being handed off to UCBSL to manufacturing components over the summer, it is important we have some time to get feedback from their machine shop. We hope to have a complete drawing package to UCBSL for review by 5/17. By doing so, we allow ourselves time to finalize drawing details and to ensure there are no issues with handing off the procurement to the UC Berkeley Space Sciences Laboratory.

9. Conclusion & Recommendations

The function of the UC Berkeley Space Sciences Laboratory's CubeSat FUV imager is highly dependent on a reliable cover design that protects the instrumentation as well as deploys to allow for measurements from the FUV imager. The fundamental requirements for the deployable cover are high alignment reliability, maintain a full 30° FOV for the FUV sensor, and deploy two exposure mirrors at 45° relative to the optical axis. The final design incorporates a stationary flat bottom mirror, a top flat mirror that purely rotates, a deployment of the front panel, and a redesign of Front Optics Assembly baffling. The mirrors are attached the structure via flexures which absorb vibrations and minimize residual stress in the mirrors. Actuation is caused by a Frangibolt which is located on the outside of the front assembly. Lockout of the top cover is performed by Delrin flexures which act as hardstops.

During initial assembly of the satellite structure, several design aspects were of concern to the Senior Project group: the spring, flexure, mirror bonding fixture, and front panel shaft design. The first major part of the design we wanted to bring to attention was the spring attachment onto the hinge shafts. Assembly was very difficult when placing the 90 degree tang end into the machined hole on both the top mirror and front door hinges. Another spring issue which was

observed during assembly was the free end of the front door spring not wanting to sit in the machined hole on the journal. For future work, the team suggests to modify the designs of the spring free ends to not interfere with the shafts upon assembly. The team also suggests to lengthen the springs in order to have the free ends held in place by compression. Second, the flexures on the bottom mirror and top mirror assembly contained many concerning design aspects which were noticed during the assembly and integration process. During the design phase, the Senior Project group used information gathered during the literature review to determine a proper size and shape of the flexure. Due to the oversight of not performing enough preliminary analyses beforehand, the flexures appeared to be too stiff for their application. The purpose of the flexures are to create a non-rigid connection between the mirror and the satellite structure. In the group's finite element analysis performed during the Fall quarter, the flexures do not deflect sufficiently and absorb the loading on the mirror. The group suggests to research ways in which the flexures could be less stiff and flex under loading, but too much and cause the brittle mirror to shatter. A more sophisticated FEA model could be created to understand the correlation between the stiffness of the flexure and the risk of damage to the mirror due to a large flexure deformation. Thirdly, the mirror bonding fixture proved to have too many degrees of freedom, making them inadequate for repeatably clocking the flexure positions onto the mirrors for bonding. The first problem that arose was the large difference between the Delrin locator and the aluminum fixture's hole meant for the Delrin locator. This led to lots of shims being stacked on one another to estimate concentricity with the aluminum walls. Because no single shim was thick enough to check the clearance between the Delrin and the aluminum fixture, we were unable to establish concentricity with confidence. Furthermore, the height of the Delrin locator was unnecessarily tall which led to the flexures having to be shimmed up excessively in order to bring them to the proper height relative to the mirror. This large stack of shims provided an unstable and nonparallel base that caused extra time to be spent ensuring that the flexures were level to the mirror and not tilted. The Delrin locator did not work as expected as it was much harder to establish concentricity of the mirror relative to the Delrin locator. We attempted to establish this by using a level on the top of the aluminum surface and then replicating this measurement on top of the mirror surface, but the level we were using was not very accurate and this relies on absolute flatness of both the bottom of the hole in the aluminum as well as the bottom of the Delrin locator itself. Overall, simplifying this mirror bonding fixture design would greatly save assembly time in the future. Finally, the front panel shaft proved to be much harder than expected to align. This is because of the split shaft nature of the design as well as the lack of support on the shafts. Because two shafts were used to operate one door, perfect axial alignment was needed in order to allow for motion which was very difficult to replicate during assembly. To make the matters worse, the shaft was only rigidly supported to the CubeSat structure via the shaft clamp on the outside of the shaft: one clamp per shaft. This allowed for angular deflection of the shaft relative to the CubeSat that had to be compensated by tightening the journal itself to provide a secondary support. A better design would be to alter the actuation subassembly to allow for a single shaft to be utilized as well as making sure that adequate—at least two—supports are provided for each shaft in the design. In conclusion, the design presented in this report shows that a reliable, two mirror design can be packaged in the space required. However, a design spin is suggested for the springs, flexures, front panel shaft, and mirror bonding fixture in order to bring it up to a flight ready design.

References

1. "ICON - Ionospheric Connection Explorer > Observatory > Instruments > FUV > FUV - How It Works." ICON Ionospheric Connection Explorer, icon.ssl.berkeley.edu/Observatory/Instruments/FUV.
2. Grillo, J., Haijar, T., & Hill, B. (2018). *Final Design Report UV Imager Application for a Cube Satellite* [PDF Document].
3. D. Busch, John & E. Purdy, William & David Johnson, A. (1992). Development of a non-explosive release device for aerospace applications.
4. Bucsan, C & Avram, Mihai & Prisacaru, Gheorghe. (2013). Servovalve with shape memory alloy wire actuator. 102-104.
5. NASA GODDARD SPACE FLIGHT CENTER. General Environmental Verification Standard (GEVS). Greenbelt, Maryland: NASA, 2013. Print.
6. NASA JOHN F. KENNEDY SPACE CENTER. Launch Services Program, Program Level Dispenser, and CubeSat Requirements documents
7. NASA's Jet Propulsion Laboratory. (2016, 06 01). Launch Tie-Down and Release Mechanism for CubeSat Spacecraft. Nasa Tech Briefs, 40(06).
8. Goddard Space Flight Center. (2015, 05 01). Diminutive Assembly for Nanosatellite deployables (DANY) Miniature Release Mechanism. NASA Tech Briefs, 39(05).
9. Cheimets, Peter. (n.d.). Hirex Off-Axis Mirror Mount. Retrieved from https://www.cfa.harvard.edu/~cheimets/projects/hirex/off_axis_mirror_mount_doc.html
10. Turin, Paul. (2014). *FUVEPR – Turret*. [Powerpoint Presentation]. UC Berkeley Space Sciences Laboratory.
11. Hasso Plattner Institute of Design at Stanford. (n.d.) Ideate Mixtape [PDF Document]. Retrieved from <https://dschool.stanford.edu/resources/>
12. Niku, Saeed (2008). *Creative Design of Products and Systems*. Chichester, UK: John Wiley and Sons Ltd.
13. Thorlabs. (2019). Zerodur® Broadband Dielectric Mirrors. (n.d.). Retrieved from https://www.thorlabs.com/newgrouppage9.cfm?objectgroup_id=9640

Appendices

A. QFD

B. Gantt Chart

C. Mirror Sizing MATLAB Code

D. Morphology Matrix Design Concepts

E. Assembly Plan

F. Indented Bill of Materials

G. Flexure Analysis Calculations

H. Bottom Mirror Assembly Plan

I. Optical Alignment Test Plan

J. Bottom Mirror Assembly Finite Element Analysis

K. Deployable Cover Drawing Package

Appendix B: Gantt Chart

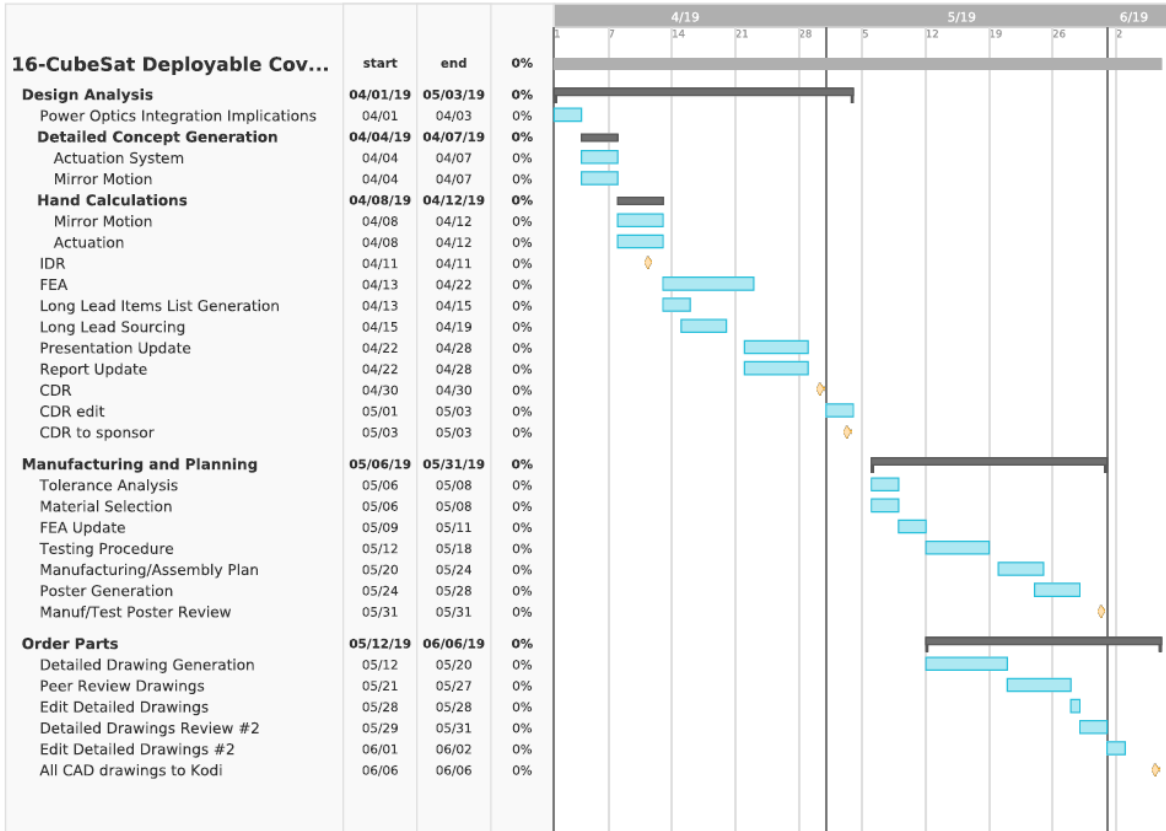
Project Q1

Printed: March 6, 2019



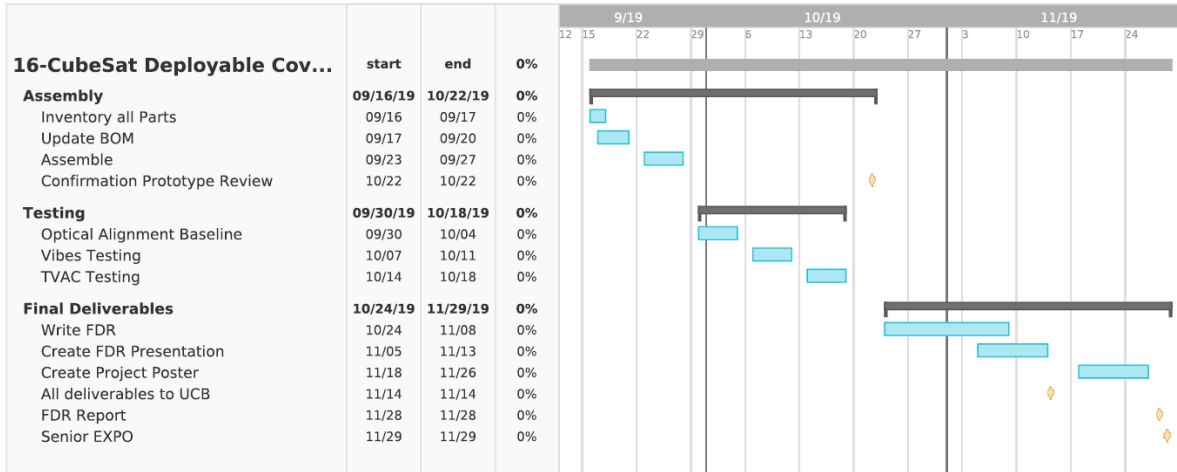
Project Q2

Printed: March 6, 2019



Project Q3

Printed: March 6, 2019



Appendix C: MATLAB Script Mirror Sizing

Written By: Team #16

```
%Description: This script will determine the size of the two mirrors inside  
%the cubesat based on the placement of the Iris and the required angles of  
%the mirrors  
clear all;  
clc;
```

Define Constants

Fixed Constants

```
theta_fov = 32;           % Angle of field of view, this is a requirement, Units are degrees  
R_i = 2.8998*10^-3;      % Radius of the iris, units are m  
theta_m1 = 45;           % angle of mirror 1 relative to bottom of satellite, units are degrees  
theta_m2 = 45;           % angle of mirror 2 relative to the bottom of satellite, units are  
degrees  
del_x_course = 0.002;    % Distance step between iteration variables, units are m  
del_x_fine = 0.003;  
x_ib = 0.015;            % Distance from Iris to Front Baffle, units are m  
h_fb = 0.085;           % Height of the front baffle, Units are m  
h_cube = 0.1;           % Height of Cube from base, units are m  
x_env = 0.05+0.0183-x_ib; % Maximum envelope in the cubesat that we are able to use,  
units are m  
  
% Define Ranges for iteration Variables - Original  
eta = [0:del_x_course:0.1]; % Height of front of cubesat, units are m  
x_m1 = [x_ib+0.005:del_x_course:0.04]; % Distance from Iris to bottom corner of mirror 1,  
Units are m  
h_oa = [0.045:del_x_course:0.055]; % Height of Optical Axis relative to the bottom of cube sat,  
units are m  
delta = [-0.01:del_x_course:0.1]; % Distance between top of cubesat and bottom corner of  
mirror 2, units are m  
  
%% Define Ranges for iteration Variables - Fine Resolution around approximate solution  
% eta = [0.075:del_x_fine:0.85]; % Height of front of cubesat, units are m  
% x_m1 = [0.025:del_x_fine:0.035]; % Distance from Iris to bottom corner of mirror 1, Units are  
m  
% h_oa = [0.05:del_x_fine:0.06]; % Height of Optical Axis relative to the bottom of cube sat,  
units are m  
% delta = [0:del_x_fine:0.1]; % Distance between top of cubesat and bottom corner of  
mirror 2, units are m
```

Calculate Mirror Lengths

Initialize loop counters

```

i = 1;

% Initialize Solution Matrix
solutions = [];

% Start loops
for n = 1:length(eta)
    for a = 1:length(x_m1)
        for b = 1:length(h_oa)
            for c = 1:length(delta)
                % Define Equation for L_m1
                L_m1(i) = (2*R_i + 2*x_m1(a)*tand(theta_fov/2))/(sind(theta_m1) -
cosd(theta_m1)*tand(theta_fov/2));

                % Define Equation for h_m1
                h_m1(i) = h_oa(b) - R_i - x_m1(a)*tand(theta_fov/2);

                % Define Equation for L_m2
                L_m2(i) = ((tand(theta_fov/2)*(2*delta(c) + 2*h_cube - 2*h_m1(i) -
L_m1(i)*cosd(theta_m1)) + L_m1(i)*sind(theta_m1)) / (sind(theta_m2))) / (1-tand(theta_fov/2));

                % Define Equation for Beta
                beta(i) = atand((x_m1(a) - x_ib) / (h_fb - h_m1(i)));

                % Define Equation for Psi
                psi(i) = atand((0.05 + x_ib - L_m1(i)*cosd(theta_m1) - x_m1(a)) / (eta(n) -
h_m1(i) - L_m1(i)*sind(theta_m1)));

                % Define Equation for Phi
                phi(i) = atand((delta(c)+h_cube-eta(n)) / ( x_env + x_ib - L_m1(i)*cosd(theta_m1)
- x_m1(a) + L_m1(i)*sind(theta_m1) + (delta(c) + (eta(n) - h_m1(i)))*tand(theta_fov/2) ));

                % Define Equation for x_m2
                x_m2(i) = (x_m1(a) - (h_cube + delta(c) - h_m1(i))*tand(theta_fov/2)) - x_ib;

                % Define final solution matrix
                solutions(i,:) = [i,eta(n), x_m1(a), h_oa(b), delta(c), L_m1(i), L_m2(i),
h_m1(i), beta(i), psi(i), phi(i), x_m2(i)];
                i = i+1;
            end
        end
    end
end
save solutions

```

Define Constraints for Solutions and Find the Best Solution

Run For loop to solve for solutions that fit all constraints

```

load solutions
% for ind = 1:i-1

```

```

% % Constraint on All Angles are greater than the required field of view
%   if ((solutions(ind,3) - x_ib) + L_m1(ind)*cosd(theta_m1) < 0.05 &&...
%       (L_m2(ind) < 0.095) && beta(ind) > theta_fov/2) &&...
%       ((psi(ind) > theta_fov/2) && phi(ind) > theta_fov/2)
%
%       % If the soltion passes all constraints save as a 1(pass) in the solution index vector
%       solution_ind(ind) = 1;
%
%   elseif ((solutions(ind,3) - x_ib) + solutions(ind,6)*cosd(theta_m1) < 0.05 &&...
%          (solutions(ind,7) < 0.095) && (solutions(ind,9) > theta_fov/2) &&...
%          (solutions(ind,10) < 0) && (solutions(ind,11) > theta_fov/2))
%
%       % If the soltion passes all constraints save as a 1(pass) in the solution index vector
%       solution_ind(ind) = 1;
%   else
%       % if the solution does not pass the constraints, save as a 0(fail) in the solution
Index vector
%       solution_ind(ind) = 0;
%   end
% end

% Run For loop to solve for solutions that fit all constraints
load solutions
for ind = 1:i-1
% For this Schenario, Beta is not a constraint
% Constraint on All Angles are greater than the required field of view
    if (solutions(ind,3) - x_ib) + L_m1(ind)*cosd(theta_m1) < 0.05 &&...
        (L_m2(ind) < 0.095) &&...
        ((psi(ind) > theta_fov/2) && phi(ind) > theta_fov/2)

        % If the soltion passes all constraints save as a 1(pass) in the solution index vector
        solution_ind(ind) = 1;

    elseif ((solutions(ind,3) - x_ib) + solutions(ind,6)*cosd(theta_m1) < 0.05 &&...
           (solutions(ind,7) < 0.095) && (solutions(ind,9) > theta_fov/2) &&...
           (solutions(ind,10) < 0) && (solutions(ind,11) > theta_fov/2))

        % If the soltion passes all constraints save as a 1(pass) in the solution index vector
        solution_ind(ind) = 1;
    else
        % if the solution does not pass the constraints, save as a 0(fail) in the solution Index
vector
        solution_ind(ind) = 0;
    end
end

solutions_ind_L_m1 = find((solutions(:,3) - x_ib) + solutions(:,6)*cosd(theta_m1) < 0.05);

solutions_ind_L_m2 = find(solutions(:,7) < 0.095);

solutions_ind_beta = find(solutions(:,9) > theta_fov/2);

solutions_ind_psi = find(solutions(:,10) > theta_fov/2);

```

```
solutions_ind_phi = find(solutions(:,11) > theta_fov/2);
```

Plot Solutions for Pass and Fail of Each Variable

Define each pass and fail as either a 1 or 0 to plot Note: pf means pass fail variable so it only contains 1's and 0's

```
[nr, nc] = size(solutions);

% Define Pass fail for L_m1
L_m1_pf = zeros(nr, 1);
L_m1_pf(solutions_ind_L_m1) = 1;

% Define Pass fail for L_m2
L_m2_pf = zeros(nr, 1);
L_m2_pf(solutions_ind_L_m2) = 1;

% Define Pass fail for Beta
beta_pf = zeros(nr, 1);
beta_pf(solutions_ind_beta) = 1;

% Define Pass fail for psi
psi_pf = zeros(nr, 1);
psi_pf(solutions_ind_psi) = 1;

% Define Pass fail for phi
phi_pf = zeros(nr, 1);
phi_pf(solutions_ind_phi) = 1;

% % Define Pass fail for All Solutions
% solution_pf = zeros(nr, 1);
% solution_pf(solution_ind) = 1;

% Plot the pass-fail variables
figure(1)
% Plot L_m1
subplot(3,2,1)
bar(1:ind, L_m1_pf)
xlabel('Iteration Number')
ylabel('Pass or Fail')
title('L_{m1}')
axis([1, i-1, 0, 1])

% Plot L_m2
subplot(3,2,2)
bar(1:ind, L_m2_pf)
xlabel('Iteration Number')
ylabel('Pass or Fail')
title('L_{m2}')
axis([1, i-1, 0, 1])
```

```

% Plot Beta
subplot(3,2,3)
bar(1:ind, beta_pf)
xlabel('Iteration Number')
ylabel('Pass or Fail')
title('Beta')
axis([1, i-1, 0, 1])

% Plot Psi
subplot(3,2,4)
bar(1:ind, psi_pf)
xlabel('Iteration Number')
ylabel('Pass or Fail')
title('Psi')
axis([1, i-1, 0, 1])

% Plot Phi
subplot(3,2,5)
bar(1:ind, phi_pf)
xlabel('Iteration Number')
ylabel('Pass or Fail')
title('Phi')
axis([1, i-1, 0, 1])

% Plot Solutions
subplot(3,2,6)
bar(1:ind, solution_ind)
xlabel('Iteration Number')
ylabel('Pass or Fail')
title('Total Solutions')
axis([1, i-1, 0, 1])

% Link the x axis
linkaxes([subplot(3,2,1), subplot(3,2,2), subplot(3,2,3), subplot(3,2,4), subplot(3,2,5),
subplot(3,2,6)], 'xy')

solutions_work = solutions(find(solution_ind ==1), :);

% Loop and display valid results
% valid = [];
% for i = solution_ind
%     valid = [valid;solutions(i,:)];
% end
%
% display(valid)

```

Published with MATLAB® R2018a

Appendix D: Morphological Matrix Design Concepts

Sub Function	1	2	3	4	5	6
Concept 1	Single Bar Linkage W/ Linear Guide	Direct Frangibolt Mounting	Top Mirror Split Gasket	Retangular Flexures	Half Front Cover Deployment	Rotational Hardstop Pin
Concept 2	Single Bar Linkage W/ Linear Guide	Direct Pin-Puller Mounting	Continuous Top Mirror Gasket W/ Mirror Recess	Circular Flexures	Bottom Mirror Baffle	Linear Hardstop Block
Concept 3	Linear Guide W/ Moving Hinge	Direct Frangibolt Mounting	Top Mirror Split Gasket	Retangular Flexures	Half Front Cover Deployment	Rotational Hardstop Pin
Concept 4	Linear Guide W/ Moving Hinge	Direct Pin-Puller Mounting	Continuous Top Mirror Gasket W/ Mirror Recess	Circular Flexures	Bottom Mirror Baffle	Linear Hardstop Block
Concept 5	Pin and Slot W/Moving Hinge	Direct Frangibolt Mounting	Top Mirror Split Gasket	Retangular Flexures	Half Front Cover Deployment	Rotational Hardstop Pin
Concept 6	Pin and Slot W/Moving Hinge	Direct Pin-Puller Mounting	Continuous Top Mirror Gasket W/ Mirror Recess	Circular Flexures	Bottom Mirror Baffle	Linear Hardstop Block
Concept 7	Single Bar Linkage W/ Linear Guide	Direct Frangibolt Mounting	Continuous Top Mirror Gasket W/ Mirror Recess	Circular Flexures	Bottom Mirror Baffle	Linear Hardstop Block
Concept 8	Single Bar Linkage W/ Linear Guide	Direct Frangibolt Mounting	Top Mirror Split Gasket	Circular Flexures	Bottom Mirror Baffle	Linear Hardstop Block
Concept 9	Single Bar Linkage W/ Linear Guide	Direct Frangibolt Mounting	Top Mirror Split Gasket	Recessed Epoxy	FOA Baffle	Retaining Ring
Concept 10	Single Bar Linkage W/ Linear Guide	Direct Frangibolt Mounting	Top Mirror Split Gasket	Perimeter Bolt Pattern	Blanket Baffle	Magnetic Linkage Lockout

Appendix E: Assembly Plan

Subassemblies:

1. Bottom Mirror

Procedure 1A- Helicoil inserts:

- a. Place two-legged mount in vice, oriented with backing plate mounting surface up. Make sure not to use front leg as clamping surface to ensure datum integrity.
- b. Using Helicoil insertion tool, place M3 helicoils in both tapped holes.
- c. Turn two-legged mount in vice such that optical datum mounting surface is up. Again, follow step A warning about not clamping front leg surface.
- d. Place M3 helicoils in both legs.
- e. Place one-legged mount in vice, oriented with backing plate mounting surface up.
- f. Using Helicoil insertion tool, place M3 helicoils in both tapped holes.
- g. Turn one-legged mount so that optical datum mounting surface is up.
- h. Place M3 helicoil into leg.
- i. Use edge clamping techniques to restrain position of backing plate to a flat surface.
- j. Using Helicoil insertion tool, place M2.5 inserts into flexure holes.

Procedure 1B- Mirror mounting on backing plate:

- a. Single datum flexure mounted in tangential, radial location of the mirror.
- b. Once the epoxy on the first datum flexure is dried, take the mirror and single flexure and bolt and lock into the backing plate. Datum sides should be aligned before bolt is tightened. During this process, the mirror should be elevated off the backing plate using foam cut to approximate raised thickness (3mm) to prohibit metal-mirror contact.
- c. The remaining two flexures are loosely indexed by their respective bolt holes.
- d. The tips of the remaining two flexures are epoxied and swung to make tangential contact with the mirror. The height of the mirror is dictated during this step by lifting the mirror off the foam and placing them on the flexure pedestals.
- e. All epoxy should be allowed to dry before continuing onto the next procedure.

Procedure 1C- Backing plate mounting on legs:

- a. Place both the two-leg mount and the single leg mount standing upright onto a microflat.
- b. Taking the backing plate, carefully place into relative bolt hole locations to the mounts.

- c. Align the backing plate to the exact location relative to the mount by using a parallel bar against the back leg of the two-legged mount to align the backing plate vertically.
- d. Holding the backing plate against the parallel bar, tighten the bolts using a diagonal pattern.

2. Top Mirror and Door Hinge

Procedure 2A- Helicoil inserts:

- a. Take a moment to mark the locational surfaces of the towers with tape. This will define a no-clamp zone for the below steps.
- b. Hold the tower piece against a table by extending the kinematic mount end over the edge and C-clamping it to the table. Be careful to not clamp on the locational surfaces.
- c. Place 4x M2.5 helicoils in the kinematic mount of the tower.
- d. Repeat steps b and c with the other hinge tower.
- e. Secure the top mirror's backing plate on a table with mirror-side up using C-clamps. Make sure to avoid clamping over holes or on gasketing surface.
- f. Using the helicoil insertion tool, place 3x M2.5 helicoils in the flexure hole locations.
- g. Using the helicoil insertion tool, place 4x M2.5 helicoils in the journal mounting holes.

Procedure 2B- Mirror mounting on backing plate:

- a. Refer to procedure 1A.

Procedure 2C- Hinge tower assembly:

Note: Perform steps a-f for both hinge towers.

- a. Use a vice to restrict motion of the hinge tower. Vertical orientation should be achieved.
- b. Attach the spring to the shaft by placing the radial free end of the spring into the shaft through hole.
- c. Slide the journal over the shaft end opposite the spring-shaft connection, ensuring that axial connection remains in back of shaft so that spring tension forces journal into vertical position.
- d. Place kinematic mounts over each end of the shaft.
- e. Hand tighten all bolts into helicoils.
- f. Moving from side to side on each kinematic mount (refer to the below figure), slowly snug the kinematic mounts onto the shaft with an allen wrench.
- g. With both towers assembled, constrain the top mirror backing plate on the table with C-clamps.

- a. The next task requires two people: one holding a single tower and the other carefully watching the journal from coming into contact with the mirror as well as securing the position of the journal once located properly. Work together to locate, snug down the bolts with hands, and tightening both down firmly. Make sure the single tower is firmly held in place before repeating for the other tower.
- h. Repeat step h for the second tower.

3. Front Panel Hinge

Procedure 3A- Helicoil inserts:

- a. Set up a flat table with a static perpendicular surface to securely press the structure against.
- b. Taking the structure pressed against the perpendicular surface, place 2x M2.5 helicoil inserts into the static bottom panel.
- c. Take the front panel and securely clamp it to the table with exterior side up using C-clamps.
- d. Using the helicoil insertion tool, place 2x M2.5 helicoils into the front panel journal mating holes.

Procedure 3B- Hinge Assembly:

- a. Using a vise, secure an end journal in place with the hole oriented vertically.
- b. Take the shaft and press it through the hole. It should be snug but slide in. Do not clamp the shaft surface during this step as it will distort the rotational surface.
- c. Take the end journal out of the vise and slide a spring over the threaded end. Make sure that it is the correct orientation for deployment.
- d. Next, simply hole the shaft and slide on the center journal. The clearance on this center journal should allow for easy integration.
- e. With the center journal on, slide the other spring over. Again, it is important to make sure that it is in the correct deployment orientation before proceeding.
- f. Using two clamps at the two journals to fix the shaft to the table, secure the assembled shaft with the threaded, free end hanging off the table.
- g. Place the last end journal onto the shaft.
- h. Finish the subassembly by threading the retaining nut over the threaded end of the shaft.

Procedure 3C- Actuation Mounting

- a. Load a frangibolt into the frangibolt actuator via the specialty press, remembering to place a washer between the bolthead surface and the actuator.

- b. Take a secondary washer and put it over the other side of the frangibolt.
- c. Set a damping medium in the lower frangibolt housing and set the loaded bolthead on top of it.
- d. Take the top housing and place it on top of the lower housing. Loosely join the two parts together by snugging up the screws.
- e. Place both parts on a microflat with the flat side down. Back out the screws, press both parts flat against the microflat, and secure them back into place using a torque wrench.
- f. Place all three M3 helicoils into the frangibolt housing once they are secured together.

Master Assembly Plan:

1. Lock the keeper to the optical datum. This will define the position of everything else.
2. Using a 10mm gauge block off the keeper plane, position the bottom mirror on the optical datum. The side-to-side orientation of the bottom mirror will be located by the pedestal machined into the optical datum surface.
3. The two hinge halves should be placed loosely secured against the outside structure via their side helicoils.
4. Place the top mirror against its side gasketing surface and slide it along the surface until it can be secured to the two side journals.
5. Take the actuation assembly and mount it to the front panel.
6. Take the front panel hinge and mount it to the static front panel via the two end journals.
7. Using two people, orient the front panel to the front panel hinge and secure into place via the bolt holes. During this stage, the top door will need to be open and care should be taken to avoid frangibolt contact with internal components.

Appendix F: Indented Bill of Materials

Indented Bill of Material (BOM)										
UV Deployable Cover										
Assembly Level	Part Number	Drawing Number	Description	Vendor	Qty	Cost	Ttl Cost			
			Lvl0 Lvl1 Lvl2 Lvl3 Lvl4							
0	100000		UV Imager Assembly	----						
1	101000		Bottom Mirror Assembly	----						
2	101001		Backing Plate	UCB	1	400	400			
2	101002		Bottom Mirror	Thor Labs	1	\$177	177			
2	101003		Bottom Flexure Left Handed	Flexure Vendor	1	\$110				
2	101004		Bottom Flexure	Flexure Vendor	2	85	170			
			One Leg Mount			200				
			Two Leg Mount			200				
2			Fasteners							
2			Hex Screw 1.6x0.35x2.5mm	McMaster	3					
2			Hex Screw 3x0.5x8mm	McMaster	4					
1	102000		Top Cover Assembly	----					0	
2	102001		Top Cover Structure	UCB	1	300	300			
2	102002		Top Mirror	Thor Labs	1	\$354	354			
2	102003		Top Flexure	Flexure Vendor	2	85	170			
2	102004		Top Flexure Left Handed	Flexure Vendor	1	110	110			
			Fasteners							
			Hex Screw 1.6x0.35x2.5mm	McMaster	3					
1	103000		Top Hinge Assembly	----					0	
2	103001		Clamp Cover	UCB	4	40	160			
2	103002		Hinge Tower	UCB	2	220	440			
2	103003		Top Cover Shaft	UCB	2	60	120			
2	103006		Top Hinge Spring	Spring Vendor	2	65	130			
			Top Mirror Journal	UCB	2	600	1200			
			Fasteners							
			Hex Screw 2.4x0.45x6mm	McMaster	12				0	
1	104000		Actuation Assembly	----					0	
2	104001		Frangibolt	TiNi Aero	20	45	900			
2	104002		Frangibolt Top Housing	UCB	1	140	140			
2	104003	Bottom	Frangibolt Bottom Housing	UCB	1	140	140			
2	104004		Frangibolt Housing Damping Medium	McMaster	1	25	25			
2	104005		Frangibolt Actuator	TiNi Aero	1	100	100			
			Fasteners							
			Plain Washer 1.6mm	McMaster	2					
			Hex Screw 1.600mm	McMaster	2					
			Hex Nut M3x0.5mm	McMaster	1					
1	105000		Front Panel Assembly	----						
2	105001		Front Panel	UCB	1	60				
2	105002		Static Front Panel	UCB	1	60				
2	105003		Front Panel Journal	UCB	1	400				
2	105004		Front Panel Shaft Clamp	UCB	2	250				
2	105005		Front Panel Shaft	UCB	1	125				
			Front Panel Spring	Spring Vendor	2	60				
			Fasteners							
			Hex Nut M3x0.5mm	McMaster	2					
			Hex Screw 3x0.5x8mm	McMaster	3					
			Hex Screw 2.5x0.45x3mm	McMaster	4					
1	106000		Limit Switch Assembly	----					0	
2	ESE22MH24		Limit Switch	Digi-Key Electronics	1	0.62	0.62			
2	106001		Left Switch Mount	UCB	1	20	20			
2	106002		Right Switch Mount	UCB	1	20	20			
			Fasteners						0	
			Hex Screw 2.5x0.45x3mm		2				0	
			Fasteners TBD	McMaster Carr					0	
			3m 2216 Epoxy	Amazon	1	51.91	51.91			
Total Parts						95		5128.53		

Appendix G: Flexure Analysis Calculations

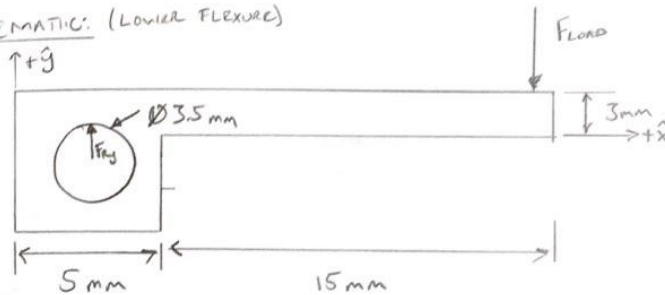
DESIGN ANALYSIS CONT'D

33

SIMPLIFIED FLEXURE ANALYSIS:

FIRST WE ASSUME THE FLEXURE IS A SIMPLIFIED CANTILEVER BEAM WITH A LOAD APPLIED TO THE END.

SCHEMATIC: (LOWER FLEXURE)



ASSUMPTIONS:

1. FLEXURE DOES NOT ROTATE (FORCE IS NOT GREAT ENOUGH TO OVERCOME PRELOAD IN PRELOADED BOLT).
2. FOR THIS ANALYSIS, ALL LOAD IS TAKEN INTO F&B1 FLEXURE FOR WORST CASE SCENARIO
3. EPOXY DOES NOT TAKE

ADDITIONAL GIVENS:

MATERIAL IS 301 SPRING-TEMPERED STAINLESS STEEL

YIELD STRENGTH, $\sigma_{max} = 147 \text{ KSI}$ (1014 MPa), $E = 28000 \text{ KSI}$

LOAD APPLIED IS 100g WHICH IS MAX EXPECTED DURING LAUNCH.

ON LOWER MIRROR FLEXURE, LOAD IS, $F_{LOAD} = 101g$ SINCE

THE MIRROR HAS A MAXIMUM WEIGHT OF 0.116 ON EARTH AT 1g.

ANALYSIS:

SINCE THIS PART IS MODELED AS A SIMPLE CANTILEVER BEAM,

WE KNOW THAT:

$$M = F(x-l) \quad (\text{Eq. 1})$$

$$y_{max} = \frac{Fl^3}{3EI} \quad (\text{Eq. 2})$$

$$\tau = \frac{V}{A} \quad (\text{Eq. 3})$$

FOR THIS APPLICATION, WE WANT A FACTOR OF SAFETY OF 2.

$$\sigma_{ALLOWED} = \frac{\sigma_{YIELD}}{F.S.} = \frac{147 \text{ KSI}}{2} = 73.5 \text{ KSI}$$

Cont'd

Appendix G: Flexure Analysis Calculations

36

LOWER MIRROR FLEXURE ANALYSIS (CONT'D)

FIND THE REQUIRED STRENGTH OF MATERIAL AND SEE IF SPRING STEEL WILL WORK,

$$\sigma_b = \frac{M c}{I}$$

SUBSTITUTE OTHER EQ'S SO EQUATION IS IN TERMS OF LOAD AND DIMENSIONS.

$$\sigma_{b \text{ ALLOWED}} = \frac{12 F(l) c}{b h^3}$$

$$* \sigma_{\text{yield}} = \frac{(F.S.) 12 F(l) c}{b h^3} \quad (\text{EQ. 4})$$

NOW FIND REQ'D YIELD STRENGTH TO SEE IF SPRING STEEL WORKS.

$$\sigma_{\text{yield}} = \frac{(2) 12 (10 \text{ lb}) (0.1279 \text{ in}) (0.5906 \text{ in})}{(0.1181 \text{ in}) (0.2559 \text{ in})^3}$$

$$\sigma_{\text{yield}} = 9160.34 \text{ psi} \left(\frac{1 \text{ KIP}}{1000 \text{ LBS}} \right)$$

$$* \sigma_{\text{yield}} = 9.15 \text{ KSI REQ'D, SPRING STEEL IS DEFINITELY STRONG ENOUGH.}$$

NOW WE MUST FIND MAXIMUM DEFLECTION,

$$y_{\text{max}} = \frac{F l^3}{3 E I}$$

$$= \frac{F l^3 12}{3 E b h^3}$$

SUBSTITUTE VALUES,

$$= \frac{(10 \text{ lb}) (0.5906 \text{ in})^3 (12)}{3 (28000000 \text{ lb/in}^2) (0.1181 \text{ in}) (0.2559 \text{ in})^3}$$

$$y_{\text{max}} =$$



Assembly Plan: Bottom Mirror Assembly

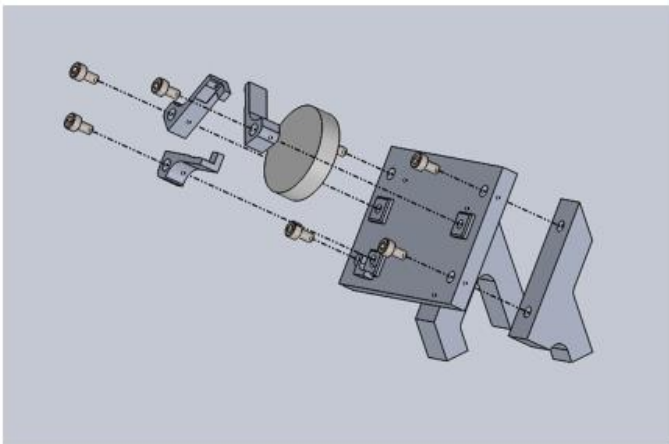
Presented By: EJ Rainville, Patrick Whitesel, Jeff Wagner

Sponsor: UC Berkley Space Sciences Laboratory

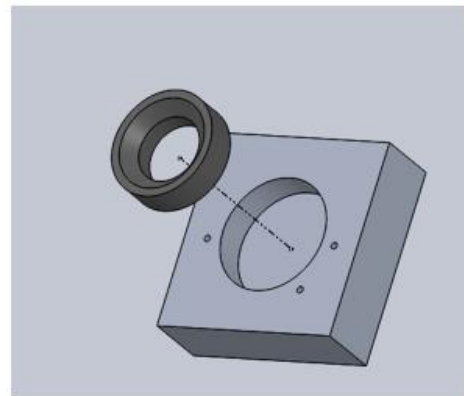
MUWI Deployable Cover - October 14, 2019

1

Overview Schematic



Overall Bottom Mirror Assembly



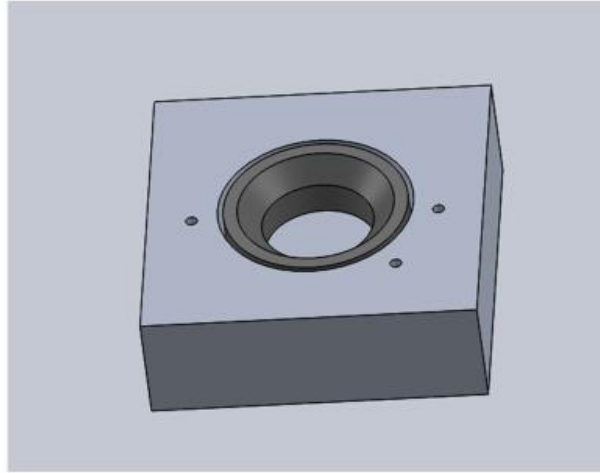
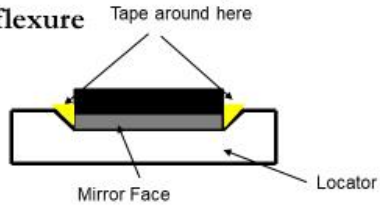
Delrin locator and Assembly Fixture

MUWI Deployable Cover - October 14, 2019

2

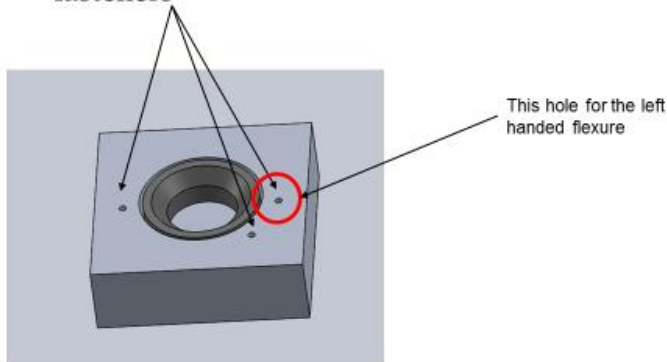
Op 20: Mirror and flexure mounting on Delrin locator

1. Place mirror face down in the Delrin locator
2. Kapton tape the half of the mirror inside the locator at the circumference
3. Shim Delrin around T6 block as necessary for flexure



Op 20: Mirror and flexure mounting on Delrin locator

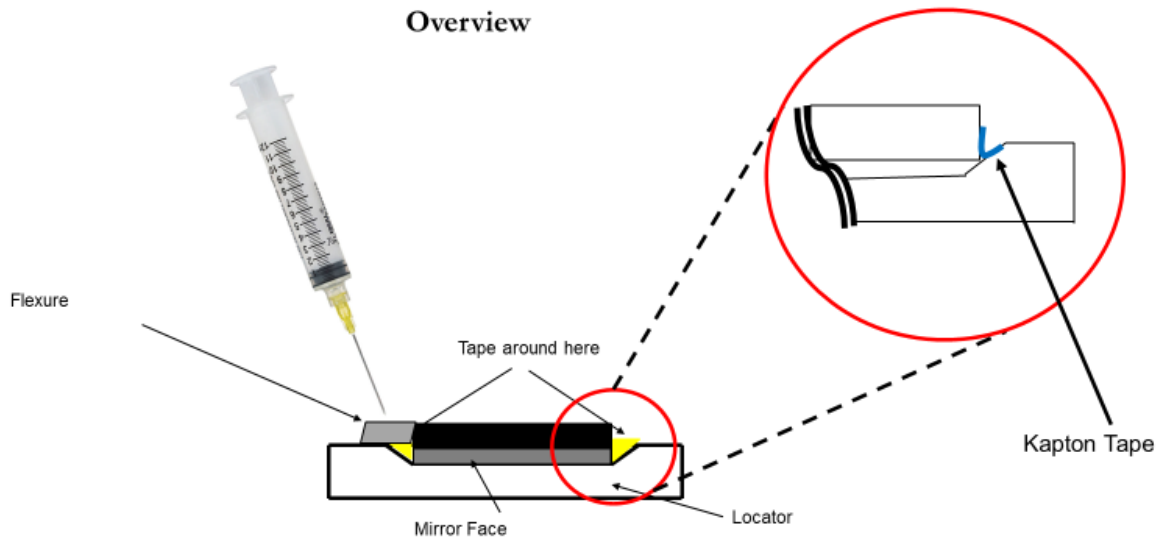
Attach flexures onto T6 block by hand tightening 2.5x0.45 fasteners



Op 30: Epoxy application and flow management



Overview



MU/VI Deployable Cover - October 14, 2019

7

Op 30: Epoxy application and flow management



Mixing and Curing Instructions

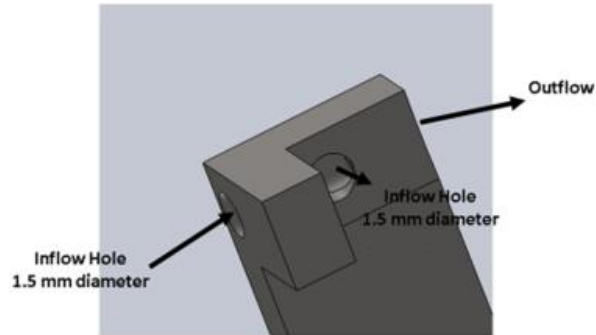
1. Prepare mixing cups, 2-part Hysol 9309 epoxy, applicator syringe, and scale
2. Measure 4 grams of Part A (larger tube) into a mixing cup
3. Measure 0.92 grams of Part B (small tube) into a mixing cup
4. Combine the measured Part B into the cup containing Part A and mix the two components together for 1 minute making sure the epoxy is completely mixed
5. Use the Applicator syringe with 20 gauge needle, load the epoxy into the syringe.
6. Apply small drop of epoxy to nearby cardboard as reference epoxy for timing
7. Apply the epoxy into the flexure flow hole through the syringe and flow until you see some epoxy coming out of bottom, Make sure to look for any unexpected epoxy flow.
8. Repeat epoxy flow for all three flexure epoxy joints
9. Wait for 30 minutes (gel-time from epoxy test case) and check the reference epoxy on the cardboard nearby, if the epoxy is tacky then remove the shims from the flexures (It will be closer to 35-40 minutes for the epoxy to actually be the correct consistency of the epoxy).
10. After 1 hour, carefully move the assembly into the composites lab oven at 180 F for 1 hour to get a complete cure.

MU/VI Deployable Cover - October 14, 2019

8

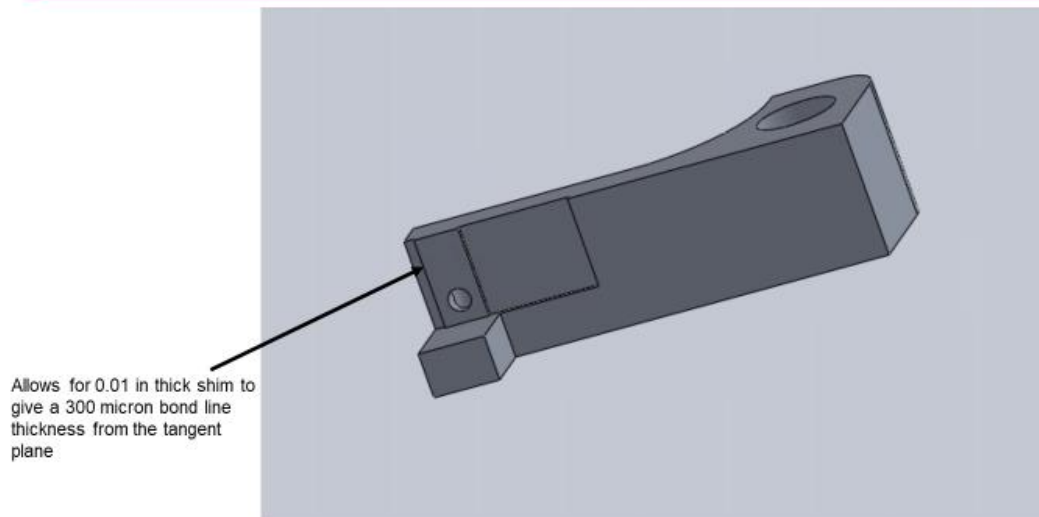
Op 30: Epoxy application and flow management

Flow from Bottom – Configuration 3



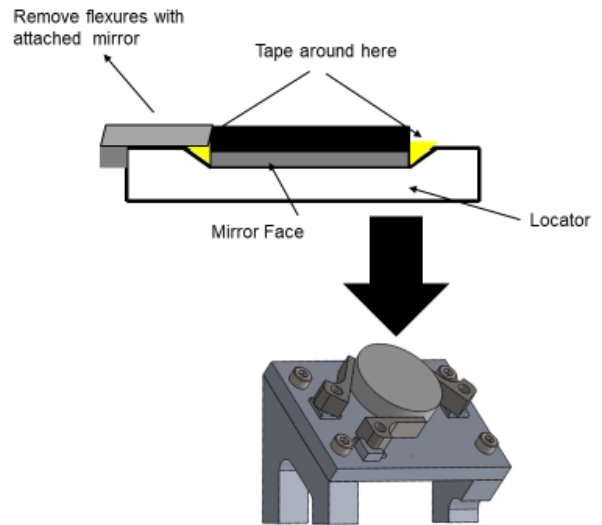
Place cloth/paper towel on outside of outflow hole to catch excess epoxy and use shims on edges to make sure that the epoxy fills the area

Op 30: Epoxy application and flow management



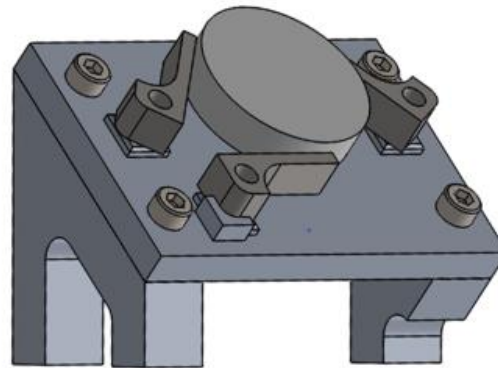
Op 40: Flexure mirror removal and reinstallation

1. Carefully remove bolts from T6 block and carefully remove the flexures with the 1 in mirror attached
2. Place flexures and mirror assembly onto the backing plate without the legs installed.



Op 50: Leg attachment

1. On a level surface, attach both the 1 leg and 2 leg mount onto the back of backing plate with the 4 M3x0.5-12mm Helicoil fasteners. Torque to 3.6 in-lbf





Optical Alignment Test Plan

By: EJ Ranlville, Patrick Whitesel, Jeff Wagner

Sponsor: UC Berkeley Space Sciences Laboratory

MUWI Deployable Cover - October 14, 2019

1

Required Tools and Materials



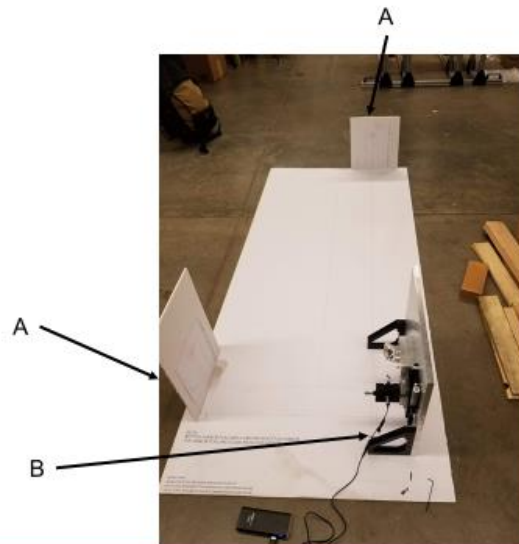
- Polar Plots for both bottom mirror as well as top mirror/laser.
- Table Topper
- GSE with laser mount and battery pack
- Metric Allen Key set

MUWI Deployable Cover - October 14, 2019

2

Step 1: Set Up Alignment Table

- A. Place Polar Placards on Marked Places per Table Topper
- B. Set GSE on Side, Lining Up Back Edge with Lines on Table Topper



MUVI Deployable Cover - October 14, 2019

3

Step 2: Align Laser

- A. Translate Laser to 50.0mm (Maximum Laser Travel)
- B. Adjust the tip/tilt of the laser using the two set screws on the front of the laser mount until the laser points directly at the bullseye in the top right corner of the far polar placard.
- C. Check to make sure that laser is level by moving far side polar placard along optical line scribed in the table topper. The laser should still hit the bullseye no matter the distance from the laser. If it starts deviating one way or another, readjust the tip/tilt of the laser.
 Note: Translation of the laser may be needed by adjusting the micrometers on the laser mount itself, not the translation table.
- D. Repeat until aligned.

Optical Line

Top Mirror Bullseye

Laser Bullseye

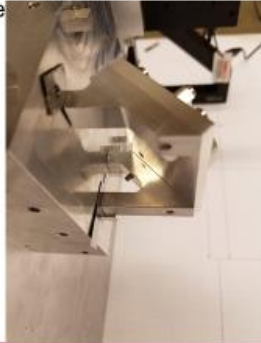


MUVI Deployable Cover - October 14, 2019

4

Step 3: Rough Alignment of Bottom Mirror

- A. Translate laser back down such that it is centered over bottom mirror (estimated to be 3.00mm on table translation micrometer)
- B. Loosen the mounting bolts from GSE legs and iteratively shim legs until laser lines up with bullseye

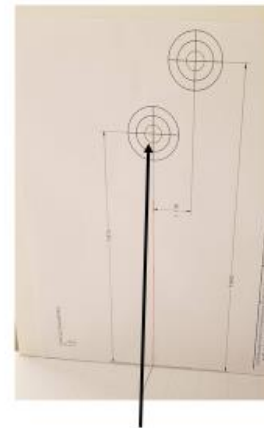


MUVI Deployable Cover - October 14, 2019

5

Step 4: Fine Tuning Dual Mirror System

- A. Remove GSE from side and mount top mirror into system (Hinge towers, mirror with backing plate, and side walls)
- B. Place GSE back on side, aligning it with the corner indicated on the tabletopper.
- C. Translate laser out to 50.00mm to double check laser alignment. Once verified, translate laser back to alignment position (~3.00mm)
- D. Iteratively adjust the lockout flexures for the top mirror assembly and shim under the hinge towers/between the hinge towers and the side wall until tolerable alignment is achieved (as indicated by the green circle on the polar plot)



Inner circle indicates deviation of .25 deg

MUVI Deployable Cover - October 14, 2019

6

Dynamic and thermal analysis of a mirror mount in a CubeSat under launch conditions resulting in high deformation, natural frequency and low thermal stresses

Authors: Edwin Rainville¹, Patrick Whitesel¹

Affiliations: ¹California Polytechnic State University, San Luis Obispo – Mechanical Engineering

Abstract

A finite element model of a mirror mount assembly within a CubeSat is developed and described. The mirror mount assembly consists of a fused silica mirror and three aluminum 6061-T6 flexures, flexible members, that are epoxied to the edges of the mirror with Hysol 9394 aerospace low outgassing epoxy. The model developed includes specific properties for the fused silica mirror and the aluminum 6061-T6 flexures. The epoxy bonds are neglected in the finite element model in order to reduce the complexity of the model and are approximated by tie constraints within the model that tie the surface nodes of the flexures to the surface nodes of the mirror. The mesh for the flexures consists of a seed size of 0.75 on the flexures and a mesh size of 1.375 for the mirror. Both the mesh for the mirror and the flexures consists of quadratic tetrahedral elements to account for the irregular geometry of both components and maintain high accuracy and reasonable computational power for the solution. Three loading scenarios were investigated including a maximum static deflection load, a dynamic load to find the natural frequency and mode shapes, and a thermal model. The maximum static deflection included a pressure over the face of the mirror of 1.91 psi which corresponds to a 100g acceleration of the mirror. During a dynamic analysis, we found the assembly to have a first mode natural frequency of 233 Hz which is high enough for the application since it is required for any structure in a CubeSat to have a first fundamental frequency of 30 Hz or higher. Using the verified model under a thermal analysis, we find low thermal stresses with a maximum stress of 5890 psi at the boundary conditions which is below the yield strength of both fused silica and aluminum 6061-T6. The low stresses caused by thermal loading suggest that the assembly will survive the expected temperature changes within the ionosphere. This analysis will be used to further inform testing methods and inform any possible redesigns necessary for the mirror mount structure to ensure the mirror survives launch and orbit conditions.

Background and Motivation

The earth's auroras (borealis and australis) are a phenomenon that are currently of great interest to space scientists and alike. Previous studies of the auroras have required large scale satellites with accurate coverage but relatively little simultaneous coverage of the earth such as University of California, Berkeley - Space Sciences Laboratory's (UCBSSL) ICON satellite. Now that the technology is developed for the large satellite, we want to develop a smaller scale satellite that will use very similar technology but is simplified. The overall goal of this project is to design a small scale, cost effective solution to map the earth's auroras with multiple deployed small satellites rather than one large satellite to increase map coverage.

As a senior project team at Cal Poly, we have been tasked with taking UC Berkeley Space Sciences Lab's ICON technology and scaling it down into a 2U (20cm x 10cm x 10cm) form factor. The specific portion of this downsizing project that we have been tasked with is the design of a deployable cover and a mirror/mount assembly. As a specification from the optics engineers, the satellite required two mirrors mounted each at 45° in opposing directions for filtering of light as shown in Figure 1a. The mirrors are mounted to the structure using a flexure, flexible member shown in Figure 1b, to reduce stress on the mirror during launch and orbital vibration which is what will be studied during this project¹.

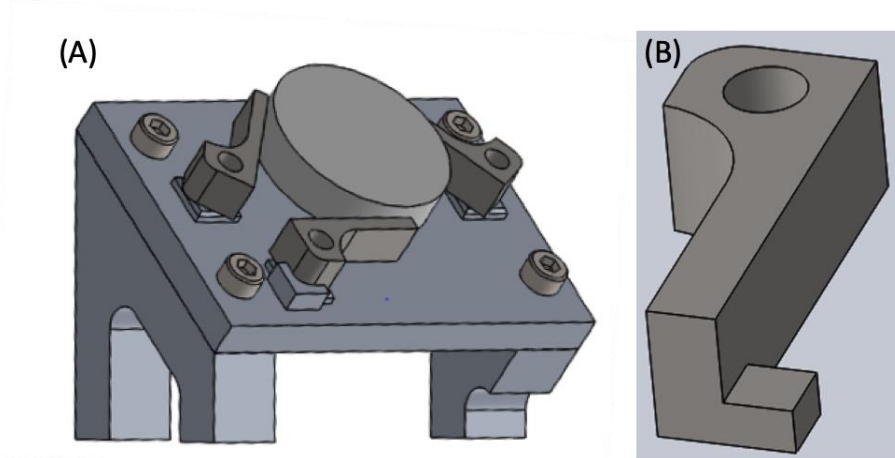


Figure 1. (A) Overall structure of the FUV imager CubeSat, showing the upper and lower mirror mounts. Mirrors are attached to the structure via flexure. (B) Lower mirror mount flexure.

The main motivation for this study is that many components in satellites require some type of vibration and thermal stress isolation, especially in optics designs, however, there are no clear guidelines for the design of these types of components and how they behave in launch and orbital conditions. Due to the necessity of this type of design in aerospace applications and the lack of resources surrounding this type of design, we intend to define a model that will inform this design for both our project and for others in the future.

Hypothesis

In order to define a simplified model of the mirror flexure to find an approximate range of solutions, we modeled the flexure as a simple cantilever beam with the major dimensions of the flexure which are 0.787 in. long, 0.07. wide and 0.24 in. thick. The original design was based on being a simple cantilever beam but additional features were added to allow for correct epoxy bonding to the mirror and holes for mounting to the backing plate. Since the load from the mirror is split amongst the three flexures, we assume for the simplified model that the flexure takes approximately 1/3 of the load from the mirror as a conservative estimate rather than splitting the load in exactly even thirds. The dynamic load on the flexure is 0.5 lbf for a 100g acceleration of the mirror and the temperature range is approximately 32-104°F. Under the dynamic load case, we expect the mirror flexure to have a maximum deflection of approximately 1.008×10^{-4} in. based on Euler-Bernoulli elastic beam theory with hand calculations attached in attachments 1 and 2. We also expect to see a first fundamental frequency at approximately 205.8 Hz using the bending stiffness of the cantilever beam model and the effective mass of the 100g acceleration of the mirror.

Model Development

The flexure-mirror assembly model was developed according to standard practices for performing FEA on structural parts at UCBSSL. The standard procedure is to create a static model with loading representing 100 times the structure mass times the acceleration of gravity. This is what the lab uses as the static representation of the maximum dynamic loading during space flight. The geometry was modeled in Solidworks and imported into Abaqus as a .step file. In the static loading case, we decided to load the face of the mirror with a pressure load to approximate the 100g acceleration that we expect the mirror to

experience. The pressure applied to the face of the mirror was 1.91 lbf/in^2 which is calculated using the mass of the mirror, the area of the face of the mirror, and the 100g acceleration as shown in Attachment 1. In order to approximate the deformation of the flexures, we made a simplified model of the flexure as a cantilever beam with slightly simplified geometry, and then solved for the maximum deflection in the flexure. Then, the analytical model could be compared to the finite element model to validate the finite element model. The beam theory calculation resulted in a maximum deflection of 1.008×10^{-4} in which the finite element model resulted in a maximum deflection, averaged between the three flexures, of 6.6×10^{-4} in. The finite element deflection differed from the expected, simplified model however is on the same order of magnitude, and is a very small deflection. While the finite element model agrees with the simplified model, we will need more experimental data to further fully verify the finite element model for future analyses. For the purposes of this study, we will assume that since the simplified analytical model and the finite element model agree, the finite element model is representing the expected scenario.

The boundary conditions on the mirror consist of pin connections on the inner surfaces of the flexure bolt holes which do not allow for any deflection of the surfaces or rotations about the minor axis of the bolt, however, rotation is allowed about the major axis of the bolt hole. In order to model the mass participation of the fused silica mirror we assembled the mirror with the three flexures bonded to the outer mirror surface through tie constraints. The tie constraints bind the nodes from the flexures to the mirror, effectively modeling a rigid connection between the two surfaces in a similar fashion to the actual epoxy bond that will combine the flexures to the mirror.

All material properties will be defined as homogeneous and isotropic. The flexures are made out of aluminum 6061-T6 and will be modeled with an elastic modulus of 10,000 ksi and a Poisson's ratio of 0.33. The mirror is fabricated out of fused silica which will be modeled with an elastic modulus of 10,590 ksi and a Poisson's ratio of 0.17^[2]. For the dynamic model, the densities of Fused Silica and 6061-T6 were input into the model as 2.06×10^{-4} and $2.52 \times 10^{-4} \text{ lbf*s}^2/\text{in}^4$ respectively. The coefficient of the thermal expansion for fused silica is $1 \times 10^{-6} \text{ }^\circ\text{F}^{-1}$ and the coefficient of thermal expansion is $10.31 \times 10^{-6} \text{ }^\circ\text{F}^{-1}$ ^[2].

Mesh Development and Convergence

In order to develop a reasonable finite element model, we needed to develop a well-defined and effective mesh for the model of the mirror and flexure subassembly. The best element type for this model was a quadratic tetrahedral due to the high accuracy we wanted to achieve as well as the irregular geometry of the flexures and mirror. Hexahedral elements were not able to be generated with the irregular geometry our model. Since the main goal of this project is to determine the deflection of the flexures, we developed the mesh for the flexures with two convergences studies. The first convergence study, shown in Figure 2a, was for the flexure with a pressure load applied to the foot of the flexure. The second convergence study, shown in Figure 2b, was for the flexure loading applied to the face of the flexure in the transverse direction of the flexure.

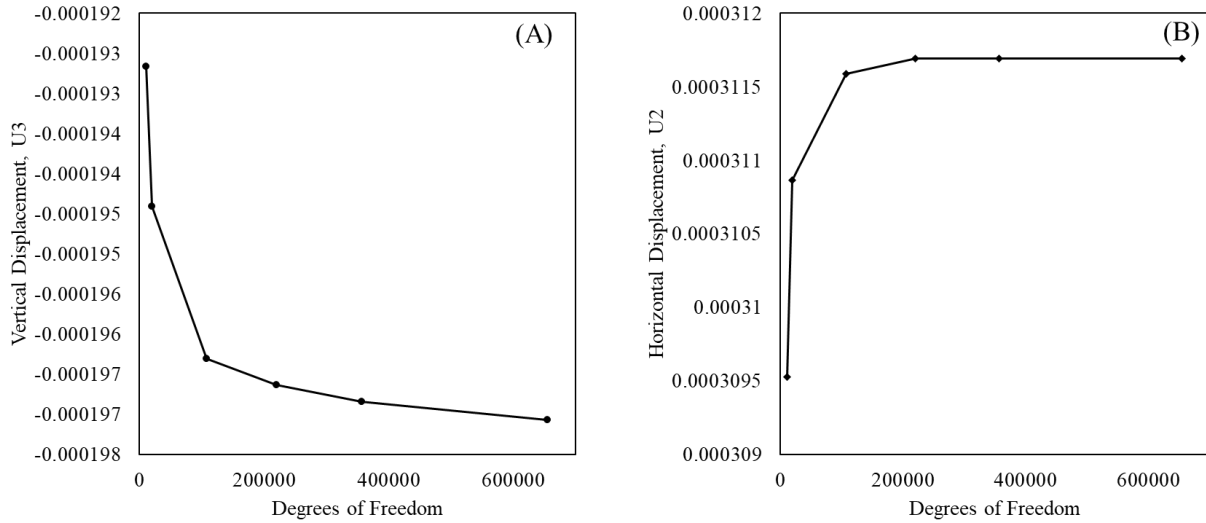


Figure 1. Mesh convergence study on flexure component for downward and transverse load applied to foot and the face of the flexure

The mesh for this flexure model converged to a solution at approximately 150,000 degrees of freedom which corresponds to a seed size of approximately 0.5.

The mesh size for the mirror was less crucial than that of the flexures and thus we decided upon a courser mesh to improve the computation time of the model. A convergence study for the mirror was computed by fixing one side of the mirror and applying a pressure of 2 psi to the face of the mirror resulting in the convergence study shown in Figure 2.

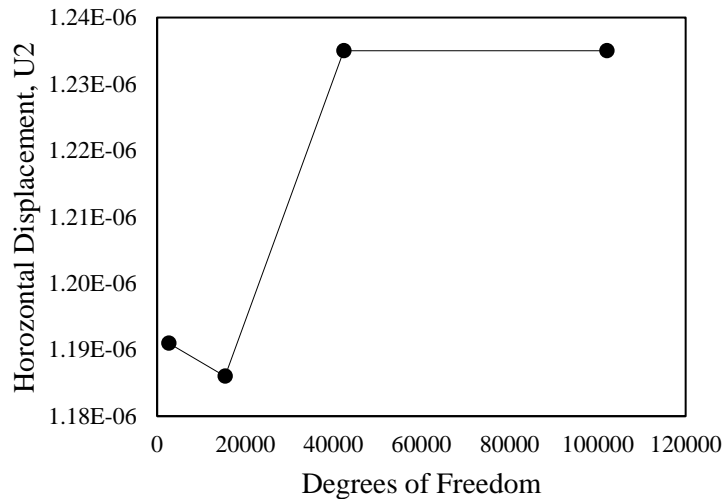


Figure 2. Convergence study to develop mesh size necessary for the mirror using a uniform pressure of 2 psi applied to the face of the mirror and the back of the mirror completely fixed.

The mesh we decided upon for the mirror was had a seed size of 1.375 based on the convergence study which corresponded to approximately 37,000 degrees of freedom which is on the low end of the convergence zone; however due to computational constraints we were required to run less degrees of freedom in the overall model. After attempting to solve the fully assembled model with all four components and tie constraints with the desired mesh size for all the components, the model required more computational power than the lab computers could offer, and the job was aborted. In order to solve

this problem, we reduced the mesh density and used a seed size of 0.75 which is still within the converged range for the flexure models, shown in Figure 2 but is on the lower end of the converged range. The final mesh that was used in the rest of the model used quadratic tetrahedral elements for both the mirror and flexures, where the mirror mesh has a seed size of 1.375 and the flexures have a mesh size of 0.75. This mesh resulted in 153,318 degrees of freedom and 31,894 elements in the model. There were no distorted elements in this model and all elements met minimum and maximum angle and aspect ratio criteria. Therefore, we decided the mesh was of high enough quality to proceed.

Analysis

Once the correlation was made between the hand calculation and static model, the dynamic representation of the loading could be implemented into Abaqus. The Lanczos eigensolver was used in the model which allowed us to compute the first 30 modes of vibration through a spectral transformation. It is important to note that the eigensolver used in the analysis can only be used to determine simple eigenvalues, which is appropriate for our application since loading is generally in the principal directions. In addition, the Lanczos solver was used to visually display the approximate mode shapes of the geometry. These modal shapes help us understand the mass participation of the flexure-mirror assembly.

A thermal model was also formed upon convergence and correlation of the static model. Unlike the static or dynamic model, the thermal FEA contained no pressure loading on the mirror face. The only loading on the assembly was the thermal temperature variation which was separated into two cases: temperature change from 104°F to 32°F, and vice versa to see if there were any hysteresis effects of thermal loading on the mirror. The goal of the thermal model was to understand the stresses within the structure caused by a large temperature change as expected during launch and orbital conditions. Understanding stress concentrations and stress magnitudes inform us of whether or not the mirror will survive the hostile conditions it will be subjected to.

A few warnings were observed in the dynamic model which are worth noting. When the model ran, a number of nodes were outside of the specified range of the three tie constraints, producing a warning. This warning is a concern as the number of nodes within the tie constraints was much greater than the number outside of the range. Another warning received in the dynamic analysis was the required history output request for the Lanczos solver was not specified. This warning was easily corrected with modifying the history output request.

Results

Under the dynamic loading case, we solved for the vibration modes and corresponding natural frequencies of the assembly and found that the first mode natural frequency occurred at 233 Hz which differed from the hand calculated natural frequency of a flexure by 13.6%. The natural frequency of the full assembly was higher than that of the hand calculations since the overall assembly is expected to have a higher stiffness than a single flexure. The first 5 modes of the mirror mount assembly were calculated and then tabulated in Table 1.

Table 1. Mirror mount assembly vibration mode and corresponding natural frequency of the mode.

Mode Number	FE Mode Frequency [Hz]	Analytical Mode Frequency [Hz]	Difference [%]
1	233	206	13.1
2	300	1289	76.7
3	416	3612	88.5
4	472		
5	562		

The frequency of each successive mode is significantly above the required minimum natural frequency for CubeSat hardware. Modal shapes were extracted and examined in the dynamic model. In order to further verify this model, we will want to eventually test the mirror mount structure to compare actual modal frequencies to the modeled; however, this study will provide a preliminary estimation for the expected natural frequencies to inform testing procedures.

In the thermal model, the maximum stresses for the cool down and heat up models were found to be 40 ksi and 60 ksi, respectively. The maximum stresses were found to be at the location of the applied boundary conditions. These stress locations are concerning for the validity of the model as the boundary conditions could be causing a stress concentration.

Discussion

A sufficient correlation was found between the static finite element model and analytical calculation. While the group wanted a stronger correlation with the static model, the more complicated dynamic model was developed for quantitative and qualitative purposes. From the dynamic model, the modal shapes could be extracted and examined qualitatively. Figure 3 highlights the first four mode shapes of the structure. With this figure, we can be more informed on possible failure modes upon frequency excitation upon launch. There appears to not be any concerning shapes which would cause failure to the geometry. The shapes appear to be fairly uniform in nature allowing for even weight distribution of the mirror.

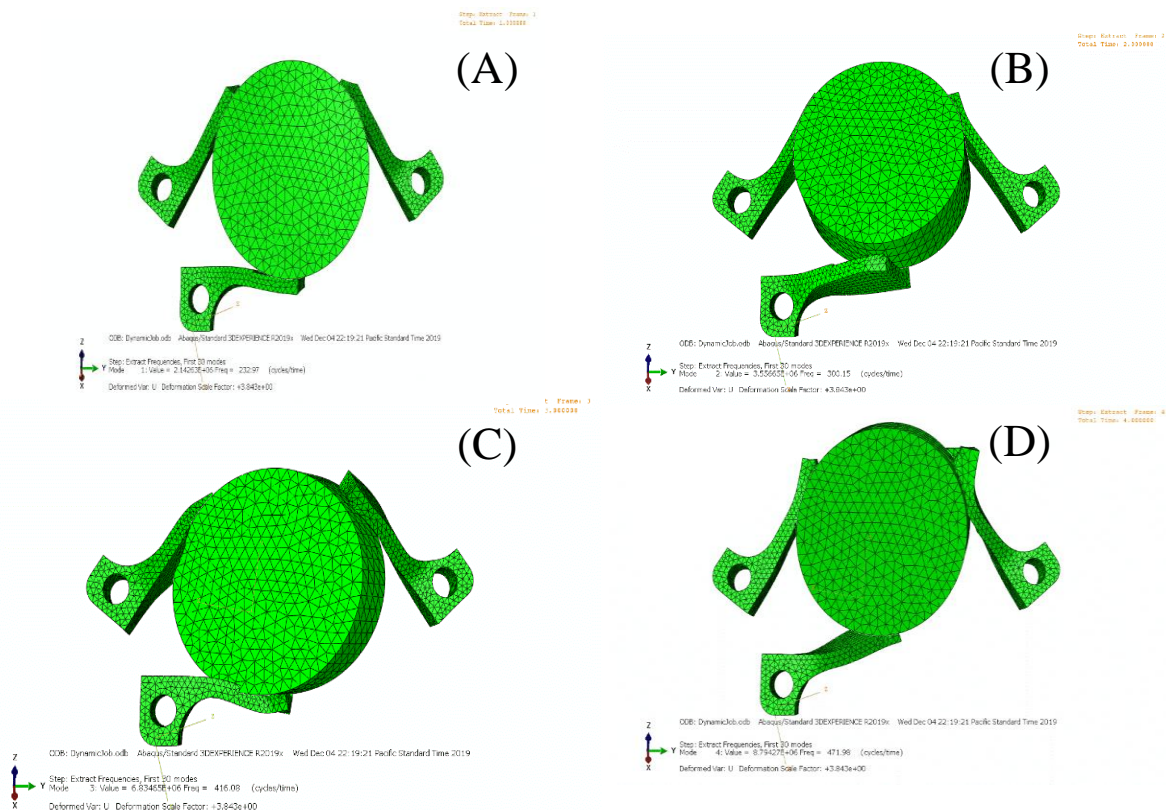


Figure 3. Mode shapes of the mirror assembly under the dynamic loading scenario (A) first mode, (B) second mode, (C) third mode, and (D) fourth mode where the scale factor on the analysis is 3.843 and the material properties and model characteristics defined previously.

There is a slight discrepancy between the computed and analytical fundamental frequencies within the study. Large contributing factors to this discrepancy is the complicated modeled geometry and the lack of experimental data. Since the geometry was very complicated, it proved to be difficult to match a simplified analytical model which contained similar boundary conditions and loading. Experimental vibration data would have been excellent in authenticating the fundamental frequency of the complex assembly, but no previous work was able to be leveraged in this study. With experimental data, the quality of the model could be verified.

Using the statically verified model conditions, we changed the loading condition to a thermal study where the mirror mount assembly was heated from 32°F to 104°F and then cool over the same temperature range. The thermal stress under this loading scenario are concentrated at the bolt holes for the mirror mount as shown in Figure 4.

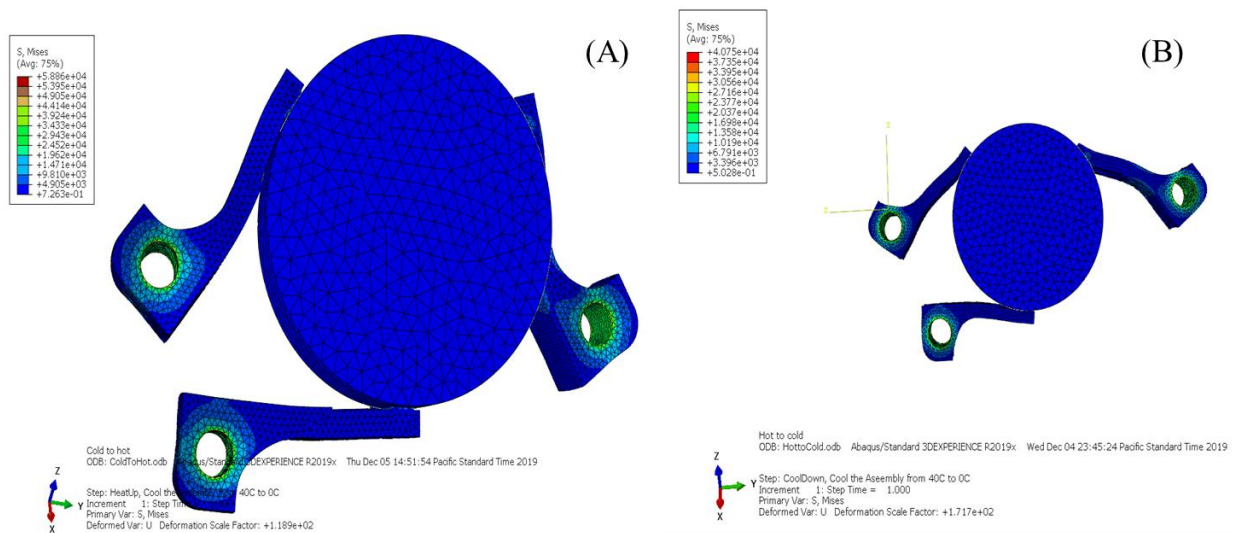


Figure 4. Thermal stresses on the mirror mount assembly during (A) heating up and (B) cooling down of the assembly between 32-104°F. The scale factor for these images is 171.

This result is convoluted since we expect the bolt holes to have stress concentrations but we are not able to decouple this result from the potential that the model boundary conditions are causing extra stress concentrations in this region. Since we verified this model statically and there were no stress concentrations present at the boundary conditions we assume that this model is representative of the true loading scenario. There is a hysteresis effect on the mirror mount assembly cooling and heating where higher stresses occur during the heat up process; however, both stresses were highly comparable. These results will help to inform the testing procedures to look for potential hysteresis effects and thoroughly investigate the stresses at the bolt holes to further verify.

Conclusion

During a dynamic analysis we found the assembly to have a first mode natural frequency of 233 Hz which is well above the required minimum natural frequency for a CubeSat structure. Using the verified model under a thermal analysis, we find low thermal stresses with a maximum stress of 5890 psi which is below the yield strength of both fused silica and aluminum 6061-T6 and the stresses were located at the bolt holes on the aluminum during the thermal loading. The low thermal stresses suggest

that the assembly will survive the expected temperature changes within the ionosphere. Further model development could be made with vibrational test data or a more sophisticated analytical model. This analysis will be used to further inform testing methods and inform any possible redesigns to the mirror mount structure.

Broader Impacts

Many aerospace applications require stress and vibration isolation to structural members; however, there are no clear guidelines for the design and performance of these types of members. This study will be used to inform UCB-SSL and the larger aerospace community on the performance of a flexible member used to mount optics and sensitive elements and the performance of the flexure under launch and orbital conditions.

Attachments

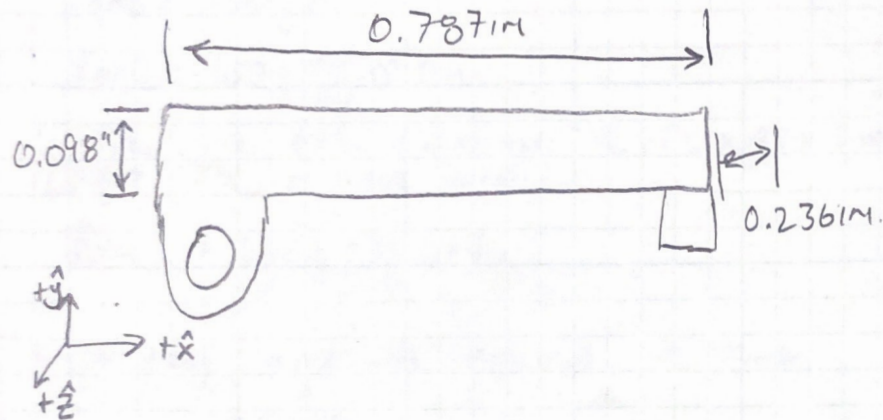
- [1] Hand Calculations for Flexure Maximum Deflection
- [2] MATLAB hand Calculation code for maximum deflection and natural frequency

References

- [1] Vukobratovich et al. 1988, *Optomechanical and Electro-Optical Design of Industrial System*
- [2] “Young's Modulus - Tensile and Yield Strength for Common Materials.” *Engineering ToolBox*, www.engineeringtoolbox.com/young-modulus-d_417.html.
- [3] Israr, Asif. (2014). Vibration and Modal Analysis of Low Earth Orbit Satellite. *Shock and Vibration*. 2014. 8. 10.1155/2014/740102.

SIMPLIFIED FLEXURE MODEL.

SCHEMATIC / MODEL:



DIMENSIONS OF MIRROR:

$$L_f = 0.7871 \text{ IN}$$

$$W_f = 0.098 \text{ IN}$$

$$t_f = 0.2361 \text{ IN}$$

ASSUMPTIONS FOR MODEL:

1. ISOTROPIC MATERIALS
2. MIRROR LOAD IS TAKEN EVENLY BY FLEXURES.
3. CONSTANT CROSS-SECTIONAL AREA

ANALYSIS:

STATIC LOAD CASE,

THE EXPECTED LOAD IS AT AN ACCELERATION OF $100g$ ON THE MIRROR WHICH IS COMMON DURING A ROCKET LAUNCH.

FIRST CALCULATE THE MASS OF THE MIRROR,

$$M_m = \rho V_{ol}$$

$$M_m = \rho \frac{\pi}{4} D^2 t_m \quad (\text{EQ. 1})$$

CONT'D

(STATIC LOAD CONT'D)

NOW WE WANT TO FIND THE 100g LOAD,

$$\text{LOAD} = 100 \text{ gm}$$

$$\text{LOAD} = 100 \text{ g} \frac{\pi}{32} D^2 t_m$$

SINCE WE ARE ASSUMING THE FLEXURES EQUALLY CARRY THE MIRROR LOAD,

$$\text{LOAD}_F = \frac{100}{3} \text{ g} \frac{\pi}{32} D^2 t_m$$

FROM CODE IN MATLAB ATTACHED WE FIND,

$$\text{LOAD}_F = 0.5002$$

FOR THE SIMPLIFIED MODEL OF THE FLEXURE WE WILL ASSUME THE FLEXURE IS A SIMPLE CANTILEVER BEAM AND WE WILL USE EULER-BERNOULLI BEAM THEORY TO ESTIMATE THE TIP DEFORMATION,

$$\delta_F = \frac{FL^3}{3EI}$$

WE WILL THEN ASSUME THE CROSS SECTION OF THE FLEXURE IS CONSTANT, WHICH IT MOSTLY IS, THUS,

$$I = \frac{bh^3}{12} \quad \text{WHERE } b = 0.098 \text{ IN, } h = 0.236 \text{ IN}$$

USING THESE CALCULATIONS IN MATLAB, WE FIND,

$$\delta_F = 1.008 \times 10^{-4} \text{ IN.}$$

Flexure Load and FEA Hand Calculations

Written by: Edwin Rainville, Patrick Whitesel

```
clear all, close all, clc

% Define Constants
g = 32.2;           % Gravitational Constant, units are ft/s^2
rho_fs = 2.202;    % Density of Fused Silica, Units are g/cm^3
rho_al = 0.1;      % Density of Aluminum, Units are lbf/in^3
D_m = 1;           % Diameter of the Mirror, Units are Inches
t_m = 0.24;        % Thickness of the Mirror, Units are Inches
g2slug = 1/14593.9; % Conversion from grams to slugs
in32cm3 = 2.54^3;  % Conversion from cubic inches to cubic cm

% Define Flexure Properties
L = .787 ;         % Length of the Flexure, units are in
b = 0.07;          % Thickness of the flexure, units are in
h = 0.24;          % Width of Flexure, units are in
I_f = b*(h^3)/12; % Moment of Intertia of Cross Section
E = 10000000;     % Elastic Modulus of Aluminum 6061-T6

% Calculate Load of Flexure
Load_m = (100)*g*rho_fs*(pi/4)*D_m^2*t_m*g2slug*in32cm3;
Load_f = Load_m/3;
A_m = pi/4*D_m^2;
Load_press = Load_m/A_m;

% Calculate Deformation at Tip of Flexure
delta_f = Load_f*L^3/(3*E*I_f); % Deformation of tip of the
flexure

% Natural Frequency of Cantilever Beam
freq_f = (1/(2*pi))*1.875^2*sqrt((E*I_f)/((Load_f/g)*L^4));

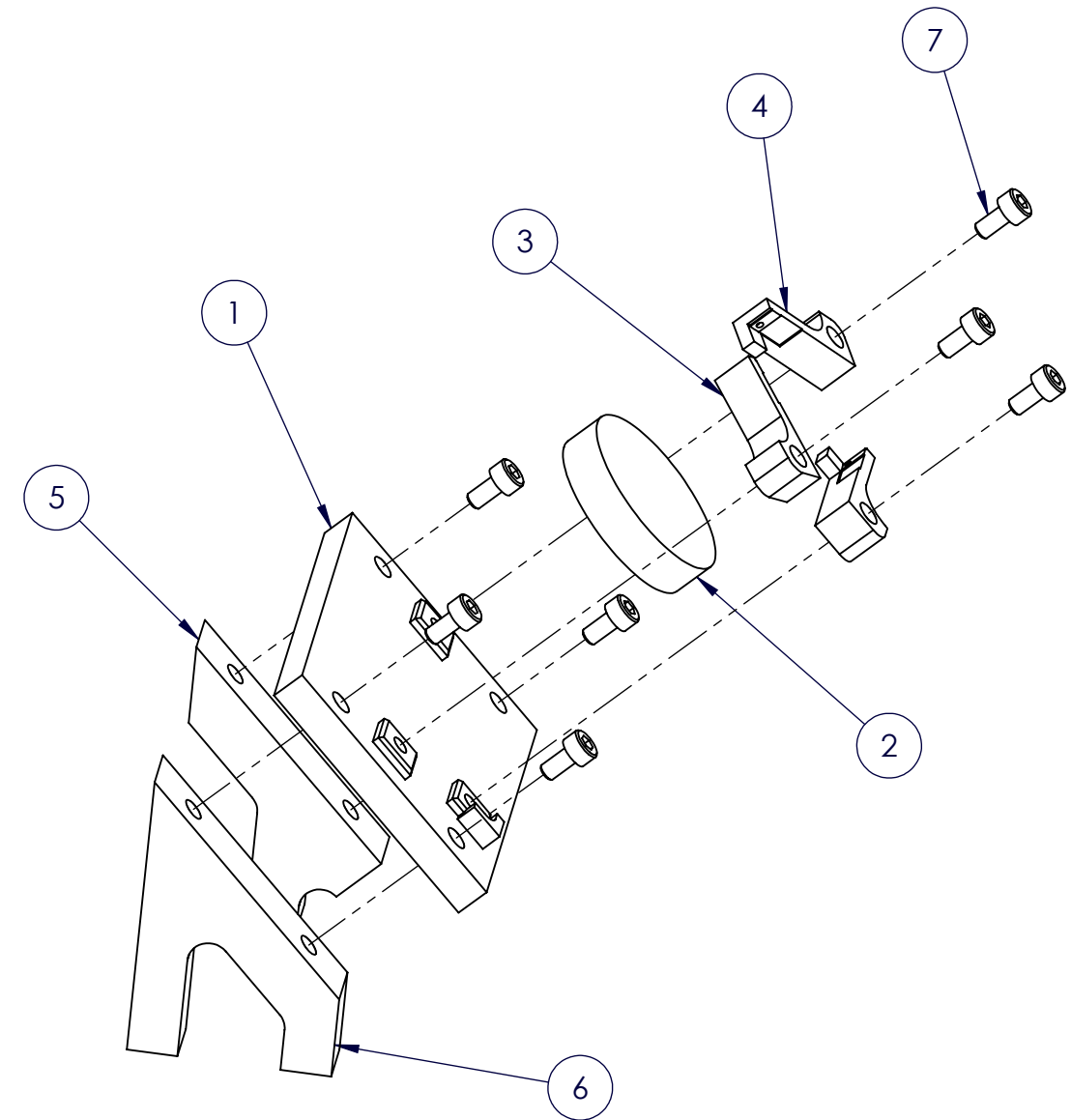
% Stiffness of Flexure
k_f = Load_f/delta_f; % Linear Spring stiffness assumption
k_eff = 3*k_f; % Three flexure springs in parallel
freq_assembly = (1/(2*pi))*sqrt(k_eff/(Load_m/g));

% Determine Average Deflection for dynamic load
delta_f_fea = [ 6.10, 5.87, 7.83]*10^-4;
delta_f_fea_avg = mean(delta_f_fea);
delta_f_diff = (delta_f- delta_f_fea_avg)/delta_f *100;
```

Published with MATLAB® R2019a

NOTES, UNLESS OTHERWISE SPECIFIED:

1. MATERIAL: ALUMINUM 6061-T651 PER AMS 4027 AND AMS 4150. FOR OTHER MATERIALS, SEE BOM.
2. BREAK EXTERNAL EDGES AND CORNERS .005 IN MAX UNLESS NOTED.
3. INTERNAL CORNER AND FILLET RADII .005 MAX UNLESS NOTED.
4. INSTALL HELICAL COIL INSERT PER NASM33537. REMOVE TANG.
5. DRAWING IS THE SOLE AUTHORITY FOR THE BASIC FORM, LOCATION, ORIENTATION, AND DIMENSIONAL CHARACTERISTICS OF ALL DESIGN FEATURES.

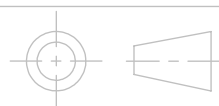


CUBE-DC-101000

ITEM NO.	PART NUMBER	DESCRIPTION	MATERIAL	QTY.
1	CUBE-DC-101001	BACKING PLATE	6061-T6 (SS)	1
2	CUBE-DC-101002	BOTTOM MIRROR, 1 INCH, THORLABS	FUSED SILICA	1
3	CUBE-DC-101003	LEFT FLEXURE FLOW FROM BOTTOM	6061-T6 (SS)	1
4	CUBE-DC-101004	BOTTOM FLEXURE FLOW FROM BOTTOM	6061-T6 (SS)	2
5	CUBE-DC-101005	ONE LEG MOUNT	6061-T6 (SS)	1
6	CUBE-DC-101006	TWO LEG MOUNT	6061-T6 (SS)	1
7	B18.3.1M - 2.5 x 0.45 x 5 Hex SHCS -- 5NHX			7

UNLESS OTHERWISE SPECIFIED:
 DIMENSIONS ARE IN INCHES
 TOLERANCES:
 FRACTIONAL $\pm 0.5^\circ$
 TWO PLACE DECIMAL ± 0.005
 THREE PLACE DECIMAL ± 0.0025

INTERPRET DRAWING
 PER ANSI Y14.5 2009



CAL POLY
SAN LUIS OBISPO

MATERIAL:
 SEE BOM

DRAWN BY:
 PATRICK WHITESEL

TITLE:
 BOTTOM MIRROR ASSEMBLY

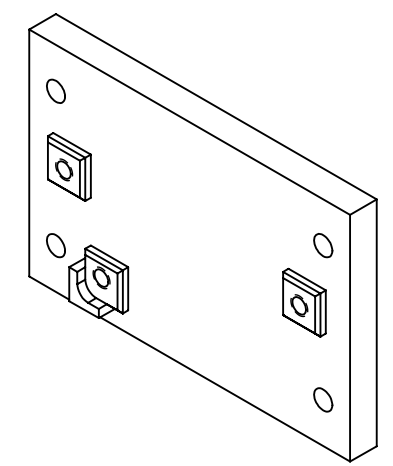
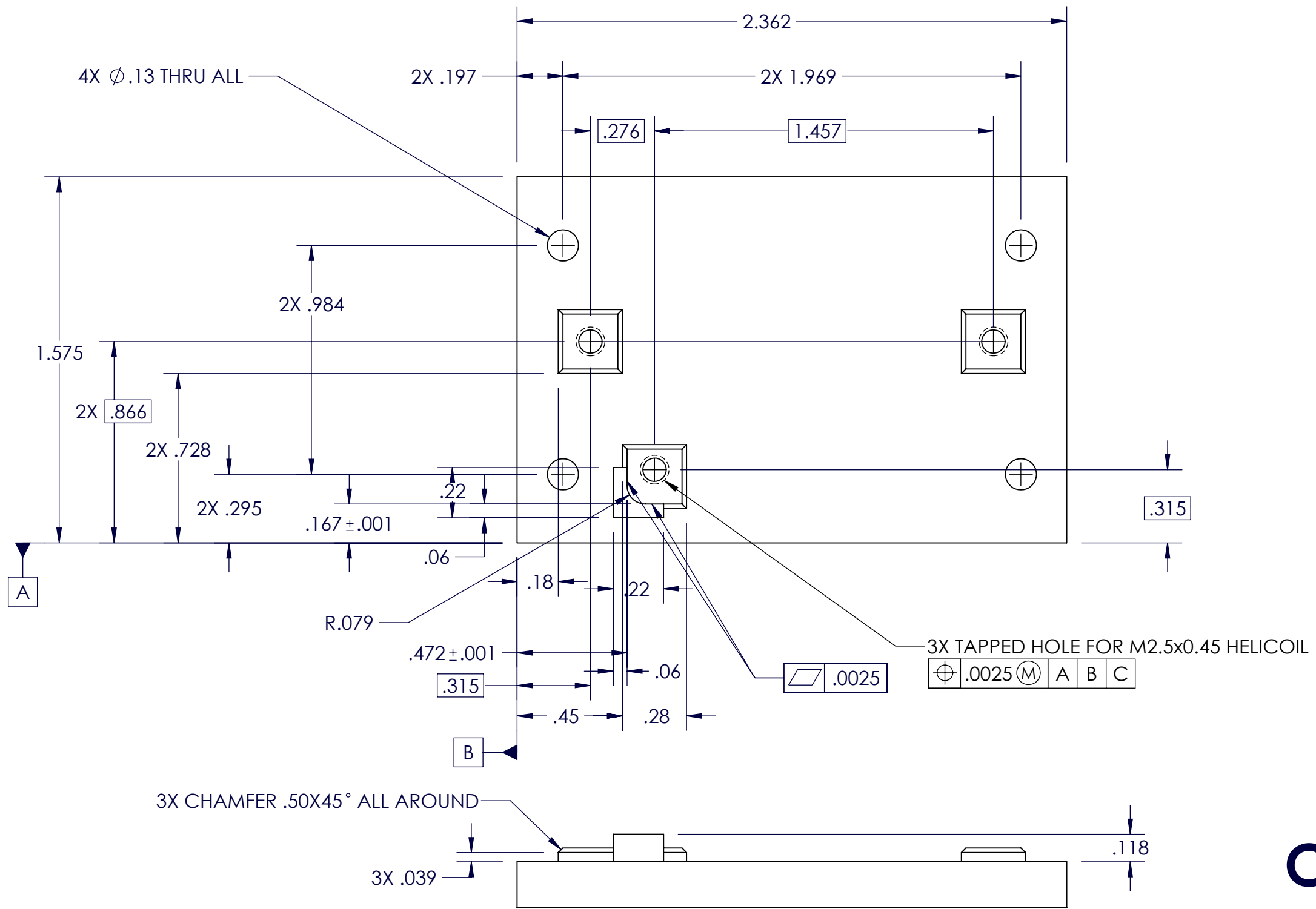
DATE:
 06-02-19

SHEET 1 OF 5

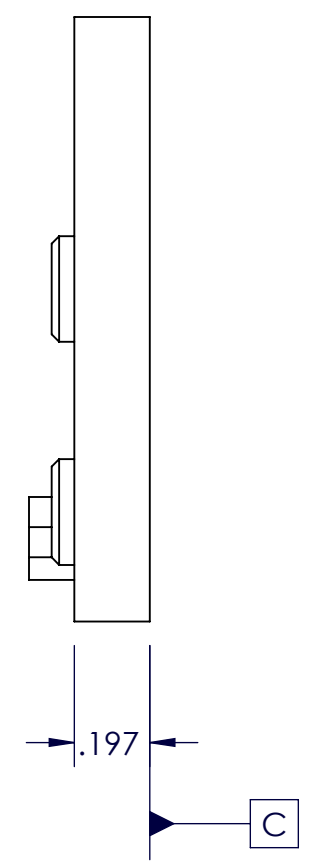
SCALE: 1:1

REV

SIZE
B

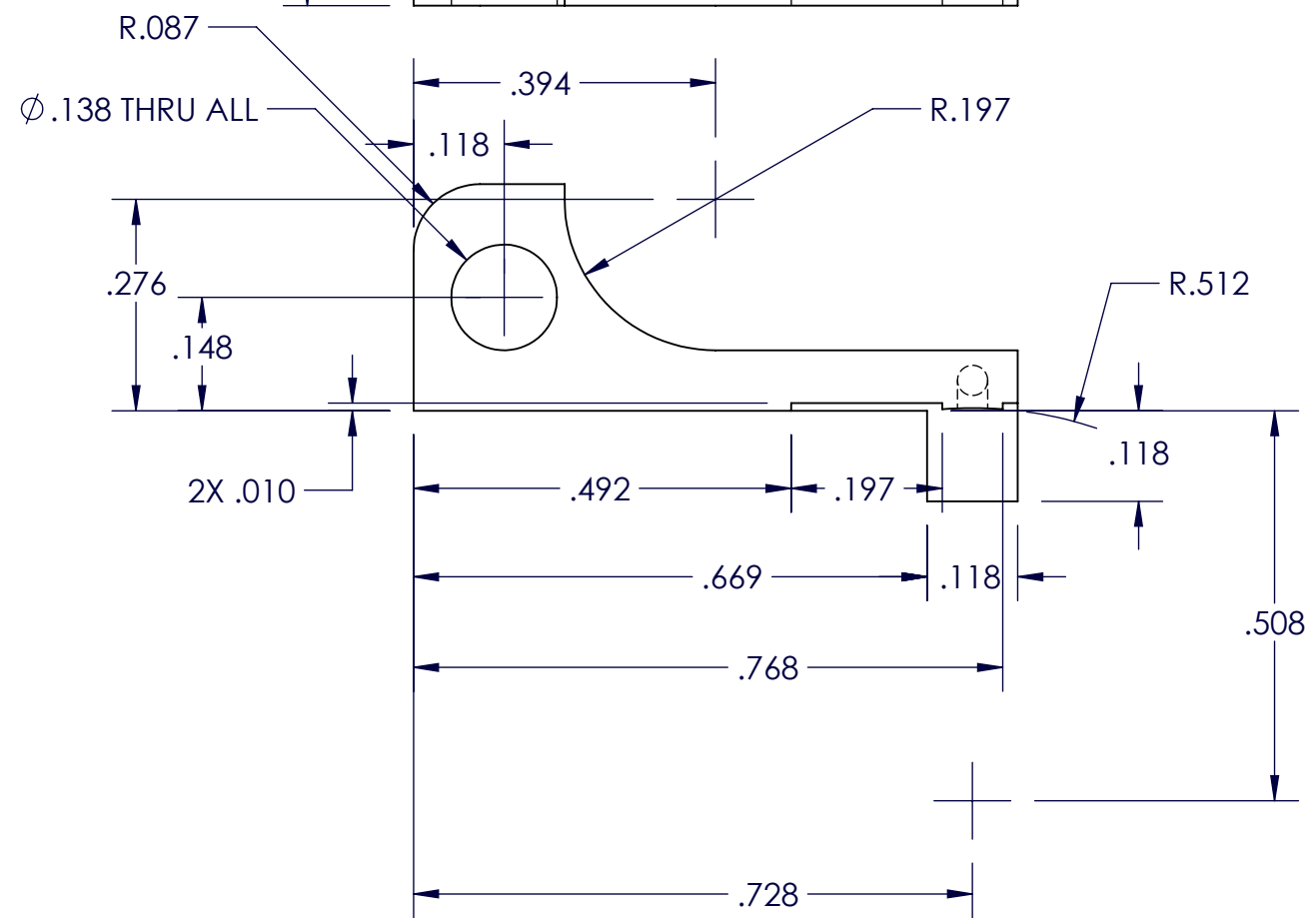
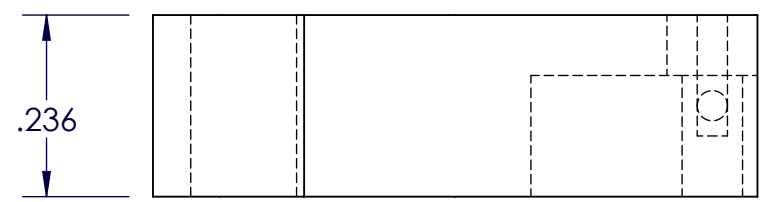
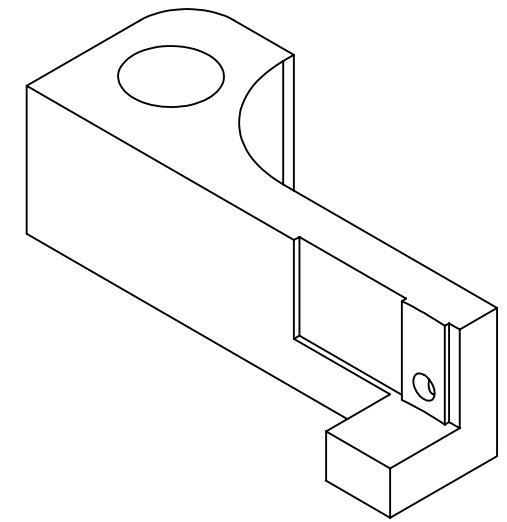
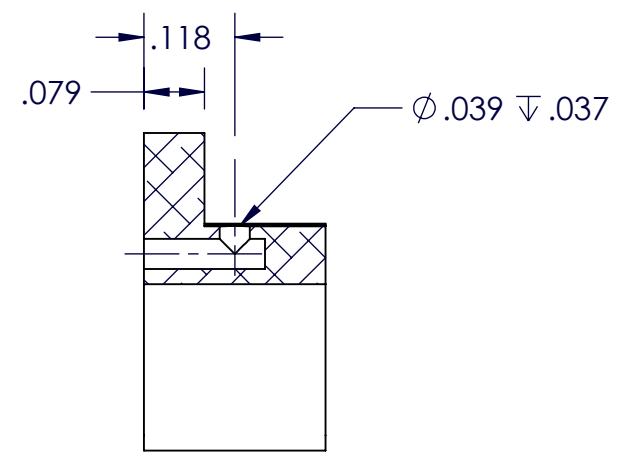
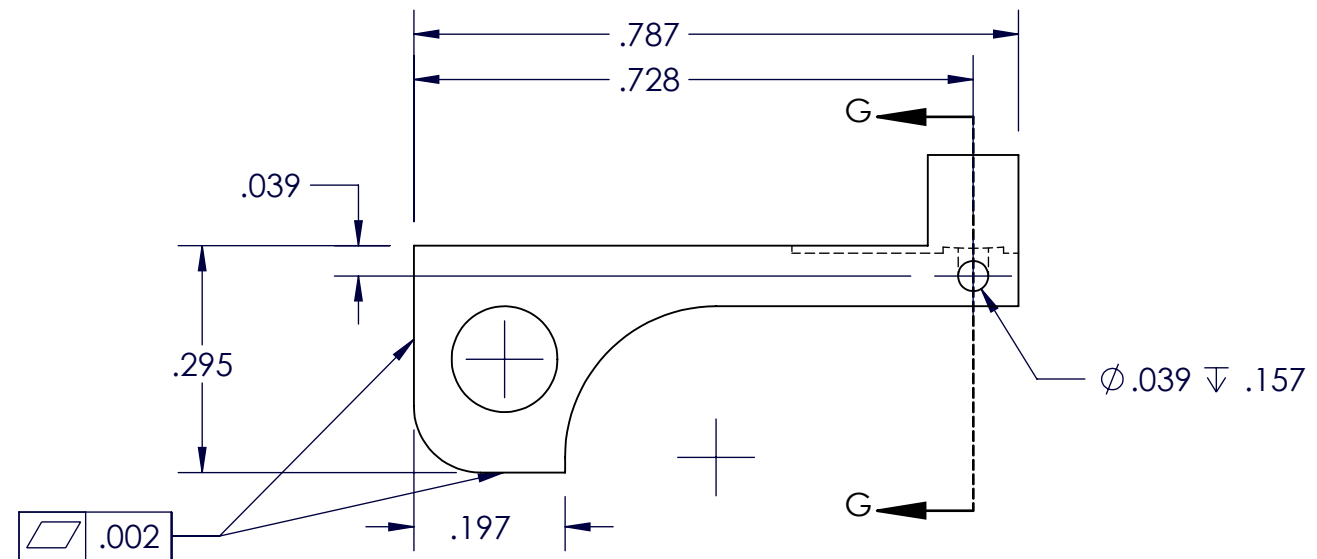


SCALE: 1:1



CUBE-DC-101001

UNLESS OTHERWISE SPECIFIED: DIMENSIONS ARE IN INCHES TOLERANCES: FRACTIONAL \pm 0.5° TWO PLACE DECIMAL \pm 0.005 THREE PLACE DECIMAL \pm 0.0025	INTERPRET DRAWING PER ANSI Y14.5 2009		MATERIAL: SEE BOM	TITLE: BACKING PLATE		SHEET 2 OF 5	SCALE: 2:1	REV	SIZE B
			DRAWN BY: PATRICK WHITESEL	DATE: 06-02-19					



CUBE-DC-101003

UNLESS OTHERWISE SPECIFIED:
 DIMENSIONS ARE IN INCHES
 TOLERANCES:
 FRACTIONAL ± 0.5°
 TWO PLACE DECIMAL ± 0.005
 THREE PLACE DECIMAL ± 0.0025

INTERPRET DRAWING
 PER ANSI Y14.5 2009

CAL POLY
SAN LUIS OBISPO

MATERIAL:
 SEE BOM
 DRAWN BY:
 PATRICK WHITESEL

TITLE:
 BOTTOM LEFT FLEXURE

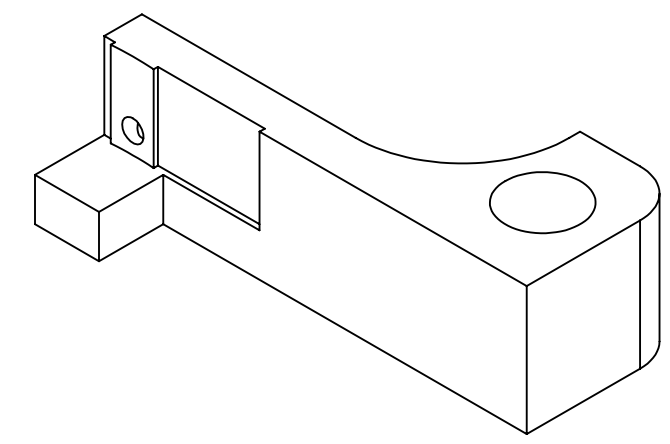
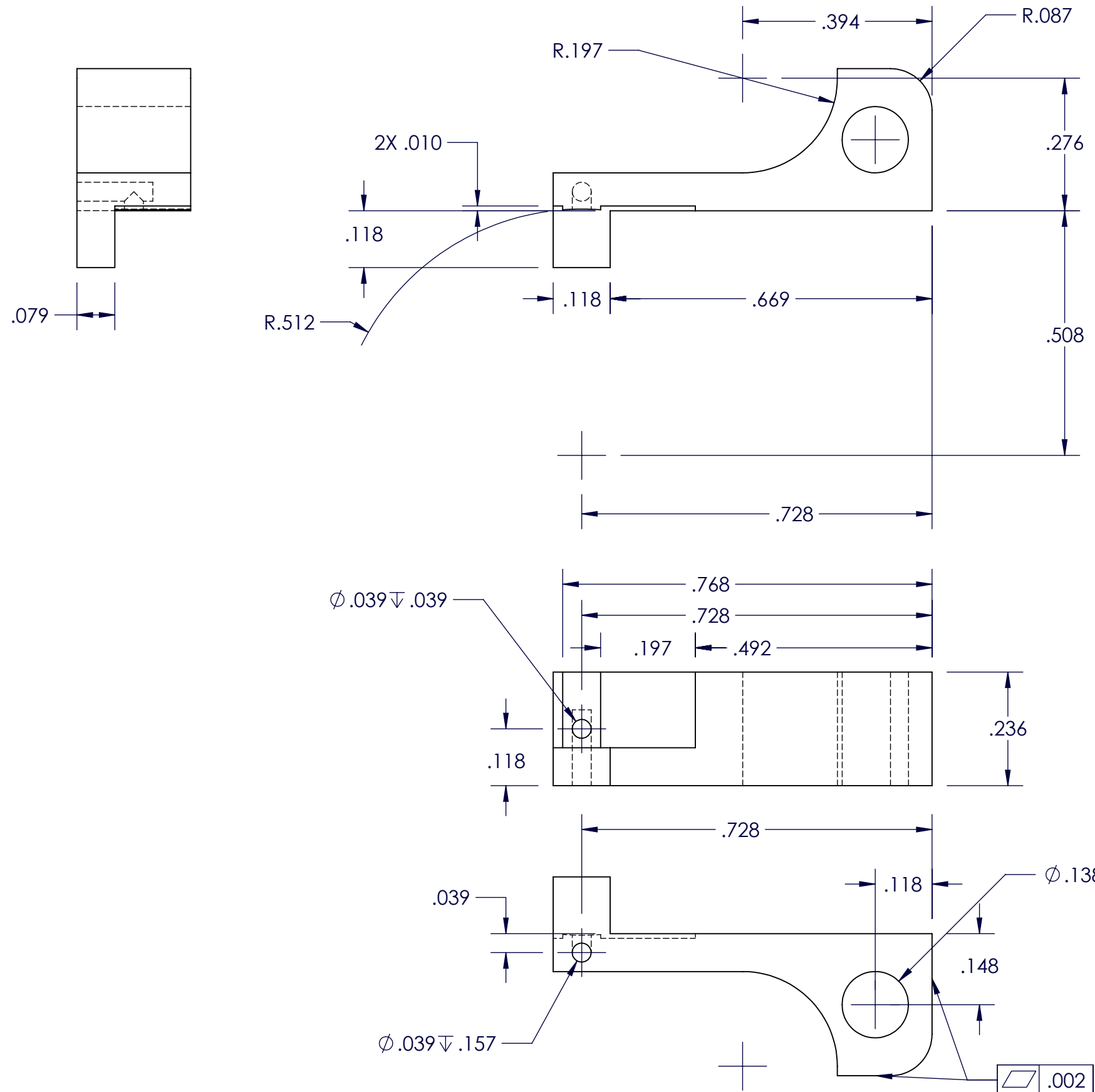
DATE:
 06-02-19

SHEET 3 OF 5


SCALE: 4:1

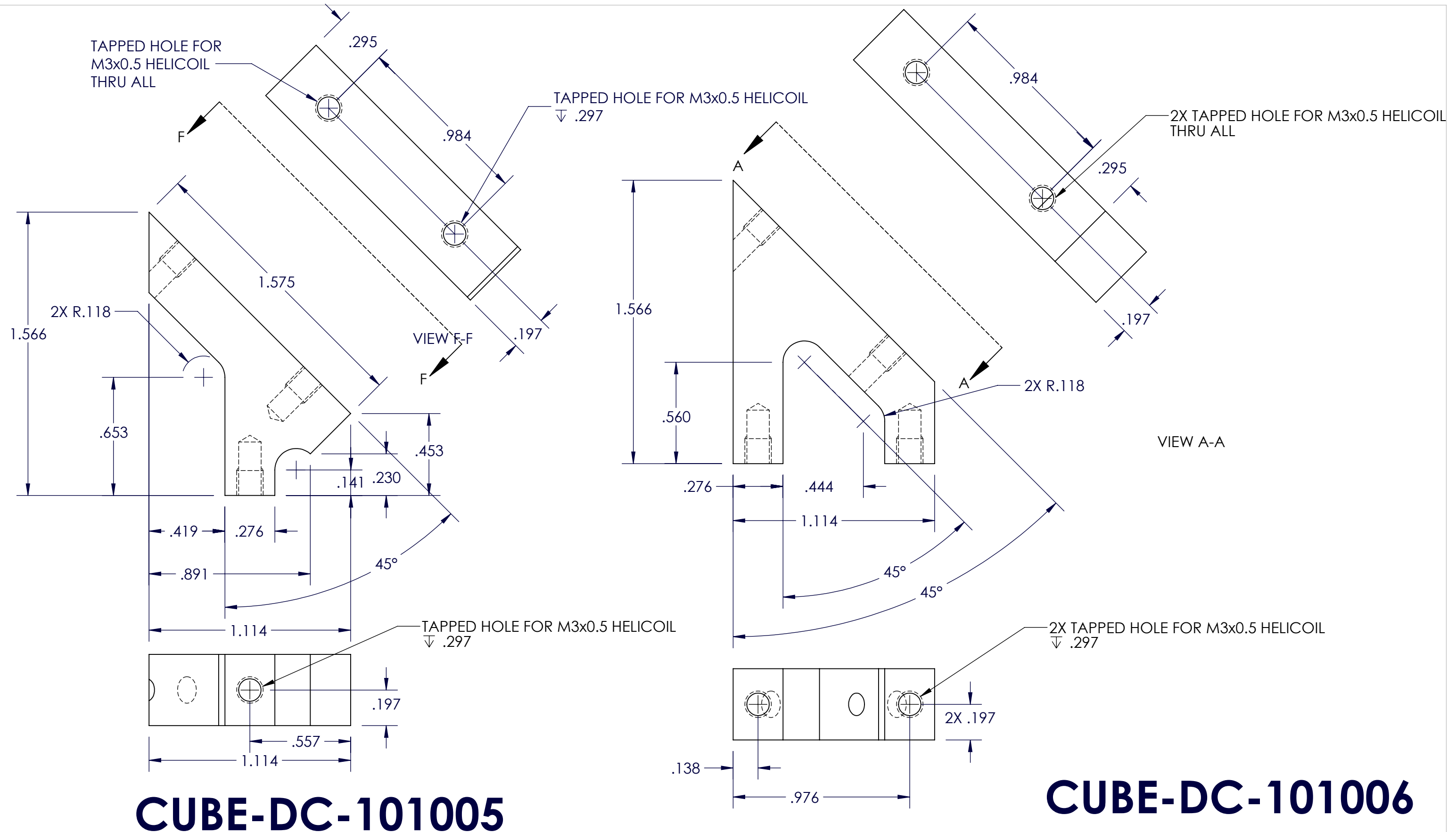
REV

SIZE
B



CUBE-DC-101004

<p>UNLESS OTHERWISE SPECIFIED: DIMENSIONS ARE IN INCHES TOLERANCES: FRACTIONAL $\pm 0.5^\circ$ TWO PLACE DECIMAL ± 0.005 THREE PLACE DECIMAL ± 0.0025</p>	<p>INTERPRET DRAWING PER ANSI Y14.5 2009</p> 	<p>CAL POLY SAN LUIS OBISPO</p>	<p>MATERIAL: SEE BOM</p> <p>DRAWN BY: PATRICK WHITESEL</p>	<p>TITLE: BOTTOM FLEXURE</p> <p>DATE: 06-02-19</p>	<p>SHEET 4 OF 5</p>	<p>SCALE: 4:1</p>	<p>REV</p>	<p>SIZE B</p>
---	---	--	--	--	---------------------	-------------------	------------	---------------------------



UNLESS OTHERWISE SPECIFIED:
 DIMENSIONS ARE IN INCHES
 TOLERANCES:
 FRACTIONAL ± 0.5°
 TWO PLACE DECIMAL ± 0.005
 THREE PLACE DECIMAL ± 0.0025

INTERPRET DRAWING
 PER ANSI Y14.5 2009

CAL POLY
SAN LUIS OBISPO

MATERIAL:
 6061-T6 - ALUMINUM

DRAWN BY:
 JEFF WAGNER

TITLE:
 ONE AND TWO LEG MOUNT

DATE:
 06-04-2019

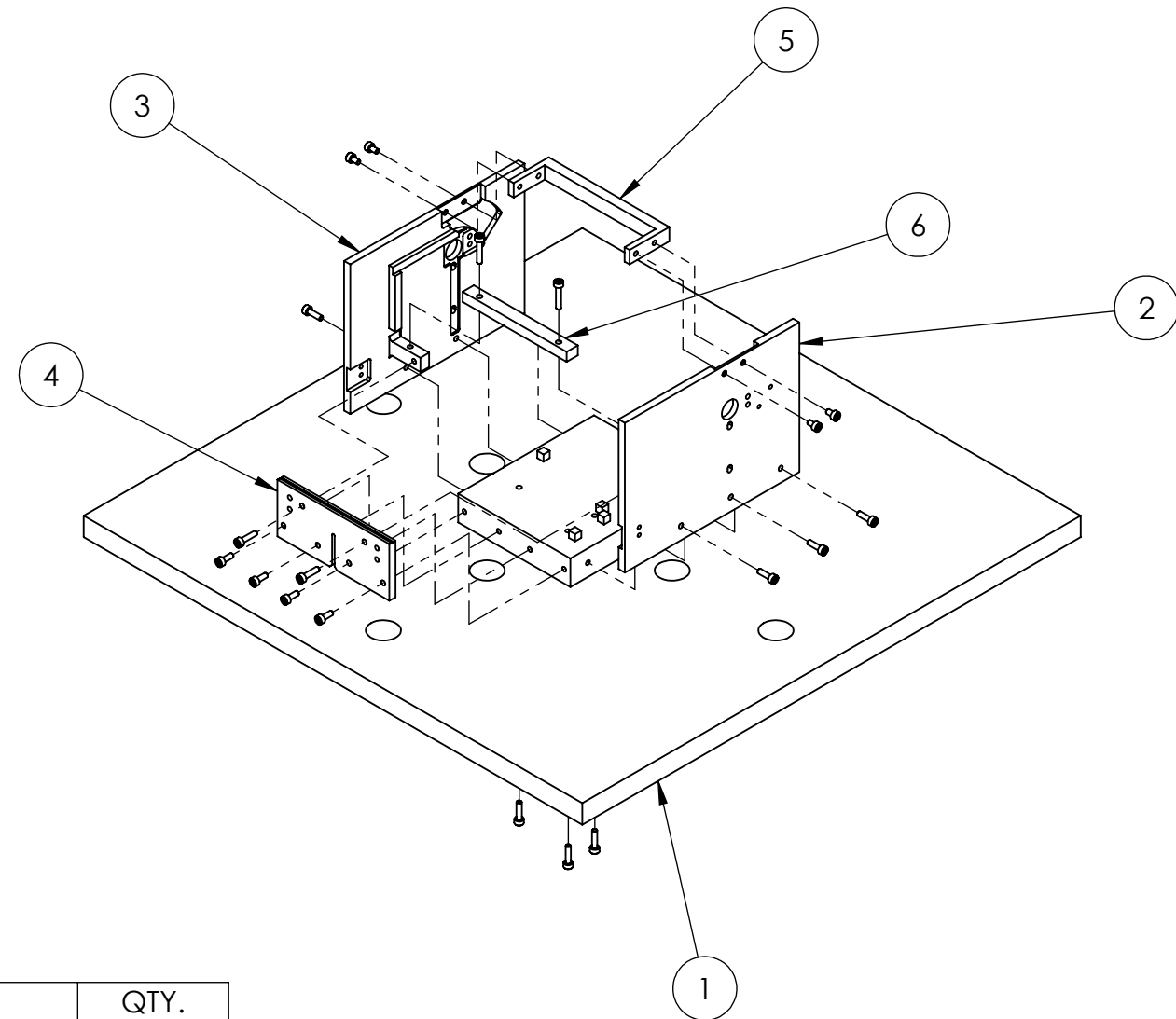
SHEET 1 OF 1

SCALE: 2:1

REV

SIZE
B

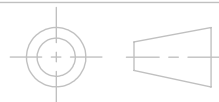
CUBE-DC-107000



ITEM NO.	PART NUMBER	DESCRIPTION	MATERIAL	QTY.
1	CUBE-DC-107001	DEPLOYABLE COVER OPTICS DATUM	6061-T6 (SS)	1
2	CUBE-DC-107002	LEFT SIDE PANEL	6061-T6 (SS)	1
3	CUBE-DC-107003	RIGHT SIDE PANEL	6061-T6 (SS)	1
4	CUBE-DC-107004	FRONT PANEL	6061-T6 (SS)	1
5	CUBE-DC-107005	TOP U BRACKET	6061-T6 (SS)	1
6	CUBE-DC-107006	FRONT CROSS BEAM	6061-T6 (SS)	1
7	B18.3.1M - 3 x 0.5 x 8 Hex SHCS -- 8NHX			4
8	B18.3.1M - 3 x 0.5 x 10 Hex SHCS -- 10NHX			6
9	B18.3.1M - 3 x 0.5 x 5 Hex SHCS -- 5NHX			4
10	B18.3.1M - 3 x 0.5 x 12 Hex SHCS -- 12NHX			5
11	B18.3.1M - 3 x 0.5 x 16 Hex SHCS -- 16NHX			2

UNLESS OTHERWISE SPECIFIED:
DIMENSIONS ARE IN INCHES
TOLERANCES:
FRACTIONAL $\pm 0.5^\circ$
TWO PLACE DECIMAL ± 0.005
THREE PLACE DECIMAL ± 0.001

INTERPRET DRAWING
PER ANSI Y14.5 2009



CAL POLY
SAN LUIS OBISPO

MATERIAL:
SEE BOM

DRAWN BY:
PATRICK WHITESEL

TITLE:
OPTICAL ALIGNMENT FIXTURE ASSEMBLY

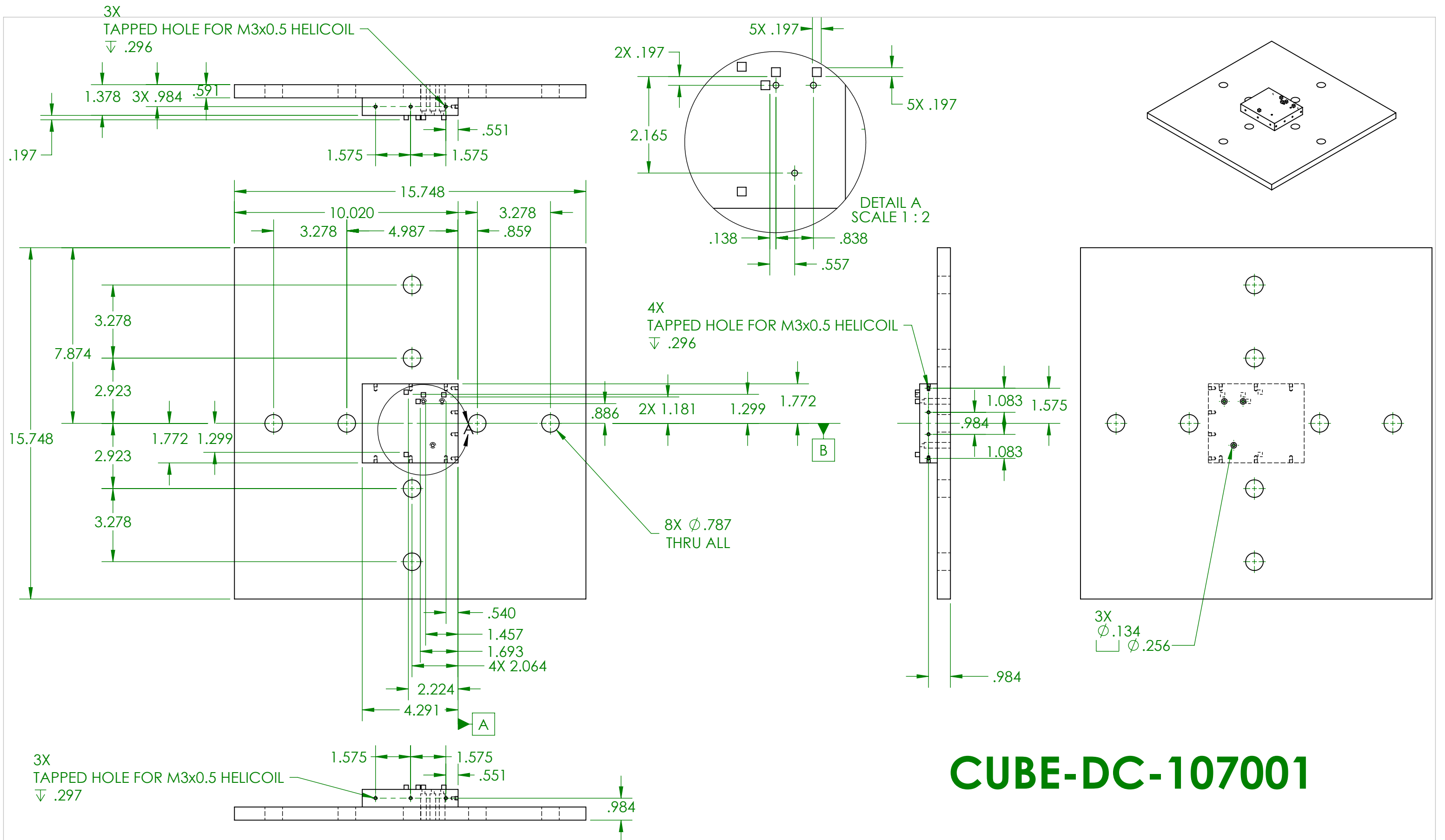
DATE:
06-02-18

SHEET 1 OF 7

SCALE: 1:4

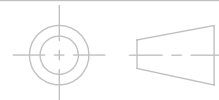
REV

SIZE
B



UNLESS OTHERWISE SPECIFIED:
 DIMENSIONS ARE IN INCHES
 TOLERANCES:
 FRACTIONAL $\pm 0.5^\circ$
 TWO PLACE DECIMAL ± 0.005
 THREE PLACE DECIMAL ± 0.001

INTERPRET DRAWING
 PER ANSI Y14.5 2009



CAL POLY
 SAN LUIS OBISPO

MATERIAL:
 SEE BOM

DRAWN BY:
 JEFF WAGNER

TITLE:
 DEPLOYABLE COVER OPTICS DATUM

DATE:
 06-02-2019

SHEET 2 OF 7

SCALE: 1:4

REV

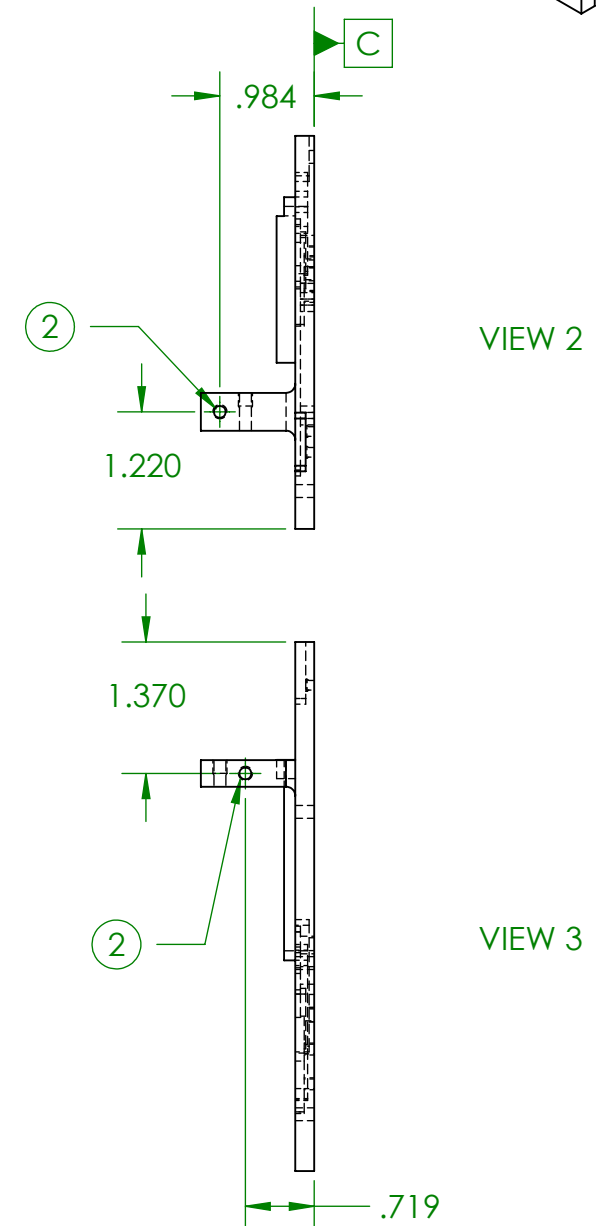
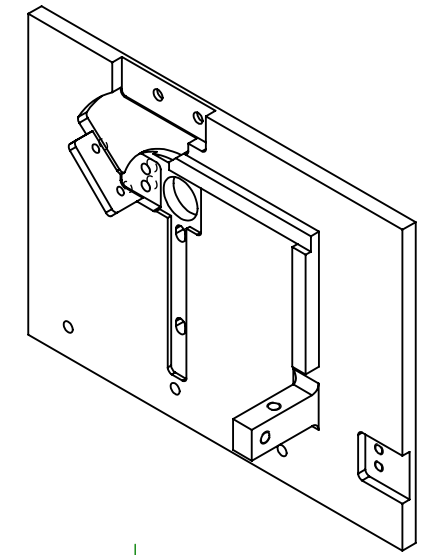
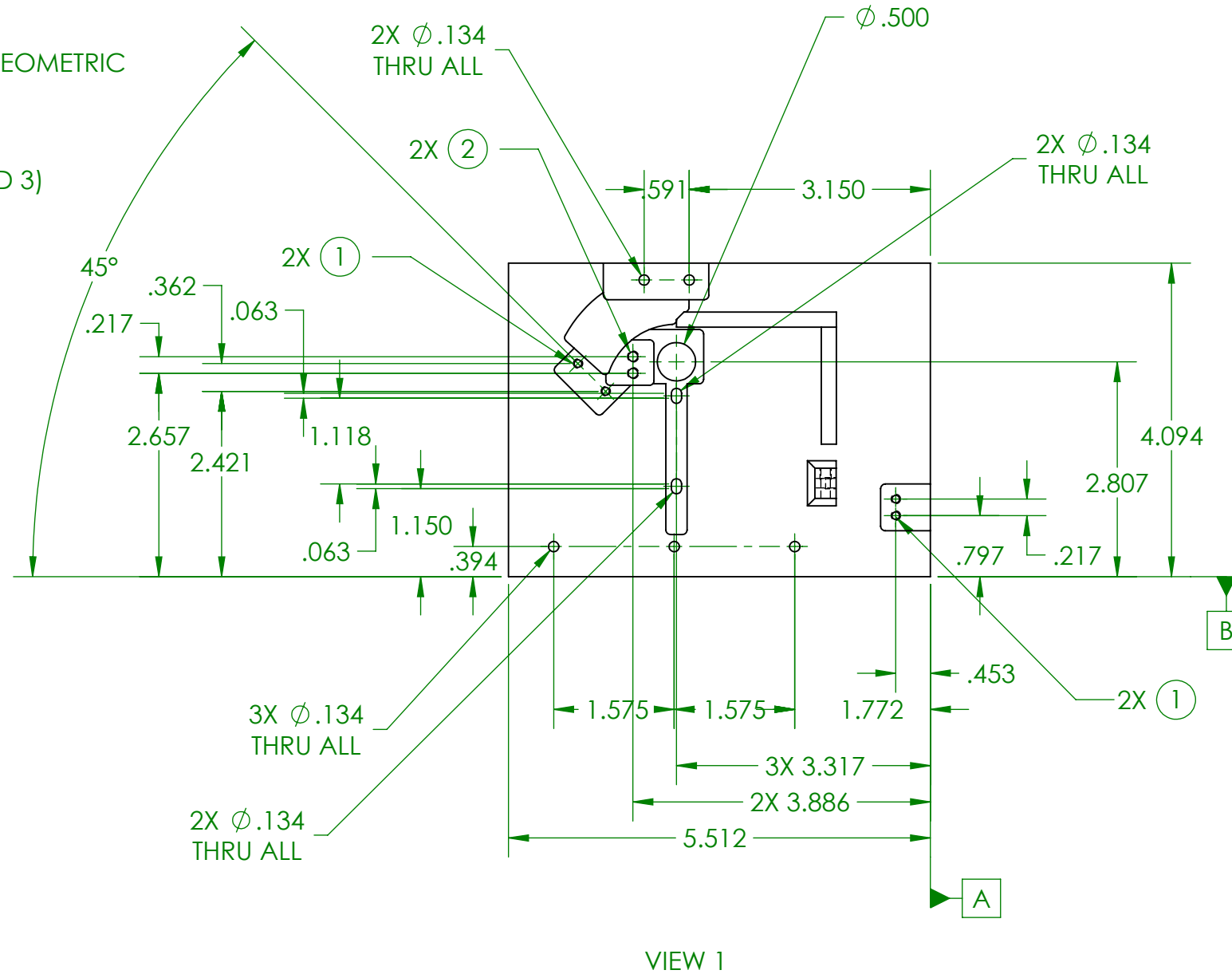
SIZE
B

NOTE:

1. SEE CAD MODEL FOR FEATURE DIMENSIONS, ONLY HOLE LOCATION AND CALLOUT PROVIDED HERE.
2. ALL DIMENSIONS ARE IN INCHES UNLESS OTHERWISE SPECIFIED
3. TOLERANCE $\pm .001$ UNLESS OTHERWISE SPECIFIED
4. (1) INDICATES FOLLOWING CALLOUT:
TAPPED HOLE FOR M2.5X0.45 HELICOIL
THRU ALL
5. (2) INDICATES FOLLOWING CALLOUT:
TAPPED HOLE FOR M3X0.5 HELICOIL
THRU ALL
6. ALL INTERIOR CORNERS: R=1.5MM
7. ALL HOLE LOCATIONS HAVE APPLIED GEOMETRIC TOLERANCE OF

$\oplus .001 \text{ (M) X X}$

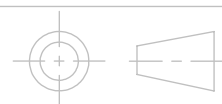
WITH RESPECTIVE DATUMS:
(A&B FOR VIEW 1, B&C FOR VIEW 2 AND 3)



CUBE-DC-107002

UNLESS OTHERWISE SPECIFIED:
DIMENSIONS ARE IN INCHES
TOLERANCES:
FRACTIONAL $\pm 0.5^\circ$
TWO PLACE DECIMAL ± 0.005
THREE PLACE DECIMAL ± 0.001

INTERPRET DRAWING
PER ANSI Y14.5 2009



CAL POLY
SAN LUIS OBISPO

MATERIAL:
SEE BOM

DRAWN BY:
JEFF WAGNER

TITLE:
LEFT SIDE PANEL

DATE:
06-02-2019

SHEET 3 OF 7

SCALE: 1:2

REV

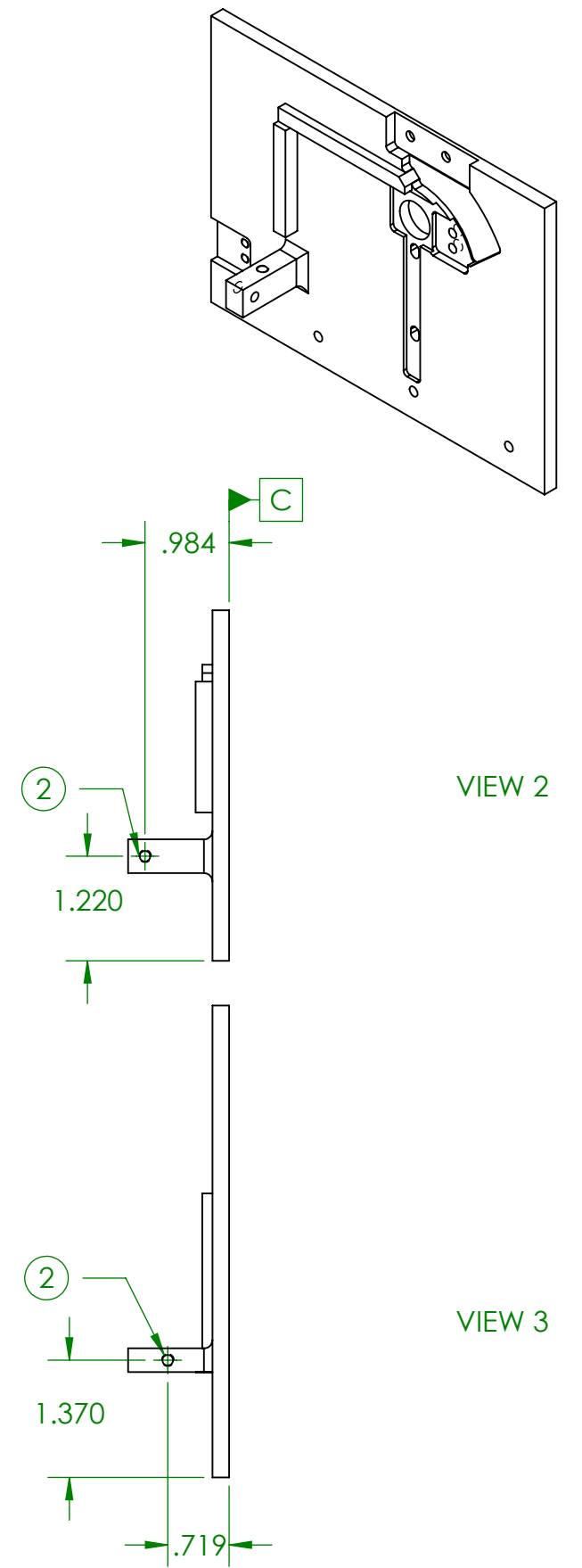
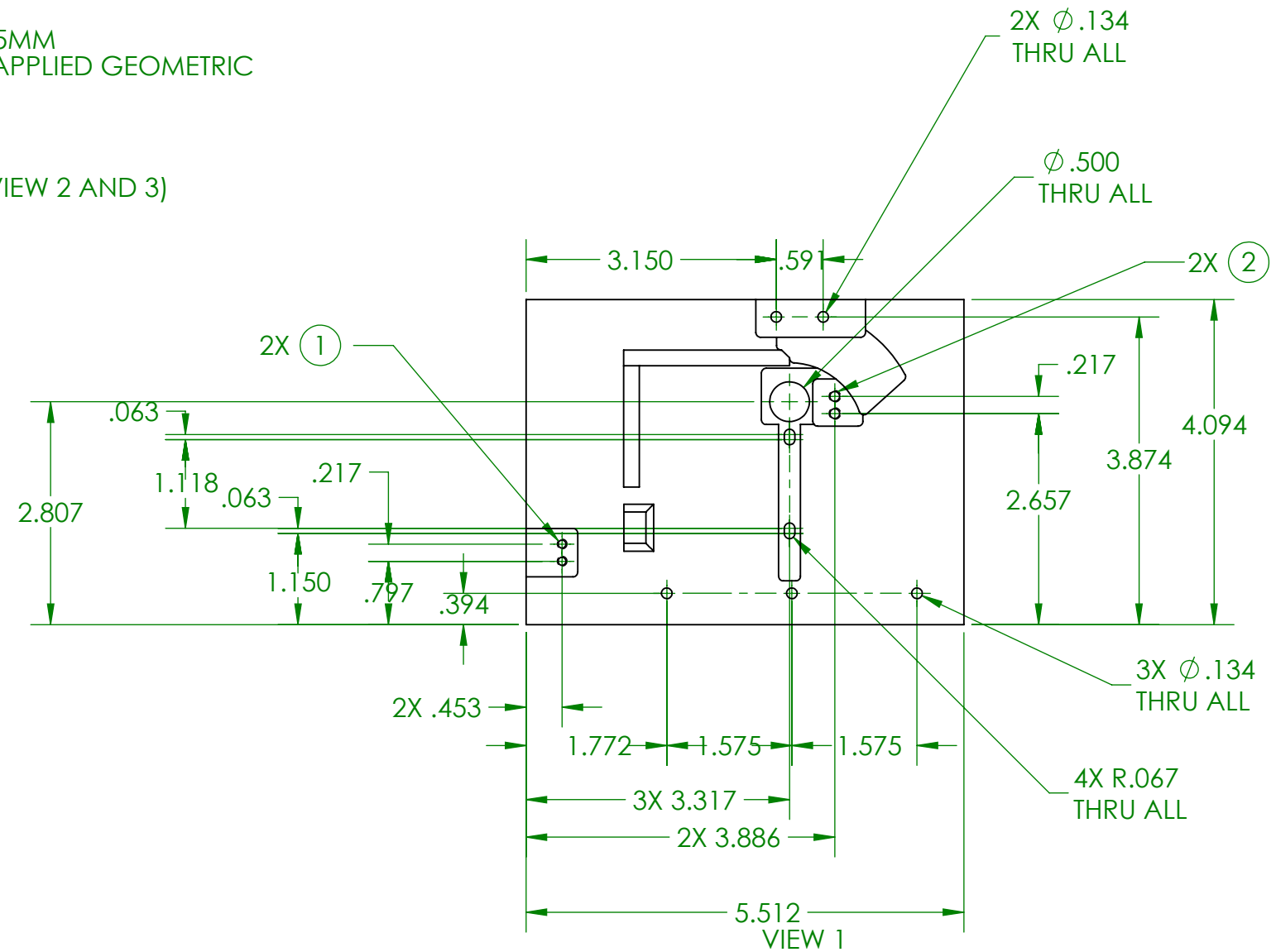
SIZE
B

NOTE:

1. SEE CAD MODEL FOR FEATURE DIMENSIONS, ONLY HOLE LOCATION AND CALLOUT PROVIDED HERE.
2. ALL DIMENSIONS ARE IN INCHES UNLESS OTHERWISE SPECIFIED
3. TOLERANCE $\pm .001$ UNLESS OTHERWISE SPECIFIED
4. (1) INDICATES FOLLOWING CALLOUT:
TAPPED HOLE FOR M2.5X0.45 HELICOIL
THRU ALL
5. (2) INDICATES FOLLOWING CALLOUT:
TAPPED HOLE FOR M3X0.5 HELICOIL
THRU ALL
6. ALL INTERIOR CORNERS: R=1.5MM
7. ALL HOLE LOCATIONS HAVE APPLIED GEOMETRIC TOLERANCE OF

$\oplus .001 \text{ (M) X X}$

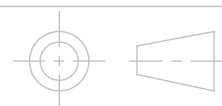
WITH RESPECTIVE DATUMS:
(A&B FOR VIEW 1, B&C FOR VIEW 2 AND 3)



CUBE-DC-107003

UNLESS OTHERWISE SPECIFIED:
DIMENSIONS ARE IN INCHES
TOLERANCES:
FRACTIONAL $\pm .5^\circ$
TWO PLACE DECIMAL ± 0.005
THREE PLACE DECIMAL ± 0.001

INTERPRET DRAWING
PER ANSI Y14.5 2009



CAL POLY
SAN LUIS OBISPO

MATERIAL:
SEE BOM

DRAWN BY:
JEFF WAGNER

TITLE:
RIGHT SIDE PANEL

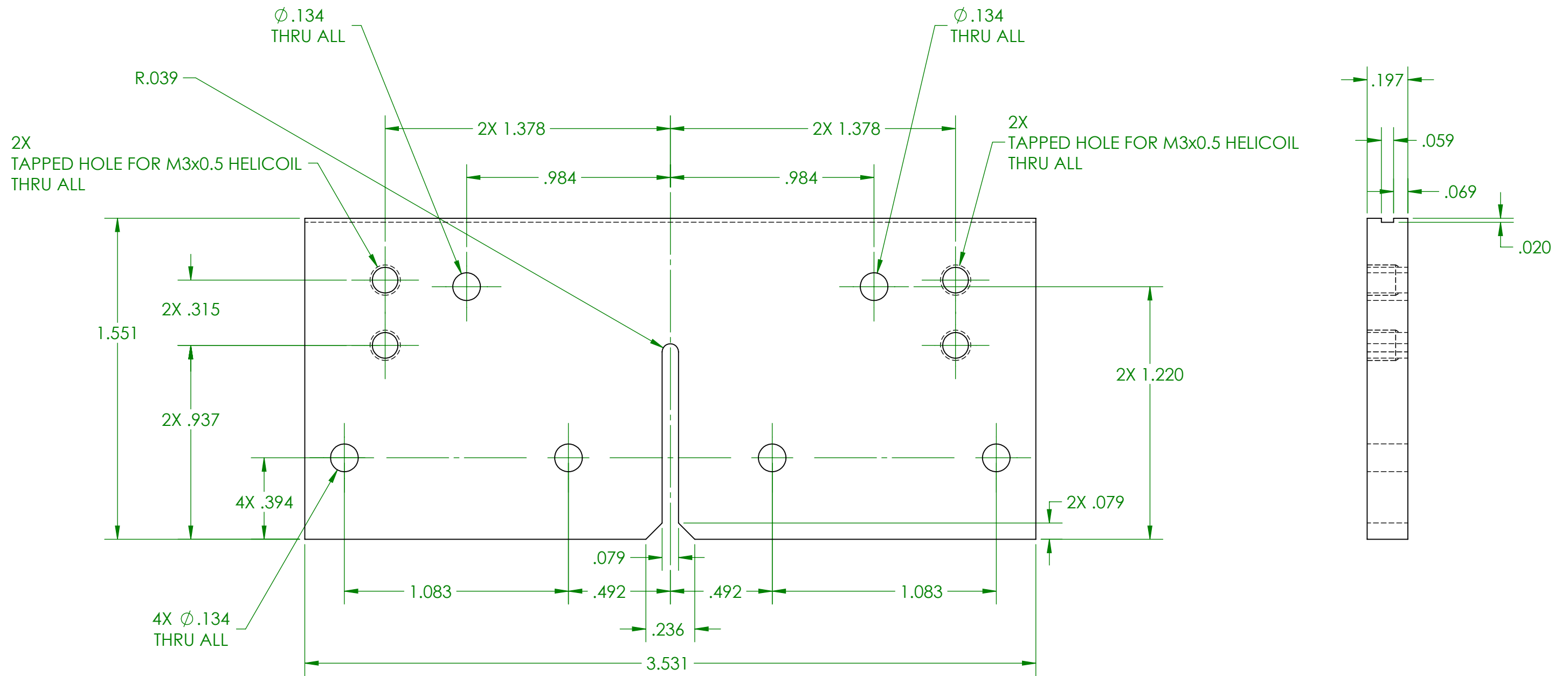
DATE:
06-02-2019

SHEET 4 OF 7

SCALE: 1:2

REV

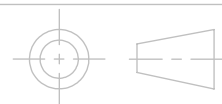
SIZE
B



CUBE-DC-107004

UNLESS OTHERWISE SPECIFIED:
 DIMENSIONS ARE IN INCHES
 TOLERANCES:
 FRACTIONAL $\pm 0.5^\circ$
 TWO PLACE DECIMAL ± 0.005
 THREE PLACE DECIMAL ± 0.001

INTERPRET DRAWING
 PER ANSI Y14.5 2009



CAL POLY
SAN LUIS OBISPO

MATERIAL:
 SEE BOM

DRAWN BY:
 JEFF WAGNER

TITLE:
 FRONT PANEL

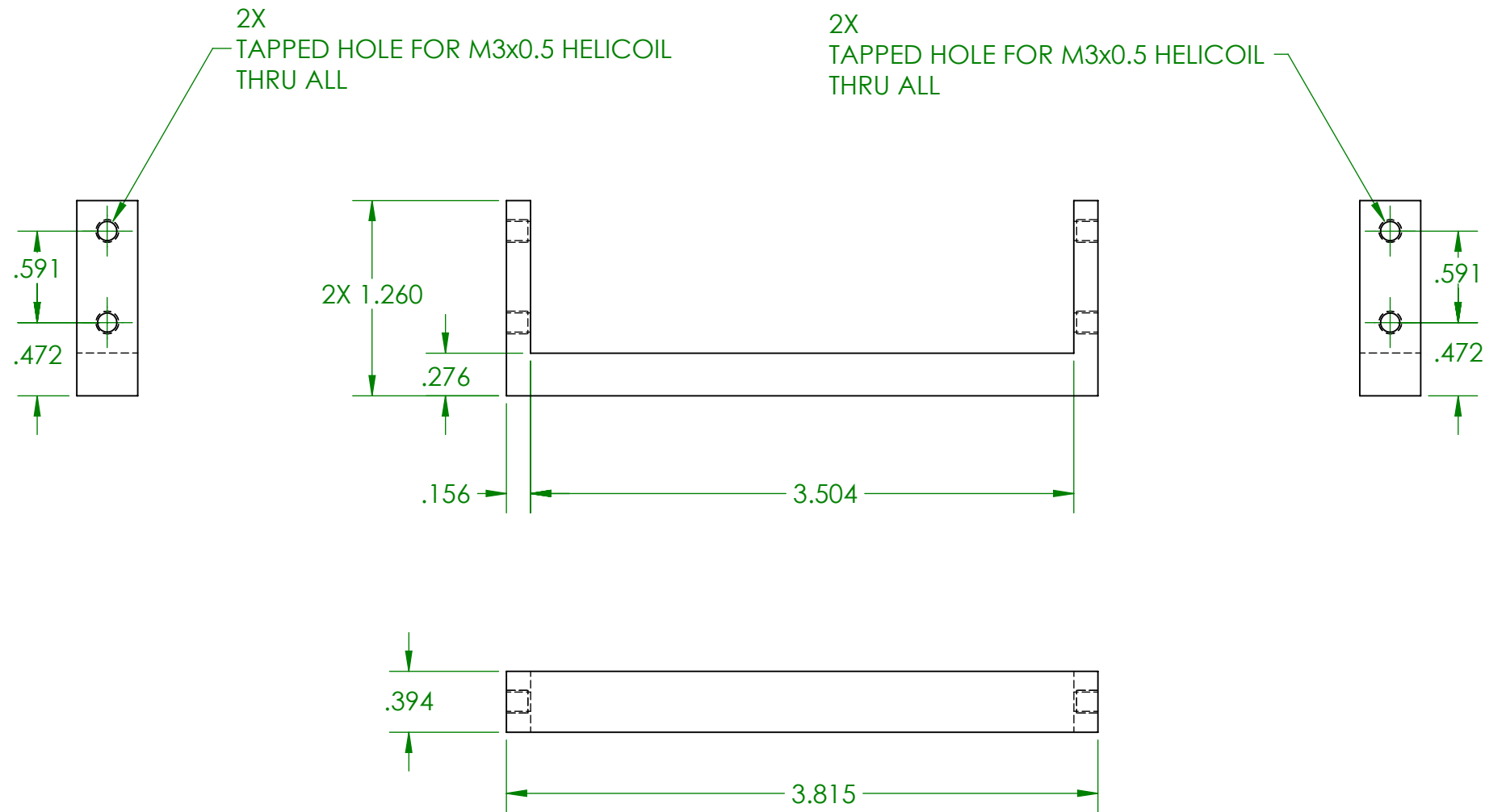
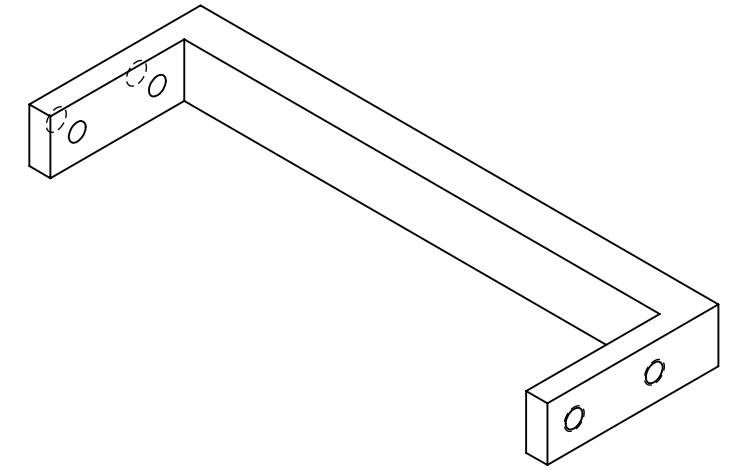
DATE:
 06-04-2019

SHEET 5 OF 7

SCALE: 2:1

REV

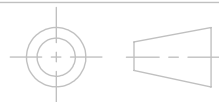
SIZE
B



CUBE-DC-107005

UNLESS OTHERWISE SPECIFIED:
 DIMENSIONS ARE IN INCHES
 TOLERANCES:
 FRACTIONAL $\pm 0.5^\circ$
 TWO PLACE DECIMAL ± 0.005
 THREE PLACE DECIMAL ± 0.001

INTERPRET DRAWING
 PER ANSI Y14.5 2009



CAL POLY
SAN LUIS OBISPO

MATERIAL:
 SEE BOM

DRAWN BY:
 JEFF WAGNER

TITLE:
 TOP U BRACKET

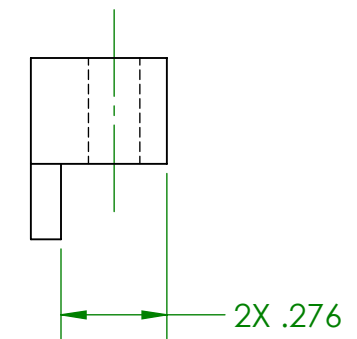
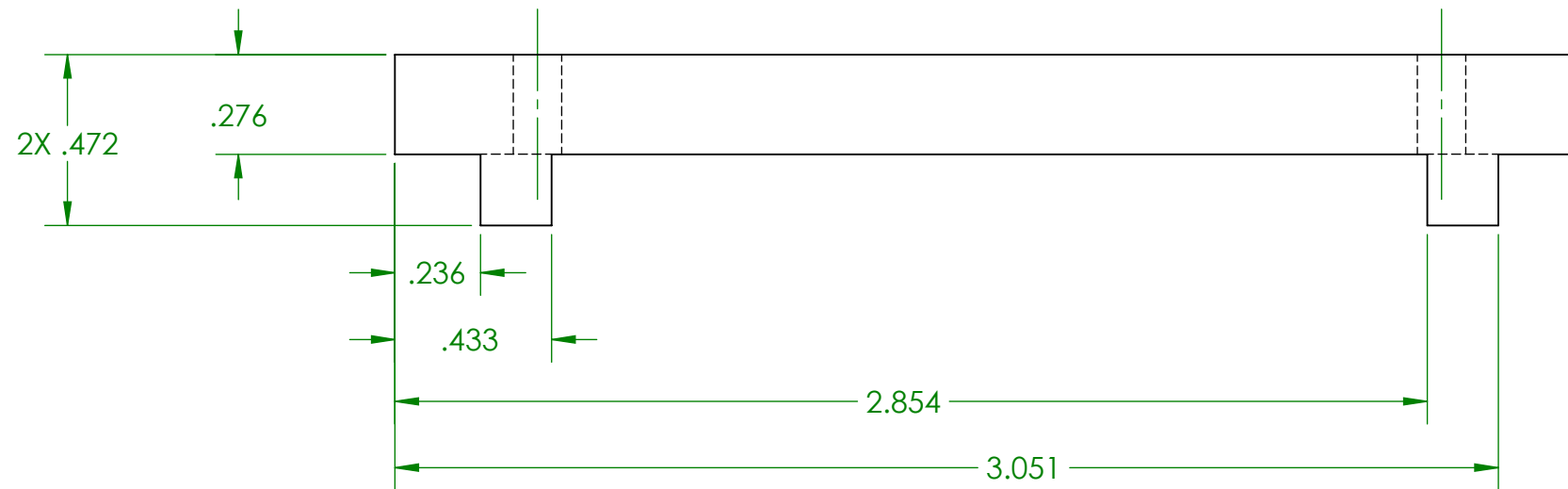
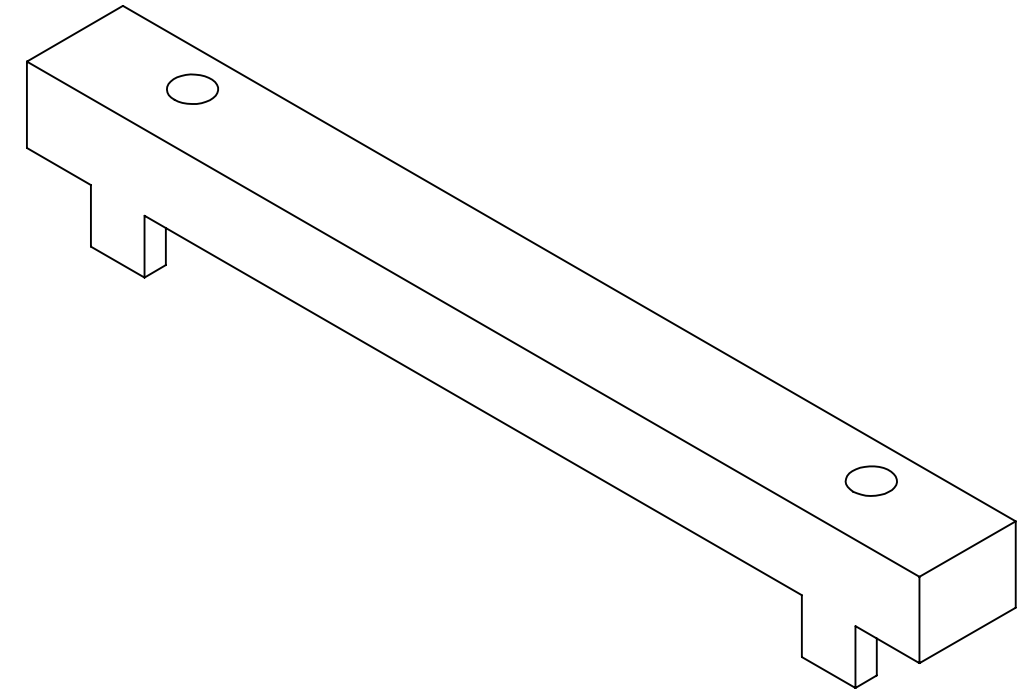
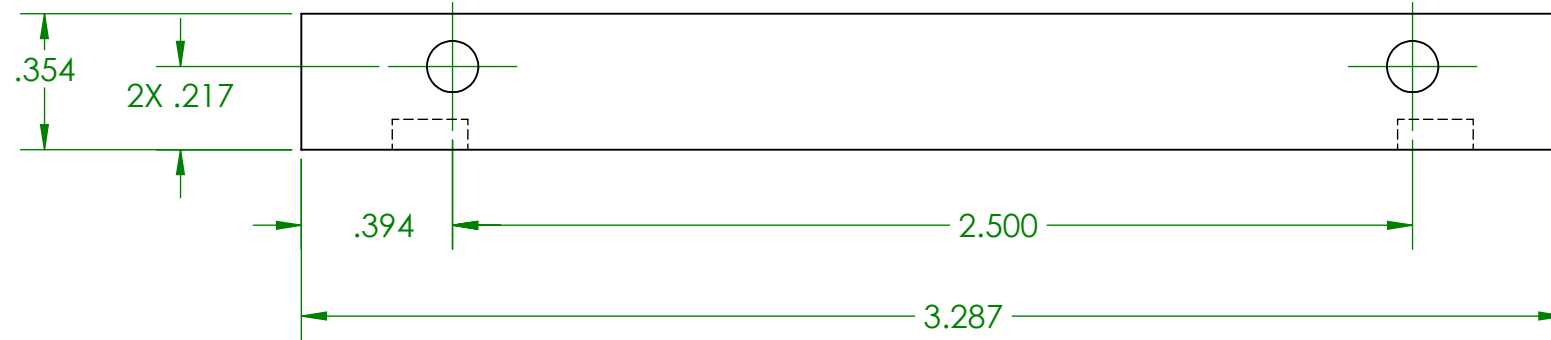
DATE:
 06-04-2019

SHEET 6 OF 7

SCALE: 1:1

REV

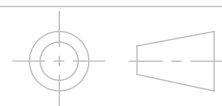
SIZE
B



CUBE-DC-107006

UNLESS OTHERWISE SPECIFIED:
 DIMENSIONS ARE IN INCHES
 TOLERANCES:
 FRACTIONAL $\pm 0.5^\circ$
 TWO PLACE DECIMAL ± 0.005
 THREE PLACE DECIMAL ± 0.001

INTERPRET DRAWING
 PER ANSI Y14.5 2009



CAL POLY
SAN LUIS OBISPO

MATERIAL:
 SEE BOM

DRAWN BY:
 JEFF WAGNER

TITLE:
 FRONT CROSS BEAM

DATE:
 06-04-2019

SHEET 7 OF 7

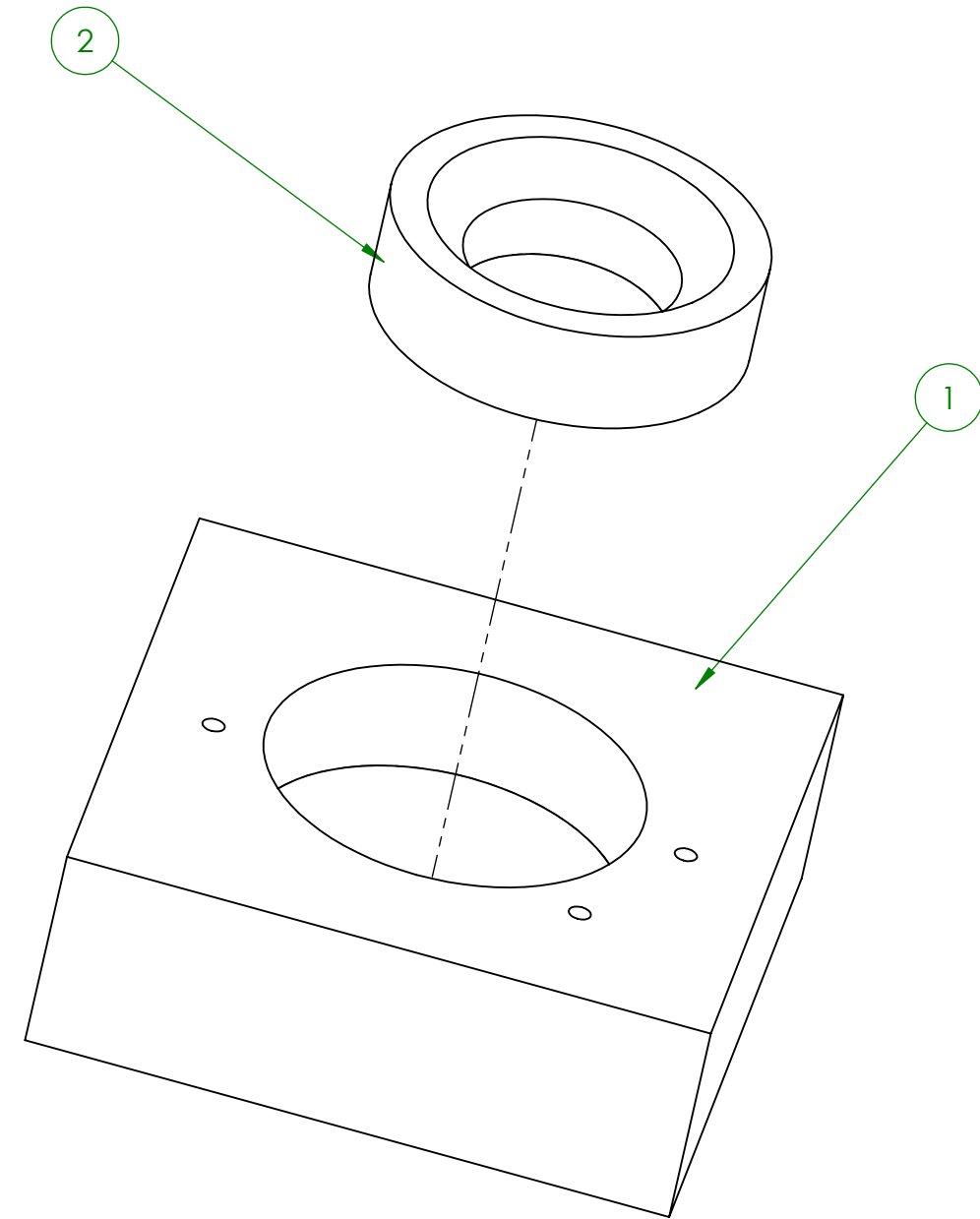
SCALE: 2:1

REV

SIZE
B

NOTES, UNLESS OTHERWISE SPECIFIED:

1. MATERIAL: ALUMINUM 6061-T651 PER AMS 4027 AND AMS 4150. FOR OTHER MATERIALS, SEE BOM.
2. BREAK EXTERNAL EDGES AND CORNERS .005 IN MAX UNLESS NOTED.
3. INTERNAL CORNER AND FILLET RADII .005 MAX UNLESS NOTED.
4. INSTALL HELICAL COIL INSERT PER NASM33537. REMOVE TANG.
5. DRAWING IS THE SOLE AUTHORITY FOR THE BASIC FORM, LOCATION, ORIENTATION, AND DIMENSIONAL CHARACTERISTICS OF ALL DESIGN FEATURES.

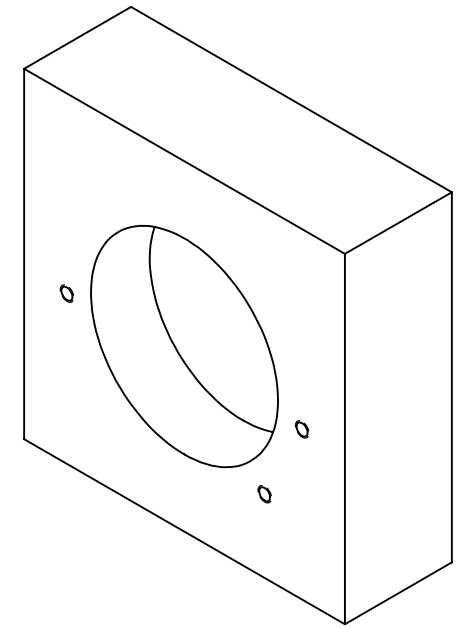
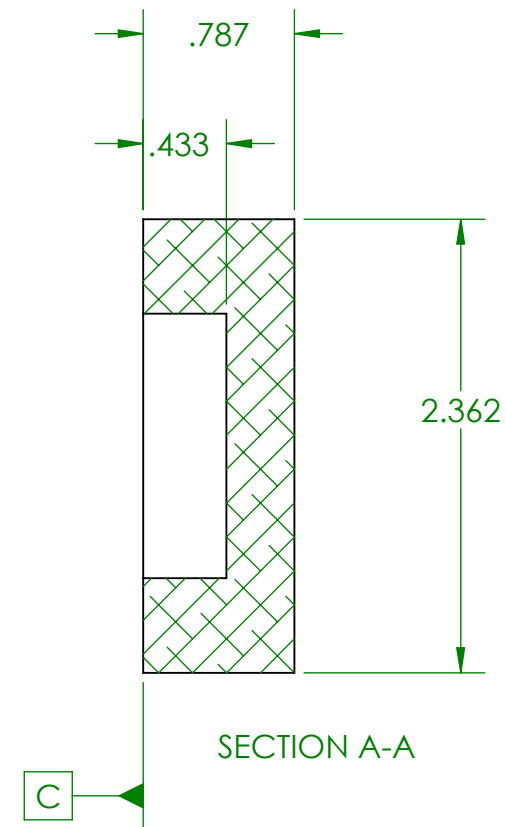
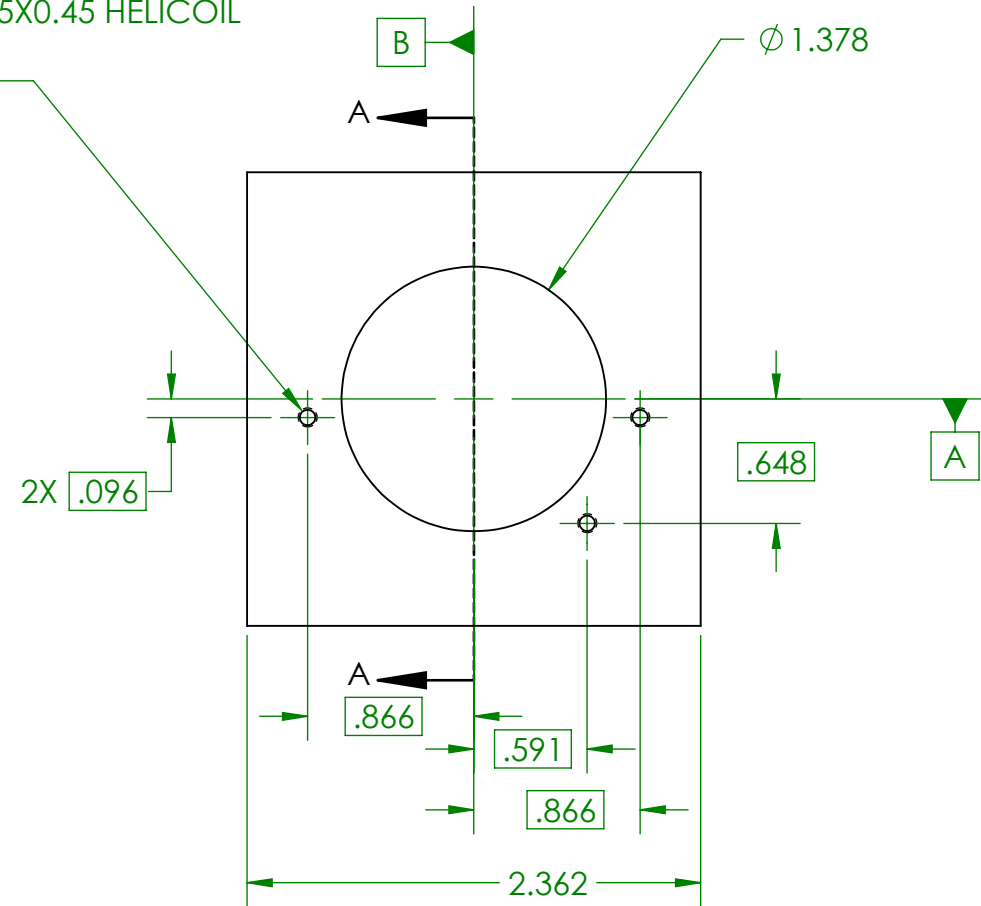


ITEM NO.	PART NUMBER	DESCRIPTION	MATERIAL	QTY.
1	CUBE-DC-108001	Bottom Mirror Flexure Aligner	6061-T6 (SS)	1
2	CUBE-DC-108002	BOTTOM MIRROR DELRIN MIRROR POSITIONER	Delrin 2700 NC010, Low Viscosity Acetal Copolymer (SS)	1

UNLESS OTHERWISE SPECIFIED: DIMENSIONS ARE IN INCHES TOLERANCES: FRACTIONAL $\pm 0.5^\circ$ TWO PLACE DECIMAL ± 0.005 THREE PLACE DECIMAL ± 0.005	INTERPRET DRAWING PER ANSI Y14.5 2009 	CAL POLY SAN LUIS OBISPO	MATERIAL: SEE BOM	TITLE: BOTTOM MIRROR BOND FIXTURE				
			DRAWN BY: JEFF WAGNER	DATE: 06-04-2019	SHEET 1 OF 3	SCALE: 3:2	REV	SIZE B

3X
TAPPED HOLE FOR M2.5X0.45 HELICOIL
↓.297

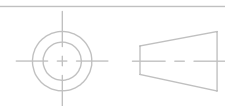
⊕.001 (M) A B C



CUBE-DC-108001

UNLESS OTHERWISE SPECIFIED:
DIMENSIONS ARE IN INCHES
TOLERANCES:
FRACTIONAL $\pm 0.5^\circ$
TWO PLACE DECIMAL ± 0.005
THREE PLACE DECIMAL ± 0.001

INTERPRET DRAWING
PER ANSI Y14.5 2009



CAL POLY
SAN LUIS OBISPO

MATERIAL:
SEE BOM

DRAWN BY:
JEFF WAGNER

TITLE:
BOTTOM MIRROR FLEXURE ALIGNER

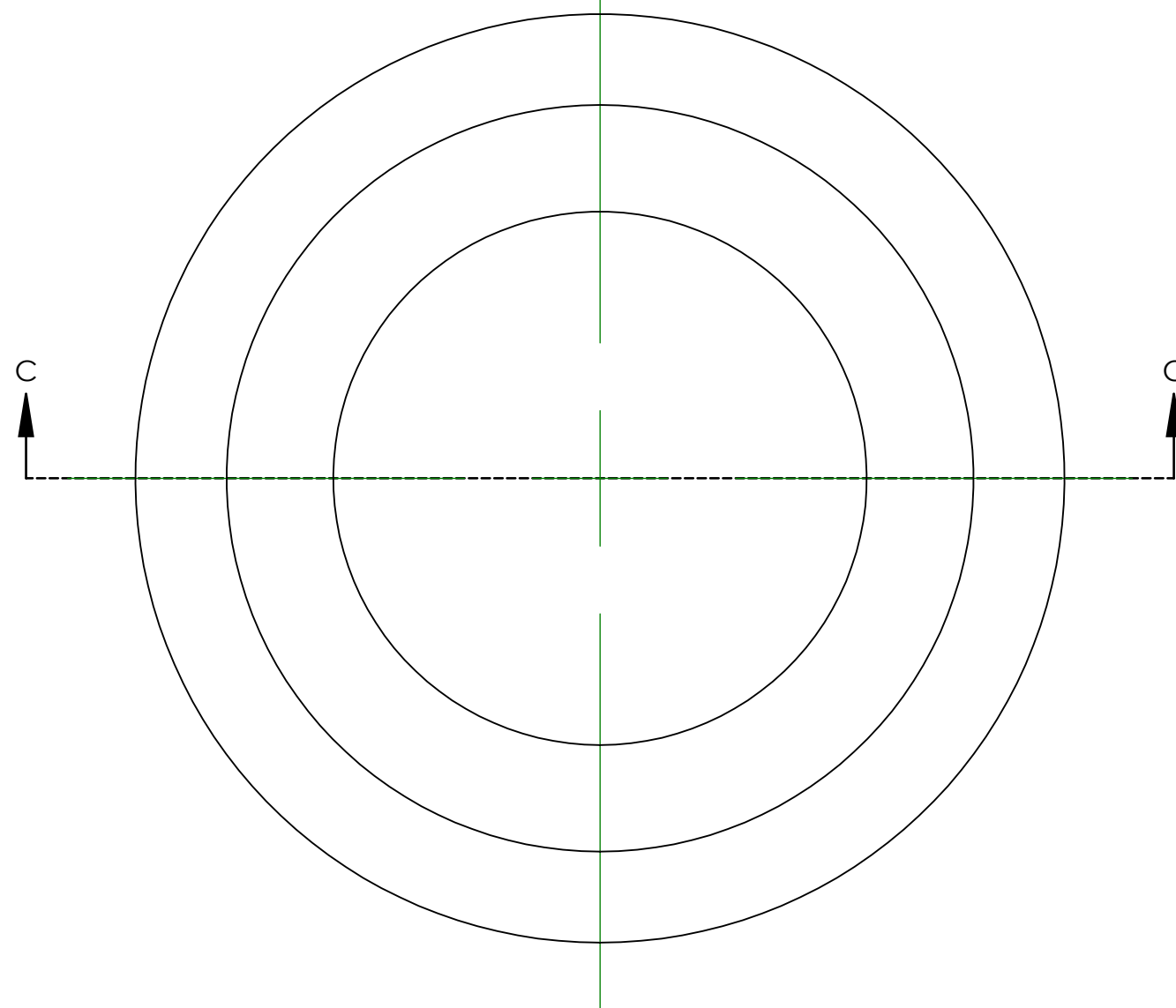
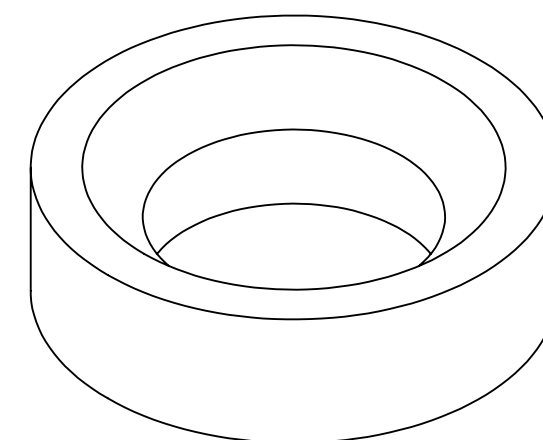
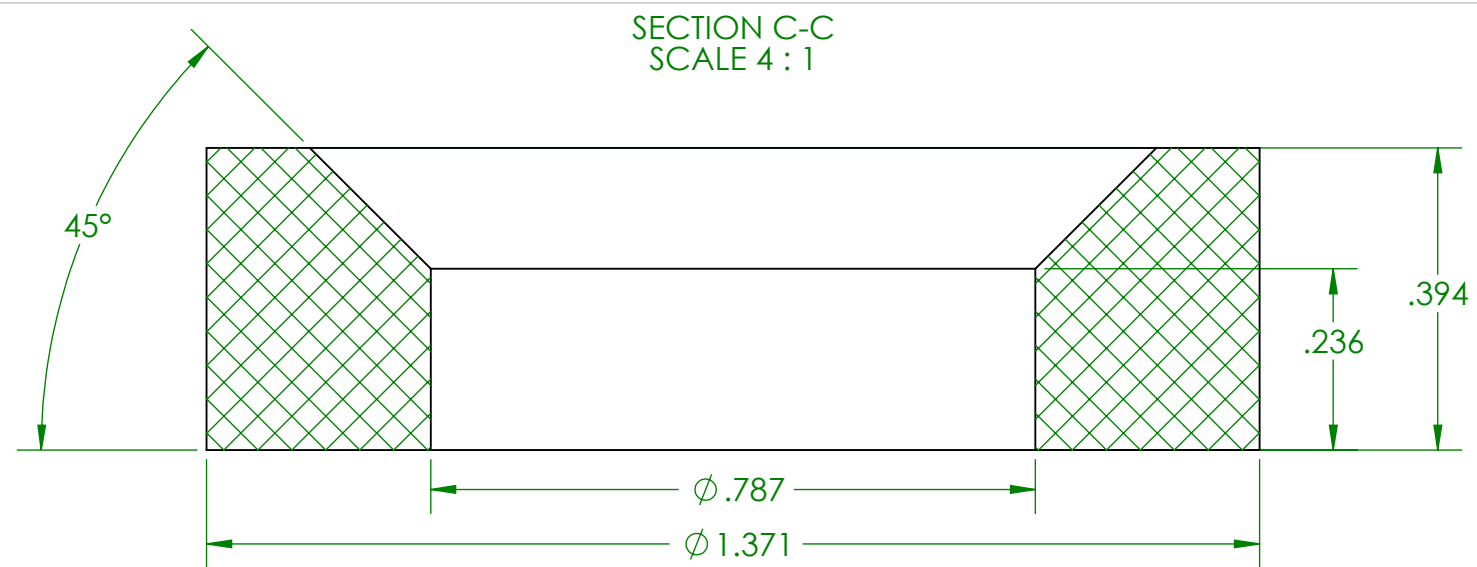
DATE:
06-04-2019

SHEET 2 OF 3

SCALE: 1:1

REV

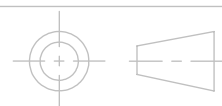
SIZE
B



CUBE-DC-108002

UNLESS OTHERWISE SPECIFIED:
DIMENSIONS ARE IN INCHES
TOLERANCES:
FRACTIONAL $\pm 0.5^\circ$
TWO PLACE DECIMAL ± 0.005
THREE PLACE DECIMAL ± 0.001

INTERPRET DRAWING
PER ANSI Y14.5 2009



CAL POLY
SAN LUIS OBISPO

MATERIAL:
SEE BOM

DRAWN BY:
JEFF WAGNER

TITLE:
BOTTOM MIRROR DELRIN MIRROR POSITIONER

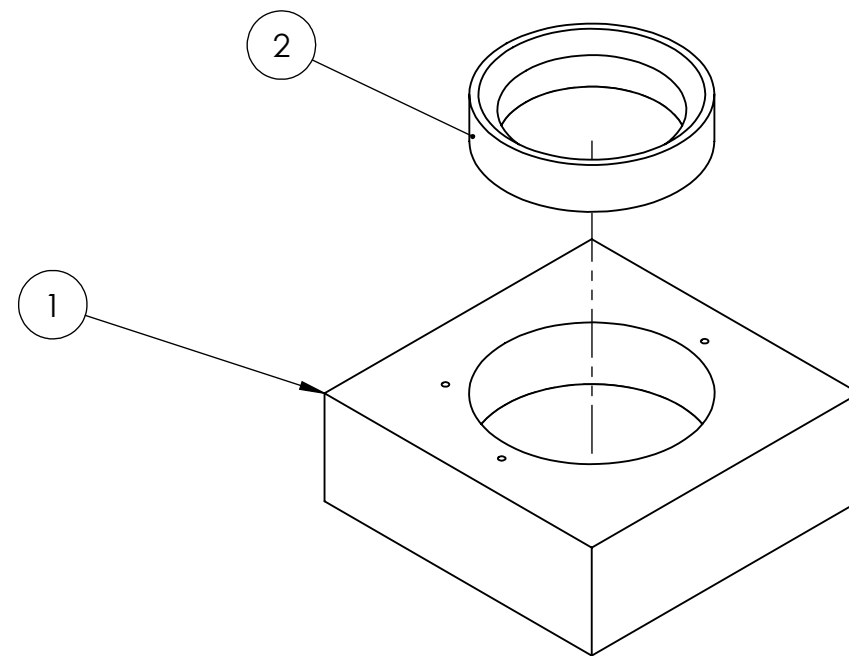
DATE:
06-04-2019

SHEET 3 OF 3

SCALE: 4:1

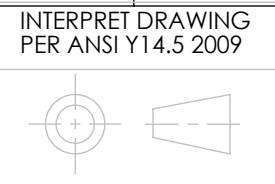
REV

SIZE
B



ITEM NO.	PART NUMBER	DESCRIPTION	MATERIAL	QTY.
1	CUBE-DC-109001	TOP MIRROR FLEXURE ALIGNER	6061-T6 (SS)	1
2	CUBE-DC-109002	TOP MIRROR DELRIN MIRROR POSITIONER	Delrin 2700 NC010, Low Viscosity Acetal Copolymer (SS)	1

UNLESS OTHERWISE SPECIFIED:
 DIMENSIONS ARE IN INCHES
 TOLERANCES:
 FRACTIONAL $\pm 0.5^\circ$
 TWO PLACE DECIMAL ± 0.005
 THREE PLACE DECIMAL ± 0.005

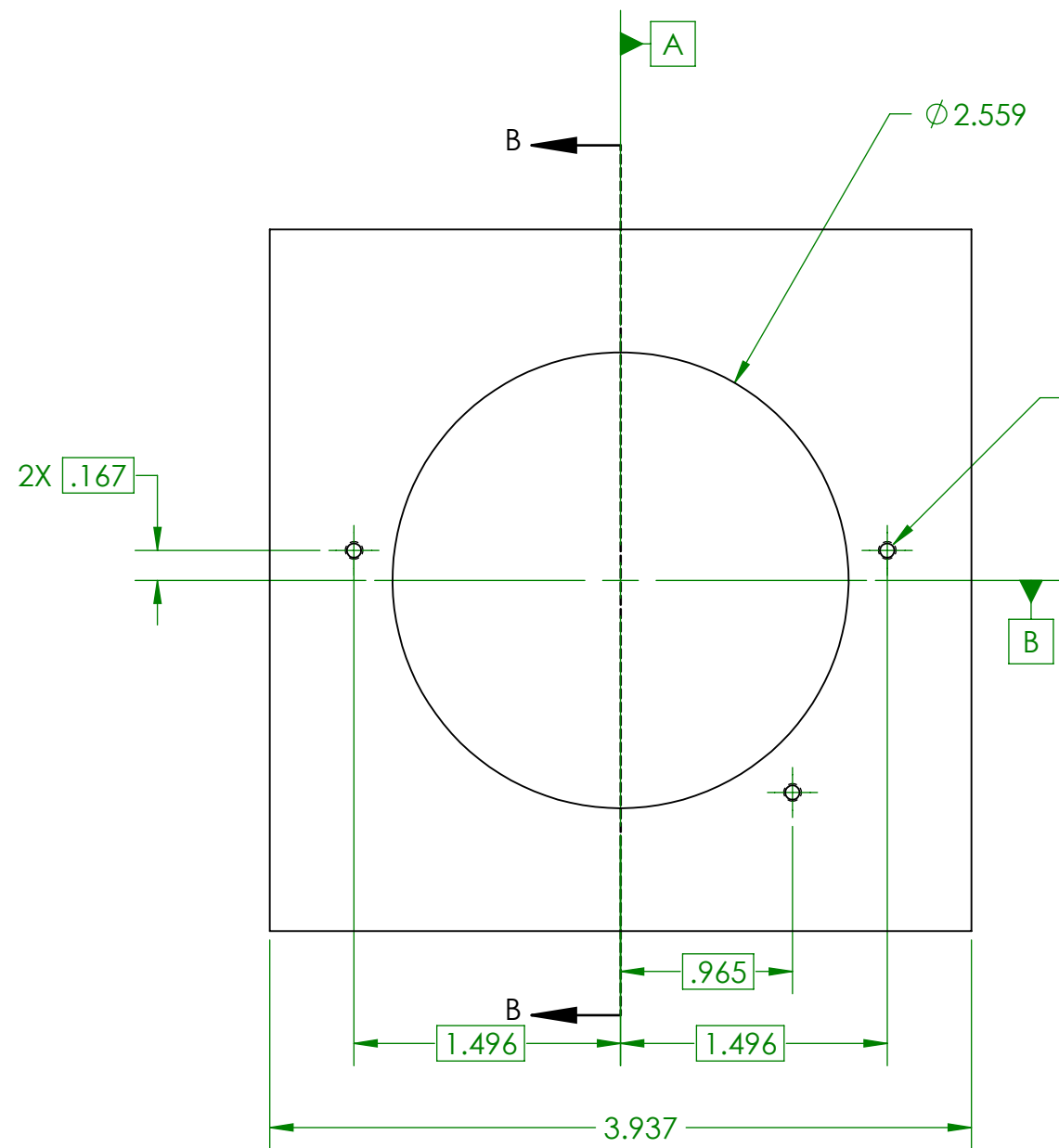


CAL POLY
SAN LUIS OBISPO

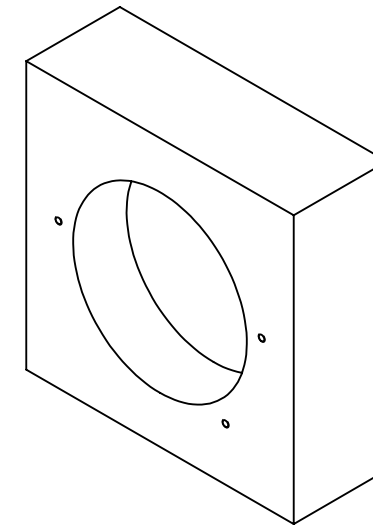
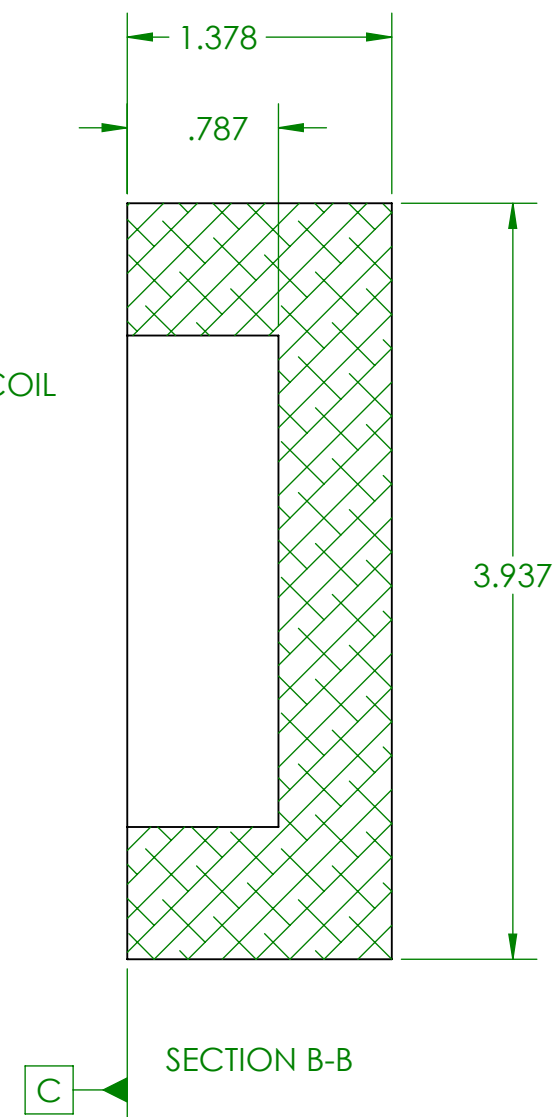
MATERIAL:
 SEE BOM

DRAWN BY:
 JEFF WAGNER

TITLE: TOP MIRROR BOND FIXTURE		DATE: 06-04-2019	SHEET 1 OF 3	SCALE: 1:2	REV	SIZE B



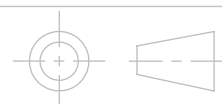
3X
TAPPED HOLE FOR M2.5x0.45 HELICOIL
↓ .297
⊕ .001 (M) A B C



CUBE-DC-109001

UNLESS OTHERWISE SPECIFIED:
DIMENSIONS ARE IN INCHES
TOLERANCES:
FRACTIONAL ± 0.5°
TWO PLACE DECIMAL ± 0.005
THREE PLACE DECIMAL ± 0.001

INTERPRET DRAWING
PER ANSI Y14.5 2009



CAL POLY
SAN LUIS OBISPO

MATERIAL:
SEE BOM

DRAWN BY:
JEFF WAGNER

TITLE:
TOP MIRROR FLEXURE ALIGNER

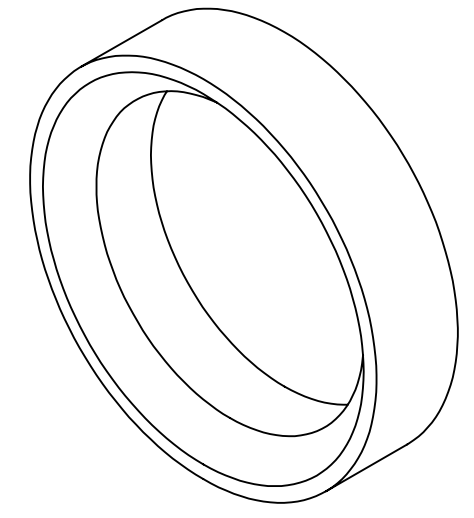
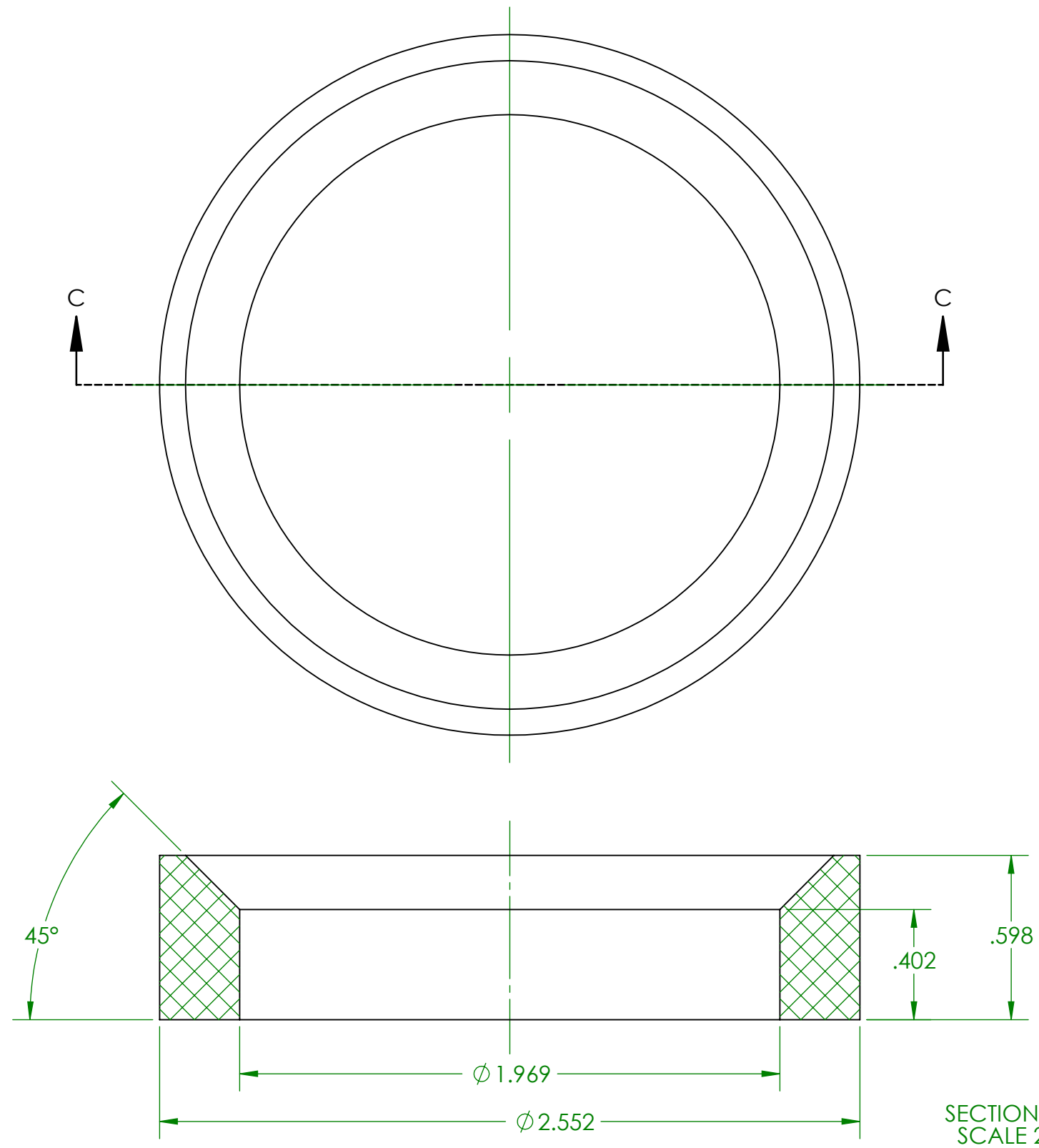
DATE:
06-04-2019

SHEET 2 OF 3

SCALE: 1:1

REV

SIZE
B



CUBE-DC-109002

UNLESS OTHERWISE SPECIFIED:
 DIMENSIONS ARE IN INCHES
 TOLERANCES:
 FRACTIONAL $\pm 0.5^\circ$
 TWO PLACE DECIMAL ± 0.005
 THREE PLACE DECIMAL ± 0.001

INTERPRET DRAWING
 PER ANSI Y14.5 2009

CAL POLY
SAN LUIS OBISPO

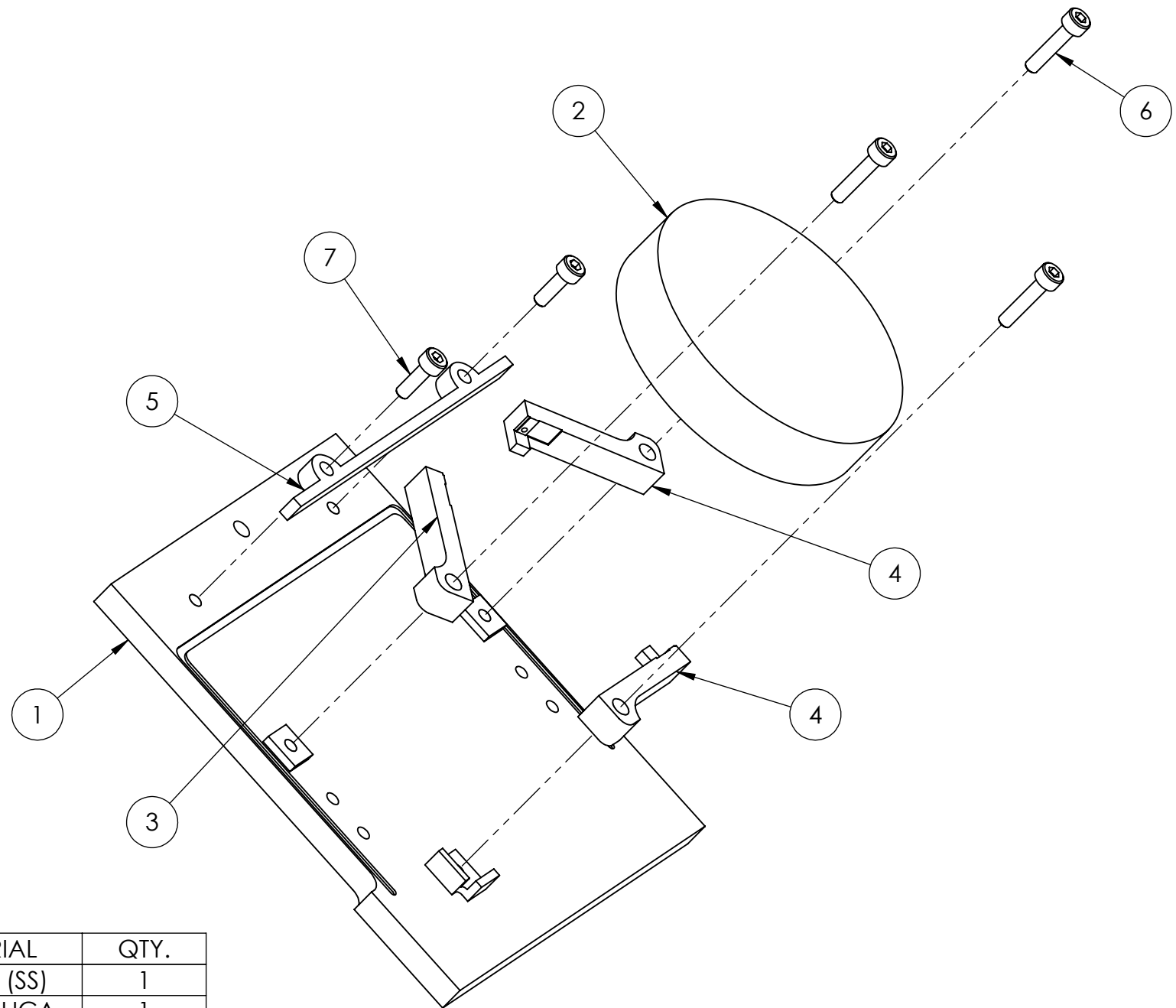
MATERIAL:
 SEE BOM
 DRAWN BY:
 JEFF WAGNER

TITLE:
 TOP MIRROR DELRIN MIRROR POSITIONER
 DATE:
 06-04-2019

SHEET 3 OF 3	SCALE: 2:1	REV	SIZE B
--------------	------------	-----	------------------

NOTES, UNLESS OTHERWISE SPECIFIED:

1. MATERIAL: ALUMINUM 6061-T651 PER AMS 4027 AND AMS 4150. FOR OTHER MATERIALS, SEE BOM.
2. BREAK EXTERNAL EDGES AND CORNERS .005 IN MAX UNLESS NOTED.
3. INTERNAL CORNER AND FILLET RADII .005 MAX UNLESS NOTED.
4. INSTALL HELICAL COIL INSERT PER NASM33537. REMOVE TANG.
5. DRAWING IS THE SOLE AUTHORITY FOR THE BASIC FORM, LOCATION, ORIENTATION, AND DIMENSIONAL CHARACTERISTICS OF ALL DESIGN FEATURES.

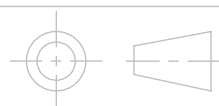


CUBE-DC-102000

ITEM NO.	PART NUMBER	DESCRIPTION	MATERIAL	QTY.
1	CUBE-DC-102001	BACKING PLATE	6061-T6 (SS)	1
2	CUBE-DC-102002	TOP MIRROR, 2 IN	FUSED SILICA	1
3	CUBE-DC-102003	LEFT HANDED FLEXURE, FLOW FROM BOTTOM	6061-T6 (SS)	1
4	CUBE-DC-102004	RIGHT HANDED FLEXURE, FLOW FROM BOTTOM	6061-T6 (SS)	2
5	CUBE-DC-102005	CLOSURE TAB	PEEK	1
6	B18.3.1M - 2.5 x 0.45 x 12 Hex SHCS -- 12NHX			3
7	B18.3.1M - 2.5 x 0.45 x 8 Hex SHCS -- 8NHX			2

UNLESS OTHERWISE SPECIFIED:
 DIMENSIONS ARE IN INCHES
 TOLERANCES:
 FRACTIONAL ± 0.5°
 TWO PLACE DECIMAL ± 0.005
 THREE PLACE DECIMAL ± 0.0025

INTERPRET DRAWING
 PER ANSI Y14.5 2009



CAL POLY
SAN LUIS OBISPO

MATERIAL:
 SEE BOM

DRAWN BY:
 PATRICK WHITESEL

TITLE:
 TOP MIRROR ASSEMBLY

DATE:
 06-02-19

SHEET 1 OF 5

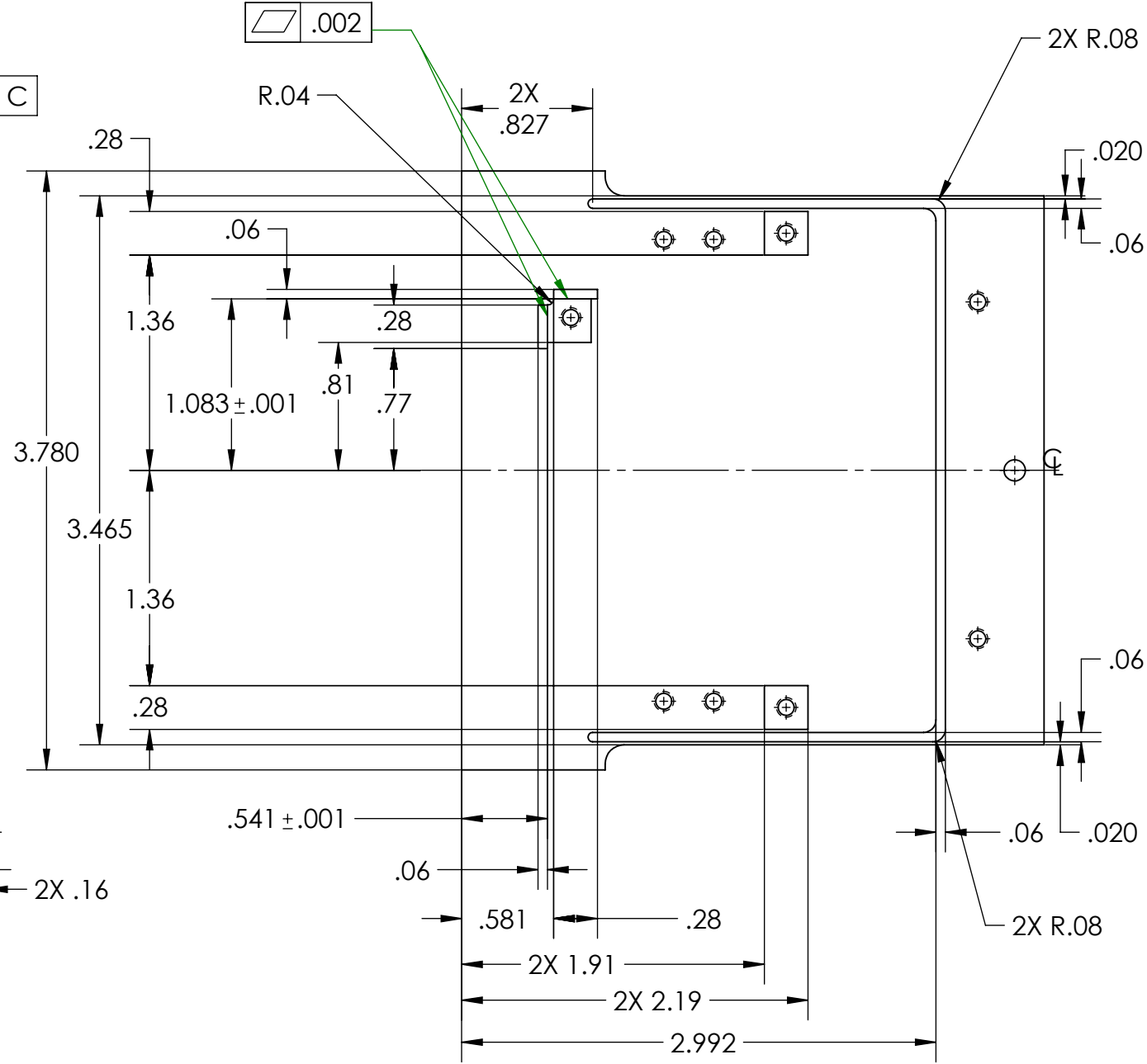
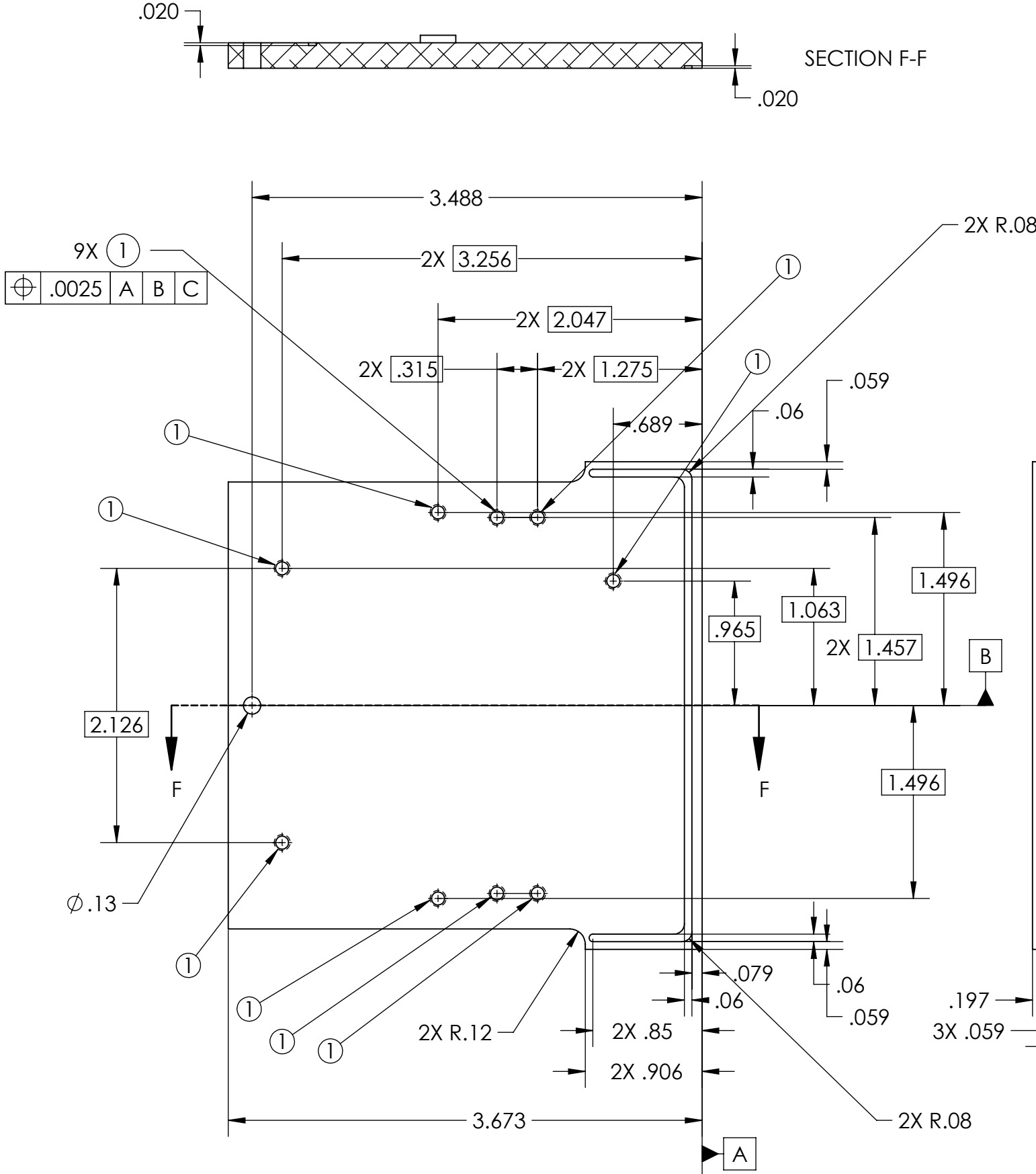
SCALE: 1:1

REV

SIZE
B

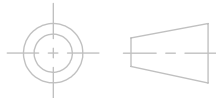
CUBE-DC-102001

- NOTE:
1. ALL DIMENSIONS IN INCHES UNLESS OTHERWISE STATED
 2. TOLERANCES UNLESS OTHERWISE STATED:
 X.X = $\pm .05$
 X.XX = $\pm .005$
 X.XXX = $\pm .001$
 3. (1) INDICATES FOLLOWING CALLOUT
 TAPPED HOLE FOR M2.5X0.45 HELICOIL
 THRU ALL



UNLESS OTHERWISE SPECIFIED:
 DIMENSIONS ARE IN INCHES
 TOLERANCES:
 FRACTIONAL $\pm 0.5^\circ$
 TWO PLACE DECIMAL ± 0.005
 THREE PLACE DECIMAL ± 0.0025

INTERPRET DRAWING
 PER ANSI Y14.5 2009



CAL POLY
SAN LUIS OBISPO

MATERIAL:
 SEE BOM

DRAWN BY:
 PATRICK WHITESEL

TITLE:
 BACKING PLATE

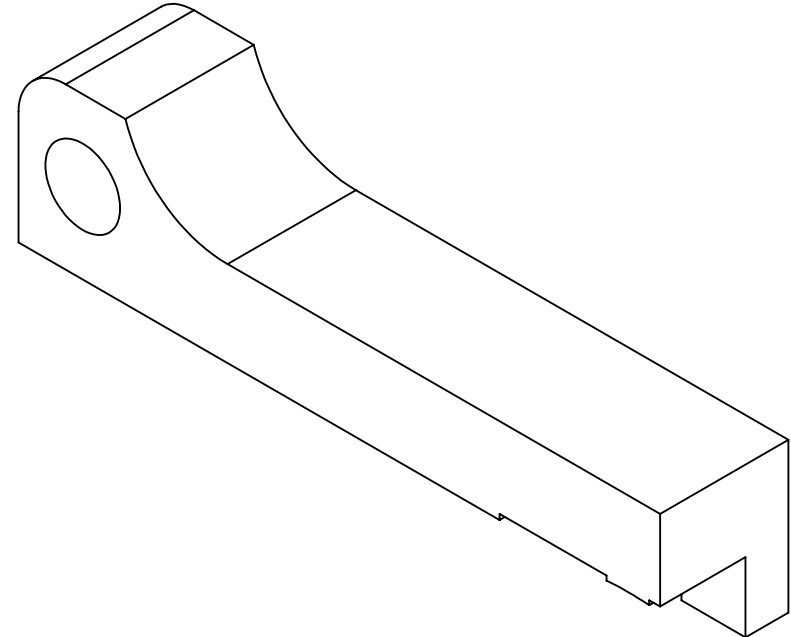
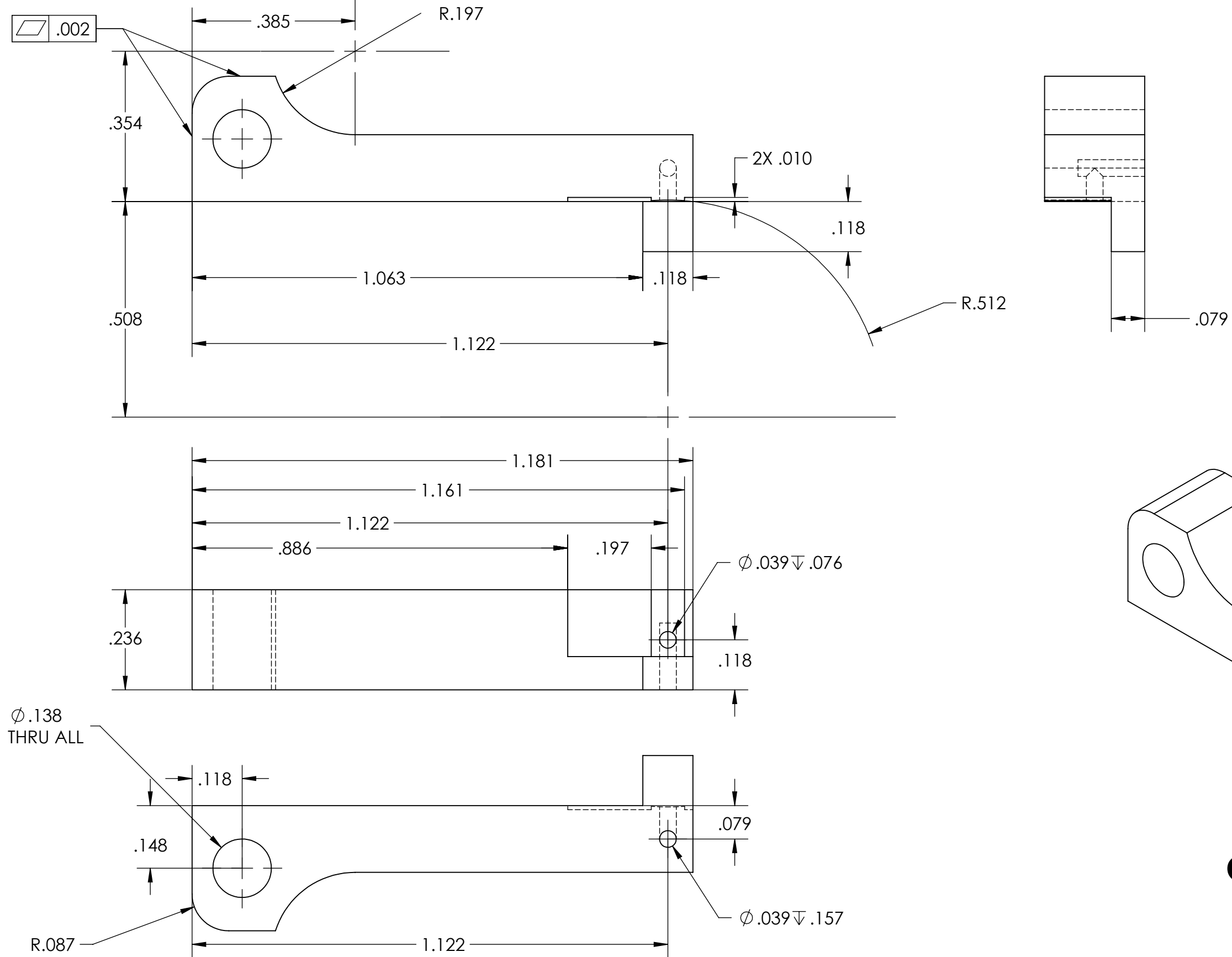
DATE:
 06-02-19

SHEET 2 OF 5


SCALE: 1:1

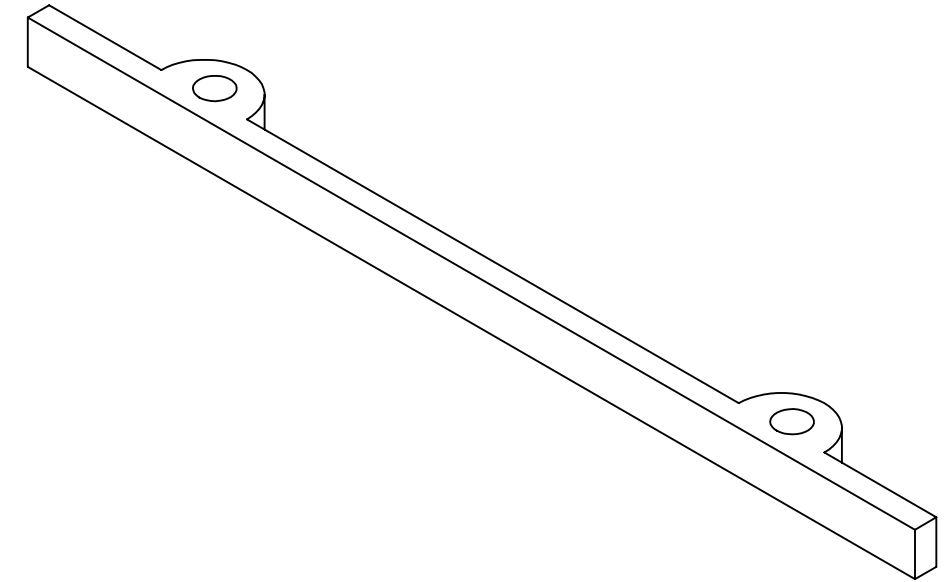
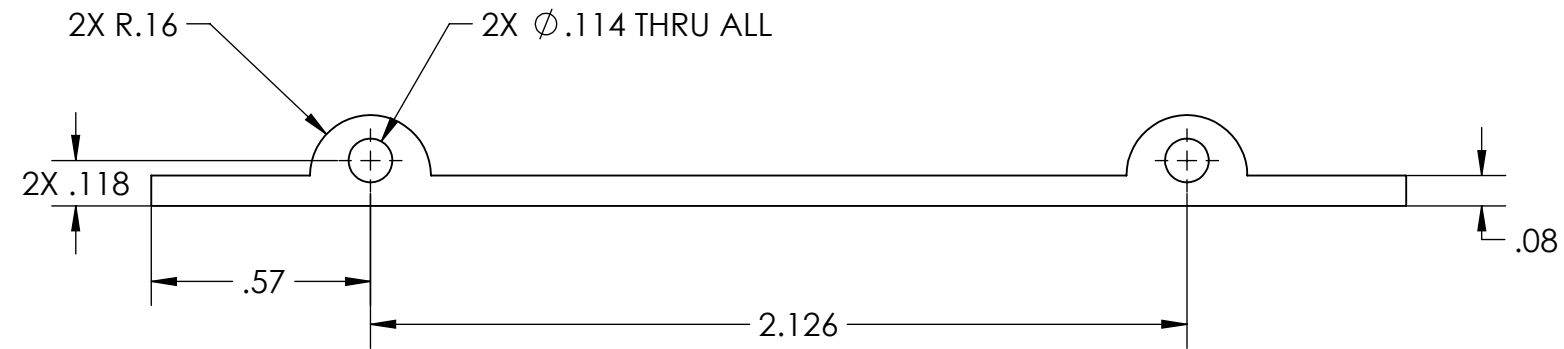
REV

SIZE
B

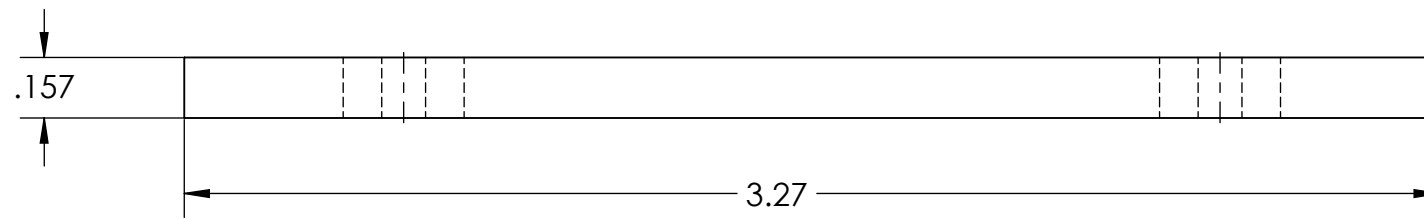


CUBE-DC-102003

<p>UNLESS OTHERWISE SPECIFIED: DIMENSIONS ARE IN INCHES TOLERANCES: FRACTIONAL ± 0.5° TWO PLACE DECIMAL ± 0.005 THREE PLACE DECIMAL ± 0.0025</p>	<p>INTERPRET DRAWING PER ANSI Y14.5 2009</p> 	<p>CAL POLY SAN LUIS OBISPO</p>	<p>MATERIAL: SEE BOM</p> <p>DRAWN BY: JEFF WAGNER</p>	<p>TITLE: LEFT HANDED FLEXURE, FLOW FROM BOTTOM</p> <p>DATE: 06-04-2019</p>	<p>SHEET 3 OF 5</p>	<p>SCALE: 4:1</p>	<p>REV</p>	<p>SIZE B</p>
---	---	--	---	---	---------------------	-------------------	------------	---------------------------

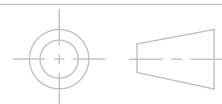


CUBE-DC-102005



UNLESS OTHERWISE SPECIFIED:
 DIMENSIONS ARE IN INCHES
 TOLERANCES:
 FRACTIONAL $\pm 0.5^\circ$
 TWO PLACE DECIMAL ± 0.005
 THREE PLACE DECIMAL ± 0.0025

INTERPRET DRAWING
 PER ANSI Y14.5 2009



CAL POLY
SAN LUIS OBISPO

MATERIAL:
 SEE BOM

DRAWN BY:
 PATRICK WHITESEL

TITLE:
 CLOSURE TAB

DATE:
 06-02-19

SHEET 5 OF 5

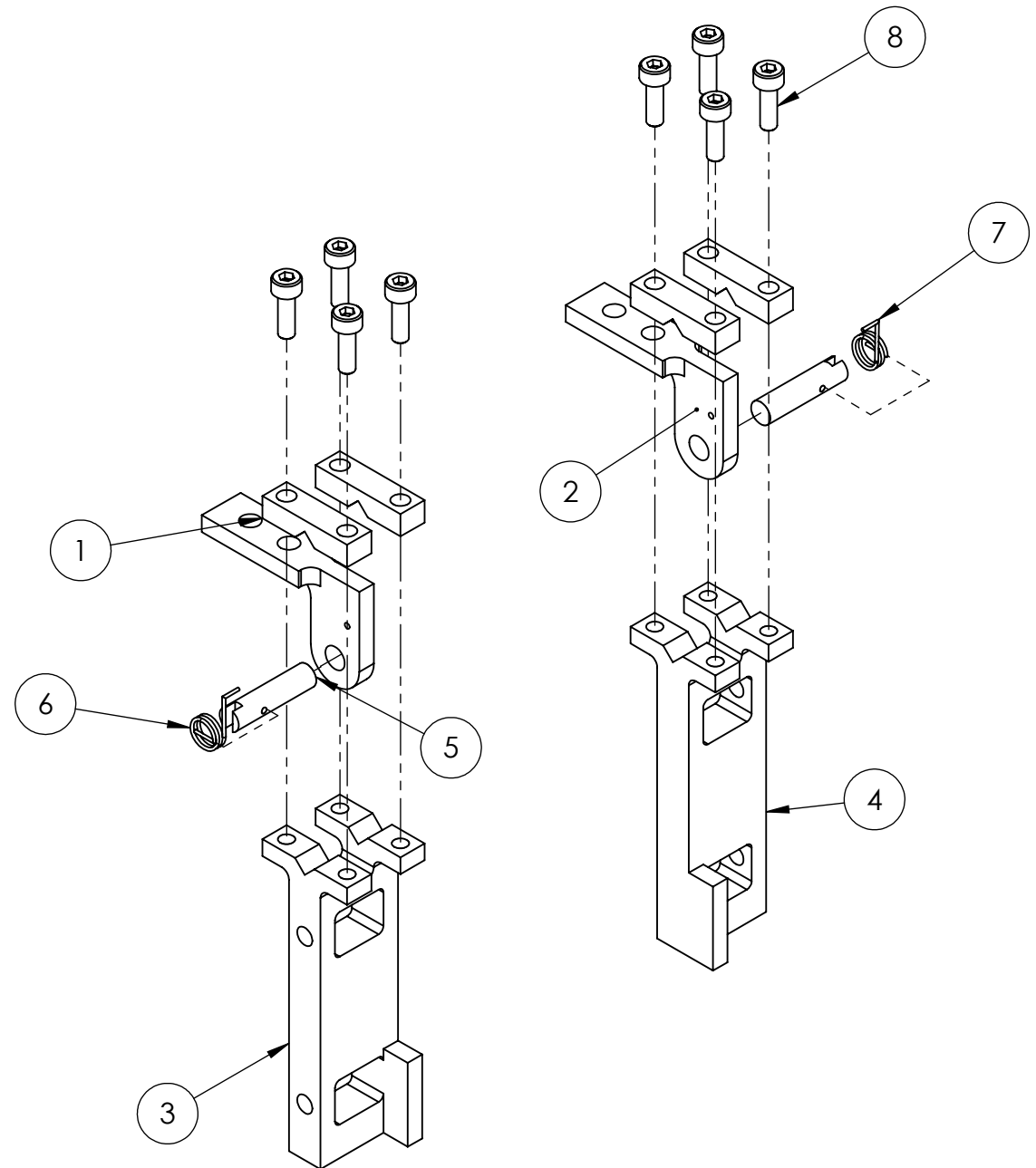
SCALE: 2:1

REV

SIZE
B

NOTES, UNLESS OTHERWISE SPECIFIED:

1. MATERIAL: ALUMINUM 6061-T651 PER AMS 4027 AND AMS 4150. FOR OTHER MATERIALS, SEE BOM.
2. BREAK EXTERNAL EDGES AND CORNERS .005 IN MAX UNLESS NOTED.
3. INTERNAL CORNER AND FILLET RADII .005 MAX UNLESS NOTED.
4. INSTALL HELICAL COIL INSERT PER NASM33537. REMOVE TANG.
5. DRAWING IS THE SOLE AUTHORITY FOR THE BASIC FORM, LOCATION, ORIENTATION, AND DIMENSIONAL CHARACTERISTICS OF ALL DESIGN FEATURES.
- 6.

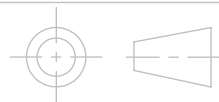


CUBE-DC-103000

ITEM NO.	PART NUMBER	DESCRIPTION	MATERIAL	Stowed/ QTY.
1	CUBE-DC-103001	CLAMP COVER	6061-T6 (SS)	4
2	CUBE-DC-103007	TOP MIRROR JOURNAL	TEFLON NICKEL PLATED STAINLESS STEEL	2
3	CUBE-DC-103002	HINGE TOWER LEFT	6061-T6 (SS)	1
4	CUBE-DC-103003	HINGE TOWER RIGHT	6061-T6 (SS)	1
5	CUBE-DC-103004	TOP COVER SHAFT	544 BRONZE	2
6	CUBE-DC-103005-03	TOP HINGE LEFT SPRING, 3 TURN	Alloy Steel (SS)	1
7	CUBE-DC-103006-03	TOP HINGE RIGHT SPRING, 3 TURN	Alloy Steel (SS)	1
8	B18.3.1M - 2.5 x 0.45 x 8 Hex SHCS -- 8NHX			8

UNLESS OTHERWISE SPECIFIED:
 DIMENSIONS ARE IN INCHES
 TOLERANCES:
 FRACTIONAL ± 0.5°
 TWO PLACE DECIMAL ± 0.005
 THREE PLACE DECIMAL ± 0.0025

INTERPRET DRAWING
 PER ANSI Y14.5 2009



CAL POLY
SAN LUIS OBISPO

MATERIAL:
 SEE BOM

DRAWN BY:
 PATRICK WHITESEL

TITLE:
 TOP HINGE ASSEMBLY

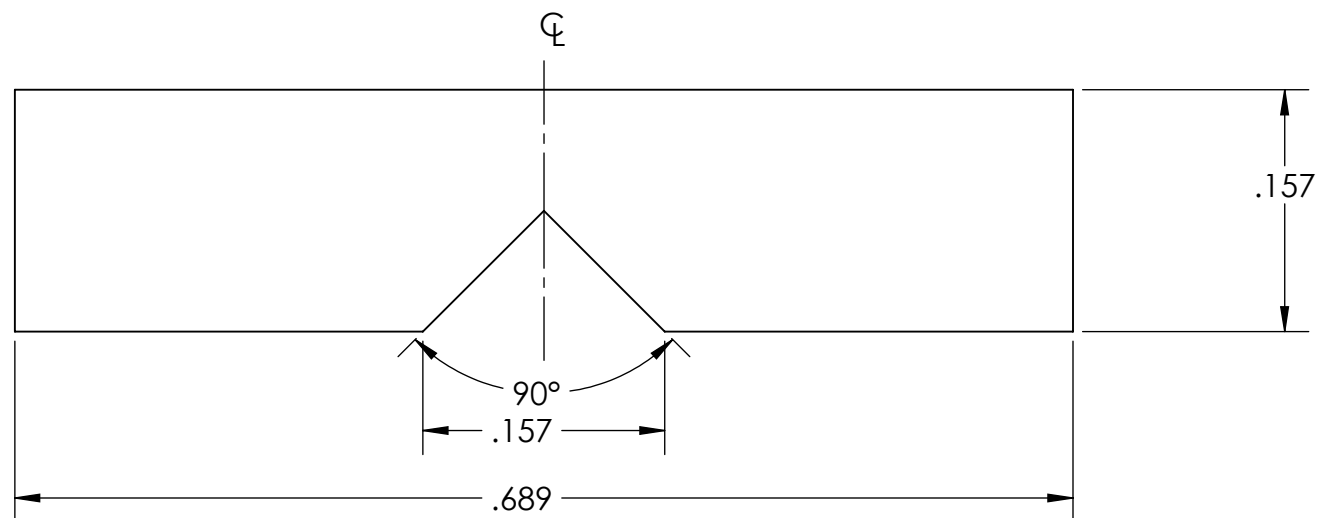
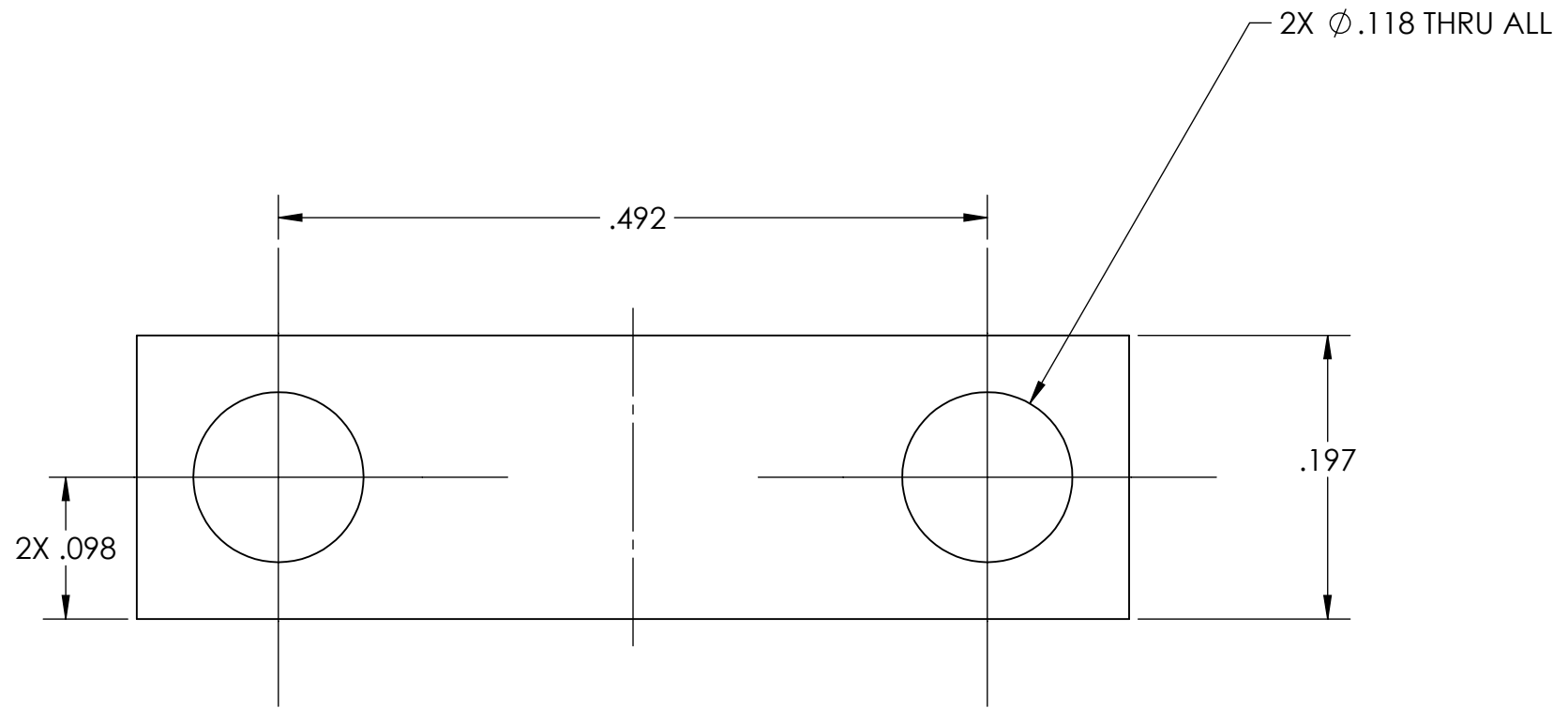
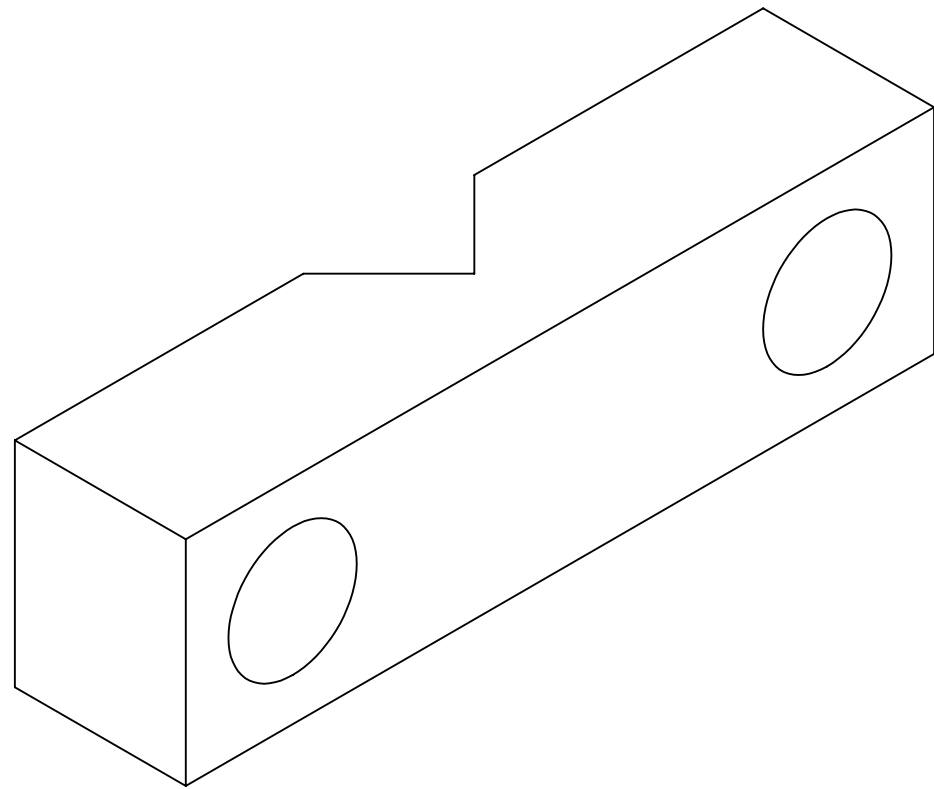
DATE:
 06-04-19

SHEET 1 OF 7

SCALE: 1:1

REV

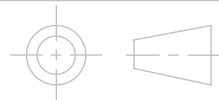
SIZE
B



CUBE-DC-103001

UNLESS OTHERWISE SPECIFIED:
 DIMENSIONS ARE IN INCHES
 TOLERANCES:
 FRACTIONAL ± 0.5°
 TWO PLACE DECIMAL ± 0.005
 THREE PLACE DECIMAL ± 0.0025

INTERPRET DRAWING
 PER ANSI Y14.5 2009



CAL POLY
SAN LUIS OBISPO

MATERIAL:
 SEE BOM

DRAWN BY:
 PATRICK WHITESEL

TITLE:
 CLAMP COVER

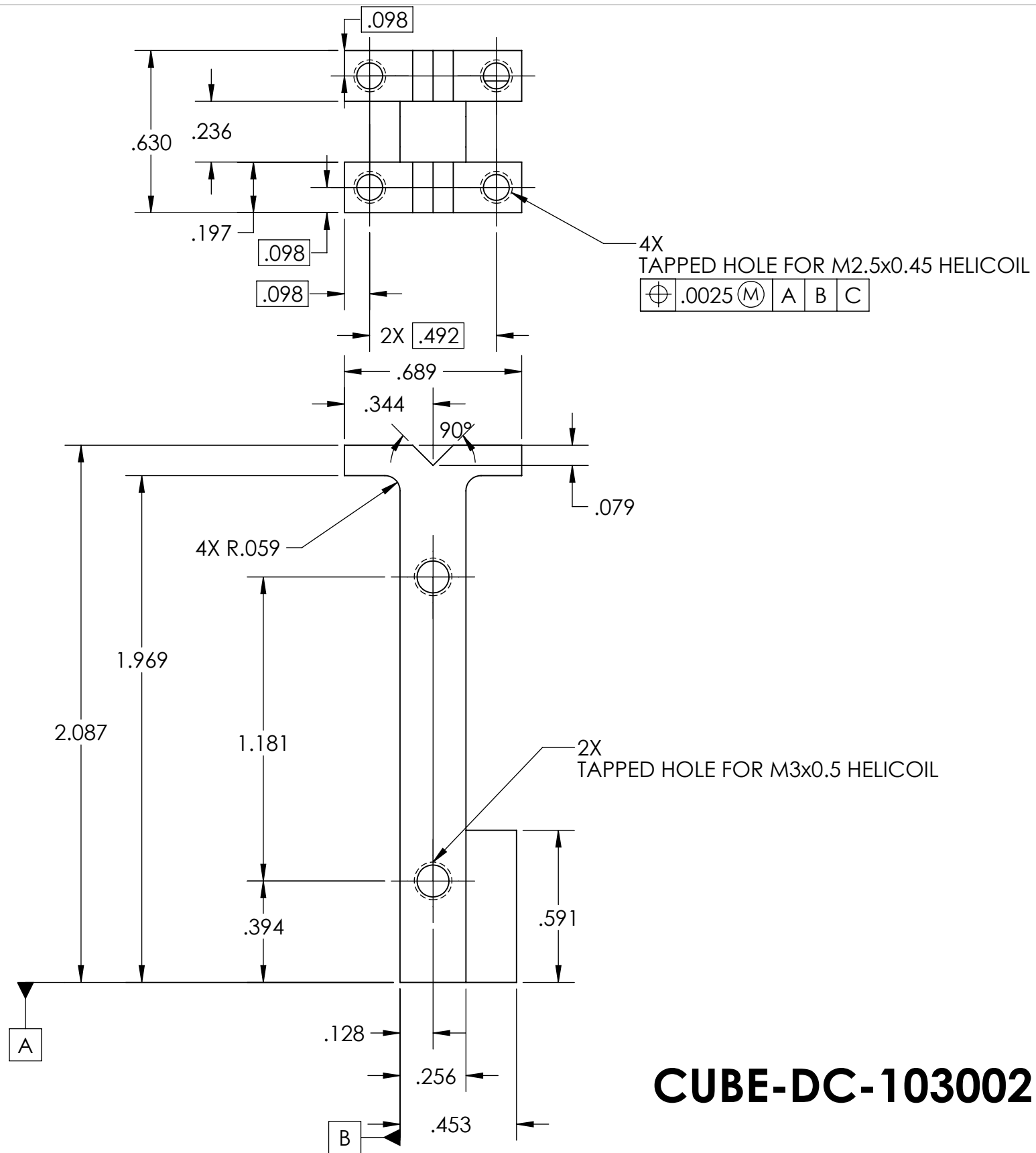
DATE:
 06-04-19

SHEET 2 OF 7

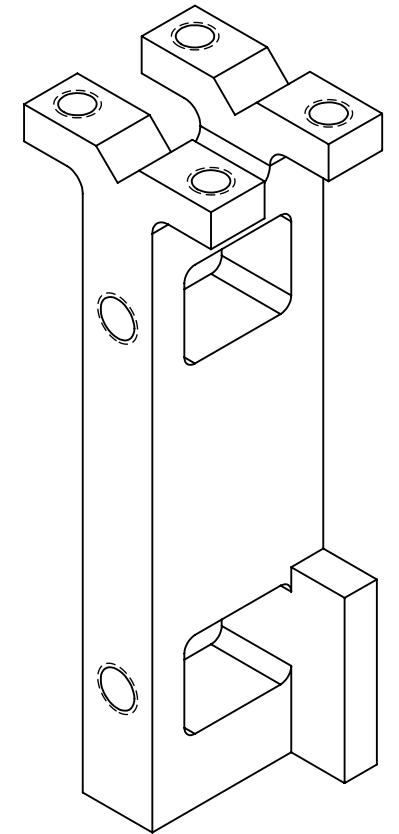
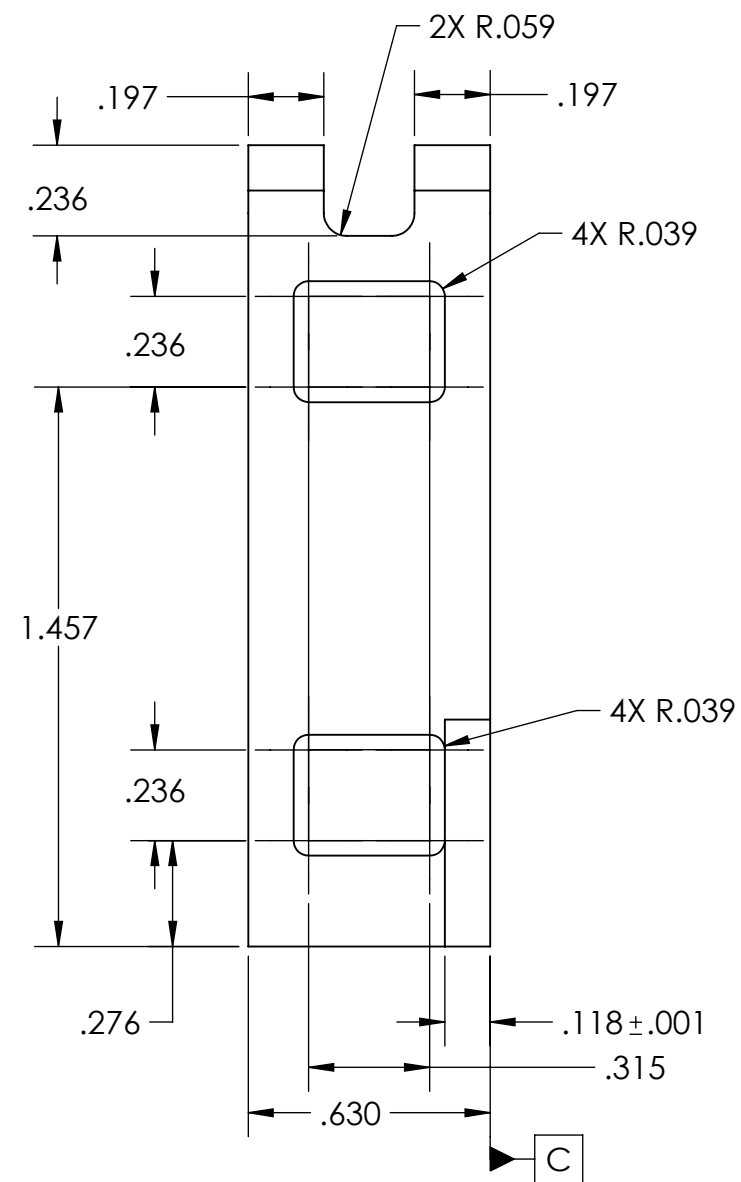
SCALE: 8:1

REV

SIZE
B

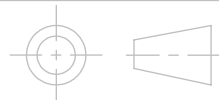


CUBE-DC-103002



UNLESS OTHERWISE SPECIFIED:
DIMENSIONS ARE IN INCHES
TOLERANCES:
FRACTIONAL $\pm 0.5^\circ$
TWO PLACE DECIMAL ± 0.005
THREE PLACE DECIMAL ± 0.0025

INTERPRET DRAWING
PER ANSI Y14.5 2009



CAL POLY
SAN LUIS OBISPO

MATERIAL:
SEE BOM

DRAWN BY:
PATRICK WHITESEL

TITLE:
HINGE TOWER LEFT

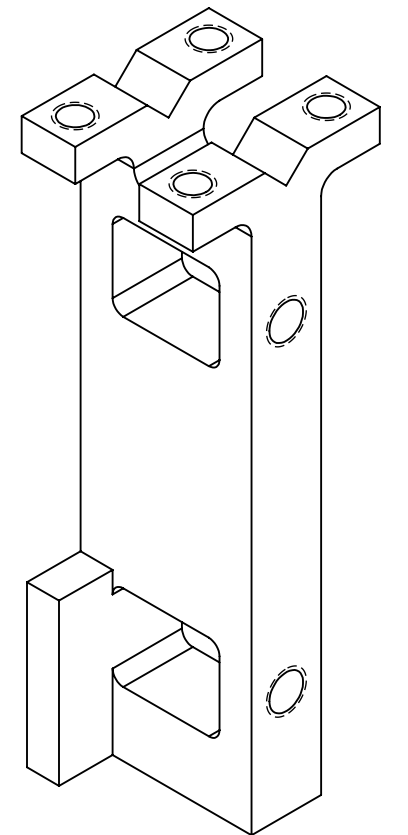
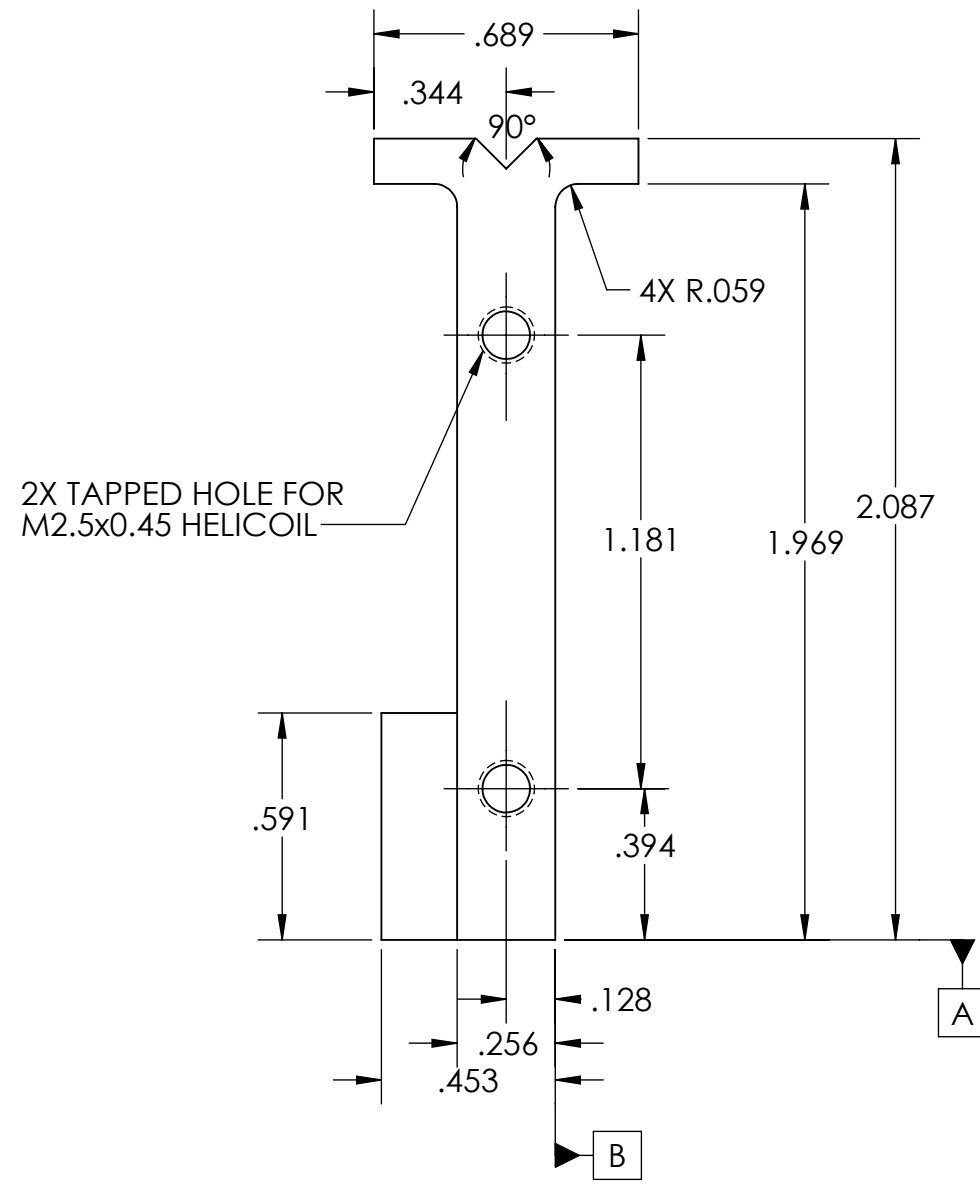
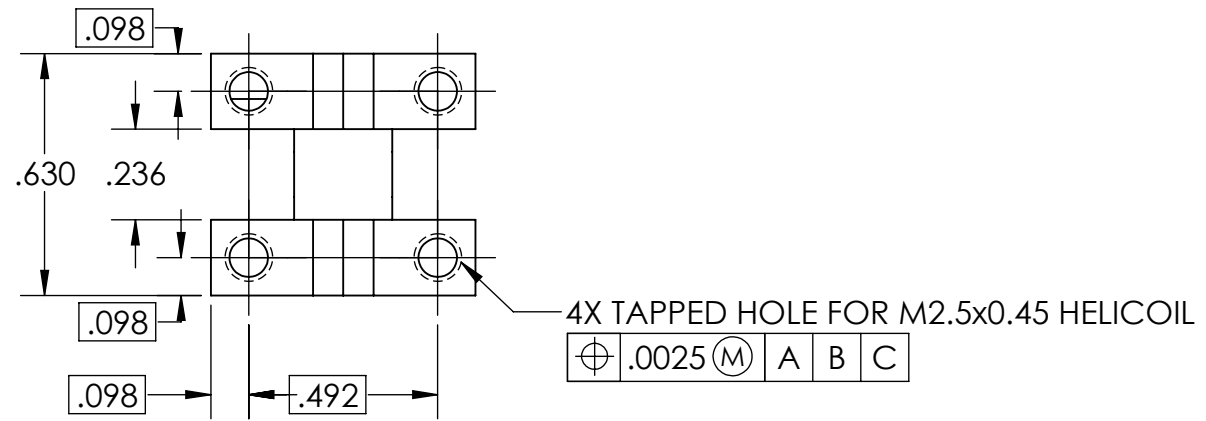
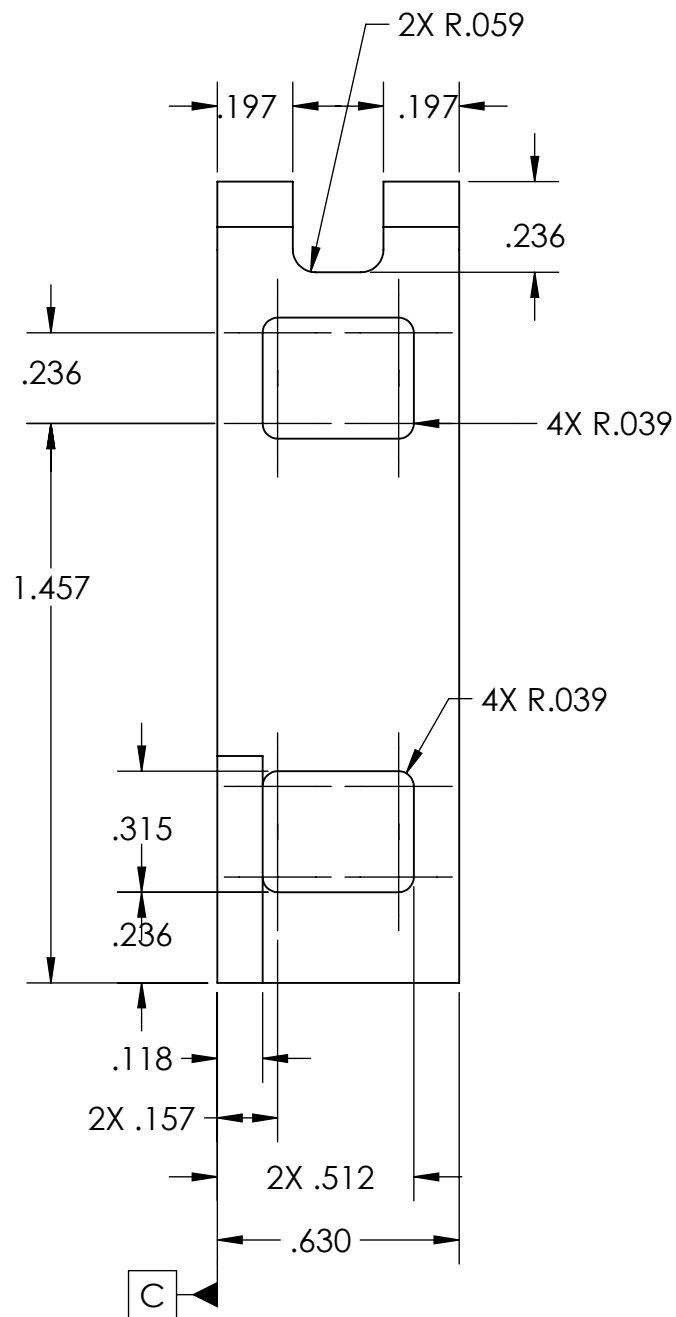
DATE:
06-04-19

SHEET 3 OF 7

SCALE: 2:1

REV

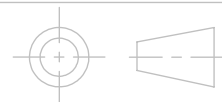
SIZE
B



CUBE-DC-103003

UNLESS OTHERWISE SPECIFIED:
 DIMENSIONS ARE IN INCHES
 TOLERANCES:
 FRACTIONAL $\pm 0.5^\circ$
 TWO PLACE DECIMAL ± 0.005
 THREE PLACE DECIMAL ± 0.0025

INTERPRET DRAWING
 PER ANSI Y14.5 2009



CAL POLY
SAN LUIS OBISPO

MATERIAL:
 SEE BOM

DRAWN BY:
 EDWIN RAINVILLE

TITLE:
 HINGE TOWER RIGHT

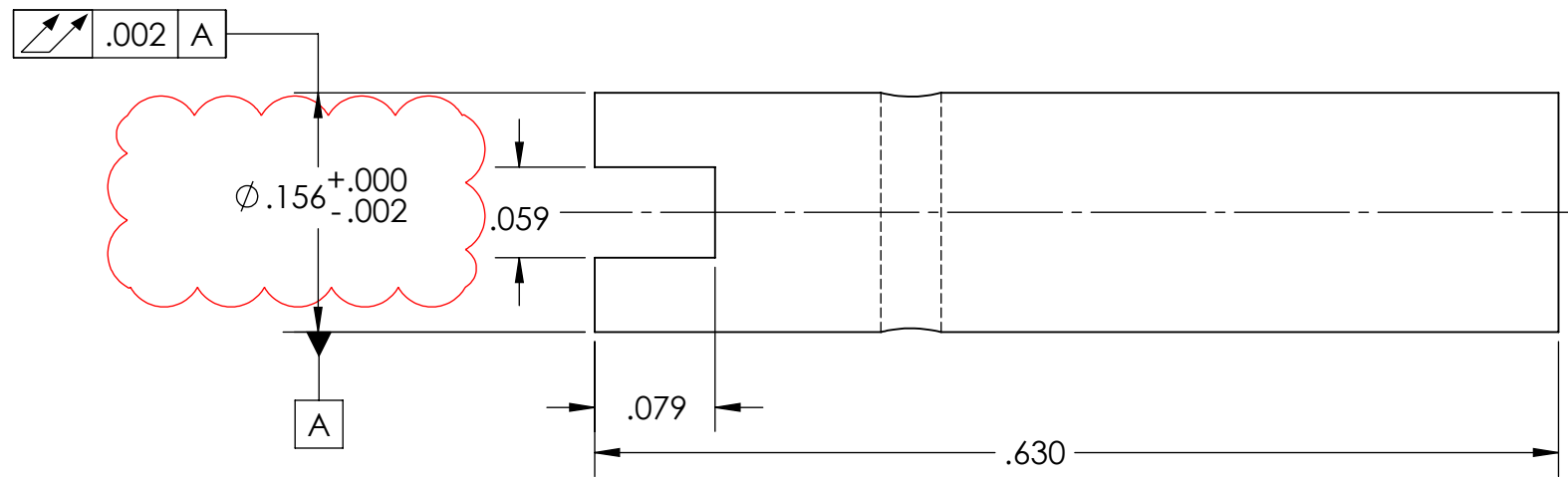
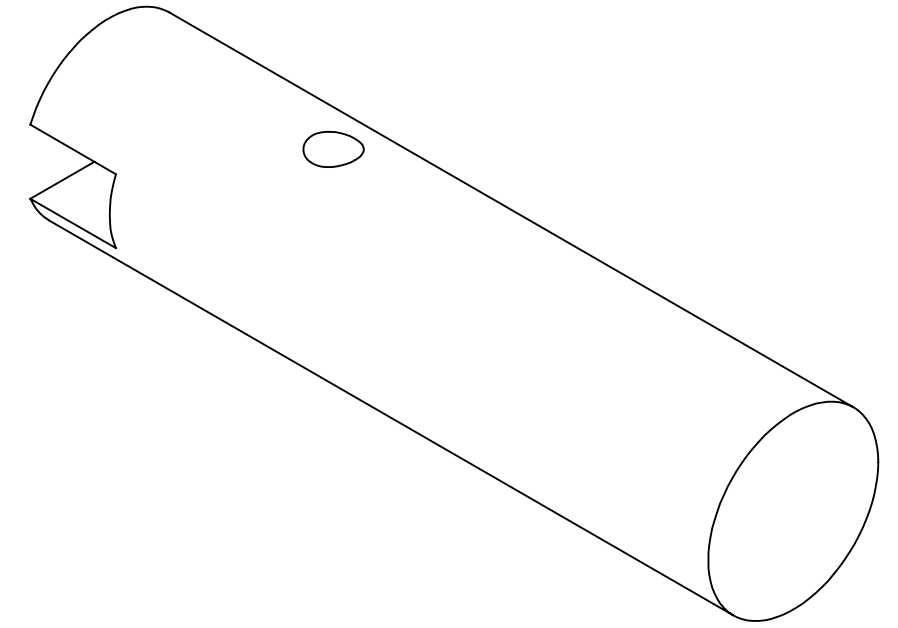
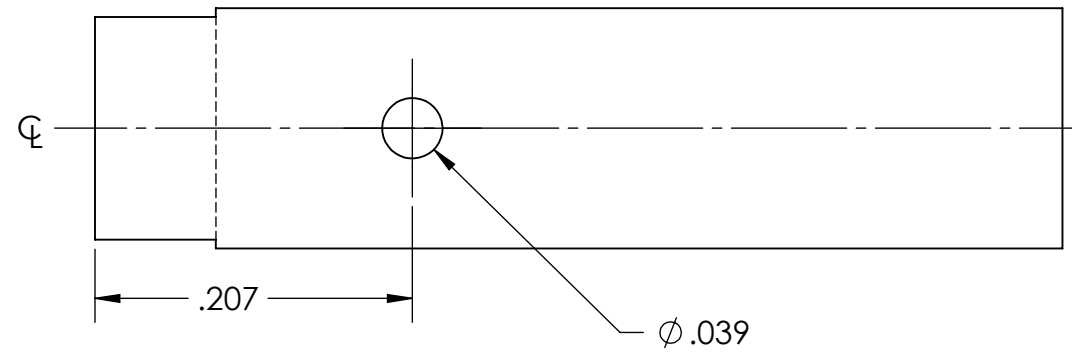
DATE:
 06-04-2019

SHEET 4 OF 7

SCALE: 2:1

REV

SIZE
B

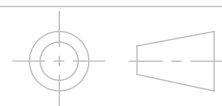


SHAFT DIMENSION CHANGED FROM M4 g6 SHAFT TO ACTUAL SHAFT DIMENSION OF SENIOR PROJECT.
TOLERANCE SHOULD BE ADJUSTED TO ENSURE FIT WITH PLATED JOURNAL.

CUBE-DC-103004

UNLESS OTHERWISE SPECIFIED:
DIMENSIONS ARE IN INCHES
TOLERANCES:
FRACTIONAL $\pm 0.5^\circ$
TWO PLACE DECIMAL ± 0.005
THREE PLACE DECIMAL ± 0.0025

INTERPRET DRAWING
PER ANSI Y14.5 2009



CAL POLY
SAN LUIS OBISPO

MATERIAL:
SEE BOM

DRAWN BY:
EDWIN RAINVILLE

TITLE:
TOP COVER SHAFT

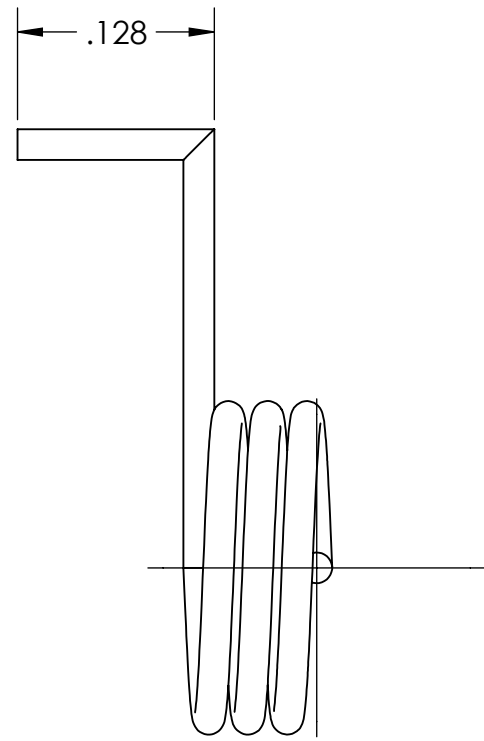
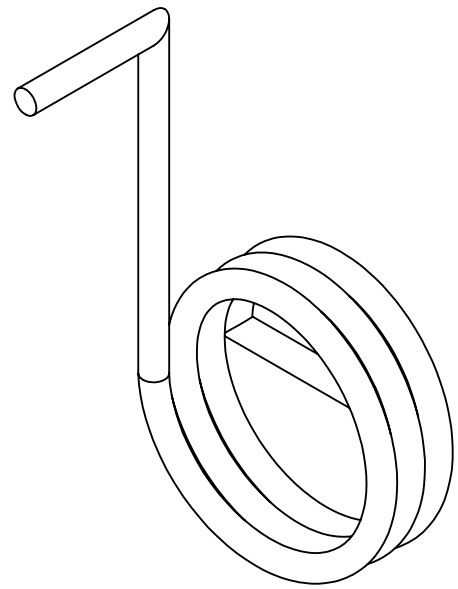
DATE:
12-04-2019

SHEET 5 OF 7

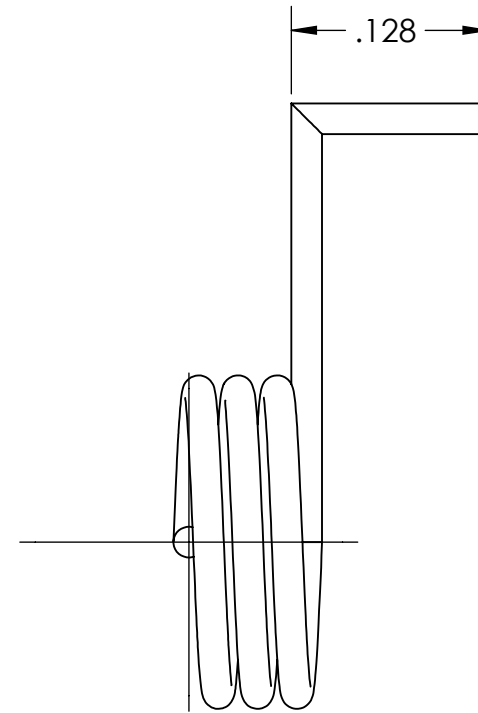
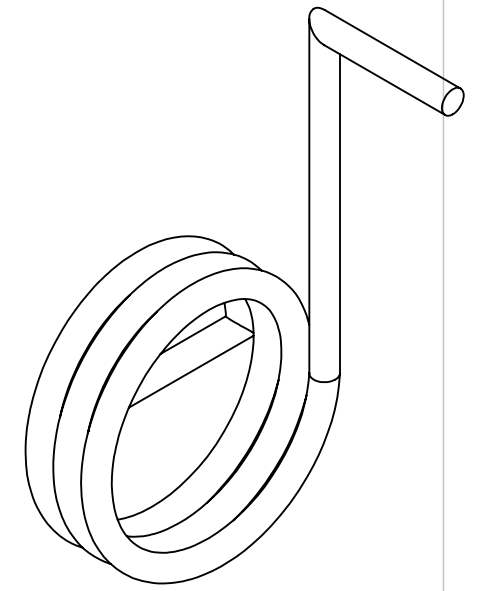
SCALE: 8:1

REV

SIZE
B



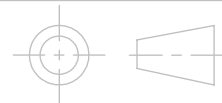
CUBE-DC-103005-03



CUBE-DC-103006-03

UNLESS OTHERWISE SPECIFIED:
 DIMENSIONS ARE IN INCHES
 TOLERANCES:
 FRACTIONAL $\pm 0.5^\circ$
 TWO PLACE DECIMAL ± 0.005
 THREE PLACE DECIMAL ± 0.0025

INTERPRET DRAWING
 PER ANSI Y14.5 2009



CAL POLY
SAN LUIS OBISPO

MATERIAL:
 SEE BOM

DRAWN BY:
 EDWIN RAINVILLE

TITLE:
 TOP HINGE LEFT AND RIGHT SPRING, 3 TURN

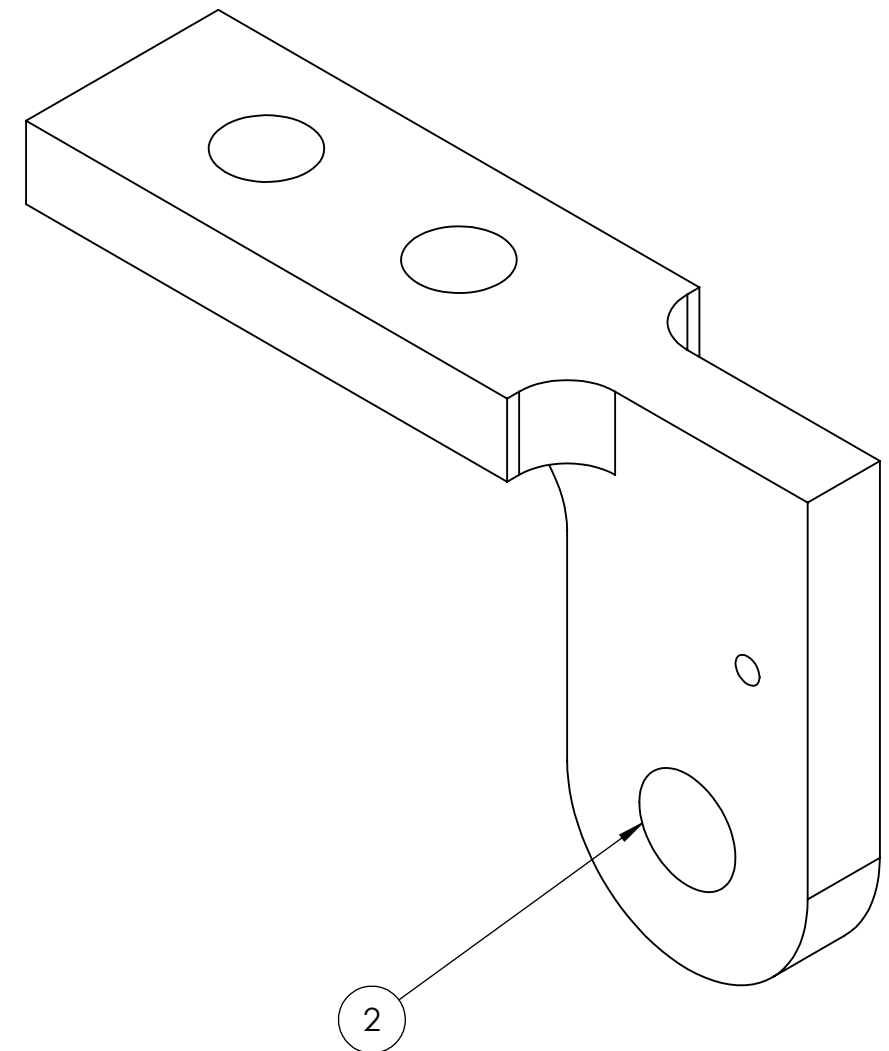
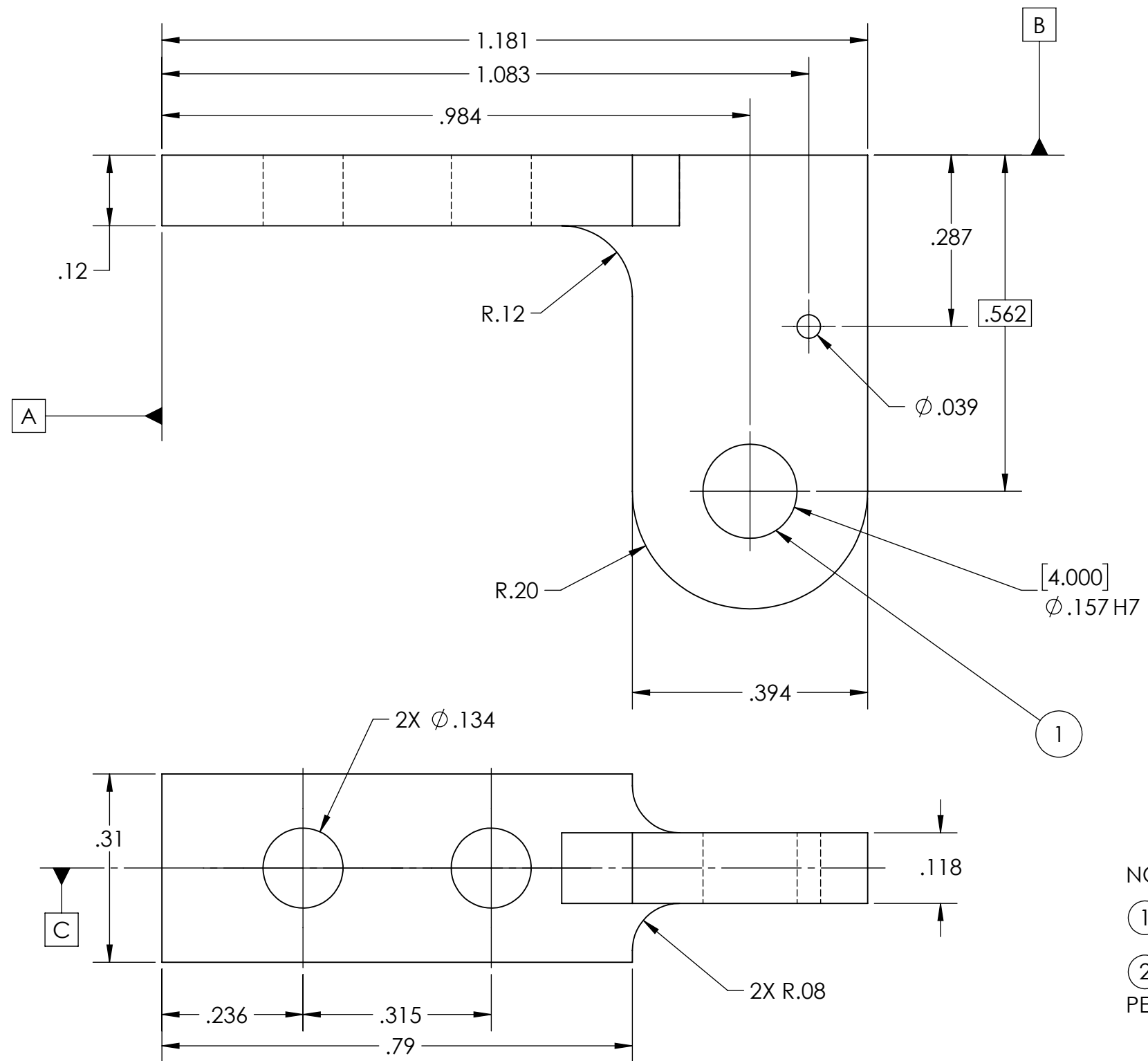
DATE:
 06-04-18

SHEET 6 OF 7

SCALE: 8:1

REV

SIZE
B



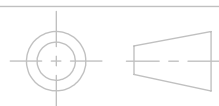
NOTE:

- ① MAKE HOLE TO 4 MM H7 STANDARD PER ANSI B4.2-1978
- ② INTERNAL SURFACE TO BE PLATED: ELECTROLESS NICKEL W/ TEFLON PER MIL-C-26074E GRADE A

CUBE-DC-103007

UNLESS OTHERWISE SPECIFIED:
 DIMENSIONS ARE IN INCHES
 TOLERANCES:
 FRACTIONAL $\pm 0.5^\circ$
 TWO PLACE DECIMAL ± 0.005
 THREE PLACE DECIMAL ± 0.0025

INTERPRET DRAWING
 PER ANSI Y14.5 2009



CAL POLY
SAN LUIS OBISPO

MATERIAL:
 SEE BOM

DRAWN BY:
 EDWIN RAINVILLE

TITLE:
 TOP MIRROR JOURNAL

DATE:
 09-30-2019

SHEET 7 OF 7

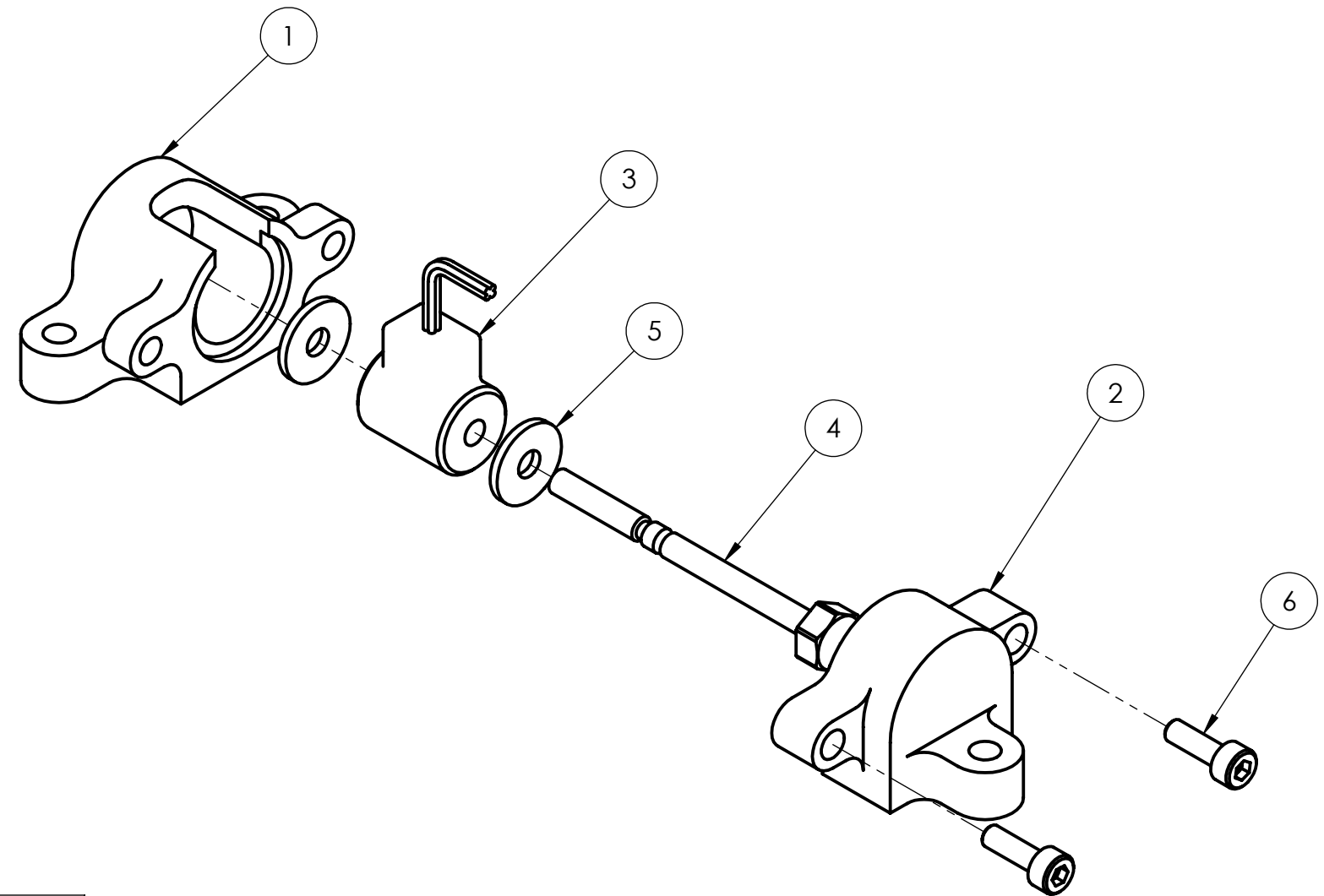
SCALE: 4.5:1

REV

SIZE
B

NOTES, UNLESS OTHERWISE SPECIFIED:

1. MATERIAL: ALUMINUM 6061-T651 PER AMS 4027 AND AMS 4150. FOR OTHER MATERIALS, SEE BOM.
2. BREAK EXTERNAL EDGES AND CORNERS .005 IN MAX UNLESS NOTED.
3. INTERNAL CORNER AND FILLET RADII .005 MAX UNLESS NOTED.
4. INSTALL HELICAL COIL INSERT PER NASM33537. REMOVE TANG.
5. DRAWING IS THE SOLE AUTHORITY FOR THE BASIC FORM, LOCATION, ORIENTATION, AND DIMENSIONAL CHARACTERISTICS OF ALL DESIGN FEATURES.

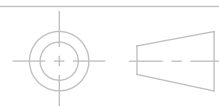


CUBE-DC-104000

ITEM NO.	PART NUMBER	DESCRIPTION	QTY.
1	CUBE-DC-104001	FRANGIBOLT HOUSING - TOP	1
2	CUBE-DC-104002	FRANGIBOLT HOUSING - BOTTOM	1
3	FRANGIBOLT ACTUATOR FD04 STD #4	FRANGIBOLT ACTUATOR	1
4	ICON-FUV-MEC-695 Frangibolt Bolt - LENGTHENED	FRANGIBOLT	1
5	flat washer type b regular_ai		2
6	B18.3.1M - 2.5 x 0.45 x 5 Hex SHCS -- 5NHX		2

UNLESS OTHERWISE SPECIFIED:
 DIMENSIONS ARE IN INCHES
 TOLERANCES:
 FRACTIONAL $\pm 0.5^\circ$
 TWO PLACE DECIMAL ± 0.005
 THREE PLACE DECIMAL ± 0.0025

INTERPRET DRAWING
 PER ANSI Y14.5 2009



CAL POLY
SAN LUIS OBISPO

MATERIAL:
 SEE BOM

DRAWN BY:
 PATRICK WHITESEL

TITLE:
 ACTUATION ASSEMBLY

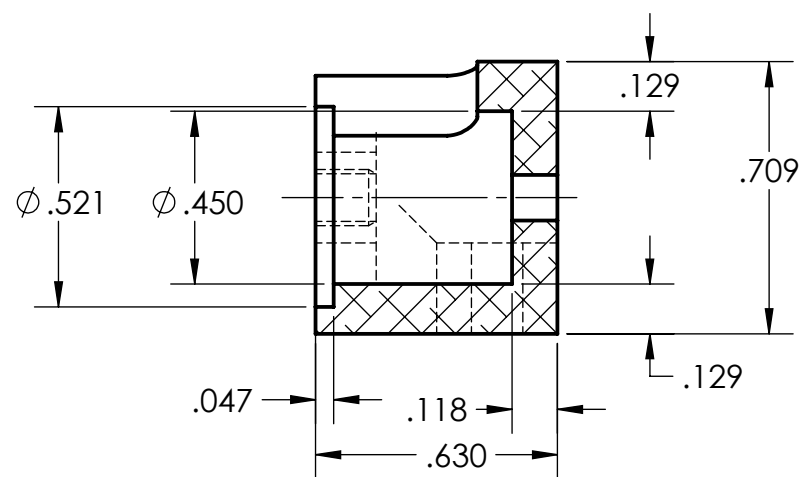
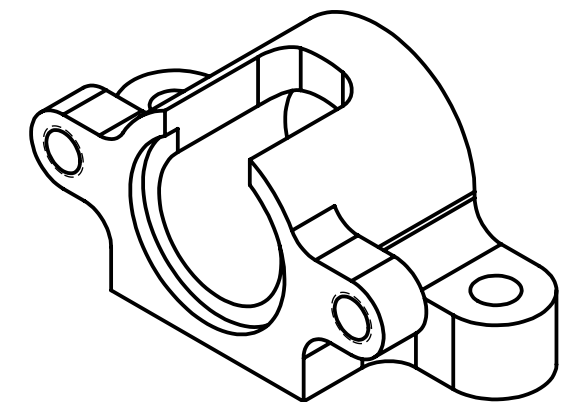
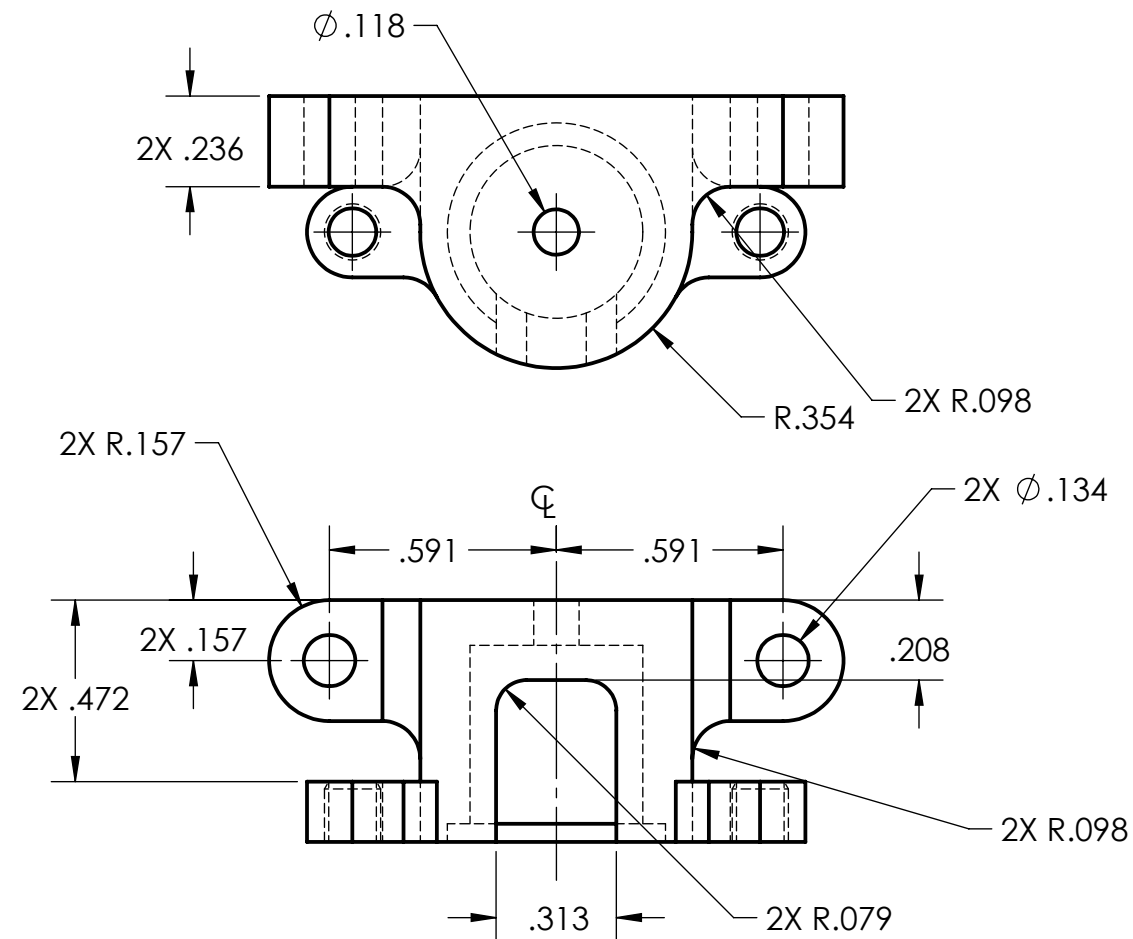
DATE:
 06-04-2019

SHEET 1 OF 4

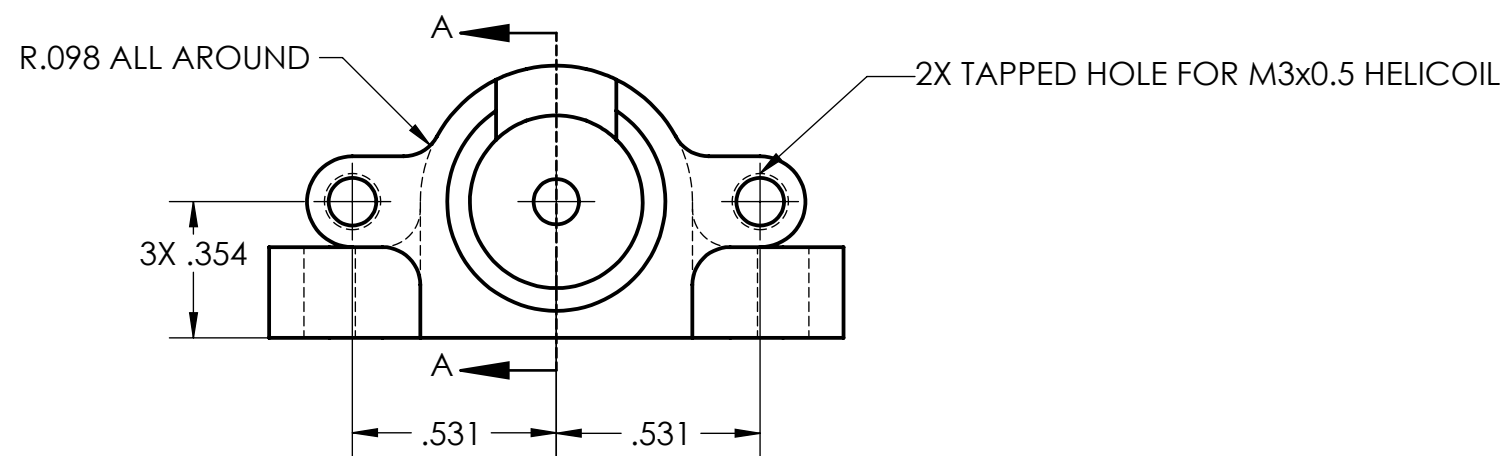
SCALE: 3:2

REV

SIZE
B



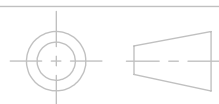
SECTION A-A
SCALE 2 : 1



CUBE-DC-104001

UNLESS OTHERWISE SPECIFIED:
DIMENSIONS ARE IN INCHES
TOLERANCES:
FRACTIONAL $\pm 0.5^\circ$
TWO PLACE DECIMAL ± 0.005
THREE PLACE DECIMAL ± 0.0025

INTERPRET DRAWING
PER ANSI Y14.5 2009



CAL POLY
SAN LUIS OBISPO

MATERIAL:
SEE BOM

DRAWN BY:
JEFF WAGNER

TITLE:
FRANGIBOLT TOP HOUSING

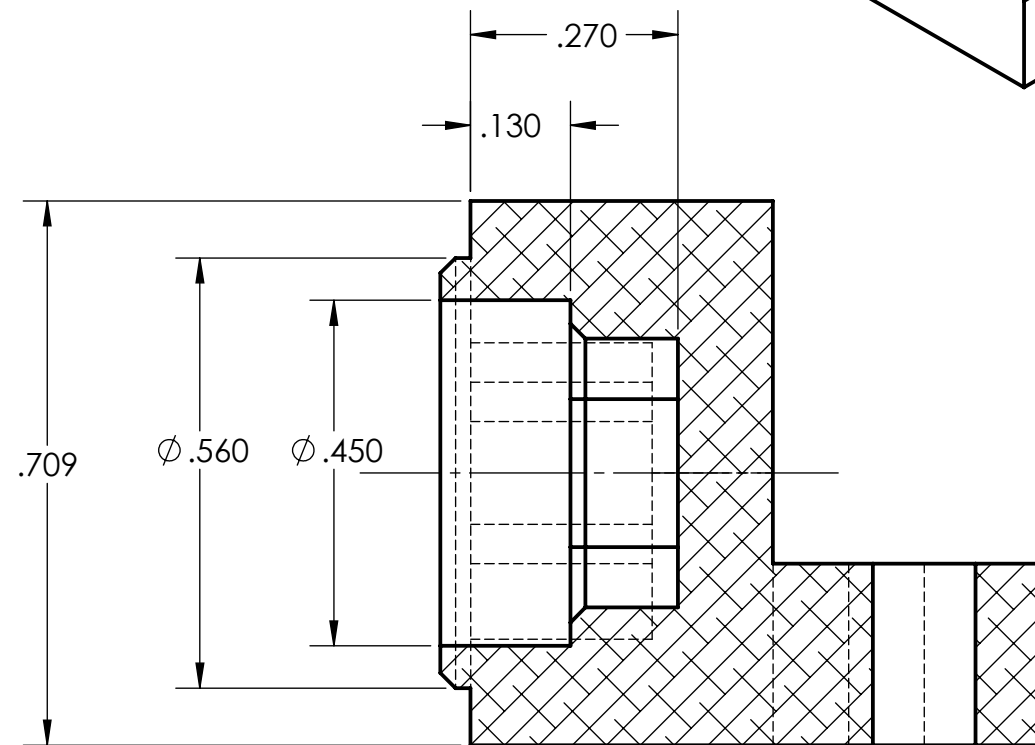
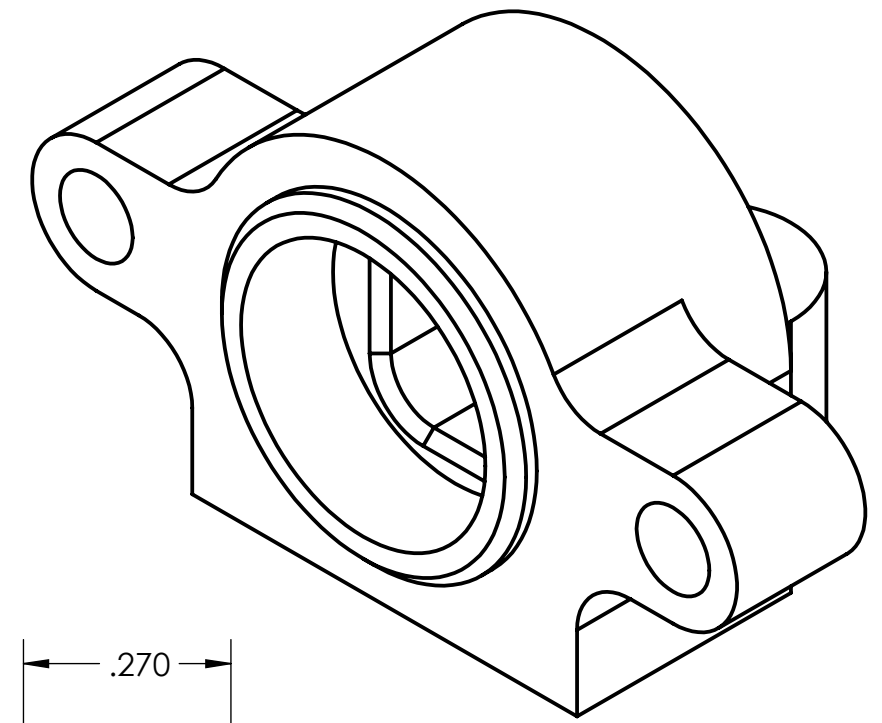
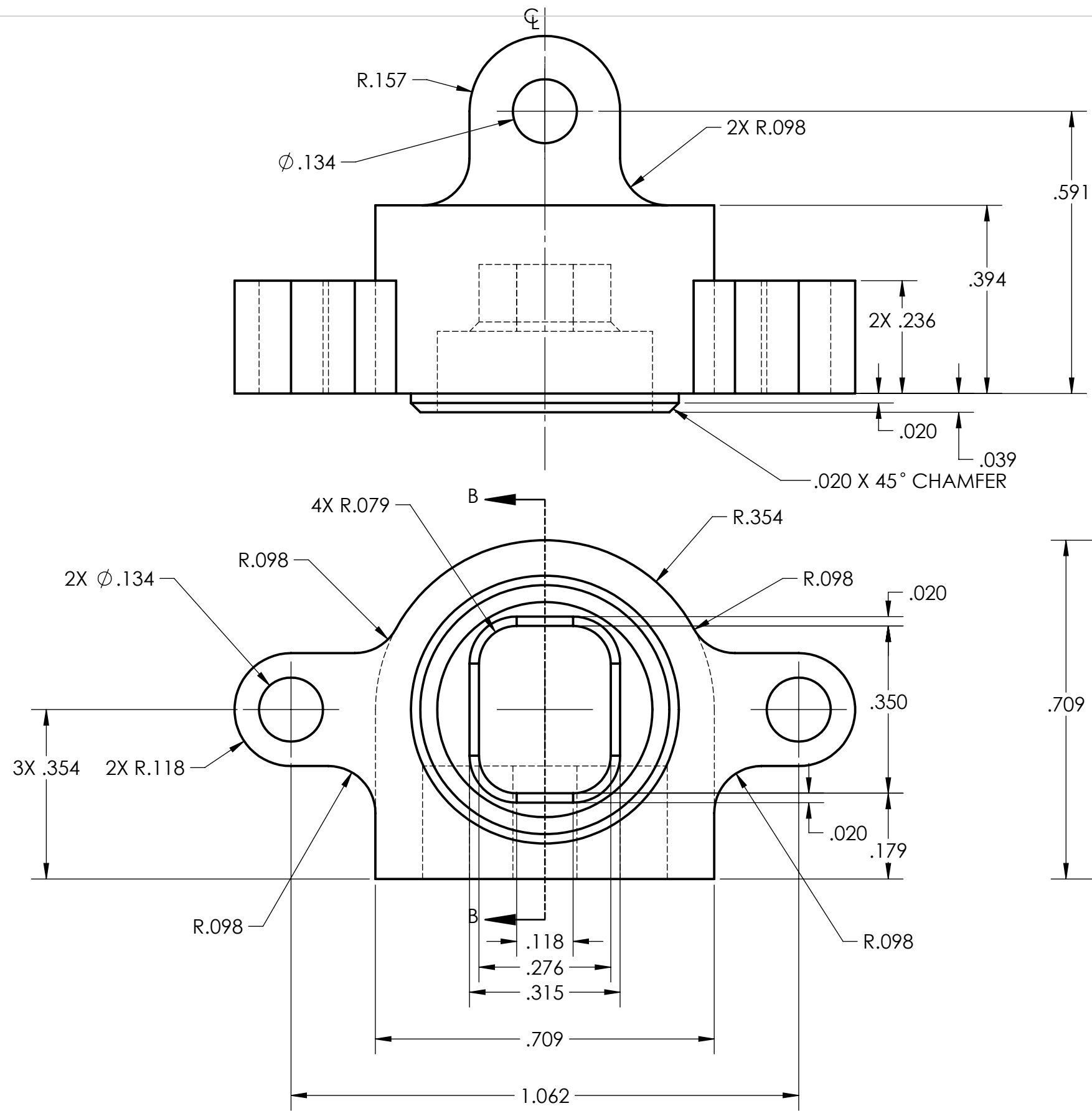
DATE:
06-04-2019

SHEET 2 OF 4

SCALE: 2:1

REV

SIZE
B

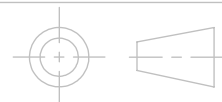


SECTION B-B

CUBE-DC-104001

UNLESS OTHERWISE SPECIFIED:
 DIMENSIONS ARE IN INCHES
 TOLERANCES:
 FRACTIONAL $\pm 0.5^\circ$
 TWO PLACE DECIMAL ± 0.005
 THREE PLACE DECIMAL ± 0.0025

INTERPRET DRAWING
 PER ANSI Y14.5 2009



CAL POLY
SAN LUIS OBISPO

MATERIAL:
 SEE BOM

DRAWN BY:
 JEFF WAGNER

TITLE:
 FRANGIBOLT BOTTOM HOUSING

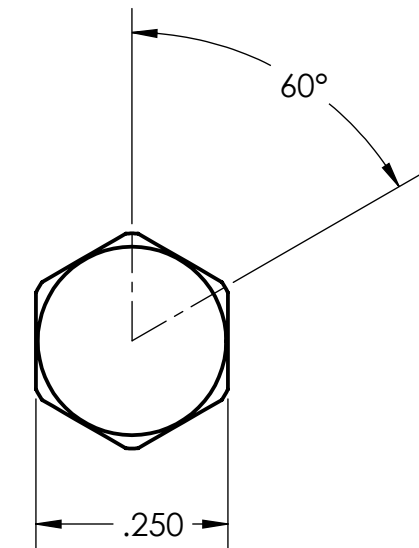
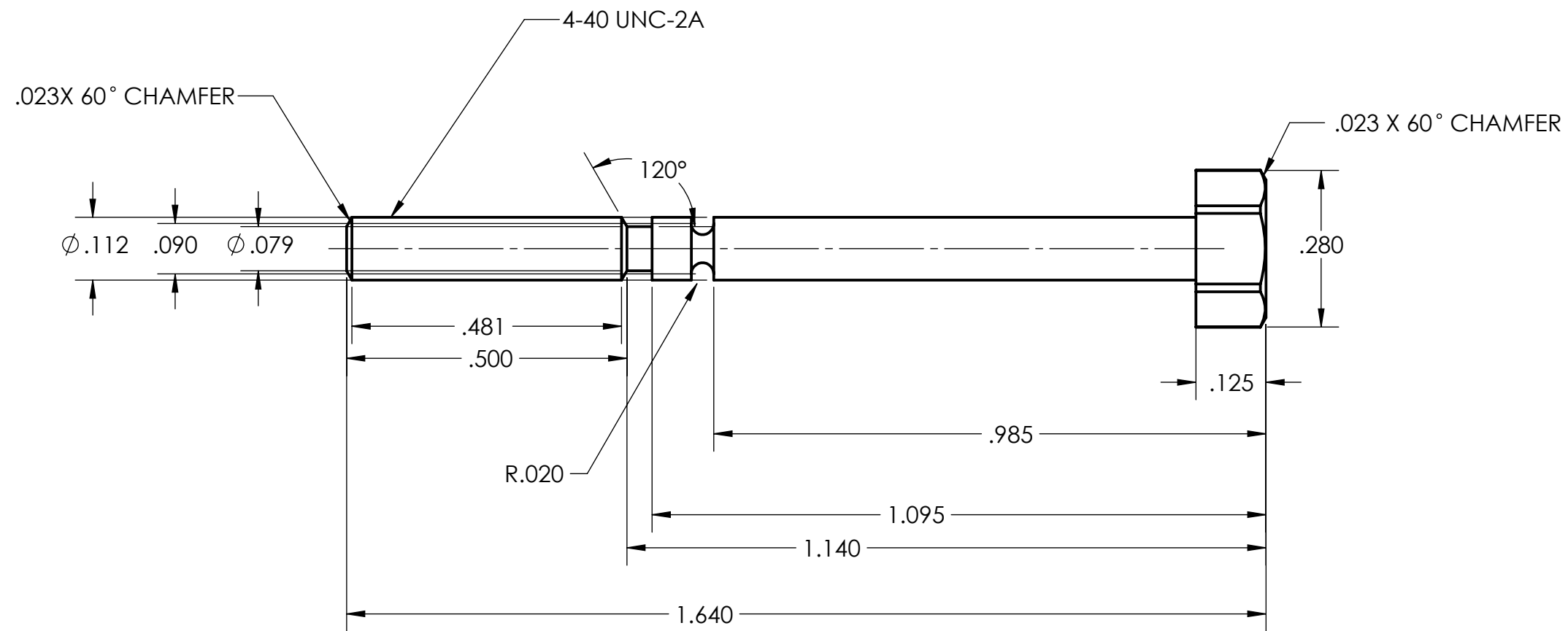
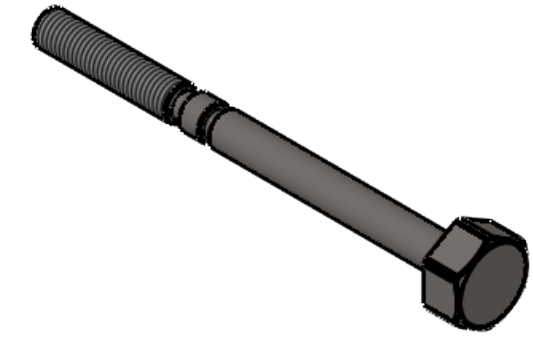
DATE:
 06-04-2019

SHEET 3 OF 4

SCALE: 4:1

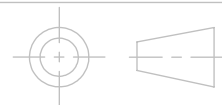
REV

SIZE
B



UNLESS OTHERWISE SPECIFIED:
 DIMENSIONS ARE IN INCHES
 TOLERANCES:
 FRACTIONAL $\pm 0.5^\circ$
 TWO PLACE DECIMAL ± 0.005
 THREE PLACE DECIMAL ± 0.0025

INTERPRET DRAWING
 PER ANSI Y14.5 2009



CAL POLY
SAN LUIS OBISPO

MATERIAL:
 SEE BOM

DRAWN BY:
 JEFF WAGNER

TITLE:
 FRANGIBOLT BOLT

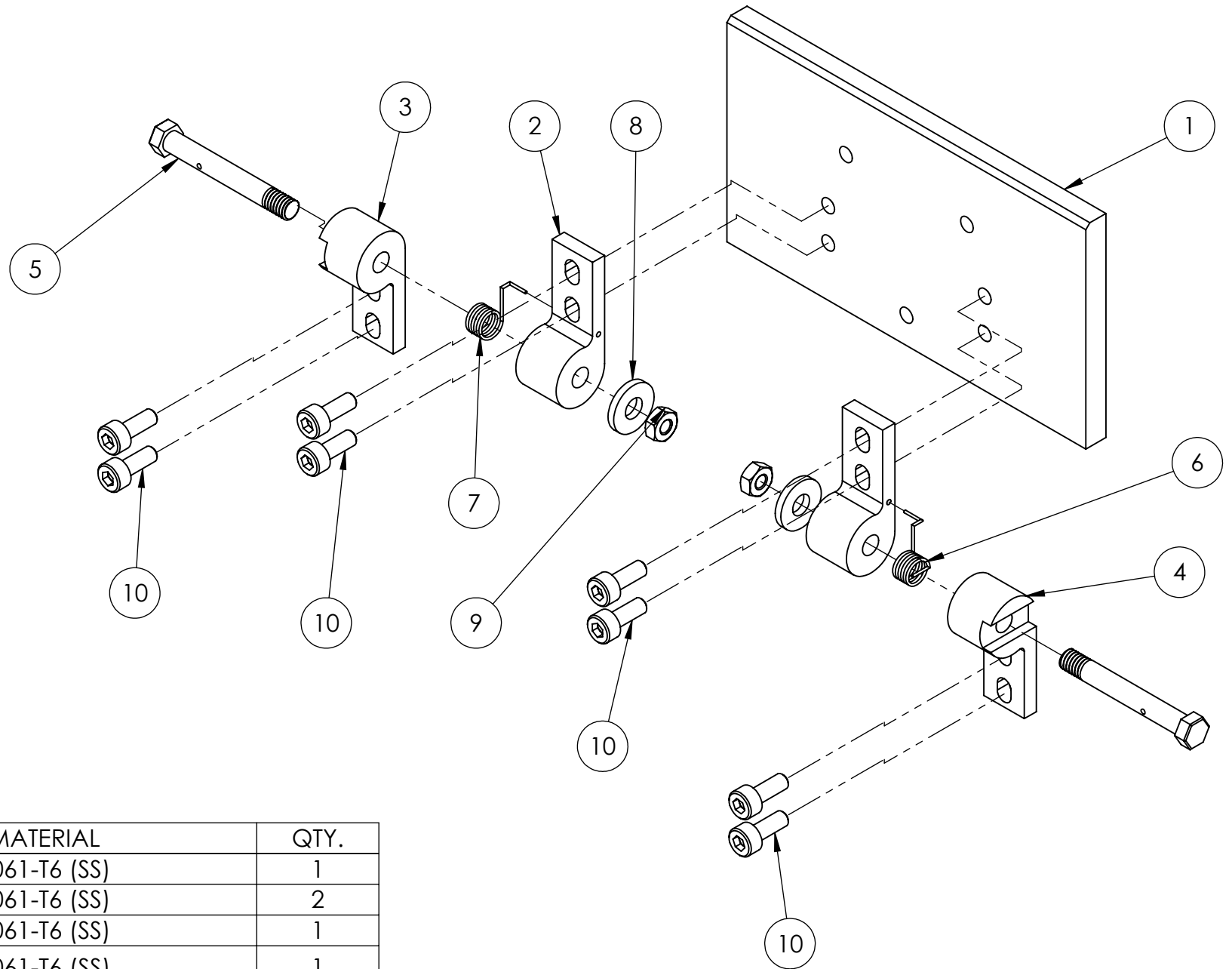
DATE:
 06-04-2019

SHEET 4 OF 4

SCALE: 4:1

REV

SIZE
B

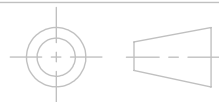


CUBE-DC-105000

ITEM NO.	PART NUMBER	DESCRIPTION	MATERIAL	QTY.
1	CUBE-DC-105001	FRONT PANEL	6061-T6 (SS)	1
2	CUBE-DC-105003	FRONT PANEL JOURNAL	6061-T6 (SS)	2
3	CUBE-DC-105004	FRONT PANEL SHAFT CLAMP	6061-T6 (SS)	1
4	CUBE-DC-105004B	FRONT PANEL SHAFT CLAMP MIRRORED	6061-T6 (SS)	1
5	CUBE-DC-105005	FRONT PANEL SHAFT	6061-T6 (SS)	2
6	CUBE-DC-105006-05	FRONT PANEL SPRING LEFT, 5 TURN	Alloy Steel (SS)	1
7	CUBE-DC-105007-05	FRONT PANEL SPRING RIGHT, 5 TURN	Alloy Steel (SS)	1
8	B18.22M - Plain washer, 3.5 mm, regular			2
9	B18.2.4.1M - Hex nut, Style 1, M3 x 0.5 --D-N			2
10	B18.3.1M - 3 x 0.5 x 8 Hex SHCS -- 8NHX			8

UNLESS OTHERWISE SPECIFIED:
DIMENSIONS ARE IN INCHES
TOLERANCES:
FRACTIONAL $\pm 0.5^\circ$
TWO PLACE DECIMAL ± 0.005
THREE PLACE DECIMAL ± 0.0025

INTERPRET DRAWING
PER ANSI Y14.5 2009



CAL POLY
SAN LUIS OBISPO

MATERIAL:
SEE BOM

DRAWN BY:
EDWIN RAINVILLE

TITLE:
FRONT PANEL

DATE:
06-04-2019

SHEET 1 OF 7

SCALE: 1:1

REV

SIZE
B

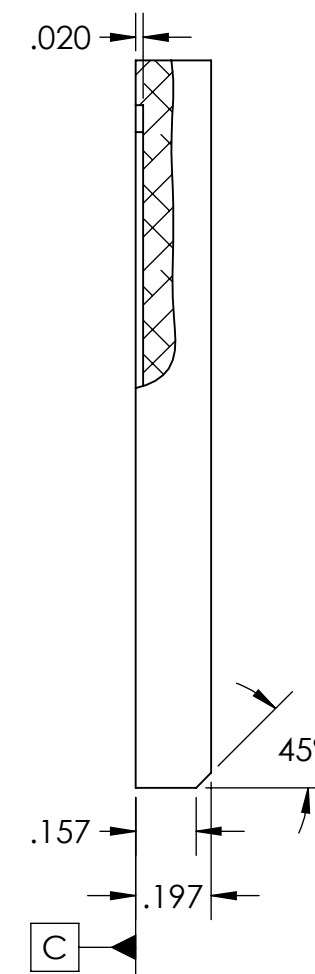
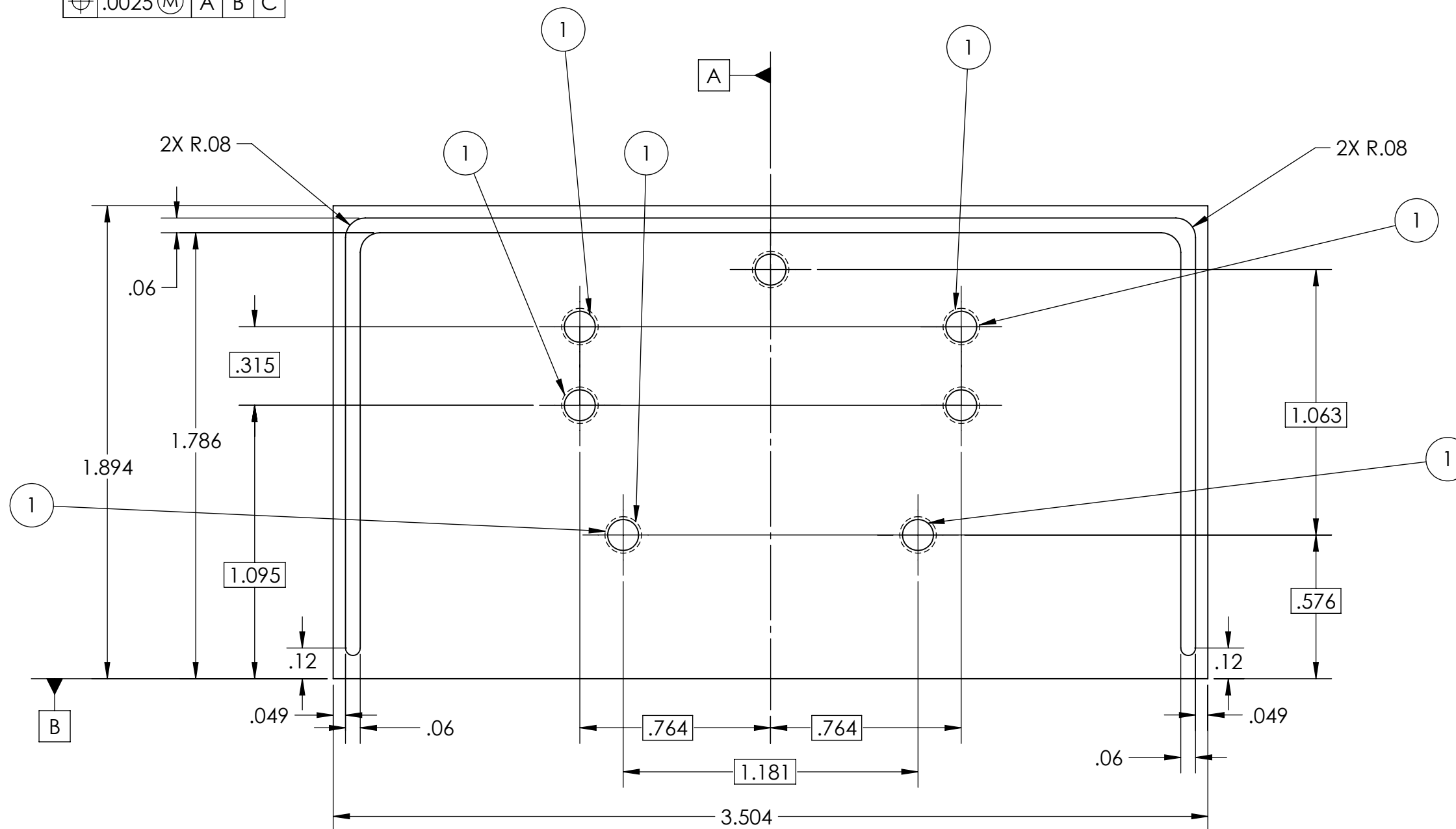
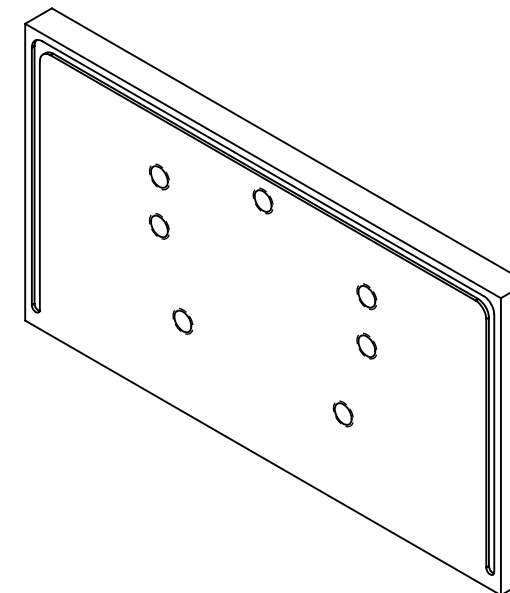
NOTE:

1. ALL DIMENSIONS IN INCHES UNLESS OTHERWISE STATED
2. TOLERANCES UNLESS OTHERWISE STATED:
 X.X = $\pm .05$
 X.XX = $\pm .005$
 X.XXX = $\pm .001$

3. (1) INDICATES FOLLOWING CALLOUT
 TAPPED HOLE FOR M3X0.5 HELICOIL
 THRU ALL

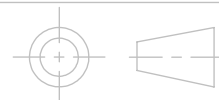
$\text{⌀} .0025 \text{ (M)}$	A	B	C
------------------------------	---	---	---

CUBE-DC-105001



UNLESS OTHERWISE SPECIFIED:
 DIMENSIONS ARE IN INCHES
 TOLERANCES:
 FRACTIONAL $\pm 0.5^\circ$
 TWO PLACE DECIMAL ± 0.005
 THREE PLACE DECIMAL ± 0.0025

INTERPRET DRAWING
 PER ANSI Y14.5 2009



CAL POLY
SAN LUIS OBISPO

MATERIAL:
 SEE BOM

DRAWN BY:
 EDWIN RAINVILLE

TITLE:
 FRONT AND BACK PANEL

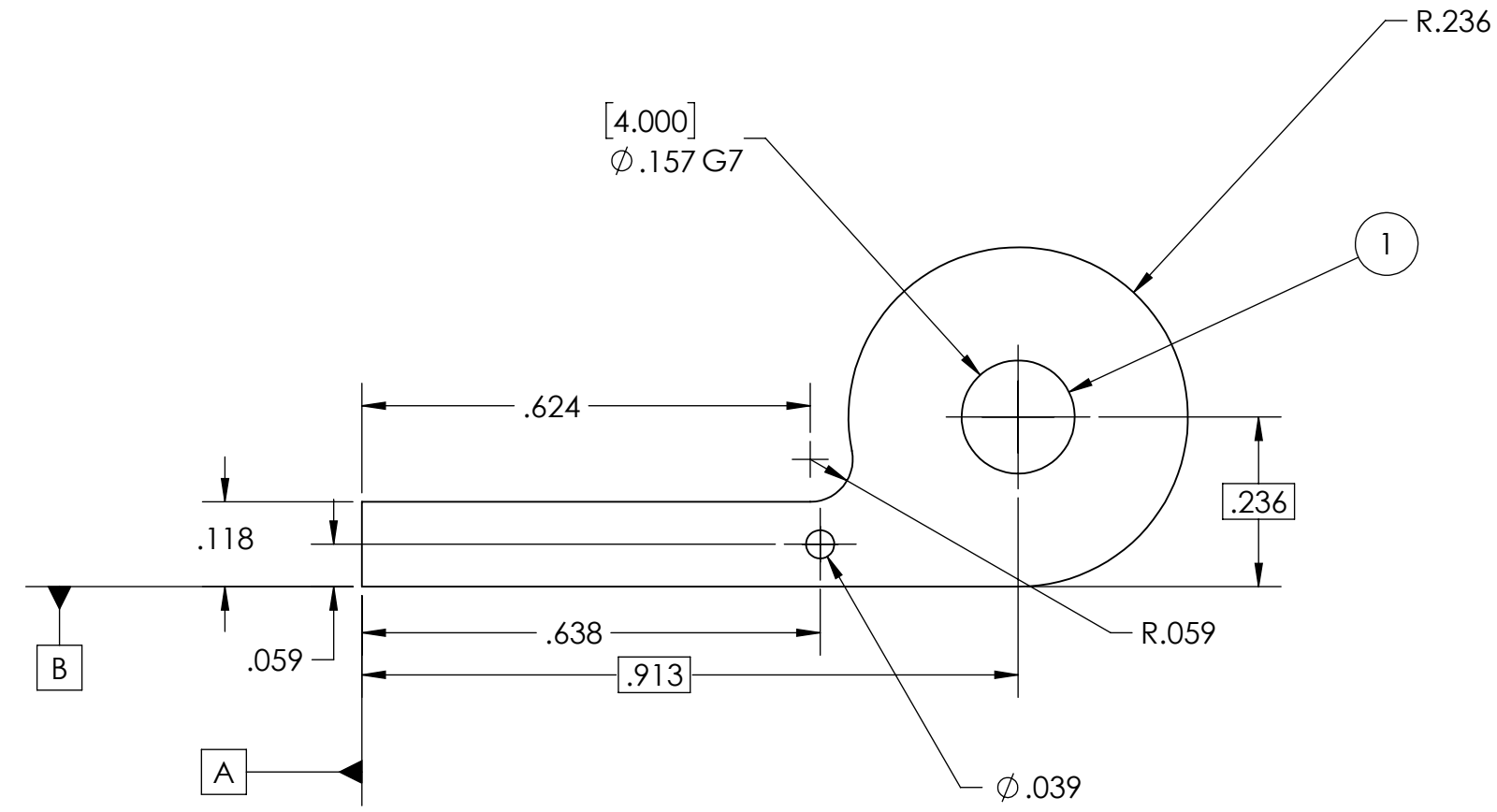
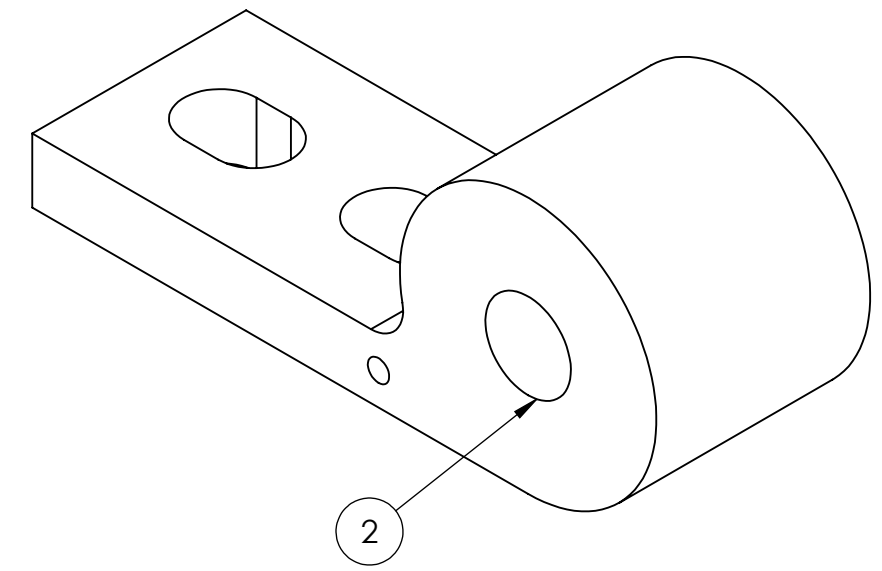
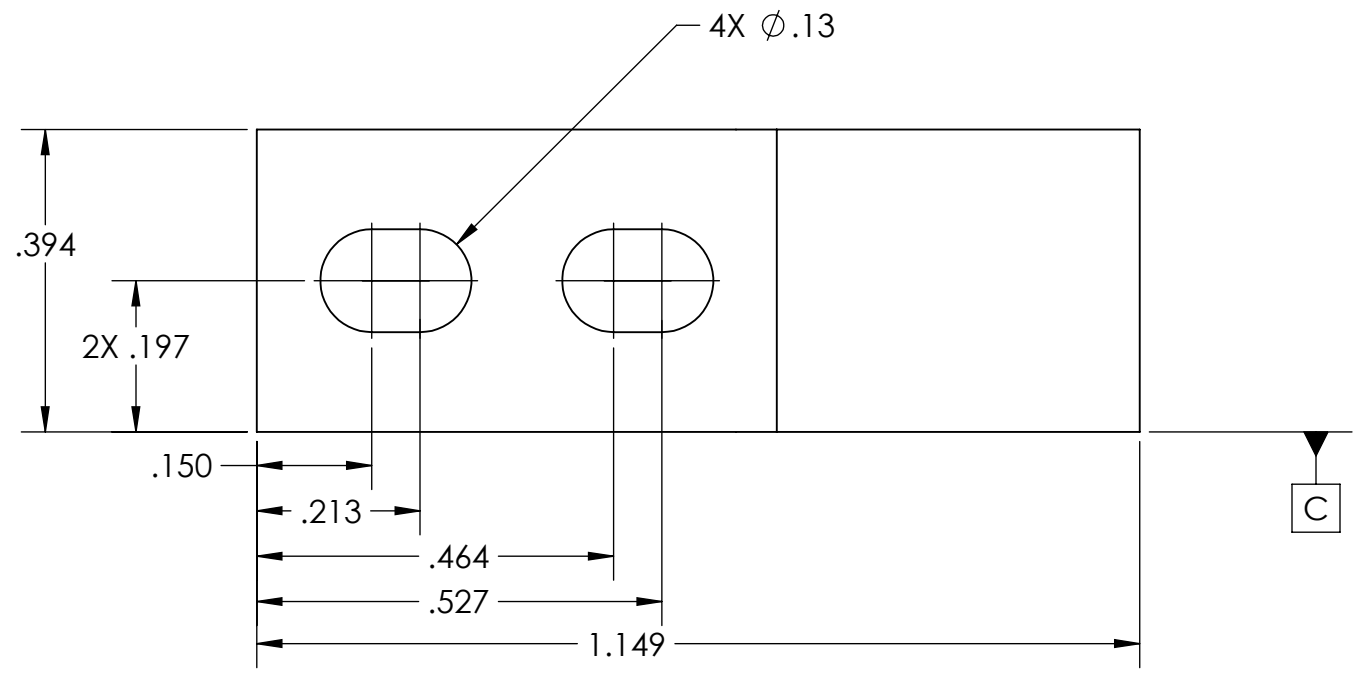
DATE:
 06-01-18

SHEET 2 OF 7

SCALE: 2:1

REV

SIZE
B

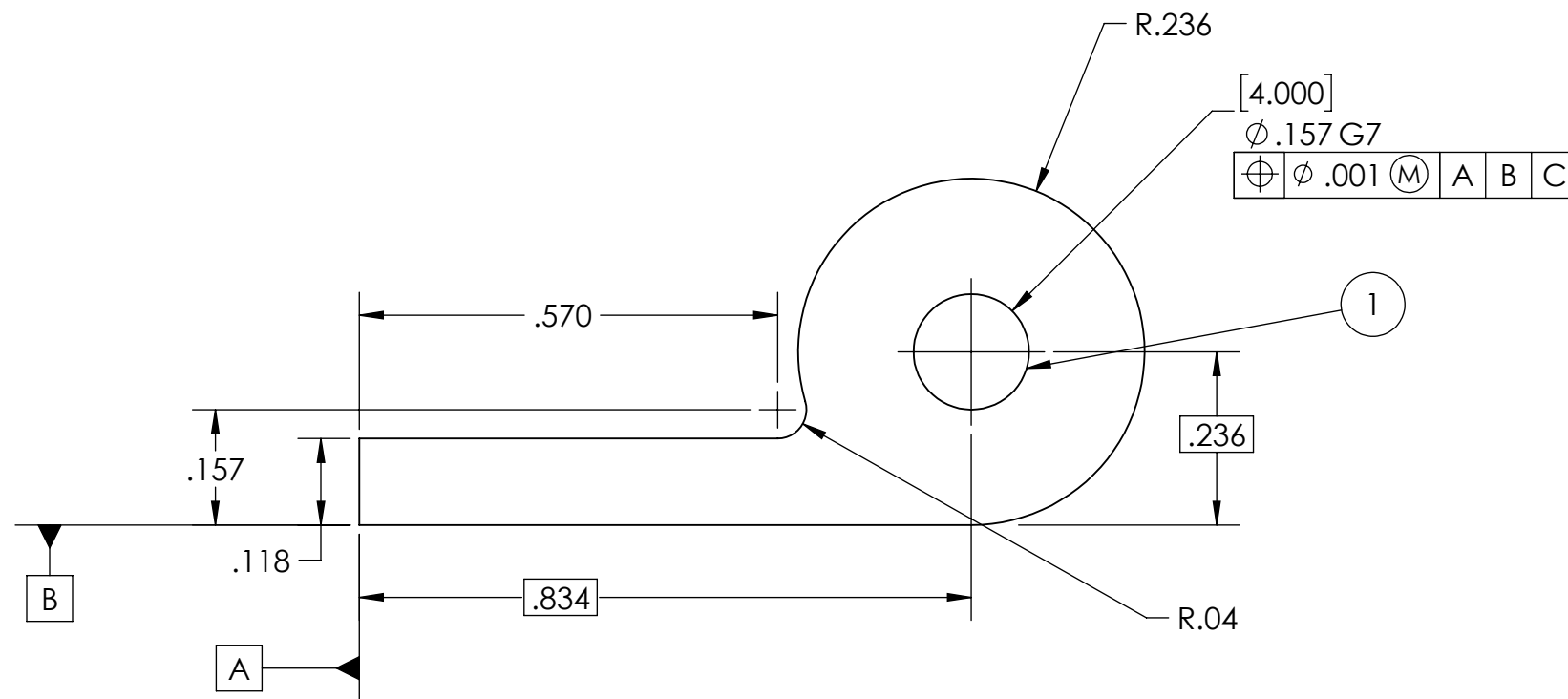
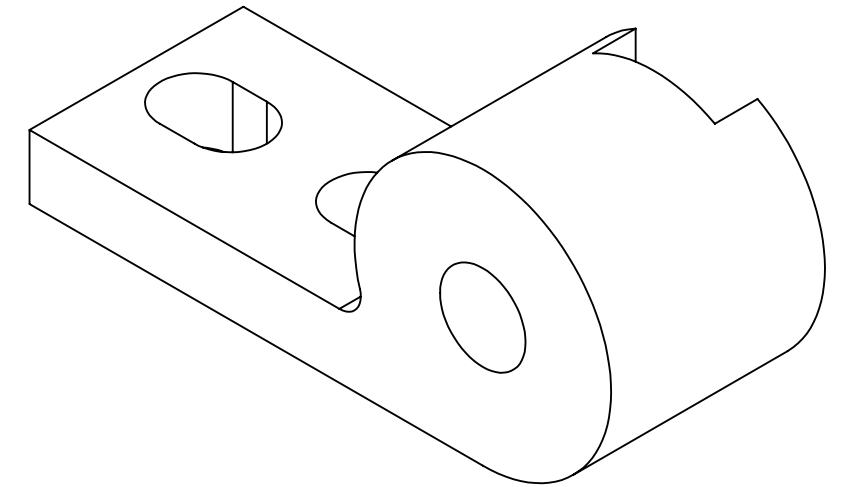
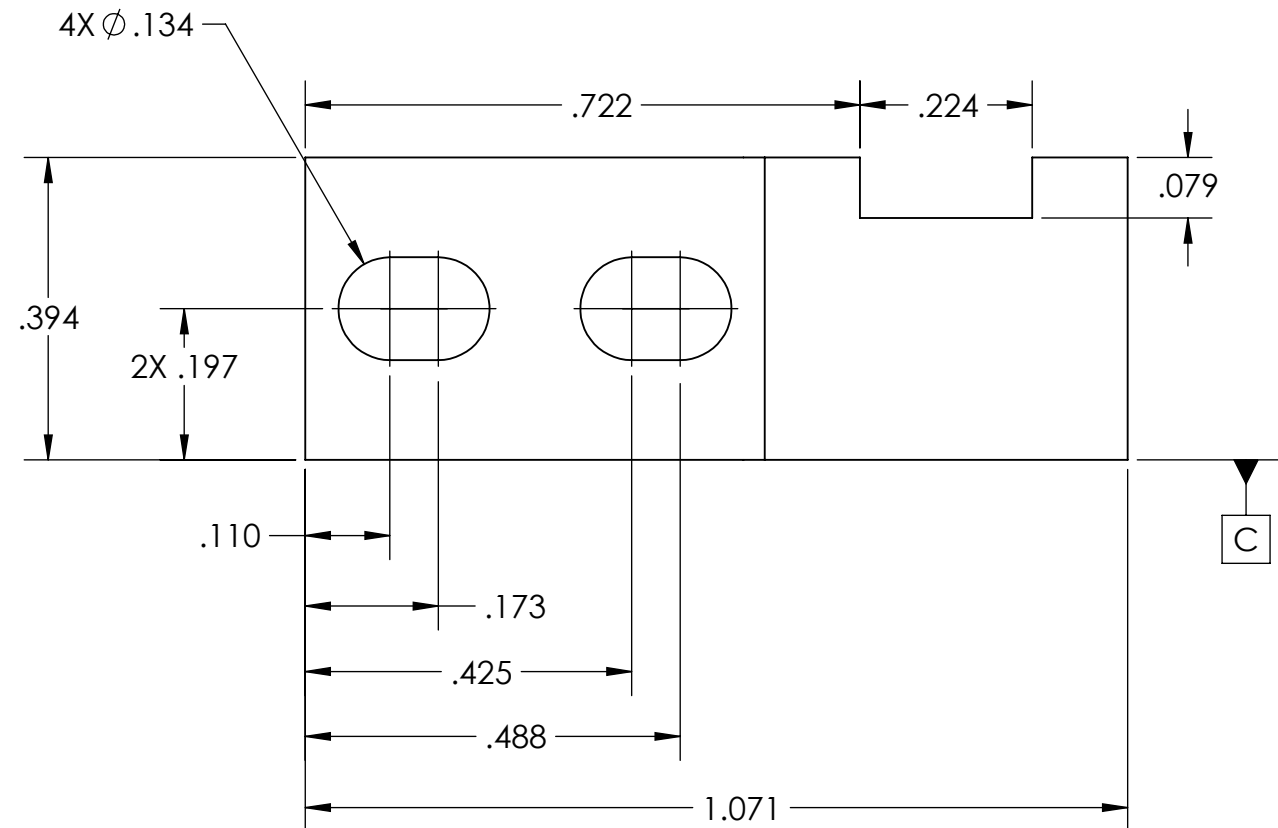


NOTE:

- ① MAKE SHAFT TO 4 MM G7 STANDARD PER ANSI B4.2-1978
- ② INTERNAL SURFACE TO BE PLATED: ELECTROLESS NICKEL W/ TEFLON PER MIL-C-26074E GRADE A

CUBE-DC-105003

UNLESS OTHERWISE SPECIFIED: DIMENSIONS ARE IN INCHES TOLERANCES: FRACTIONAL $\pm 0.5^\circ$ TWO PLACE DECIMAL ± 0.005 THREE PLACE DECIMAL ± 0.0025	INTERPRET DRAWING PER ANSI Y14.5 2009		MATERIAL: SEE BOM		TITLE: Front Panel Journal		SHEET 3 OF 7	SCALE: 4:1	REV	SIZE B
			DRAWN BY: EDWIN RAINVILLE		DATE: 09-30-2019					



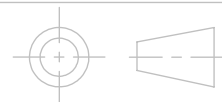
NOTE:

① MAKE HOLE TO 4 MM G7 STANDARD PER ANSI B4.2-1978

CUBE-DC-105004

UNLESS OTHERWISE SPECIFIED:
DIMENSIONS ARE IN INCHES
TOLERANCES:
FRACTIONAL $\pm 0.5^\circ$
TWO PLACE DECIMAL ± 0.005
THREE PLACE DECIMAL ± 0.0025

INTERPRET DRAWING
PER ANSI Y14.5 2009



CAL POLY
SAN LUIS OBISPO

MATERIAL:
SEE BOM

DRAWN BY:
EDWIN RAINVILLE

TITLE:
FRONT PANEL SHAFT CLAMP

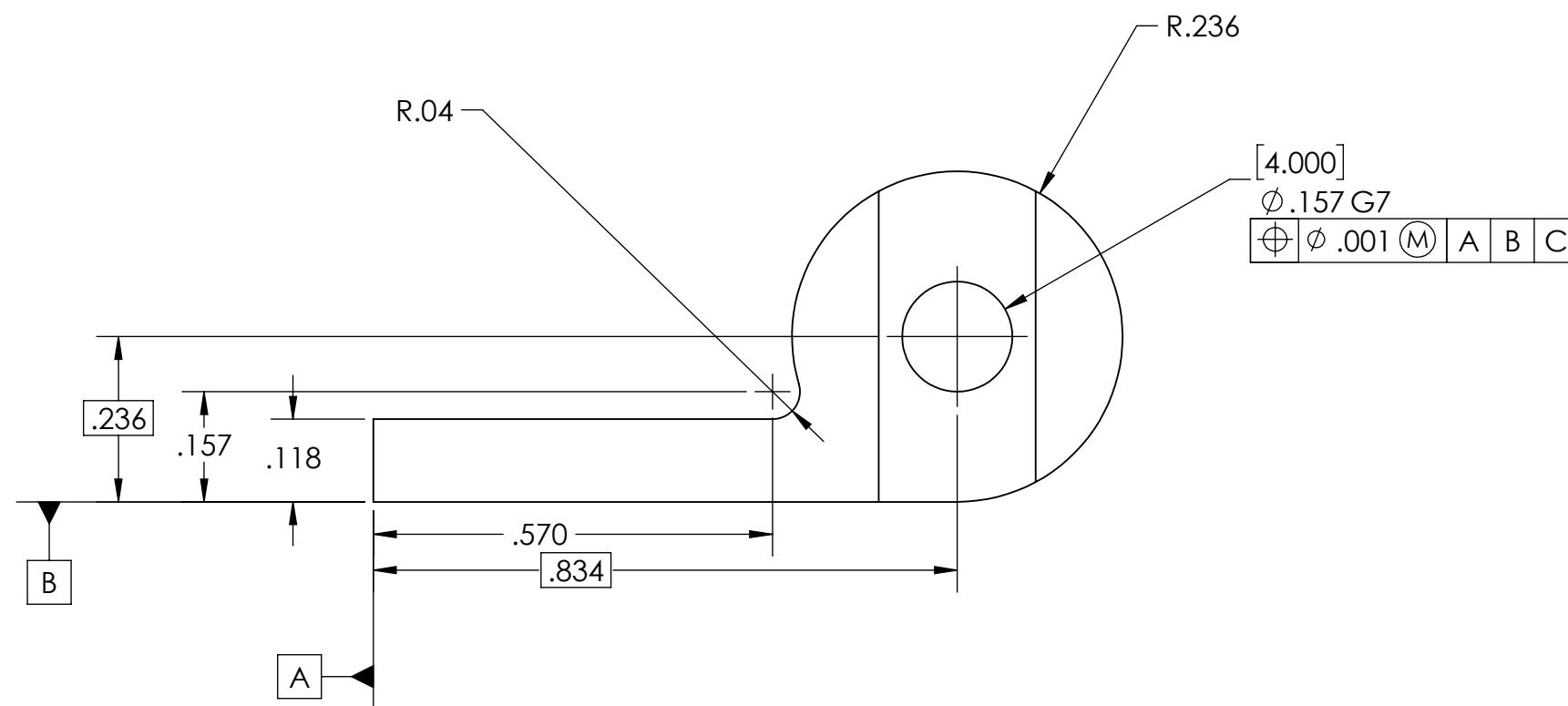
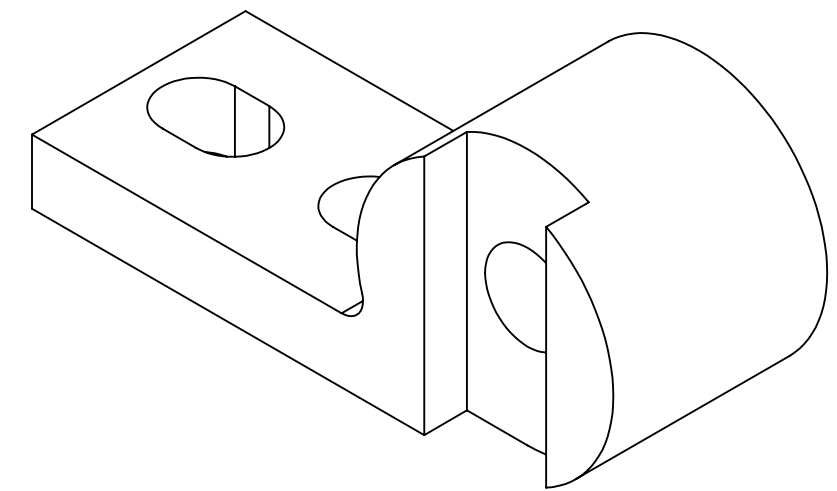
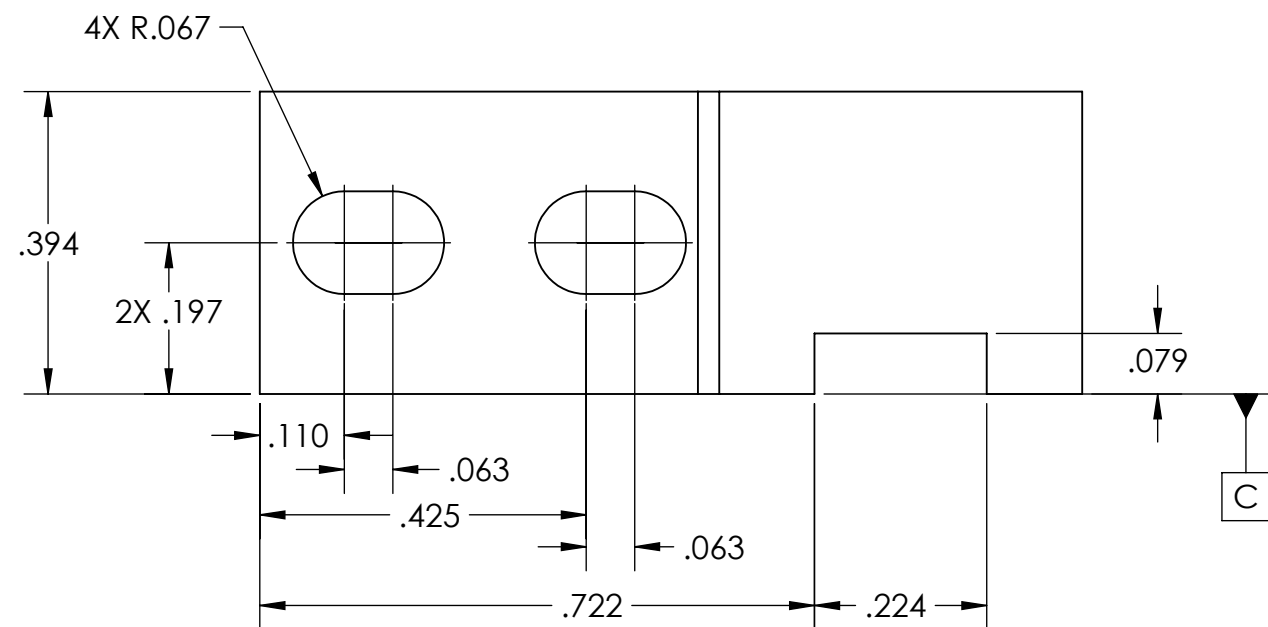
DATE:
05-10-18

SHEET 4 OF 7

SCALE: 4:1

REV

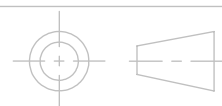
SIZE
B



CUBE-DC-105004B

UNLESS OTHERWISE SPECIFIED:
 DIMENSIONS ARE IN INCHES
 TOLERANCES:
 FRACTIONAL $\pm 0.5^\circ$
 TWO PLACE DECIMAL ± 0.005
 THREE PLACE DECIMAL ± 0.0025

INTERPRET DRAWING
 PER ANSI Y14.5 2009



CAL POLY
SAN LUIS OBISPO

MATERIAL:
 SEE BOM

DRAWN BY:
 EDWIN RAINVILLE

TITLE:
 FRONT PANEL SHAFT CLAMP MIRRORED

DATE:
 06-03-19

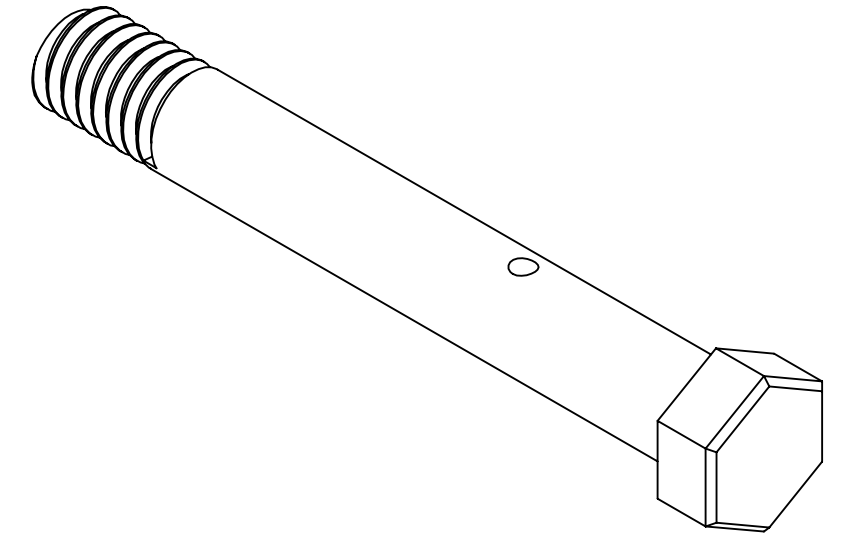
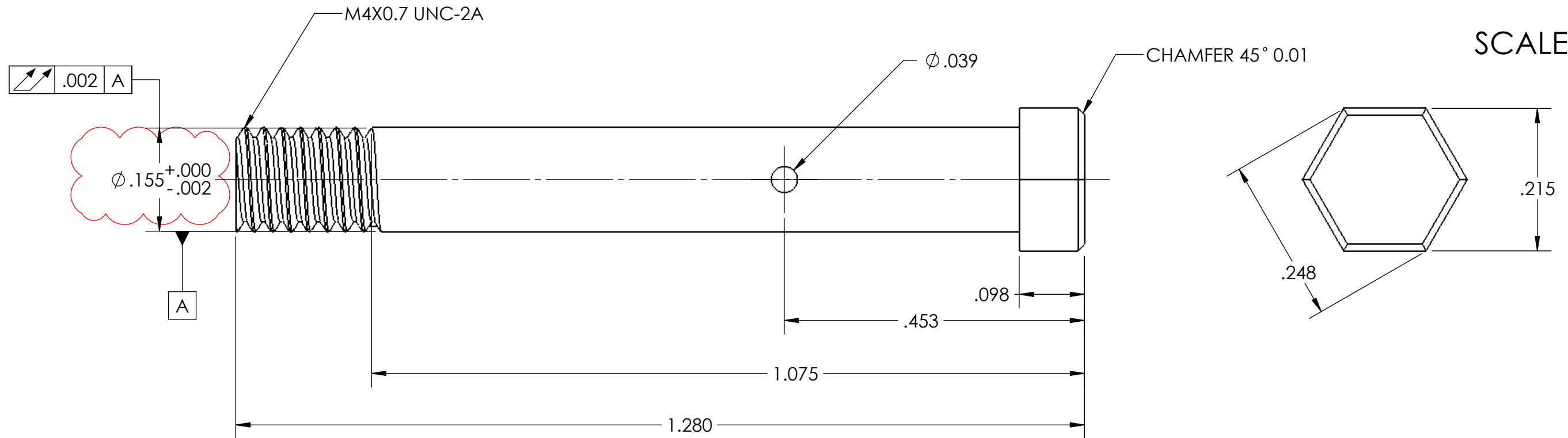
SHEET 5 OF 7

SCALE: 4:1

REV

SIZE
B

CHANGED FROM M4 g6 SHAFT. CHANGED TO ALTERED DIMENSION DURING SENIOR PROJECT.
TOLERANCE SHOULD BE ADJUSTED TO ENSURE FIT WITH PLATED JOURNAL

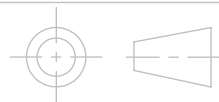


SCALE 4:1

CUBE-DC-105005

UNLESS OTHERWISE SPECIFIED:
DIMENSIONS ARE IN INCHES
TOLERANCES:
FRACTIONAL $\pm 0.5^\circ$
TWO PLACE DECIMAL ± 0.005
THREE PLACE DECIMAL ± 0.0025

INTERPRET DRAWING
PER ANSI Y14.5 2009



CAL POLY
SAN LUIS OBISPO

MATERIAL:
SEE BOM

DRAWN BY:
EDWIN RAINVILLE

TITLE:
FRONT PANEL SHAFT

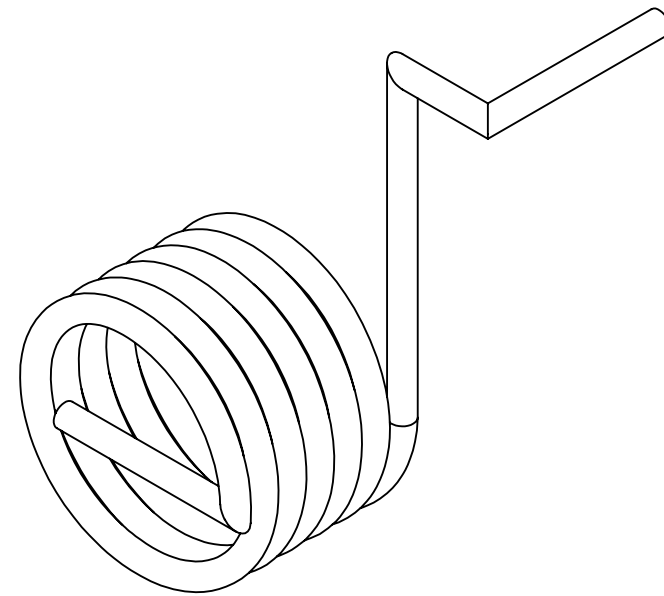
DATE:
12-04-19

SHEET 6 OF 7

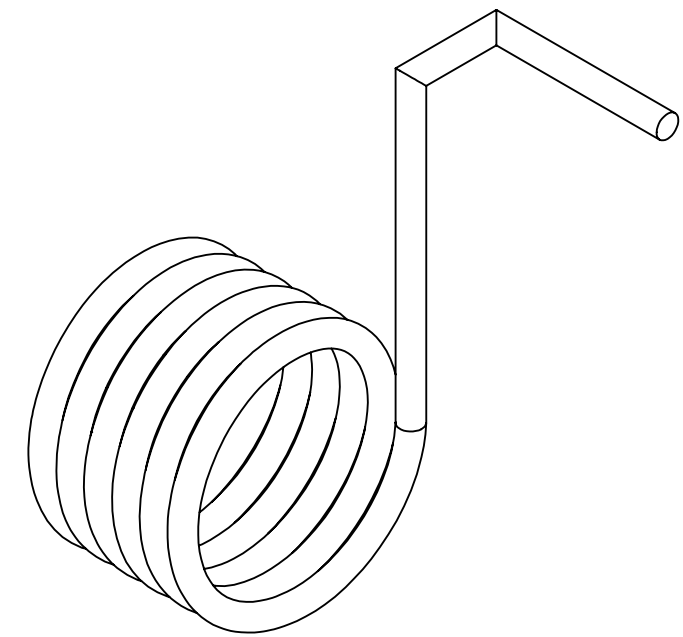
SCALE: 6:1

REV

SIZE
B



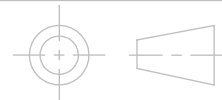
CUBE-DC-105006-05



CUBE-DC-105007-05

UNLESS OTHERWISE SPECIFIED:
 DIMENSIONS ARE IN INCHES
 TOLERANCES:
 FRACTIONAL $\pm 0.5^\circ$
 TWO PLACE DECIMAL ± 0.005
 THREE PLACE DECIMAL ± 0.0025

INTERPRET DRAWING
 PER ANSI Y14.5 2009



CAL POLY
SAN LUIS OBISPO

MATERIAL:
 SEE BOM

DRAWN BY:
 EDWIN RAINVILLE

TITLE:
 FRONT PANEL SPRINGS

DATE:
 06-04-19

SHEET 7 OF 7

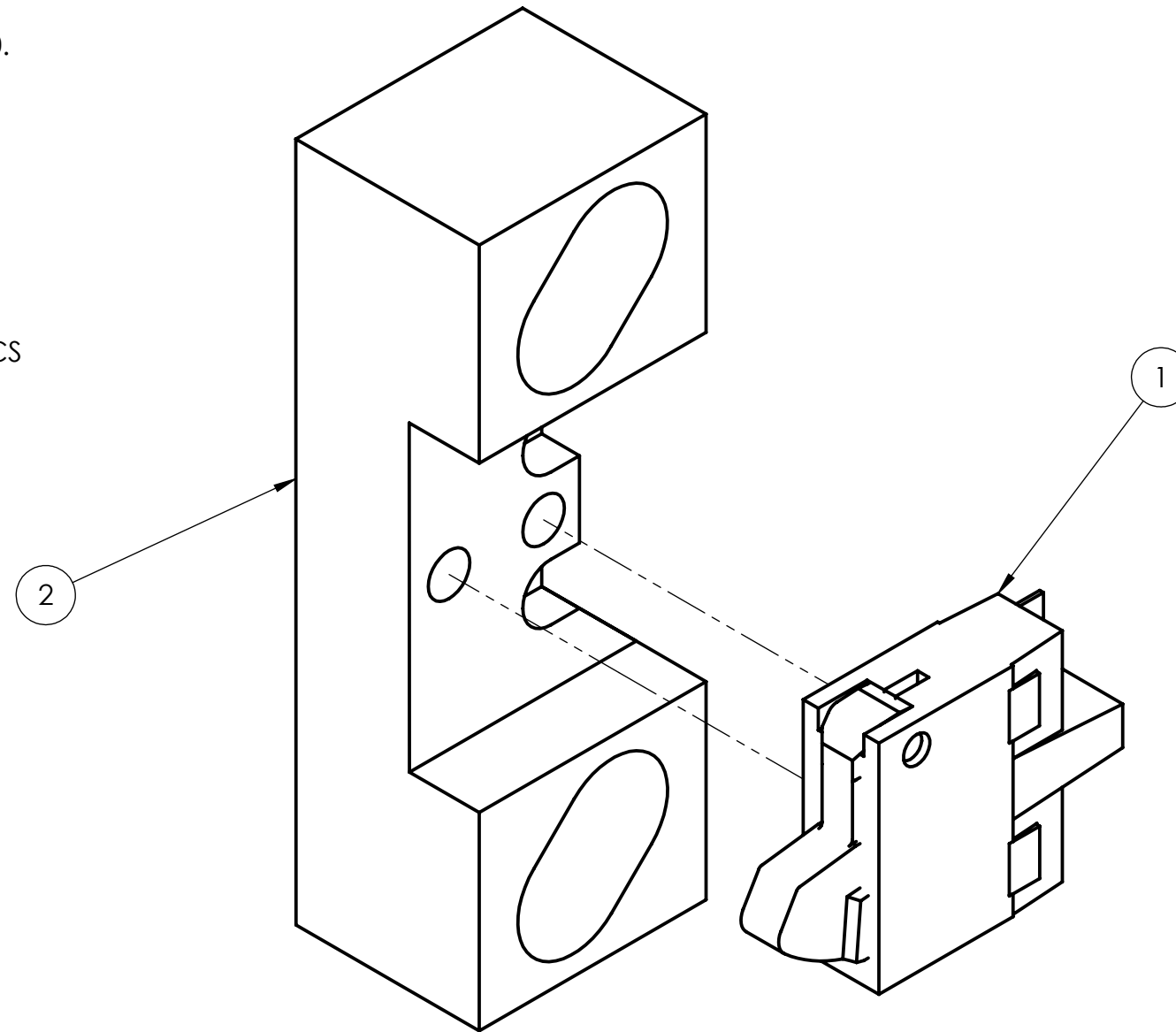
SCALE: 8:1

REV

SIZE
B

NOTES, UNLESS OTHERWISE SPECIFIED:

1. MATERIAL: ALUMINUM 6061-T651 PER AMS 4027 AND AMS 4150. FOR OTHER MATERIALS, SEE BOM.
2. BREAK EXTERNAL EDGES AND CORNERS .005 IN MAX UNLESS NOTED.
3. INTERNAL CORNER AND FILLET RADII .005 MAX UNLESS NOTED.
4. INSTALL HELICAL COIL INSERT PER NASM33537. REMOVE TANG.
5. DRAWING IS THE SOLE AUTHORITY FOR THE BASIC FORM, LOCATION, ORIENTATION, AND DIMENSIONAL CHARACTERISTICS OF ALL DESIGN FEATURES.

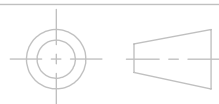


CUBE-DC-106000

ITEM NO.	PART NUMBER	DESCRIPTION	QTY.
1	ESE22MH24	LIMIT SWITCH	1
2	CUBE-DC-106001	LIMIT SWITCH MOUNT	1

UNLESS OTHERWISE SPECIFIED:
 DIMENSIONS ARE IN INCHES
 TOLERANCES:
 FRACTIONAL $\pm 0.5^\circ$
 TWO PLACE DECIMAL ± 0.005
 THREE PLACE DECIMAL ± 0.0025

INTERPRET DRAWING
 PER ANSI Y14.5 2009



CAL POLY
SAN LUIS OBISPO

MATERIAL:
 SEE BOM

DRAWN BY:
 PATRICK WHITESEL

TITLE:
 LIMIT SWITCH ASSEMBLY

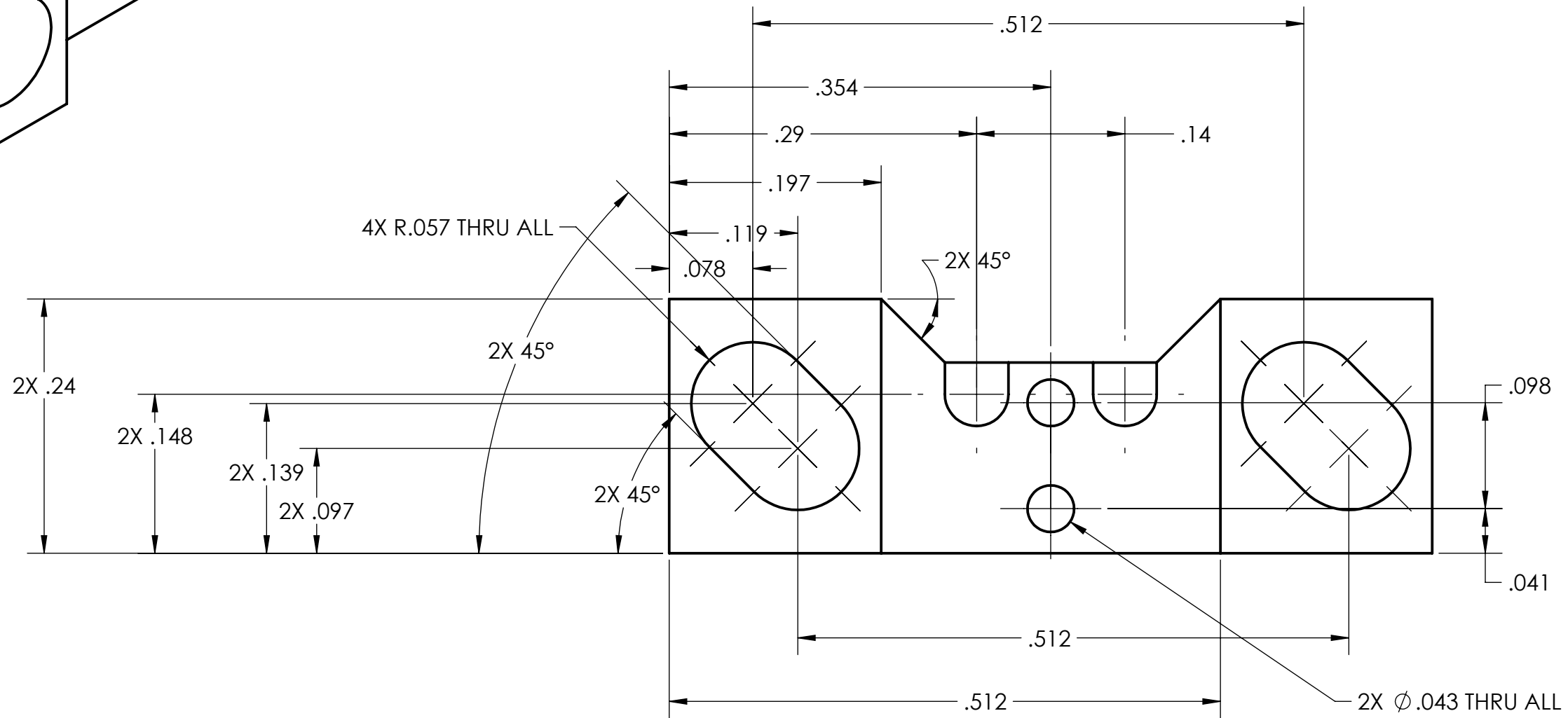
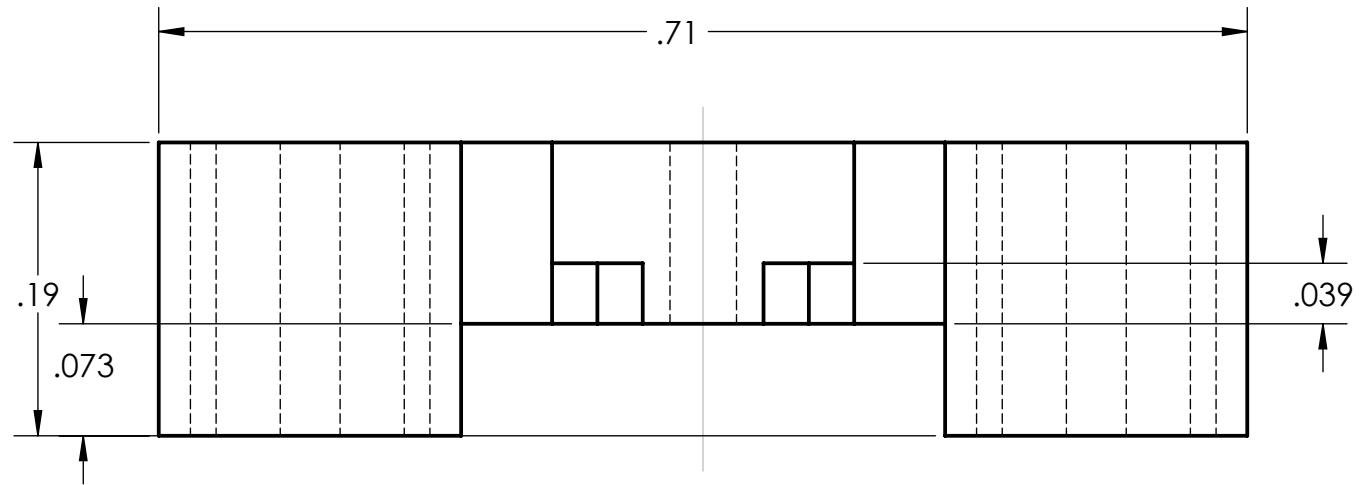
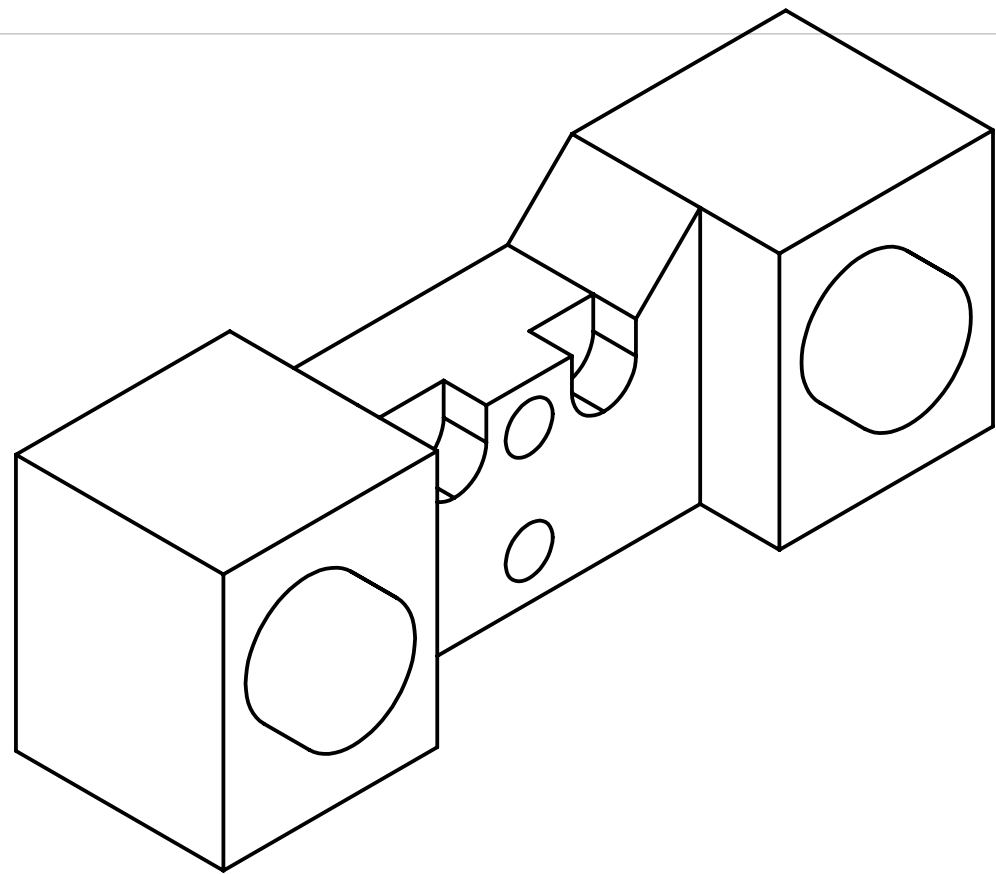
DATE:
 06-02-19`

SHEET 1 OF 2

SCALE: 8:1

REV

SIZE
B



CUBE-DC-106001

UNLESS OTHERWISE SPECIFIED:
 DIMENSIONS ARE IN INCHES
 TOLERANCES:
 FRACTIONAL $\pm 0.5^\circ$
 TWO PLACE DECIMAL ± 0.005
 THREE PLACE DECIMAL ± 0.0025

INTERPRET DRAWING
 PER ANSI Y14.5 2009



CAL POLY
SAN LUIS OBISPO

MATERIAL:
 SEE BOM

DRAWN BY:
 PATRICK WHITESEL

TITLE:
 LIMIT SWITCH MOUNT

DATE:
 06-04-2019

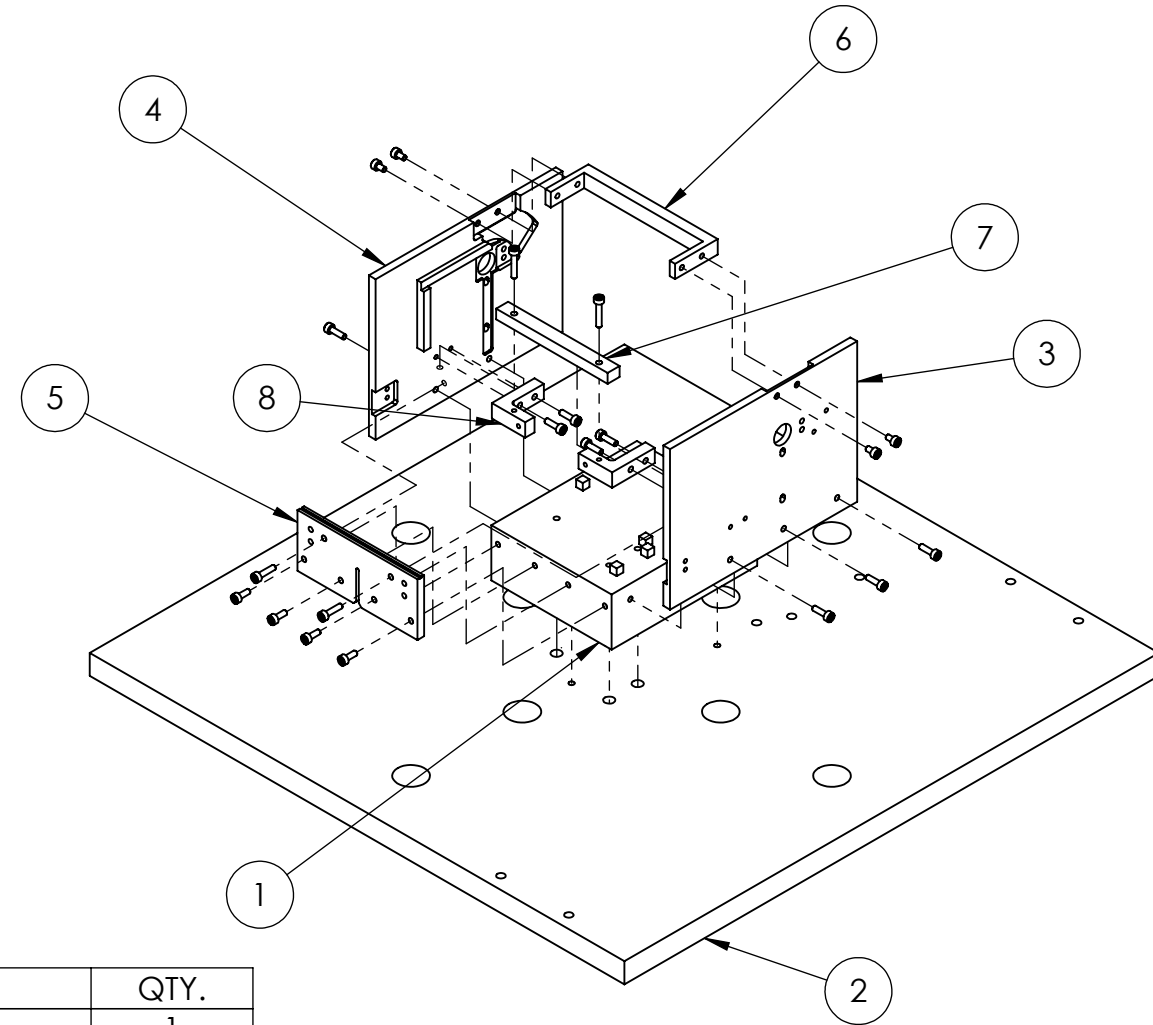
SHEET 1 OF 1

SCALE: 8:1

REV

SIZE
B

CUBE-DC-107000



ITEM NO.	PART NUMBER	DESCRIPTION	MATERIAL	QTY.
1	CUBE-DC-107001A	DEPLOYABLE COVER OPTICS DATUM	6061-T6 (SS)	1
2	CUBE-DC-107001B	DEPLOYABLE COVER OPTICS DATUM	6061-T6 (SS)	1
3	CUBE-DC-107002	LEFT SIDE PANEL	6061-T6 (SS)	1
4	CUBE-DC-107003	RIGHT SIDE PANEL	6061-T6 (SS)	1
5	CUBE-DC-107004	FRONT PANEL	6061-T6 (SS)	1
6	CUBE-DC-107005	TOP U BRACKET	6061-T6 (SS)	1
7	CUBE-DC-107006	FRONT CROSS BEAM	6061-T6 (SS)	1
8	CUBE-DC-107007	CROSS BEAM MOUNTING PLATFORM	6061-T6 (SS)	2
9	B18.3.1M - 3 x 0.5 x 8 Hex SHCS -- 8NHX			4
10	B18.3.1M - 3 x 0.5 x 10 Hex SHCS -- 10NHX			10
11	B18.3.1M - 3 x 0.5 x 5 Hex SHCS -- 5NHX			4
12	B18.3.1M - 3 x 0.5 x 12 Hex SHCS -- 12NHX			5
13	B18.3.1M - 3 x 0.5 x 16 Hex SHCS -- 16NHX			2

UNLESS OTHERWISE SPECIFIED:
DIMENSIONS ARE IN INCHES
TOLERANCES:
FRACTIONAL $\pm 0.5^\circ$
TWO PLACE DECIMAL ± 0.005
THREE PLACE DECIMAL ± 0.0025

INTERPRET DRAWING
PER ANSI Y14.5 2009



CAL POLY
SAN LUIS OBISPO

MATERIAL:
SEE BOM

DRAWN BY:
PATRICK WHITESEL

TITLE:
OPTICAL ALIGNMENT FIXTURE ASSEMBLY

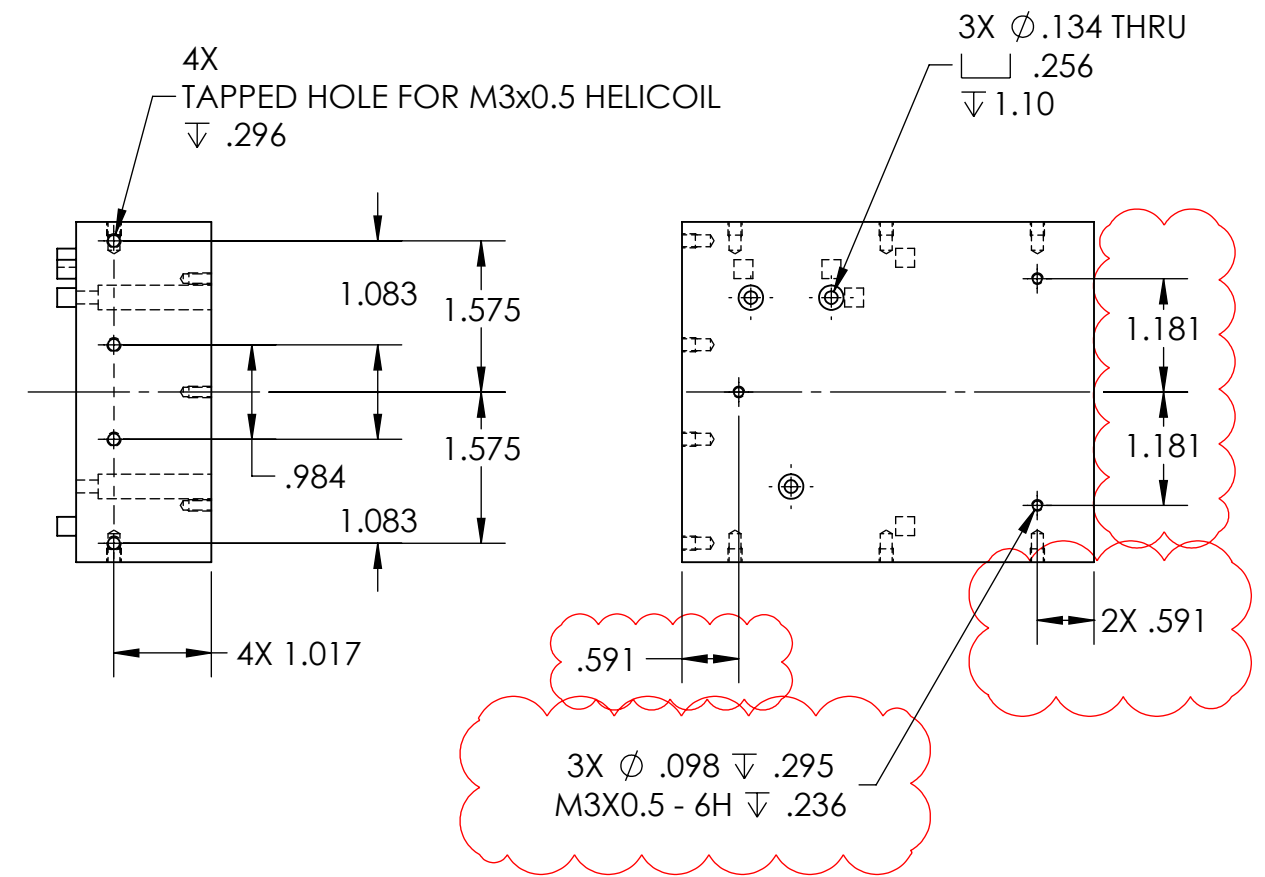
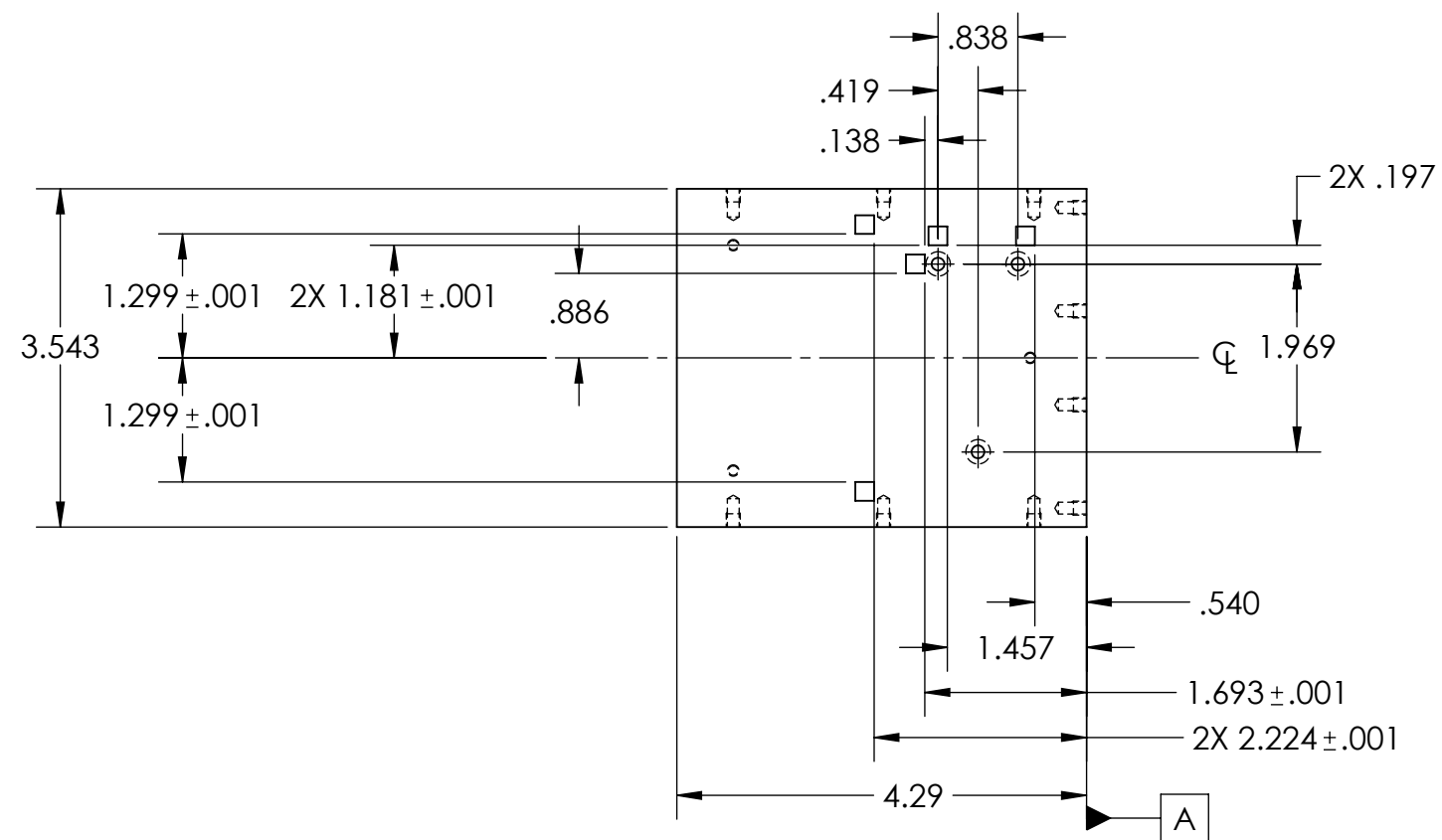
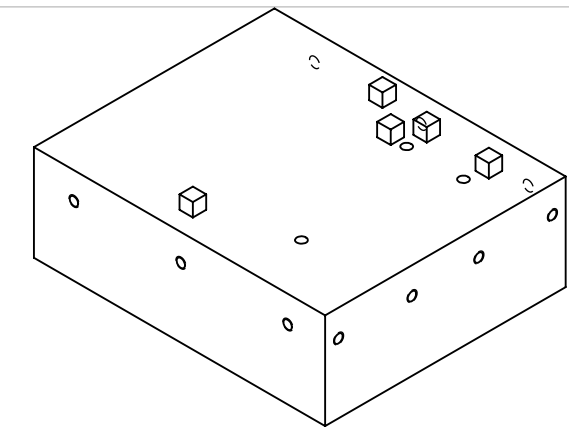
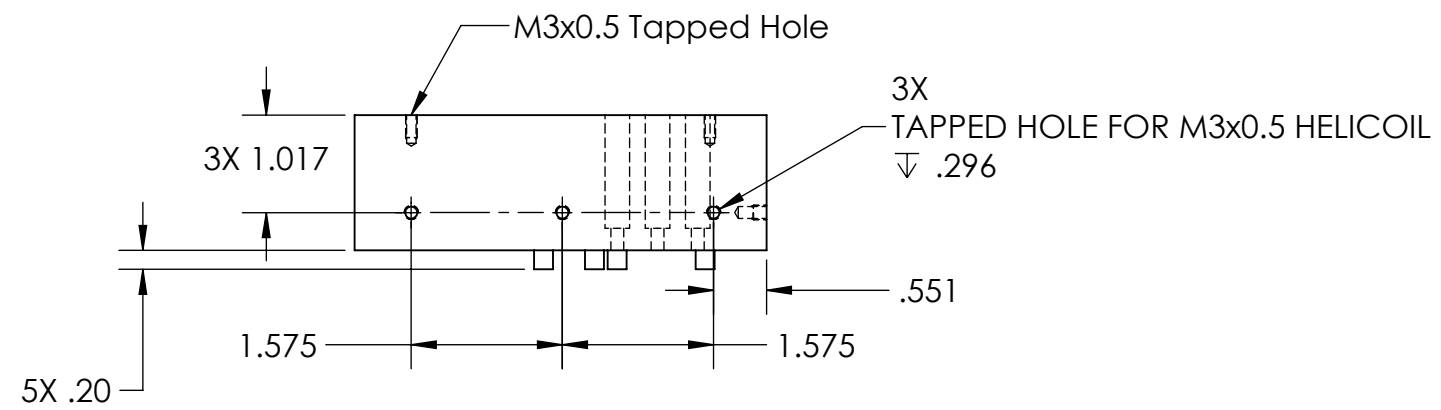
DATE:
06-02-18

SHEET 1 OF 7

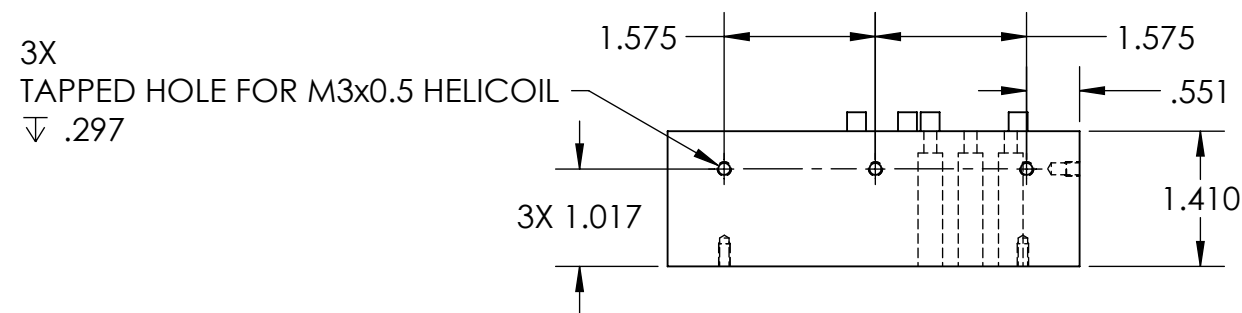
SCALE: 1:4

REV

SIZE
B



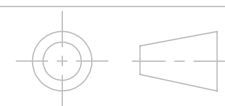
HOLES CALLED OUT



CUBE-DC-107001A

UNLESS OTHERWISE SPECIFIED:
 DIMENSIONS ARE IN INCHES
 TOLERANCES:
 FRACTIONAL ± 0.5°
 TWO PLACE DECIMAL ± 0.005
 THREE PLACE DECIMAL ± 0.0025

INTERPRET DRAWING
 PER ANSI Y14.5 2009



CAL POLY
SAN LUIS OBISPO

MATERIAL:
 SEE BOM

DRAWN BY:
 JEFF WAGNER

TITLE:
 DEPLOYABLE COVER OPTICS DATUM

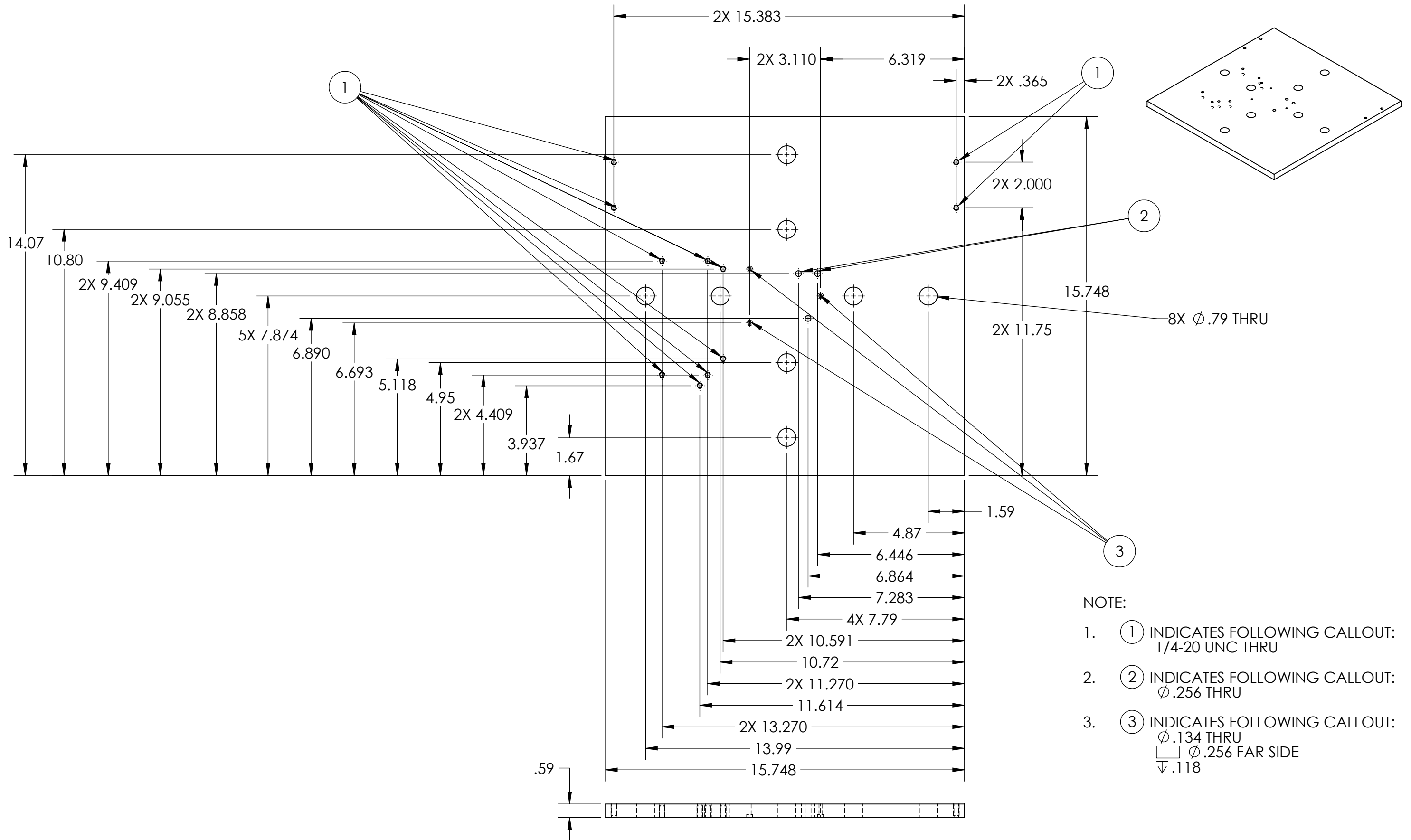
DATE:
 12-04-2019

SHEET 2 OF 7

SCALE: 1:4

REV

SIZE
B



- NOTE:
1. (1) INDICATES FOLLOWING CALLOUT:
1/4-20 UNC THRU
 2. (2) INDICATES FOLLOWING CALLOUT:
Ø .256 THRU
 3. (3) INDICATES FOLLOWING CALLOUT:
Ø .134 THRU
□ Ø .256 FAR SIDE
▽ .118

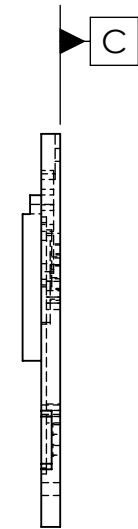
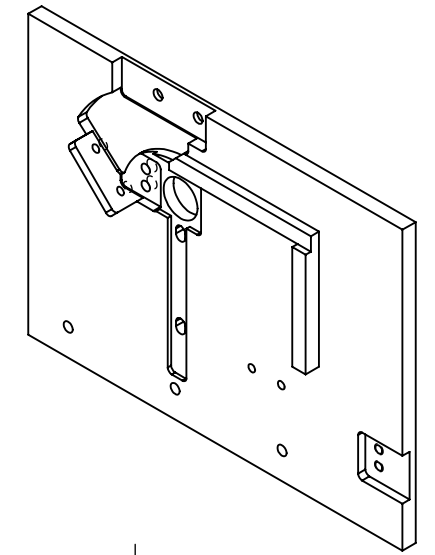
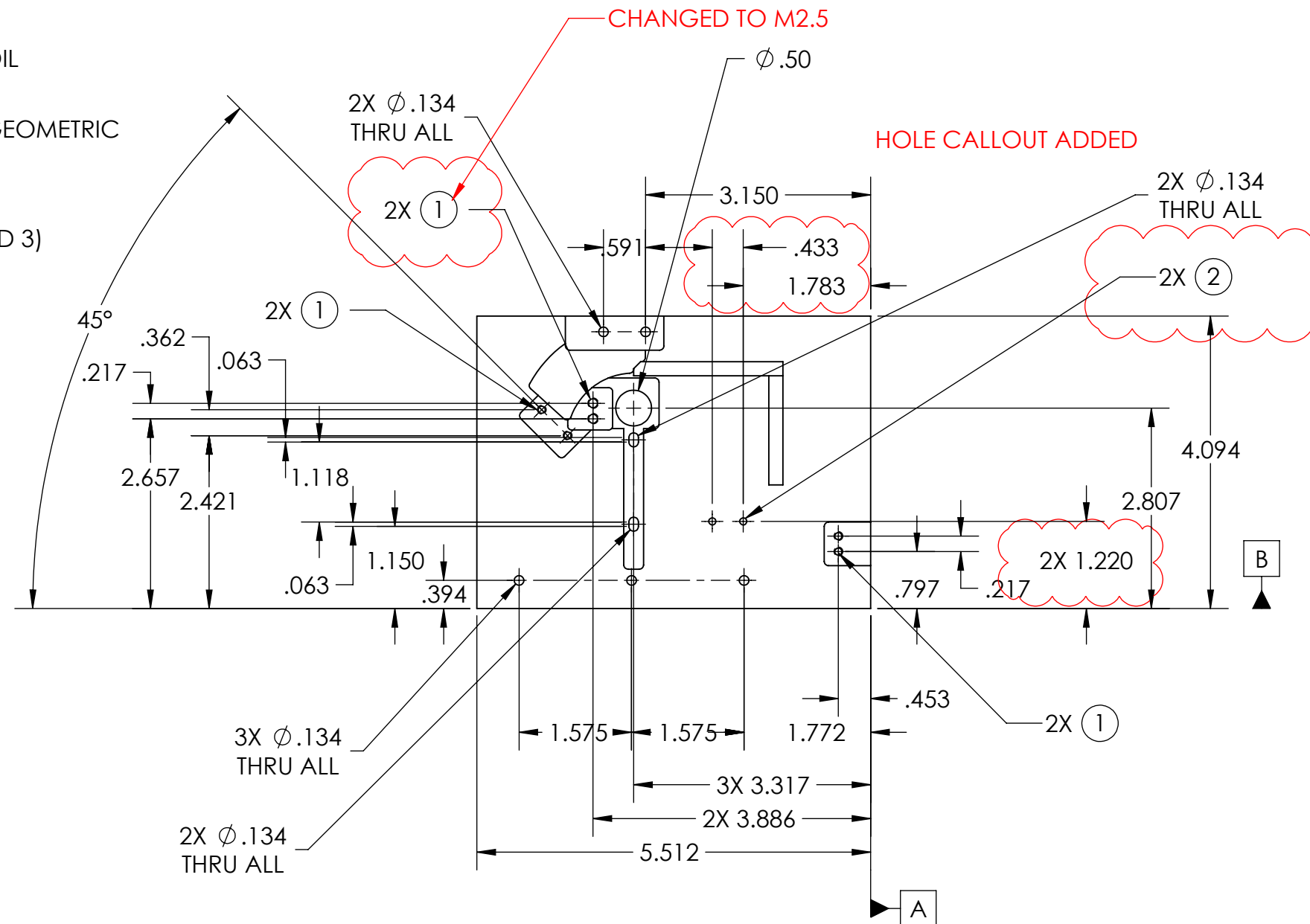
UNLESS OTHERWISE SPECIFIED: DIMENSIONS ARE IN INCHES TOLERANCES: FRACTIONAL ± 0.5° TWO PLACE DECIMAL ± 0.05 THREE PLACE DECIMAL ± 0.005	INTERPRET DRAWING PER ANSI Y14.5 2009 	CAL POLY SAN LUIS OBISPO	MATERIAL: SEE BOM	TITLE: OPTICS DATUM TRANSLATION BOARD				
			DRAWN BY: JEFF WAGNER	DATE: 06-09-2019	SHEET 1 OF 1	SCALE: 1:4	REV	SIZE B

NOTE:

1. SEE CAD MODEL FOR FEATURE DIMENSIONS, ONLY HOLE LOCATION AND CALLOUT PROVIDED HERE.
2. ALL DIMENSIONS ARE IN INCHES UNLESS OTHERWISE SPECIFIED
3. TOLERANCE $\pm .001$ UNLESS OTHERWISE SPECIFIED
4. (1) INDICATES FOLLOWING CALLOUT:
TAPPED HOLE FOR M2.5X0.45 HELICOIL
THRU ALL
5. (2) INDICATES FOLLOWING CALLOUT:
TAPPED HOLE FOR M3X0.5 HELICOIL
THRU ALL
6. ALL INTERIOR CORNERS: R=1.5MM
7. ALL HOLE LOCATIONS HAVE APPLIED GEOMETRIC TOLERANCE OF

$\oplus .0025 \text{ (M)} \text{ X X}$

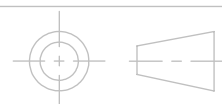
WITH RESPECTIVE DATUMS:
(A&B FOR VIEW 1, B&C FOR VIEW 2 AND 3)



CUBE-DC-107002

UNLESS OTHERWISE SPECIFIED:
DIMENSIONS ARE IN INCHES
TOLERANCES:
FRACTIONAL $\pm 0.5^\circ$
TWO PLACE DECIMAL ± 0.005
THREE PLACE DECIMAL ± 0.0025

INTERPRET DRAWING
PER ANSI Y14.5 2009



CAL POLY
SAN LUIS OBISPO

MATERIAL:
SEE BOM

DRAWN BY:
JEFF WAGNER

TITLE:
LEFT SIDE PANEL

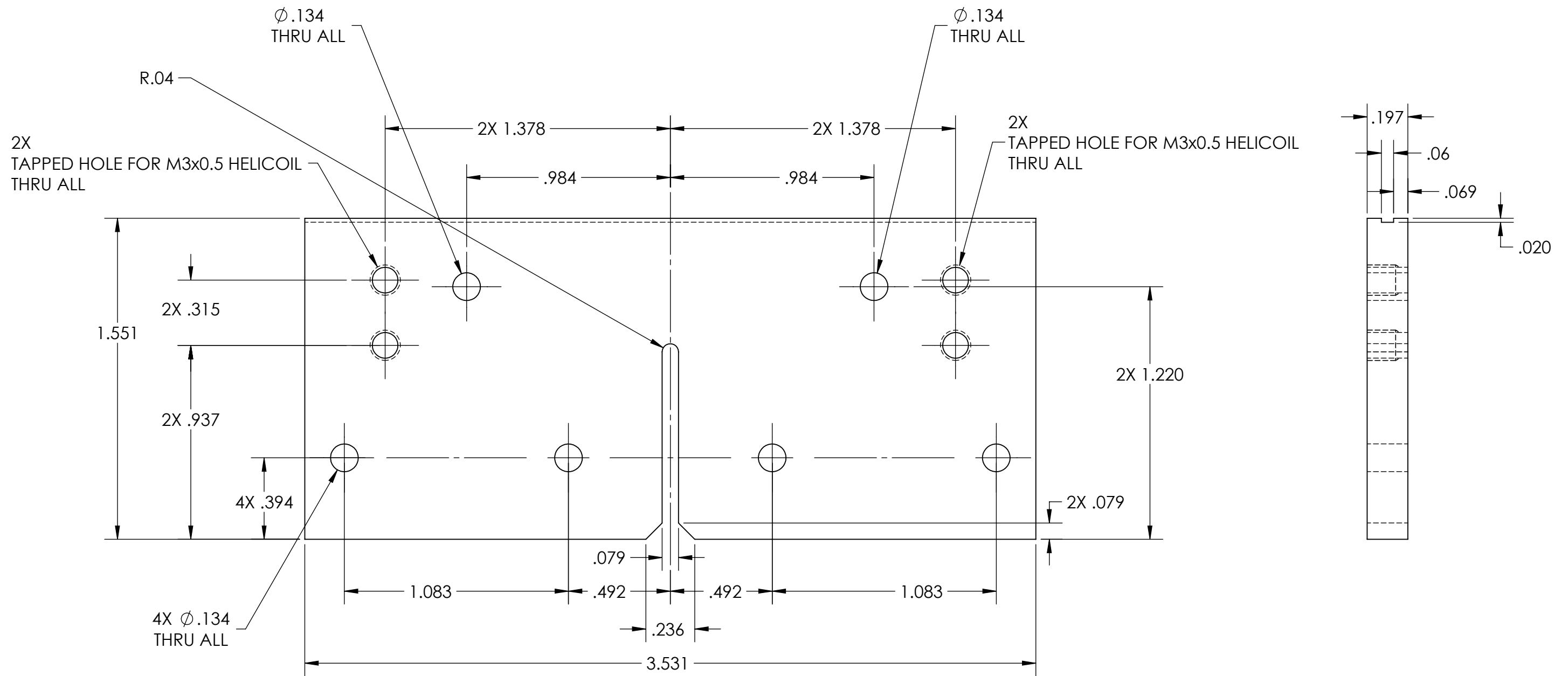
DATE:
12-04-2019

SHEET 3 OF 7

SCALE: 1:2

REV

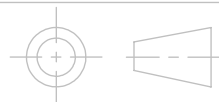
SIZE
B



CUBE-DC-107004

UNLESS OTHERWISE SPECIFIED:
 DIMENSIONS ARE IN INCHES
 TOLERANCES:
 FRACTIONAL $\pm 0.5^\circ$
 TWO PLACE DECIMAL ± 0.005
 THREE PLACE DECIMAL ± 0.0025

INTERPRET DRAWING
 PER ANSI Y14.5 2009



CAL POLY
SAN LUIS OBISPO

MATERIAL:
 SEE BOM

DRAWN BY:
 JEFF WAGNER

TITLE:
 FRONT PANEL

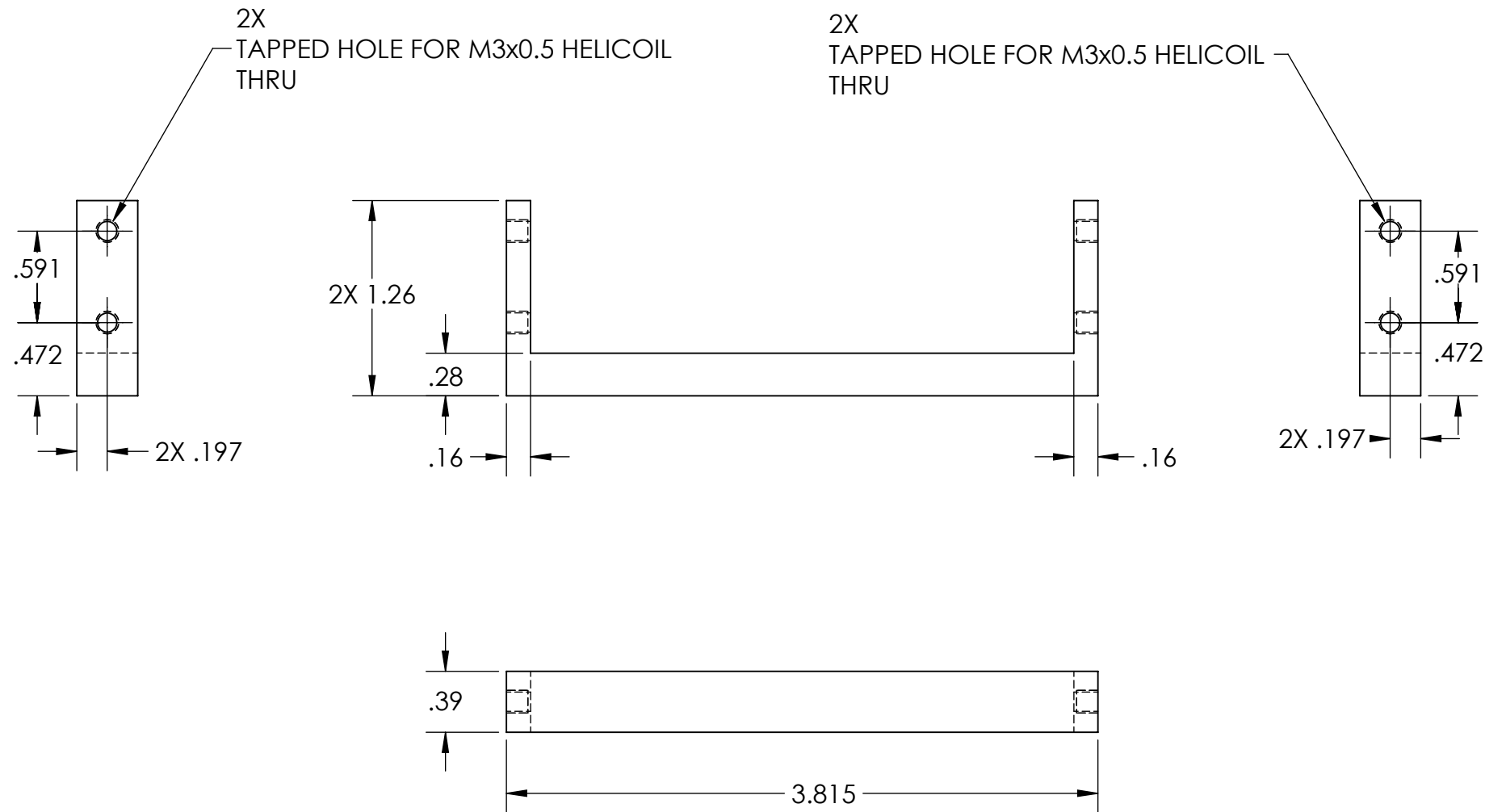
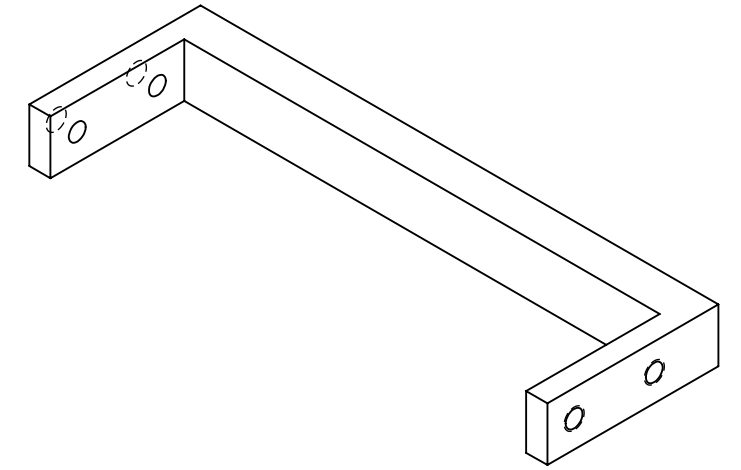
DATE:
 06-04-2019

SHEET 5 OF 7

SCALE: 2:1

REV

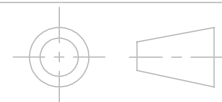
SIZE
B



CUBE-DC-107005

UNLESS OTHERWISE SPECIFIED:
 DIMENSIONS ARE IN INCHES
 TOLERANCES:
 FRACTIONAL $\pm 0.5^\circ$
 TWO PLACE DECIMAL ± 0.005
 THREE PLACE DECIMAL ± 0.0025

INTERPRET DRAWING
 PER ANSI Y14.5 2009



CAL POLY
SAN LUIS OBISPO

MATERIAL:
 SEE BOM

DRAWN BY:
 JEFF WAGNER

TITLE:
 TOP U BRACKET

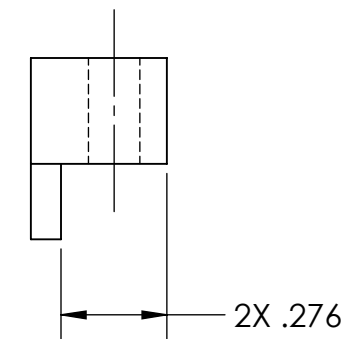
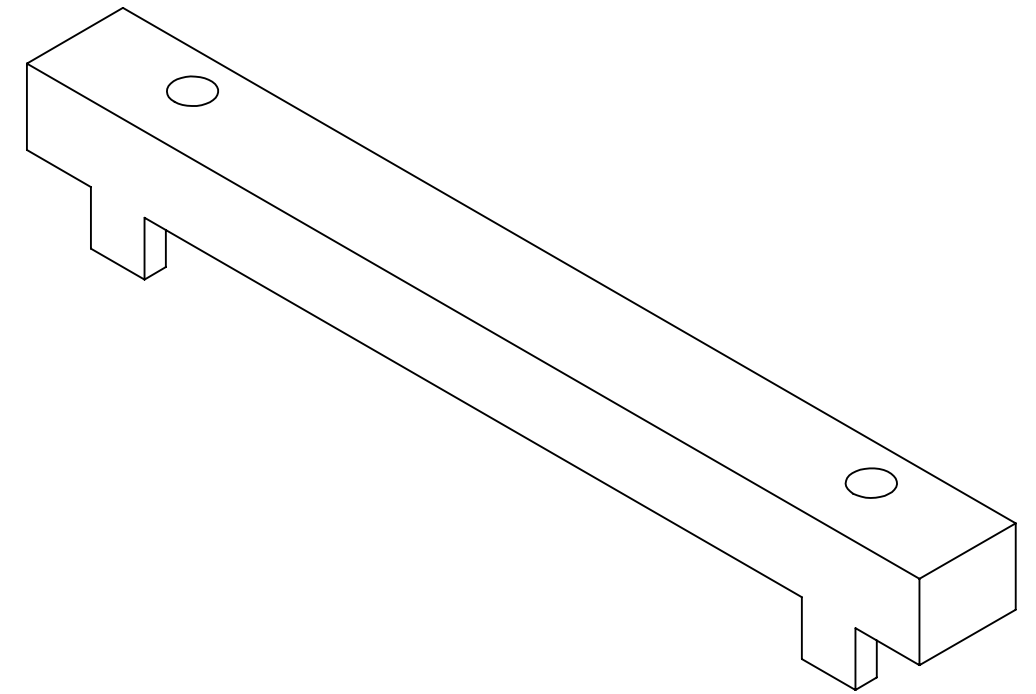
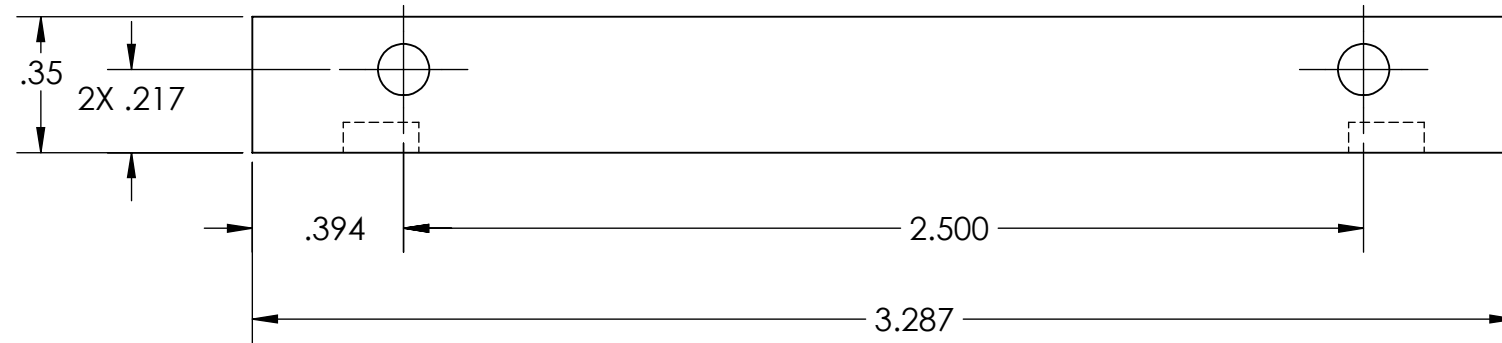
DATE:
 06-04-2019

SHEET 6 OF 7

SCALE: 1:1

REV

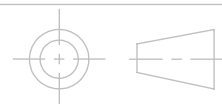
SIZE
B



CUBE-DC-107006

UNLESS OTHERWISE SPECIFIED:
 DIMENSIONS ARE IN INCHES
 TOLERANCES:
 FRACTIONAL $\pm 0.5^\circ$
 TWO PLACE DECIMAL ± 0.005
 THREE PLACE DECIMAL ± 0.0025

INTERPRET DRAWING
 PER ANSI Y14.5 2009



CAL POLY
SAN LUIS OBISPO

MATERIAL:
 SEE BOM

DRAWN BY:
 JEFF WAGNER

TITLE:
 FRONT CROSS BEAM

DATE:
 06-04-2019

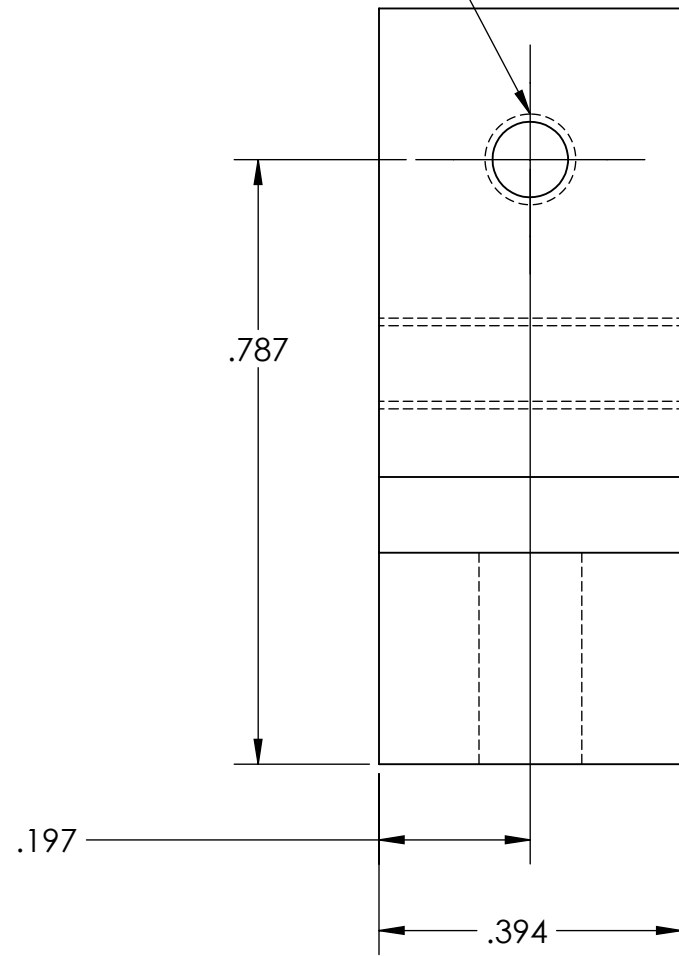
SHEET 7 OF 7

SCALE: 2:1

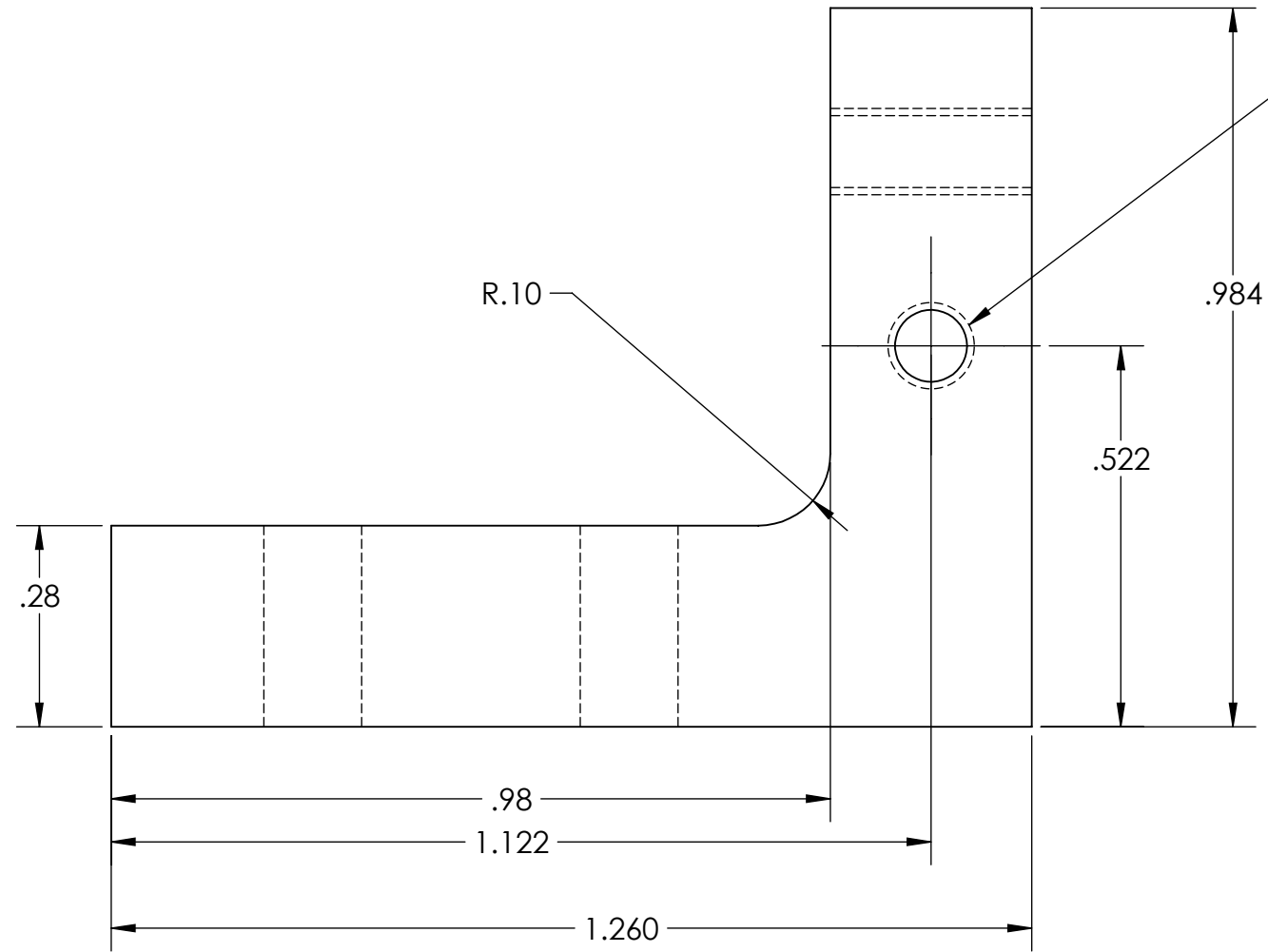
REV

SIZE
B

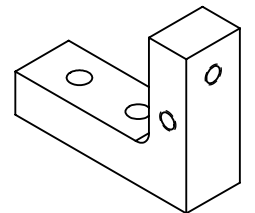
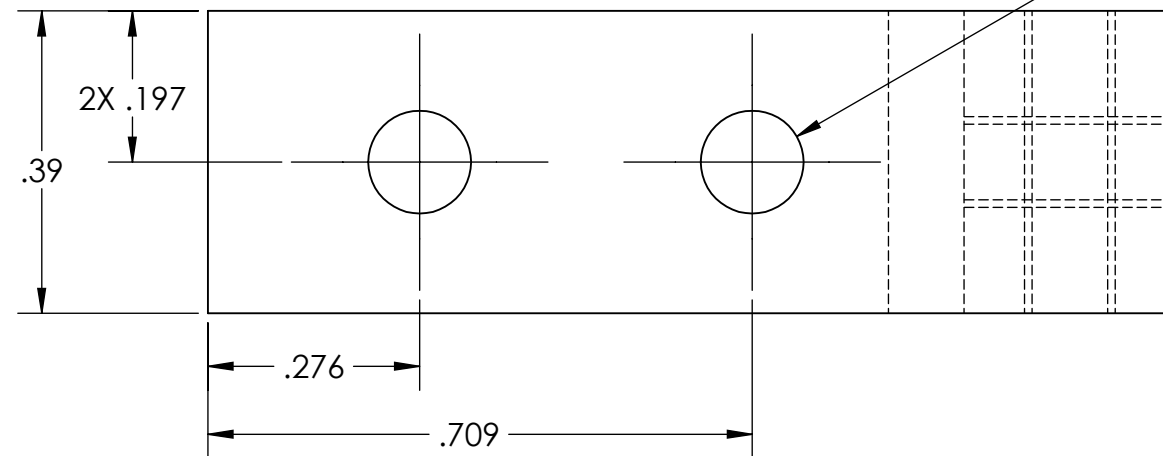
TAPPED HOLE FOR M3x0.5 HELICOIL



TAPPED HOLE FOR M3x0.5 HELICOIL

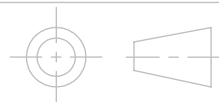


2X ϕ .134 THRU ALL



UNLESS OTHERWISE SPECIFIED:
DIMENSIONS ARE IN INCHES
TOLERANCES:
FRACTIONAL $\pm 0.5^\circ$
TWO PLACE DECIMAL ± 0.05
THREE PLACE DECIMAL ± 0.005

INTERPRET DRAWING
PER ANSI Y14.5 2009



CAL POLY
SAN LUIS OBISPO

MATERIAL:
SEE BOM

DRAWN BY:
JEFF WAGNER

TITLE:
CROSS BEAM MOUNTING PLATFORM

DATE:
06-09-2019

SHEET 1 OF 1

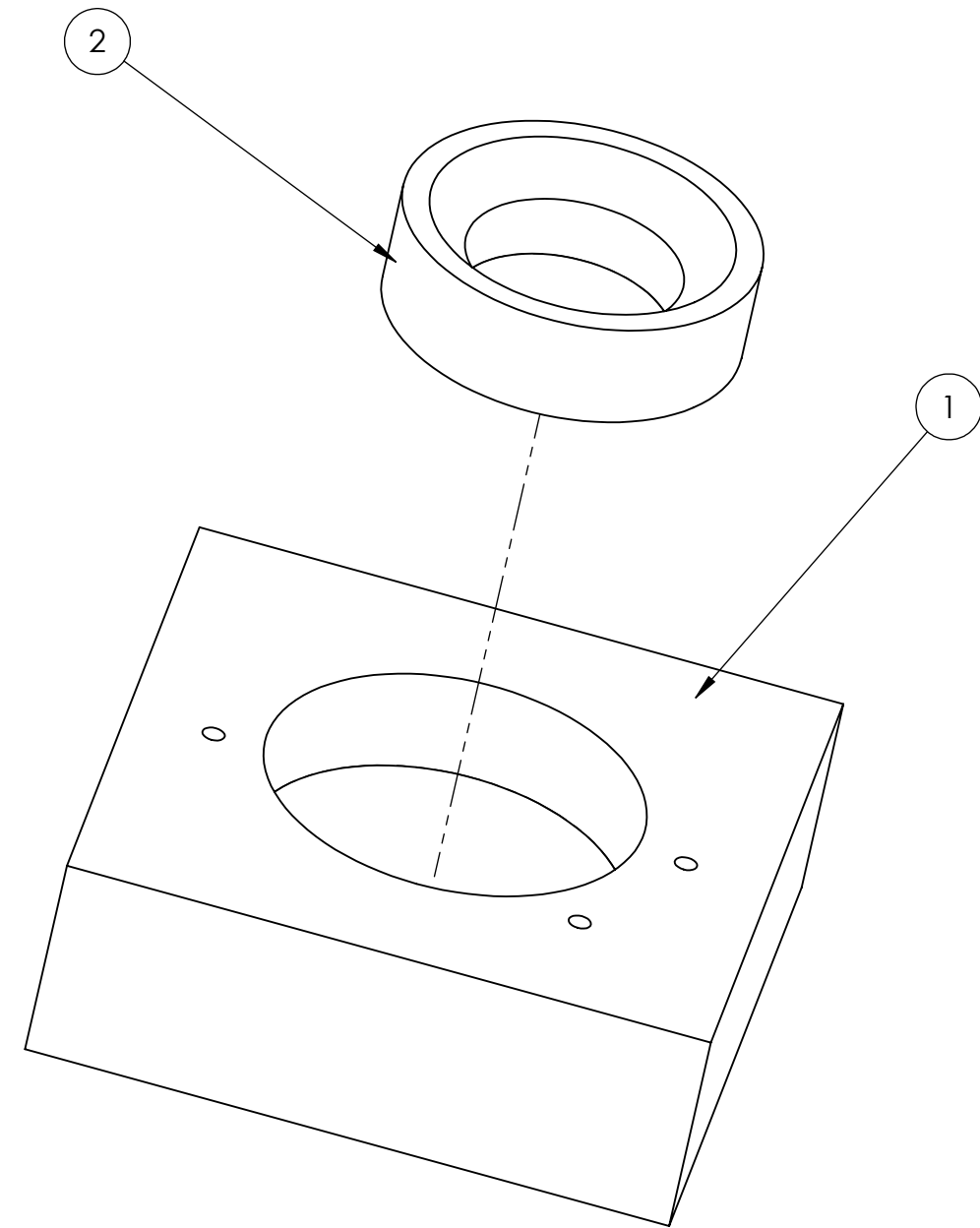
SCALE: 2:1

REV

SIZE
B

NOTES, UNLESS OTHERWISE SPECIFIED:

1. MATERIAL: ALUMINUM 6061-T651 PER AMS 4027 AND AMS 4150. FOR OTHER MATERIALS, SEE BOM.
2. BREAK EXTERNAL EDGES AND CORNERS .005 IN MAX UNLESS NOTED.
3. INTERNAL CORNER AND FILLET RADII .005 MAX UNLESS NOTED.
4. INSTALL HELICAL COIL INSERT PER NASM33537. REMOVE TANG.
5. DRAWING IS THE SOLE AUTHORITY FOR THE BASIC FORM, LOCATION, ORIENTATION, AND DIMENSIONAL CHARACTERISTICS OF ALL DESIGN FEATURES.



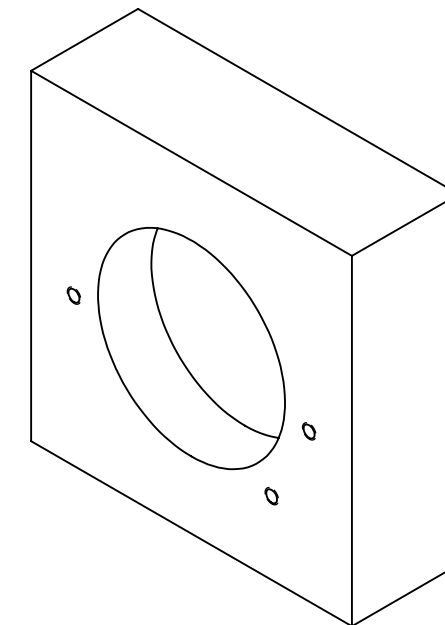
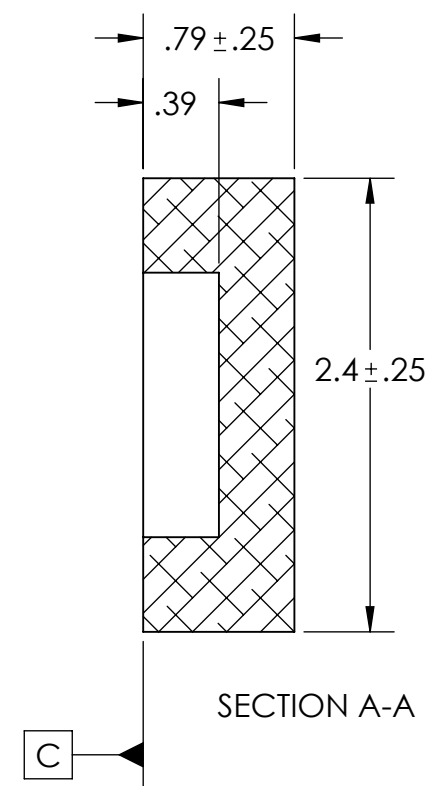
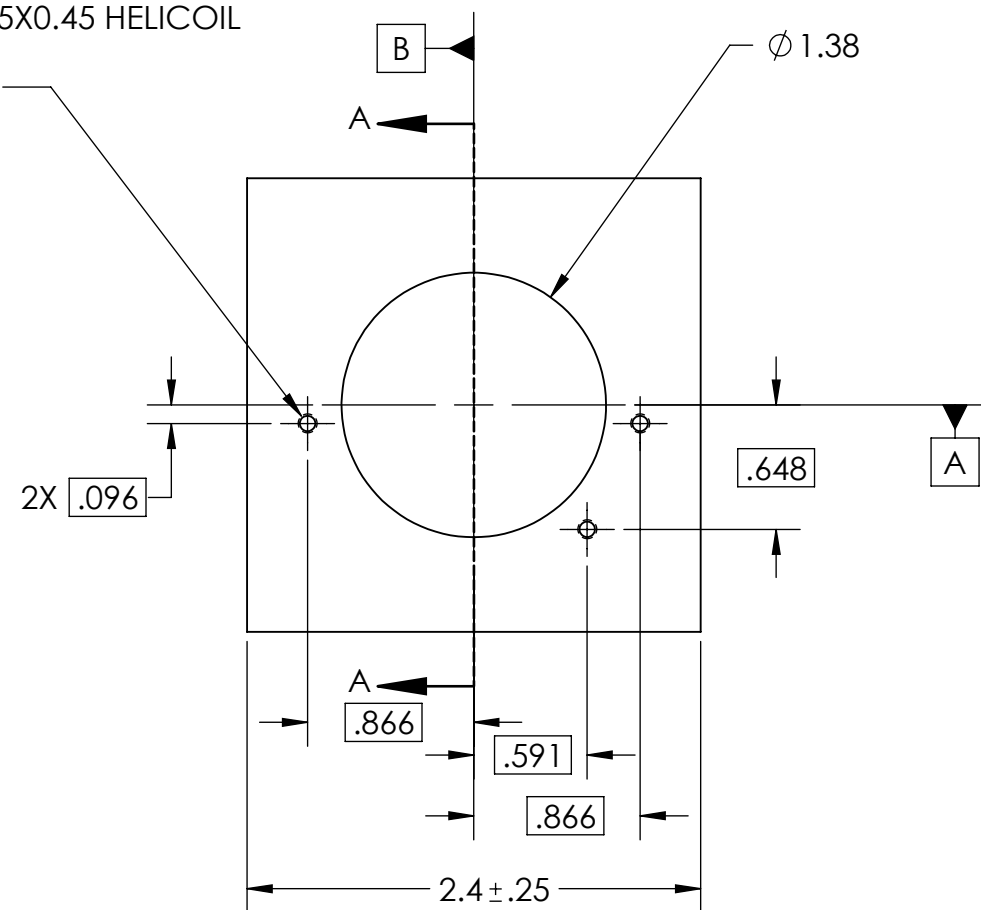
CUBE-DC-108000

ITEM NO.	PART NUMBER	DESCRIPTION	MATERIAL	QTY.
1	CUBE-DC-108001	Bottom Mirror Flexure Aligner	6061-T6 (SS)	1
2	CUBE-DC-108002	BOTTOM MIRROR DELRIN MIRROR POSITIONER	Delrin 2700 NC010, Low Viscosity Acetal Copolymer (SS)	1

UNLESS OTHERWISE SPECIFIED: DIMENSIONS ARE IN INCHES TOLERANCES: FRACTIONAL $\pm 0.5^\circ$ TWO PLACE DECIMAL ± 0.005 THREE PLACE DECIMAL ± 0.0025	INTERPRET DRAWING PER ANSI Y14.5 2009 	CAL POLY SAN LUIS OBISPO	MATERIAL: SEE BOM	TITLE: BOTTOM MIRROR BOND FIXTURE				
			DRAWN BY: JEFF WAGNER	DATE: 06-04-2019	SHEET 1 OF 3	SCALE: 3:2	REV	SIZE B

3X
TAPPED HOLE FOR M2.5X0.45 HELICOIL
▽.297

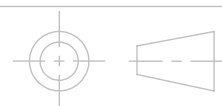
⊕.0025 (M) A B C



CUBE-DC-108001

UNLESS OTHERWISE SPECIFIED:
DIMENSIONS ARE IN INCHES
TOLERANCES:
FRACTIONAL $\pm 0.5^\circ$
TWO PLACE DECIMAL ± 0.005
THREE PLACE DECIMAL ± 0.0025

INTERPRET DRAWING
PER ANSI Y14.5 2009



CAL POLY
SAN LUIS OBISPO

MATERIAL:
SEE BOM

DRAWN BY:
JEFF WAGNER

TITLE:
BOTTOM MIRROR FLEXURE ALIGNER

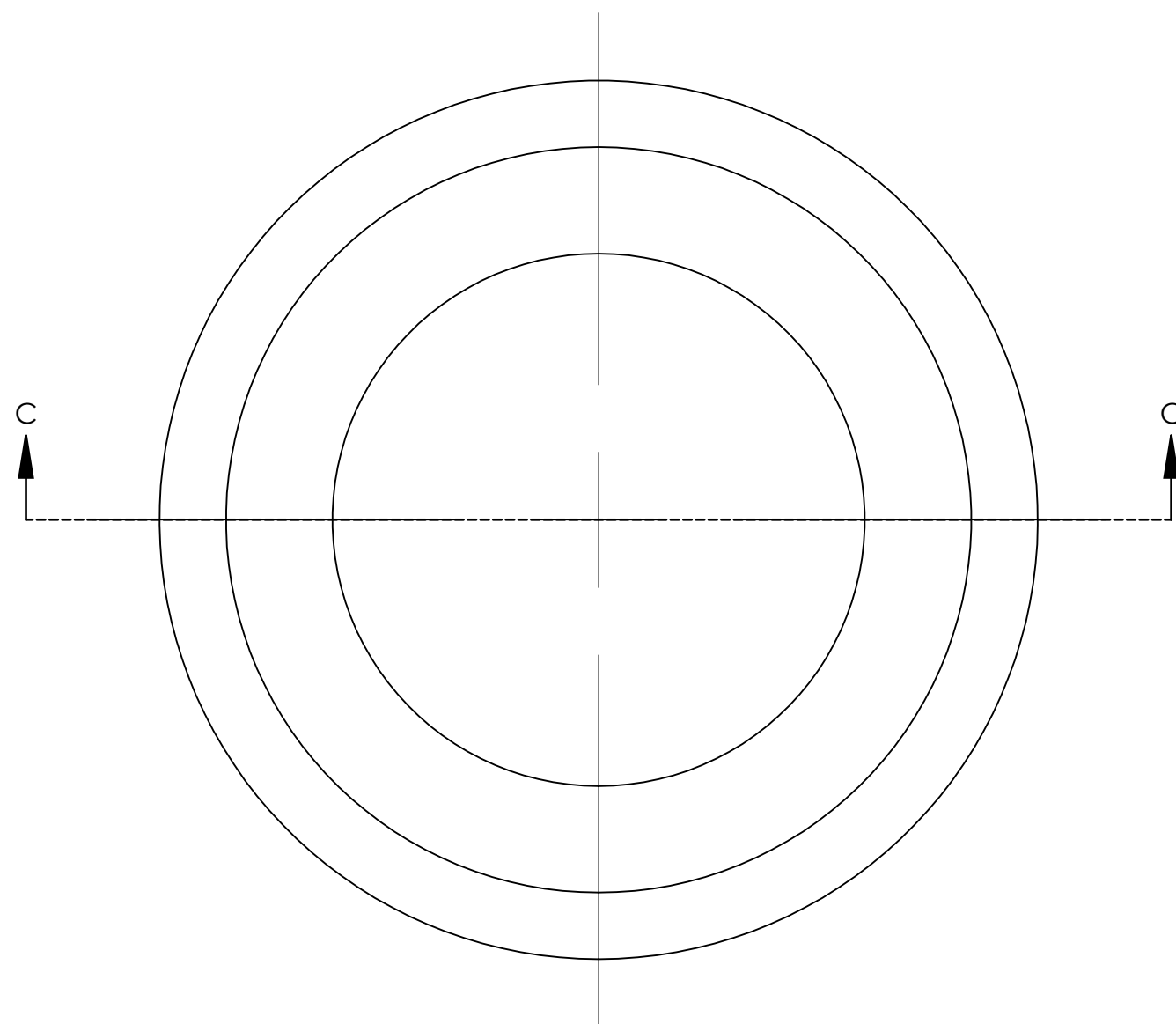
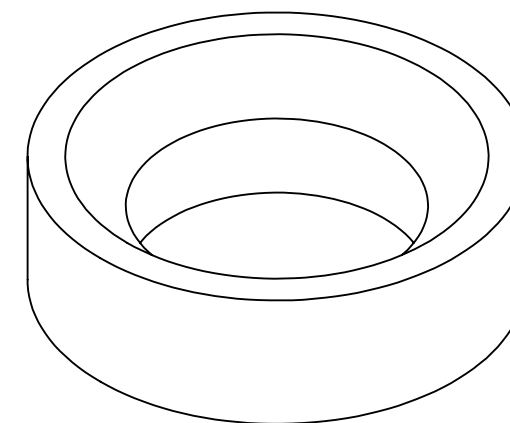
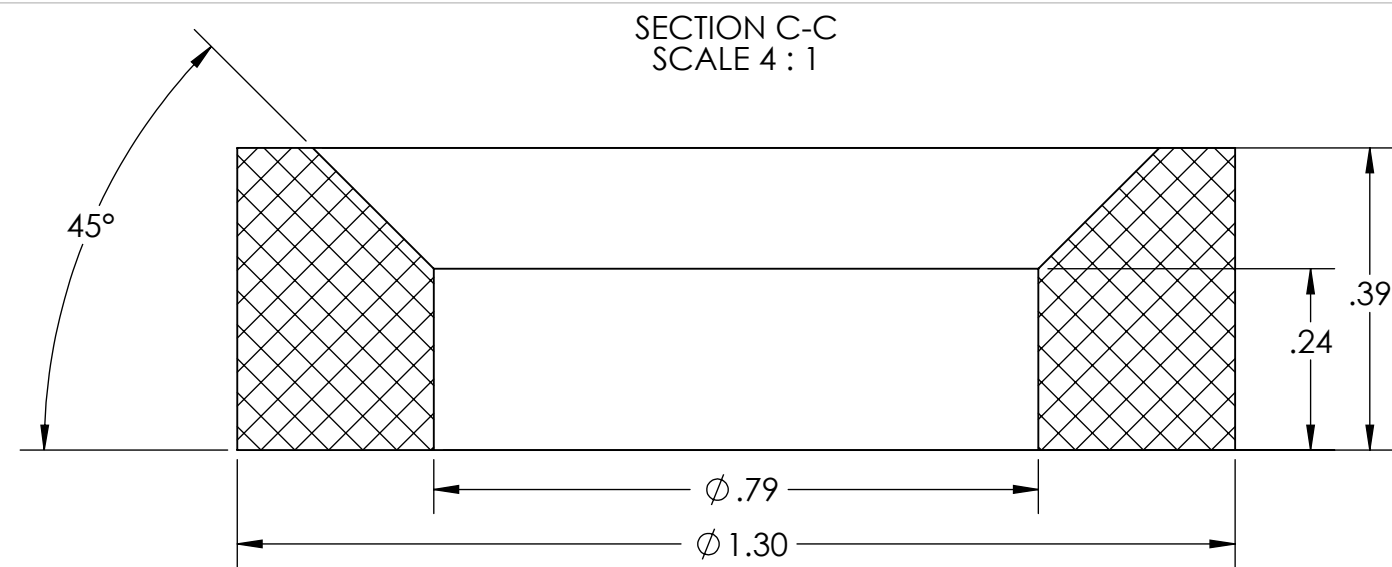
DATE:
06-04-2019

SHEET 2 OF 3

SCALE: 1:1

REV

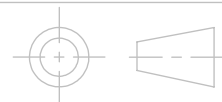
SIZE
B



CUBE-DC-108002

UNLESS OTHERWISE SPECIFIED:
DIMENSIONS ARE IN INCHES
TOLERANCES:
FRACTIONAL $\pm 0.5^\circ$
TWO PLACE DECIMAL ± 0.005
THREE PLACE DECIMAL ± 0.0025

INTERPRET DRAWING
PER ANSI Y14.5 2009



CAL POLY
SAN LUIS OBISPO

MATERIAL:
SEE BOM

DRAWN BY:
JEFF WAGNER

TITLE:
BOTTOM MIRROR DELRIN MIRROR POSITIONER

DATE:
06-04-2019

SHEET 3 OF 3

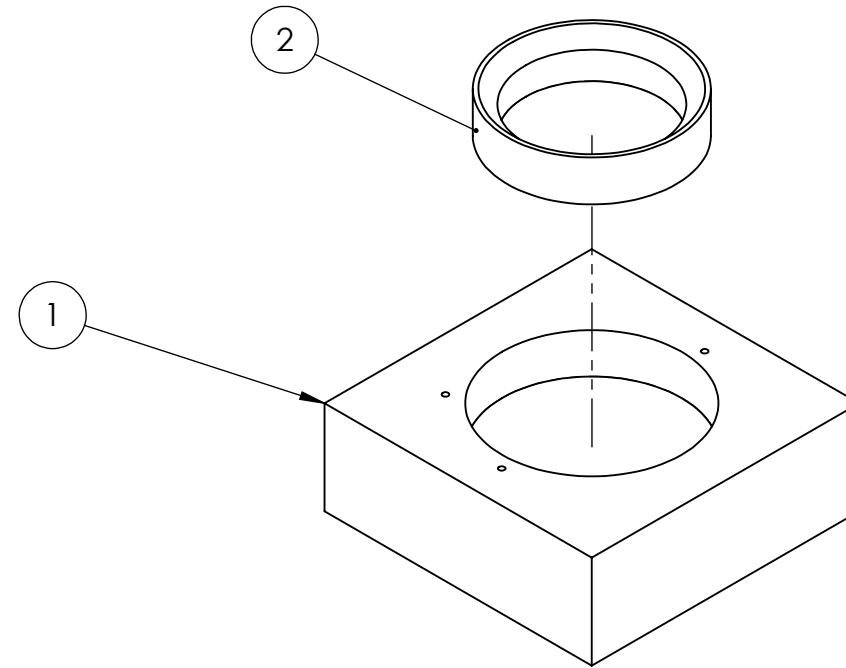
SCALE: 4:1

REV

SIZE
B

NOTES, UNLESS OTHERWISE SPECIFIED:

1. MATERIAL: ALUMINUM 6061-T651 PER AMS 4027 AND AMS 4150. FOR OTHER MATERIALS, SEE BOM.
2. BREAK EXTERNAL EDGES AND CORNERS .005 IN MAX UNLESS NOTED.
3. INTERNAL CORNER AND FILLET RADII .005 MAX UNLESS NOTED.
4. INSTALL HELICAL COIL INSERT PER NASM33537. REMOVE TANG.
5. DRAWING IS THE SOLE AUTHORITY FOR THE BASIC FORM, LOCATION, ORIENTATION, AND DIMENSIONAL CHARACTERISTICS OF ALL DESIGN FEATURES.

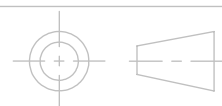


CUBE-DC-109000

ITEM NO.	PART NUMBER	DESCRIPTION	MATERIAL	QTY.
1	CUBE-DC-109001	TOP MIRROR FLEXURE ALIGNER	6061-T6 (SS)	1
2	CUBE-DC-109002	TOP MIRROR DELRIN MIRROR POSITIONER	Delrin 2700 NC010, Low Viscosity Acetal Copolymer (SS)	1

UNLESS OTHERWISE SPECIFIED:
 DIMENSIONS ARE IN INCHES
 TOLERANCES:
 FRACTIONAL $\pm 0.5^\circ$
 TWO PLACE DECIMAL ± 0.005
 THREE PLACE DECIMAL ± 0.0025

INTERPRET DRAWING
 PER ANSI Y14.5 2009



CAL POLY
SAN LUIS OBISPO

MATERIAL:
 SEE BOM

DRAWN BY:
 JEFF WAGNER

TITLE:
 TOP MIRROR BOND FIXTURE

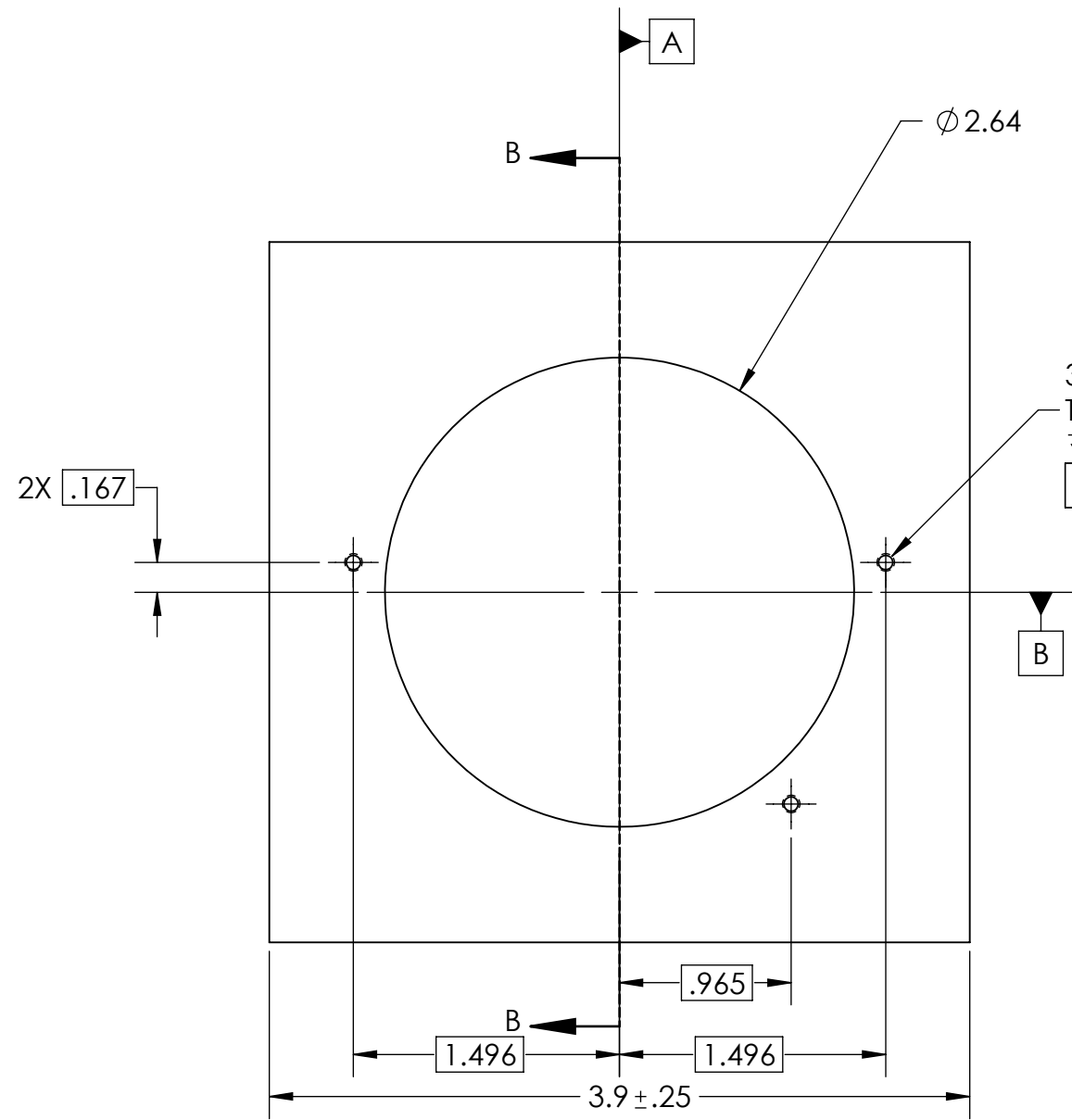
DATE:
 06-04-2019

SHEET 1 OF 3

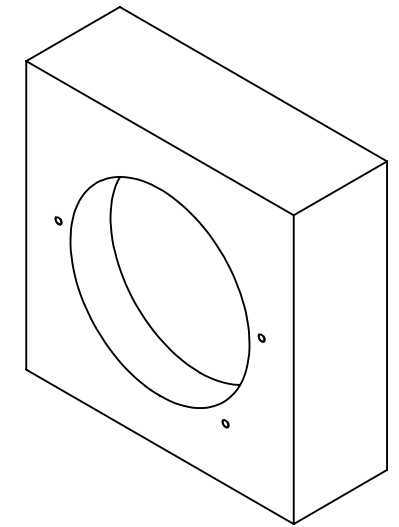
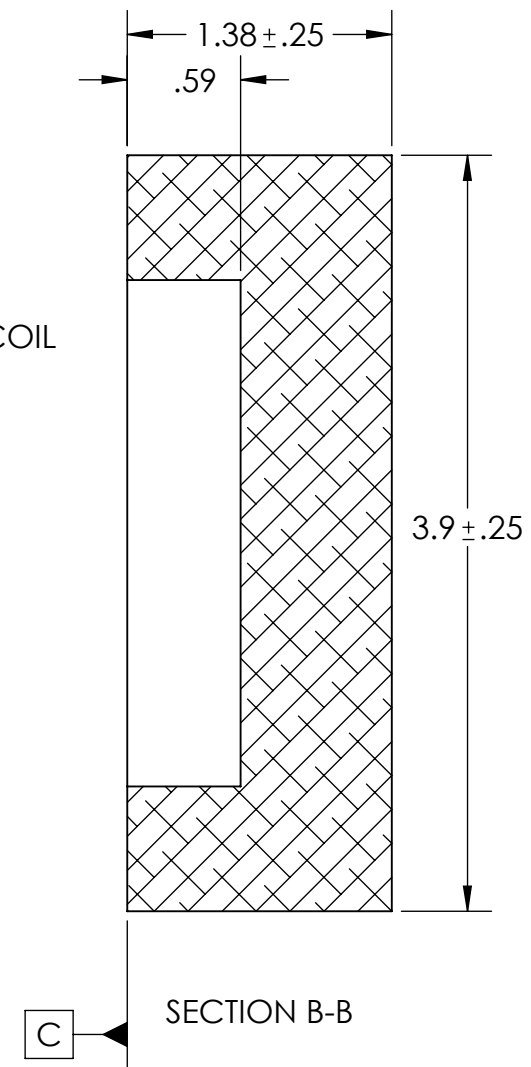
SCALE: 1:2

REV

SIZE
B



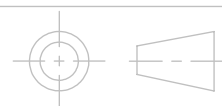
3X
TAPPED HOLE FOR M2.5x0.45 HELICOIL
↓ .297
⊕ .0025 (M) A B C



CUBE-DC-109001

UNLESS OTHERWISE SPECIFIED:
DIMENSIONS ARE IN INCHES
TOLERANCES:
FRACTIONAL ± 0.5°
TWO PLACE DECIMAL ± 0.005
THREE PLACE DECIMAL ± 0.0025

INTERPRET DRAWING
PER ANSI Y14.5 2009



CAL POLY
SAN LUIS OBISPO

MATERIAL:
SEE BOM

DRAWN BY:
JEFF WAGNER

TITLE:
TOP MIRROR FLEXURE ALIGNER

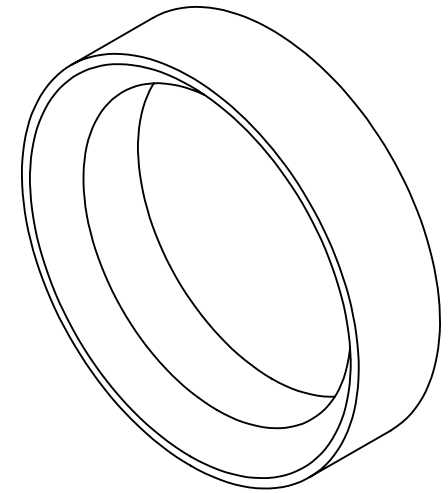
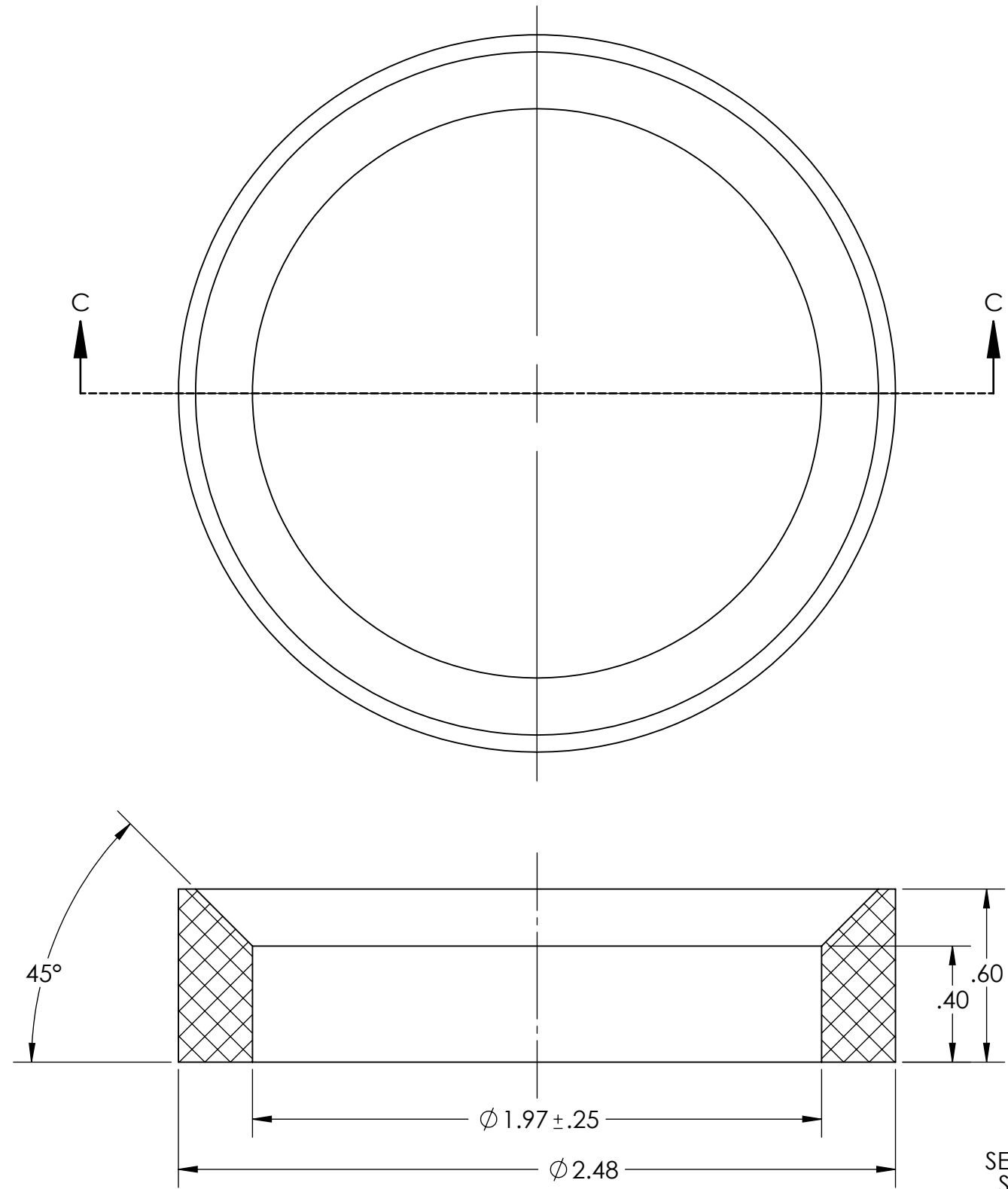
DATE:
06-04-2019

SHEET 2 OF 3

SCALE: 1:1

REV

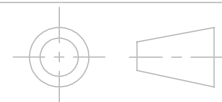
SIZE
B



CUBE-DC-109002

UNLESS OTHERWISE SPECIFIED:
 DIMENSIONS ARE IN INCHES
 TOLERANCES:
 FRACTIONAL $\pm 0.5^\circ$
 TWO PLACE DECIMAL ± 0.005
 THREE PLACE DECIMAL ± 0.0025

INTERPRET DRAWING
 PER ANSI Y14.5 2009



CAL POLY
SAN LUIS OBISPO

MATERIAL:
 SEE BOM

DRAWN BY:
 JEFF WAGNER

TITLE:
 TOP MIRROR DELRIN MIRROR POSITIONER

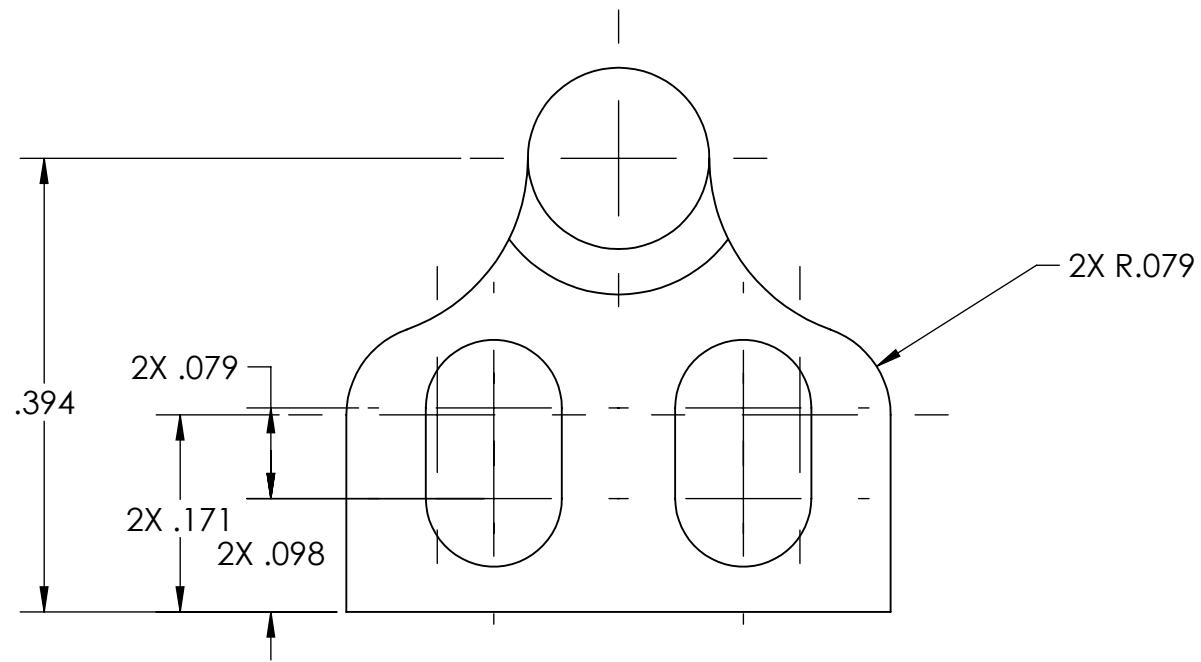
DATE:
 06-04-2019

SHEET 3 OF 3

SCALE: 2:1

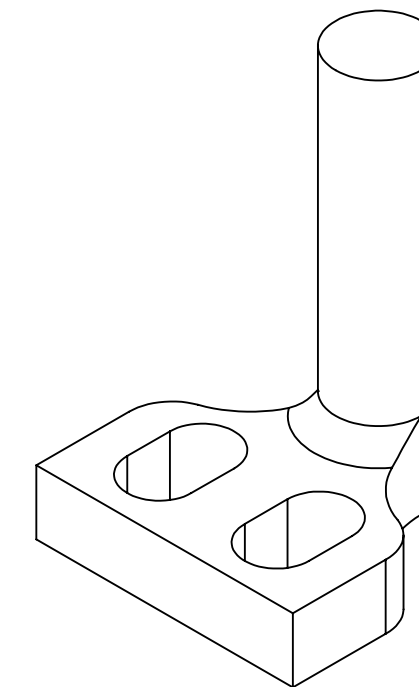
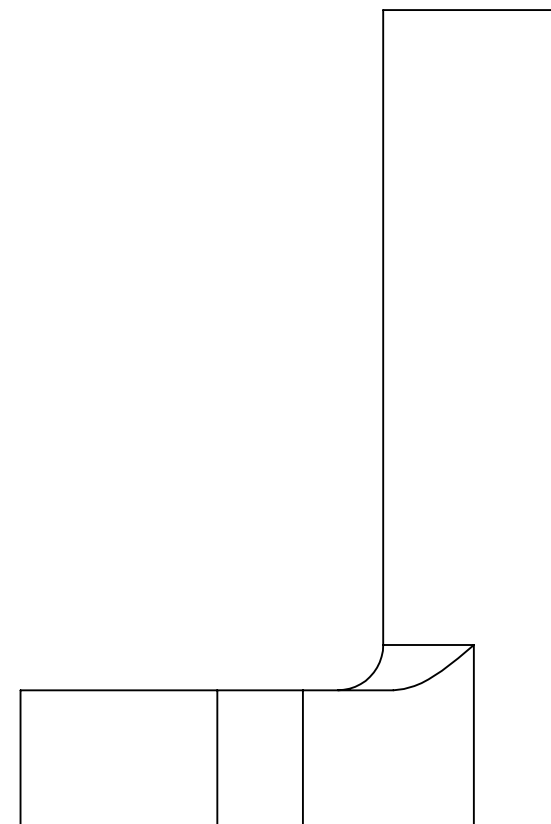
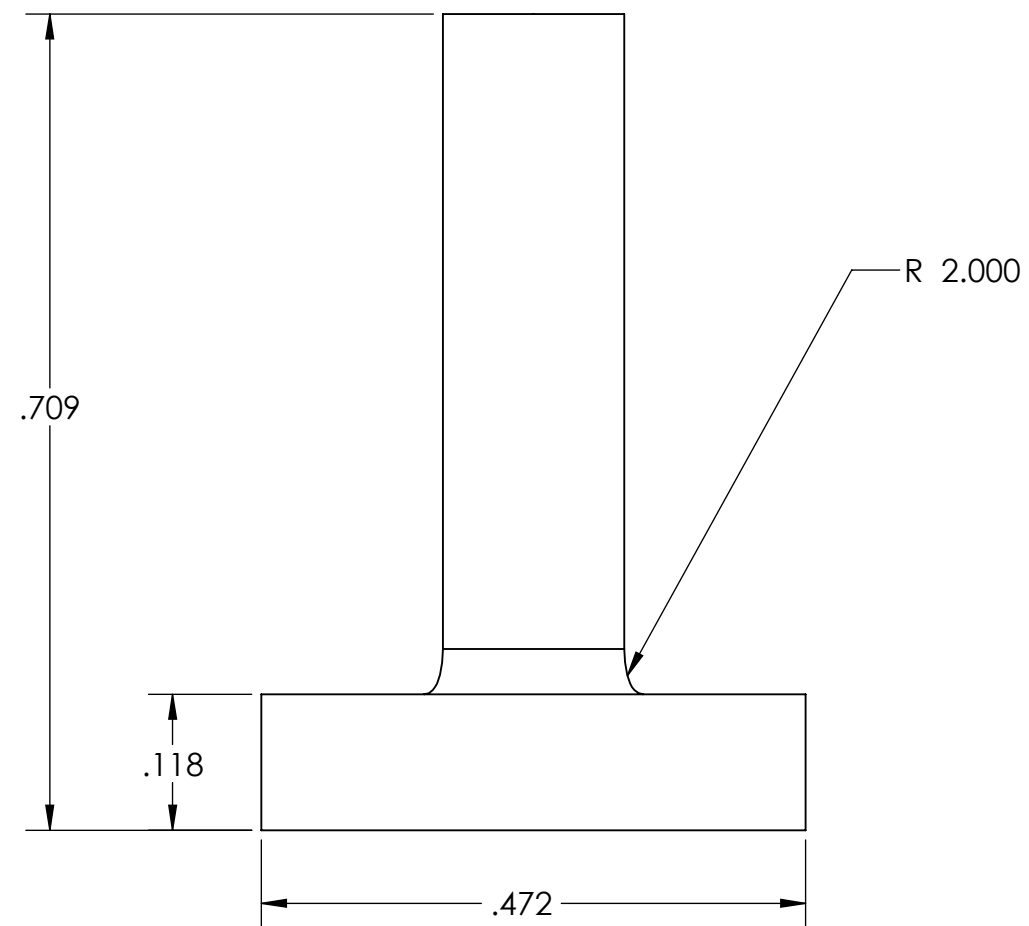
REV

SIZE
B



NOTES, UNLESS OTHERWISE SPECIFIED:

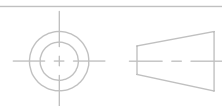
1. MATERIAL: STANDARD SLA RESIN
2. BREAK EXTERNAL EDGES AND CORNERS .005 IN MAX UNLESS NOTED.
3. INTERNAL CORNER AND FILLET RADII .005 MAX UNLESS NOTED.
4. DRAWING IS THE SOLE AUTHORITY FOR THE BASIC FORM, LOCATION, ORIENTATION, AND DIMENSIONAL CHARACTERISTICS OF ALL DESIGN FEATURES.



CUBE-DC-110000

UNLESS OTHERWISE SPECIFIED:
 DIMENSIONS ARE IN INCHES
 TOLERANCES:
 FRACTIONAL ± 0.5°
 TWO PLACE DECIMAL ± 0.005
 THREE PLACE DECIMAL ± 0.0025

INTERPRET DRAWING
 PER ANSI Y14.5 2009



CAL POLY
SAN LUIS OBISPO

MATERIAL:
 SEE BOM

DRAWN BY:
 PATRICK WHITESEL

TITLE:
 LOCKOUT FLEXURE

DATE:
 06-06-19

SHEET 1 OF 1

SCALE: 6:1

REV

SIZE
B